STUDIES OF CARBON, OXYGEN AND STRONTIUM ISOTOPES IN TOOTH ENAMEL: EVALUATING PALEOENVIRONMENTAL CHANGE IN SOUTH AFRICA AND EXPANDING THE PALEOCLIMATE TOOL KIT

by
Sophie B. Lehmann

A dissertation submitted to The Johns Hopkins University in conformity with the requirements for the degree of Doctor of Philosophy

Baltimore, Maryland
October 2016

ABSTRACT

Anthropogenic-driven climate change has and will continue to influence Earth's ecosystems and environments. Major regional and global climate events have been observed throughout the geological record. We need to determine how natural systems responded to climate in the past and the possible interactions between mammalian species, including humans, and their environment, if we are to have perspective on how natural systems will respond to changes in climate both currently and in the future. Evaluating past climate and environment can be a useful way to evaluate if and how past landscapes, ecosystems and animal-environment interactions may have been influenced by climatic change.

Archeological and paleontological sites along the coastal region of southwestern South Africa preserve fossils and artifacts dating to the Pliocene and Pleistocene (within the last 5 million years). These materials indicate that southwestern South Africa was once home to large herbivorous mammalian communities and that hominins lived here since the mid-Pleistocene, at ca. 1 million years ago. However, this region is currently hot and dry and within a cool growing season. Furthermore, this region is within the fynbos biome, a biome with species that date to before the Pliocene, and is today mostly composed of woody, nutrient-poor shrub land. It is unknown how animals survived in the region during the Pliocene and Pleistocene or the composition of past vegetation and its distribution.

Here I present an evaluation of animal diet and the climate and environment of southwestern South Africa over the last 5 million years using the carbon ($\delta^{13}C$ values) and oxygen ($\delta^{18}O$ values) isotopic composition of fossil teeth. I then evaluate the

movement of animals for food in southwestern South Africa during the mid-Pleistocene and the distribution of vegetation at this time using strontium isotope ratios ($^{87}Sr/^{86}Sr$ ratios) in the fossil tooth enamel preserved at archeological site Elandsfontein. I then consider the use of triple oxygen isotopes ($\Delta^{17}O$) in the fossil record as a way to improve upon the current $\delta^{18}O$ method to determine past climate and environmental change by presenting and characterizing $\Delta^{17}O$ in modern tooth enamel.

I found that herbivores ate vegetation characteristic of a cool growing season during the Pliocene and Pleistocene, therefore southwestern South Africa was within a winter rainfall zone since at least 5 million years ago. The ecosystem and environment of southwestern South Africa would have had to support the annual growth of grass if large mammalian herbivores (specifically grazers) could have survived in this region. Deposits indicative of fluvial environments (during the Pliocene) and spring-fed environments (during the Pleistocene) are preserved at fossil sites in the region. These environments would have been extremely important for the survival of animals in southwestern South Africa. The $^{87}Sr/^{86}Sr$ ratios of fossil teeth from mid-Pleistocene Elandsfontein suggest that large herbivores not only stayed within southwestern South Africa for food, but that they did not necessarily leave the area surrounding the fossil site.

The $\Delta^{17}O$ values of modern tooth enamel samples cover a greater span and include more negative values in arid environments than in humid environments, regardless of the oxygen isotopic composition of meteoric water and latitude. This record indicates the future potential of applying triple oxygen isotopes to the fossil record for reconstructing aridity, atmospheric pCO_2 and diagenesis.

Faculty Advisor and First Reader:
Professor Naomi E. Levin
Morton K. Blaustein Department of Earth and Planetary Sciences
The Johns Hopkins University

Second Reader:
Professor Kevin W. Lewis
Morton K. Blaustein Department of Earth and Planetary Sciences
The Johns Hopkins University

Acknowledgments

Firstly, I would like to thank Dr. Naomi Levin for her support and patience throughout my time at Johns Hopkins University. How lucky I have been to have Naomi as an advisor and mentor and I have learned a great deal from her. I largely attribute my personal growth during my graduate experience to her.

Ben Passey has worked closely with me, has been involved in all of my committees and has also been an integral part of my education in the lab. His creative and thoughtful approach to science has been a formative example for how to produce meaningful work that fits into a bigger picture. My lab mates (Greg Henkes, Rebecca Kraft, Huanting Hu, Haoyuan Ji, Nikki DeLuca, Dana Brenner, Shuning Li and Zelalem Bedaso) have created an exciting and noncompetitive atmosphere in which to explore research interests. Those in the Stable Isotope group do not cease to amaze me in their abilities and their willingness to teach one another.

Robyn Pickering has been a friend and mentor to me since I first met her in 2012. She has taken it upon herself to be interested in my work and has on many occasions selflessly offered her time to me as I finish up my graduate career. Judy Sealy has taken an interest in my work and has helped form project ideas, collect and process samples and sponsor projects not only I was visiting in South Africa, but also from a far. She has been welcoming and has consistently treated me as a colleague and as an individual scientist from whom she can learn, and for that I am grateful. Dave Braun has been the source of many of my graduate career opportunities as he has been the direct connection to my main field site and to the majority of the fossil samples analyzed from

South Africa. He has been enthusiastic sounding board for every project in this thesis and his constant drive is an inspiration.

The Department of Earth and Planetary Sciences graduate program has been so very supportive and has been invested in me both as a scientist and as a person with broad interests and goals. I have been provided with the opportunities that go beyond the topics of my thesis and prepare me for a career in Earth Sciences, one in which I see myself as more than the projects that have defined this thesis. In particular, I would like to thank those faculty and staff who have shown interest and supported me: Drs. Kathy Szlavecz, Linda Hinnov, Anand Gnanadesikan and Grace Brush have taken time out of their own schedules to check in with me, discuss research and have shown support. Kevin Lewis took his responsibility as a proxy advisor above and beyond that which could have possibility been expected of him and has been a kind and helpful mentor to me in these last few months. Kristen Gaines, Teresa Healy, Jean Light and Kim Trent often work quietly behind the scenes and whose kindness and generosity have not gone unnoticed or unappreciated.

The funding for the work including travel to South Africa, field work and sample analysis, sample transport, were provided by the Department of Earth and Planetary Sciences Palmer travel grants and other internal funds such as by N.E. Levin's John Hopkins University Catalyst Grant. Research pertaining to the evaluation of southwestern South African paleoclimate and paleoenvironment would not have even begun without grants from the National Science Foundation (BCS 1219494 and BCS 1219455) and also directly supported the work at Elandsfontein as well as my part in it, clearance provided by the Heritage Western Cape (Permit No: 2008/11/003), permission

from the West Coast Fossil Park and the owners and staff of Elandsfontein property (now Elandsfontein Exploration and Mining) to do field work and from the Iziko Museums of South Africa for allowing us to sample fossil teeth from their collection (2010), field assistance from the students that attend the University of Cape Town, Department of Archeology field course at Elandsfontein (2008 to 2014), and the efforts of Jessica Plasket and Kathryn Braun who each played a major role in the excavations and the collection of fossil teeth.

The coauthors for each thesis chapter have added enormous insight and have allowed for the research to even occur. Coauthors include: K.J. Dennis, D.B. Patterson, D.D. Stynder, L.C. Bishop, F. Forrest, P. le Roux, M. Zhu, B.H. Passey, H. Hu, T.E. Cerling, K. Hoppe, J. Miller, L. Arpee, and S. Hynek. In addition, it would have been impossible to have completed the work needed for Chapter 3 and Chapter 4 (strontium and triple oxygen isotopes) without the samples provided by United States State Park rangers, graduate students and professors from the United States, Finland, East Africa and South Africa.

Lastly I would like to thank my family and friends whose love and believe in me often far surpass my own. My sisters and parents have always encouraged me to follow my own path, that we alone decide our own destiny, and to remember that creativity and serenity can be part of everything. In particular, my father has always shown interest in what I do in his actions which range from researching a topic and asking questions about that which he might not understand, to finding the JHU website that explains thesis formatting.

I would like to thank all of the people and institutions that have played roles in my graduate career. The acknowledgments above can only begin to name the relevant people as can it only scratch the surface of the gratitude I feel for everyone involved.

Table of Contents

List of Tables

List of Figures

CHAPTER 1

1. Introduction

A major field in Earth Sciences is evaluating how climate change affected organisms, landscapes and environments in the past. The effects and imminent consequences of anthropogenic-driven climate change on ecosystems and environments have become of immediate concern and these appear to be caused largely by the increased burning of fossil fuels resulting in increasing atmospheric pCO_2 and in turn increasing global temperatures. However, both regional and global climates have fluctuated substantially throughout Earth's history (e.g., Marlow et al., 2000; Zachos, 2001). Reconstructions of past climate provide perspective on how natural systems will respond to present and future climate change; this includes the interactions between animals and environments as well interactions between the human species and environment.

Materials from marine and terrestrial systems can be influenced by different aspects of climate. When these materials are preserved in the geological record they can hold a signal of some aspect of the climate for times in the past, such as temperature or atmospheric pCO_2 (e.g., Tipple et al., 2010). Marine sediment cores can preserve terrestrial materials (e.g., pollen, leaf wax, sediments) that are used to capture aspects of past terrestrial climate and environment, such as vegetation type (deMenocal, 2004; Dupont et al, 2013). These cores also preserve material originating in the marine system itself that is used for evaluating ocean circulation and sea surface temperature change in relation to regional and global climate change (Marlow et al., 2000). Marine-based terrestrial records can have high temporal resolution, however these records are not local

to one region and instead combine materials that can span subcontinental spatial scales; furthermore, the origin of the terrestrial materials in marine sediment cores is dependent upon the direction of atmospheric and oceanic currents and so material may travel long distances before being deposited. Terrestrial-based records provide a more local perspective of the hydrological setting, vegetation and climate of a landscape across a region or site, but these records are seldom continuous and can have low temporal resolution (Cerling et al., 2013; Levin et al., 2015). It is important, however, to analyze terrestrial-based climate and environment proxy records to understand how both landscape and associated organisms responded to climate change. These terrestrial records can be then used in tandem with marine records to evaluate if and how regional and global climatic change resulted in terrestrial climate and environmental change and in turn how these changes influenced organisms within the region.

Various materials preserved at the landscape surface, including soils, sediments and fossils, can be used to evaluate the past terrestrial climate and environment of a region or site. These materials preserve information about the past climate on different time scales. For example, fossils can represent precise periods of time (i.e., the life span of an animal) while other records average climate and environment over 100s to > 100,000s of years, and even longer (e.g., the formation of soil and the deposition of sediments on a landscape).

Records of fossil mammals preserve information about an animal's diet and have been used to indicate environment and climate during the time they were alive (Luyt et al., 2000; Franz-Odendaal et al., 2002; Braun et al., 2010; Patterson et al., 2016). These records represent a snapshot in time on a specific landscape (i.e., at longest, the period of

time an animal was alive). The type of vegetation consumed by animals can be evaluated using both the morphology of a tooth which is used to understand the vegetation type an herbivore had evolved to consume, and the scrapes and scratches on the chewing surface of teeth, which is indicative of the dietary behavior of an animal in a region, irrespective of tooth morphology (e.g., Stynder, 2011). Isotope ratios in bones and teeth record the type of vegetation an animal consumed (using carbon isotopes), whether an animal traveled away from where the fossil was found for food (using strontium isotopes) and information about the water an animal consumed (using oxygen isotopes) (e.g., Luyt et al., 2000; Hoppe et al., 2006; Levin et al., 2006; Copeland et al., 2016).

The composition of vegetation in a region can be dependent upon climate. If we are to understand how organisms respond to climate change, then it is important to understand how animals utilized their landscape for food and in turn what their diets suggest about the distribution of vegetation and the environmental context of a region. In addition, in order to build and expand the tool kit for paleoclimate research, and understanding how landscapes and organisms respond to climate change, we need to develop relevant datasets from modern analogs to understand how these proxies work. This thesis addresses these concepts in detail using different isotopic systems preserved in fossil and modern teeth.

The isotopic compositions of elements in organic and inorganic carbonates (e.g., soil carbonate, tooth enamel, shells) are frequently used to reconstruct the terrestrial ecosystem response to climate change. It has long been known that that heavy and the light isotopes of a given element respond differently to various mass-dependent factors (i.e., kinetic and equilibrium effects), and therefore these isotopic effects can cause

fractionation between heavy and light isotopes. The ratio of isotopes is measurable via analysis of a molecular gas derived from a sample in a mass spectrometer. Of interest to this thesis are the distributions of carbon, oxygen and strontium isotope ratios in teeth to reconstruct terrestrial ecosystems and climate change. The $\delta^{13}C$ value (ratios of $^{13}C/^{12}C$ of a sample compared to that of a standard) of tooth enamel reflects the proportion of C_3 and C_4 plants in an animal diet, which can be used to determine the presence or the absence of C_3 and C_4 plants in the past, which in turn reflects the seasonality of rainfall (i.e., C_3 grasses occur where there is a cool growing season, while C_4 grasses grow in regions with a warm growing season) (e.g., Luyt et al., 2000). Strontium isotope ratios ($^{87}Sr/^{86}Sr$) can vary according to the mineralogical composition of a substratum, and this ratio is preserved in soils, plants and the teeth and bones of animals eating those plants, with insignificant fractionation of the strontium isotopes (e.g., Bentley, 1996). Enamel $^{87}Sr/^{86}Sr$ ratios can be used as a geochemical proxy for substrate and is often used to determine land use among mammals, including hominids, because the $^{87}Sr/^{86}Sr$ ratio from different geologic materials, or substrates, are preserved in bones and teeth. The $\delta^{18}O$ (ratios of $^{18}O/^{16}O$) value of tooth enamel is affected by a number of factors including the $\delta^{18}O$ value of ingested water, which is influenced by the $\delta^{18}O$ values of precipitation, surface and plant water and also animal physiology and behavior. Generally, animals tend to have higher $\delta^{18}O$ values of enamel in more arid environments (e.g., Hoppe et al., 2006). The aridity of terrestrial ecosystems has been evaluated using the $\delta^{18}O$ values of enamel through the comparison of $\delta^{18}O$ values of enamel from animals that are obligate drinkers and non-obligate drinkers (Levin et al., 2006).

The $\delta^{18}O$ system cannot separate the environmental effects that influence fractionation of ^{16}O and ^{18}O, therefore the application of the $\delta^{18}O$ system to fossil teeth and bones (and in the fossil record in general) can not always provide a satisfying interpretation of climate and environment. For example, when considering the $\delta^{18}O$ value of tooth enamel, the influence of evaporation on $\delta^{18}O$ value of the water an animal consumes cannot be separated from the influence of the original source water $\delta^{18}O$ value on ingested water. Specifically, kinetic and equilibrium isotopic fractionation effects on oxygen isotopes cannot be separated. Additionally, influencing factors on water $\delta^{18}O$ values are often interrelated. Nevertheless, while not ideal, the $\delta^{18}O$ values of fossil teeth and of other terrestrial carbonates have been used to define foundational environmental and climatic proxy records by which many other paleorecords are compared and that Earth scientists use to interpret major changes to the Earth's surface over time (e.g., Zachos et al., 2001; Rowley and Currie, 2006). In the evaluation past terrestrial climates and environments, another metric is needed, one that can constrain the $\delta^{18}O$ system by separating kinetic and equilibrium oxygen isotopic effects.

Triple oxygen isotope analysis ($\Delta^{17}O$) is a method that utilizes both the $^{18}O/^{16}O$ and $^{17}O/^{16}O$ ratios in a material to distinguish between kinetic and equilibrium isotope effects on the oxygen isotopic composition of enamel. $\Delta^{17}O$ reflects water availability, which cannot be distinguished by measuring $\delta^{18}O$ values alone, and therefore has the potential to be an extremely useful way to determine past environmental aridity (as reviewed in Passey et al., 2014). Water availability is an important parameter for understanding how environments and organisms responded to climate change. In

addition, the $\Delta^{17}O$ values of fossil teeth have the potential to help constrain atmospheric pCO_2 across the fossil record and also to be utilized as a method by which to evaluate whether the primary oxygen isotopes in a sample have been preserved (Gehler et al., 2011; Pack et al., 2013; Gehler et al., 2016). However, it is extremely important to first understand how $\Delta^{17}O$ in tooth enamel relates to geographic, biological, and environmental parameters today before we use this method for understanding climate and environment in the past.

The southwestern coast of South Africa has a complex and unique ecosystem and little is known about the regional environment and vegetation prior to the Last Glacial Maximum or how this region responded to global climate change over the last 5 million years, a period of major climatic change. Fossils are preserved in this region and indicate the presence of mammalian communities composed of extinct and extant animals across this time (Stynder, 2001; Klein et al., 2007). Technologically-advanced stone tools produced by hominins are preserved at the archeological site Elandsfontein in southwestern South Africa and date to ~ 1 million years ago (Braun et al., 2013). These tools point to a period of behavioral change at ~ 1million years ago and make this region a hotspot for the history of human evolution. Hominins living in southwestern South Africa would have had to contend with the surrounding environments and any changes to these environments during the Pliocene and Pleistocene. Therefore, evaluating past environment and the composition of vegetation in southwestern South Africa is particularly relevant to understanding present and future climate change because it helps build perspective for future human-environment interactions (Braun et al., 2013). It is, however, unknown how hominins and other mammals could have survived in

southwestern South Africa in the past and what the environment conditions would have been during the mid-Pleistocene at Elandsfontein. There is no modern anolog of the paleoenvironment at Elandsfontein; instead southwestern South Africa is today a dry and hostile environment in which the animal communities that once occupied the region could not possibly survive.

Fossil teeth preserved in sedimentary strata from known Pliocene and Pleistocene fossil sites in southwestern South Africa have the potential to provide evidence for the local environmental response to climate change. Records of enamel $\delta^{13}C$ values and $\delta^{18}O$ values as well as the enamel $^{87}Sr/^{86}Sr$ ratios from these fossil teeth are used in this dissertation to reconstruct the complex ways that terrestrial systems respond to climate change both on different spatial scales and over time.

In the following chapters I present three studies that take advantage of different isotope records ($^{13}C/^{12}C$, $^{18}O/^{16}O$, $^{17}O/^{16}O$ and $^{87}Sr/^{86}Sr$) that have been preserved in tooth enamel carbonate and discuss how these records can contribute to understanding past climate and environment. In this thesis, I consider the changes in environment and landscape of southwestern South Africa since 5 million years ago and how these changes may have related to global and regional climate. In Chapter 2, I present carbon and oxygen isotope data from fossil teeth from the mid-Pleistocene in southwestern South Africa and compare these records to other environment and climate proxy records from southern Africa that represent times within the last 5 million years. In Chapter 3, I consider how mammalian herbivores from mid-Pleistocene Elandsfontein moved around the region to find resources (i.e. food and water). The movement of animals can help understand the variation of vegetation in a region and help to determine whether the

proposed features of vegetation and environment at Elandsfontein, as described in Chapter 2 and that were derived from analysis of the teeth obtained at Elandsfontein, are plausible. Here I have sampled the enamel of several large herbivore teeth (animals that have the potential to migrate for food) along their tooth growth axis and analyzed their strontium isotope composition to determine if there was any indication of a change in the substrates on which they browsed and grazed. If the strontium isotope ($^{87}Sr/^{86}Sr$) ratios of these teeth were characteristic of the marine sands at Elandsfontein then it is likely that, 1) these animals did not travel to other locations in the region for food because there were adequate resources at Elandsfontein and 2) that at ~ 1 million years ago the landscape and spring-fed environment at Elandsfontein would have provided the conditions that supported the annual growth of C_3 grasses within a winter rainfall zone.

The studies presented in Chapter 2 and Chapter 3 have expanded upon previous interpretations of climate, environment and landscape change in southwestern South Africa at times since ~ 5 Ma. In these studies, I paint a picture of the regional variation of vegetation during the mid-Pleistocene, a time when hominins lived in this region, and proposed that animals and hominins were drawn to Elandsfontein because this site had enough vegetation of sufficient quality to feed diverse populations of large mammalian herbivores. I attribute the vegetative composition at and around Elandsfontein ~ 1 million years ago to a spring-fed environment as indicated by ancient spring deposits preserved at the site. The presence of springs would have provided standing water throughout the year within a region when there was only winter rain. While southwestern South Africa is considered to have become more arid since the Pliocene based on marine-based climate

and vegetation proxies, the $^{18}O/^{16}O$ ratios of fossil teeth from Elandsfontein can not be used to determine changes in aridity compared with other environmental changes.

In Chapter 4, I consider the limitations of the conventional oxygen isotope record in biominerals (e.g., teeth, bone and eggshells) for understanding past climate and environment. I discuss the importance of utilizing all three oxygen isotopes preserved in a biomineral (where the rare isotope ^{17}O is measured along with ^{16}O and ^{18}O) as a way to distinguish between different factors that influence the oxygen isotope record, constrain past pCO_2, evaluate aridity and assess diagenesis of the primary oxygen isotope composition in teeth. In addition, I present the modern range of triple oxygen isotope values of enamel from different animal species that come from various latitudes and environments and have a variety of dietary behaviors. The data provide a record of tooth enamel $\Delta^{17}O$ values that are linked to known climatic and environmental parameters.

The $\Delta^{17}O$ values of fossil teeth could be valuable for evaluating the effects of diagenesis on the fossil tooth oxygen isotope records, adding to the suite of information about diagenesis based on $^{18}O/^{16}O$ ratios of fossil teeth. In addition, evaluating the change in aridity during the mid-Pleistocene could provide a new perspective about aridity in the region, where aridity represents water balance and water balance is an important element to understand how landscapes respond to climate change.

By understanding the broader context of climate change and resource availability in the southwestern coastal region of South Africa during the mid-Pleistocene, it might be possible to understand why Elandsfontein attracted large herbivores and at the same time start to characterize how vegetation on the western coast reflected or responded to changes in regional ocean circulation and global climate change.

CHAPTER 2: Stable isotopic composition of fossil mammal teeth and environmental change in southwestern South Africa during the Pliocene and Pleistocene

ABSTRACT

The past 5 million years mark a global change from the warmer, more stable climate of the Pliocene to the initiation of glacial-interglacial cycles during the Pleistocene. Marine core sediment records located off the coast of southwestern Africa indicate aridification and intensified upwelling in the Benguela Current over the Pliocene and Pleistocene. However, few terrestrial records document environmental change in southwestern Africa over this time interval. Here we synthesize new and published carbon and oxygen isotope data of the teeth from large mammals (>6 kg) at Langebaanweg (~5 million years ago, Ma), Elandsfontein (1.0 – 0.6 Ma), and Hoedjiespunt (0.35 – 0.20 Ma), to evaluate environmental change in southwestern Africa between the Pliocene and Pleistocene. The majority of browsing and grazing herbivores from these sites yield enamel $\delta^{13}C$ values within the range expected for animals with a pure C_3 diet, however some taxa have enamel $\delta^{13}C$ values that suggest the presence of small amounts C_4 grasses at times during the Pleistocene. Considering that significant amounts of C_4 grasses require a warm growing season, these results indicate that the winter rainfall zone, characteristic of the region today, could have been in place for the past 5 million years. The average $\delta^{18}O$ value of the herbivore teeth increases ~4.4‰ between Langebaanweg and Elandsfontein for all taxa except suids. This increase may solely be a function of a change in hydrology between the fluvial system at

Langebaanweg and the spring-fed environments at Elandsfontein, or a combination of factors that include depositional context, regional circulation and global climate. However, an increase in regional aridity or global cooling between the early Pliocene and mid-Pleistocene cannot explain the entire increase in enamel $\delta^{18}O$ values. Spring-fed environments like those at Elandsfontein may have provided critical resources for mammalian fauna in the mid-Pleistocene within an increasingly arid southwestern Africa ecosystem.

2.1. Introduction

The Pliocene-Pleistocene climatic transition is marked by a global shift from relatively warm and stable climate conditions in the Pliocene to colder and more variable conditions in the Pleistocene (Imbrie et al., 1992; Zachos et al., 2001). Over the course of this transition African landscapes are considered to have become more arid (e.g., deMenocal, 2004; Dupont et al., 2013). In southwestern Africa, intensified upwelling of cold bottom waters in the Benguela Current System has been linked with increased regional aridity and the onset, expansion and speciation of the endemic Cape flora since the Miocene (Marlow et al., 2000; Dupont et al., 2005; 2011; Etourneau et al., 2009). While marine-based records indicate major changes in vegetation and climate in southern Africa, terrestrial-based records could provide a more local perspective of the hydrological setting, vegetation and climate of southwestern South Africa since the Pliocene; currently there are few archives of environmental change in this region during the last 5 million years (myr) (Roberts et al., 2011; Eze and Meadows, 2014).

Sedimentary strata from known Pliocene and Pleistocene fossil sites in southwestern South Africa have the potential to provide direct evidence for the local environmental response to climate change (Table 2.1). Sedimentary records indicate a transition from fluvial to spring-fed and eolian deposition in southwestern South Africa (Roberts et al., 2011; Eze and Meadows, 2014). Data from pre-Holocene mammalian fossils suggest the presence of significant amounts of surface water and a vegetated landscape composed of a fynbos shrubland and grassland mosaic, interspersed with trees and broad-leafed bush, which contrasts the dry, eolian landscapes that are prevalent in

southwestern South Africa today (e.g., Luyt et al., 2000; Franz-Odendaal et al., 2002; Stynder, 2009; 2011; Braun et al., 2013).

Here we use the carbon and oxygen isotopic composition of fossil herbivore tooth enamel obtained from paleontological and archaeological sites in southwestern South Africa to investigate trends in regional climate and hydrology, vegetation and animal diet between the Pliocene and Pleistocene. Together with marine archives off the coast of southern Africa that record broader, regional-scale climate and vegetation, we use these terrestrial-based data to improve upon the understanding of how environments in southwestern South Africa responded to global climatic changes during the Pliocene and Pleistocene.

2.2. Background

2.2.1. South African climate and vegetation

South Africa is predominantly semiarid with three distinct rainfall zones and corresponding vegetation zones (Fig. 2.1; Cowling et al., 2002). The winter rainfall zone of western South Africa encompasses an area of ~200-km^2 where ~65% of mean annual precipitation (MAP) occurs between April and September. The summer rainfall zone is affected by the warm Agulhas Current that flows along the eastern coast of South Africa. At the intersection of these two major meteorological zones, situated along the South Coast of South Africa, there is a region that receives rainfall during both the summer and winter. This annual rainfall zone spans from the southern coast of the Eastern Cape

Province of South Africa into the Western Cape Province (e.g., Chase and Meadows, 2007).

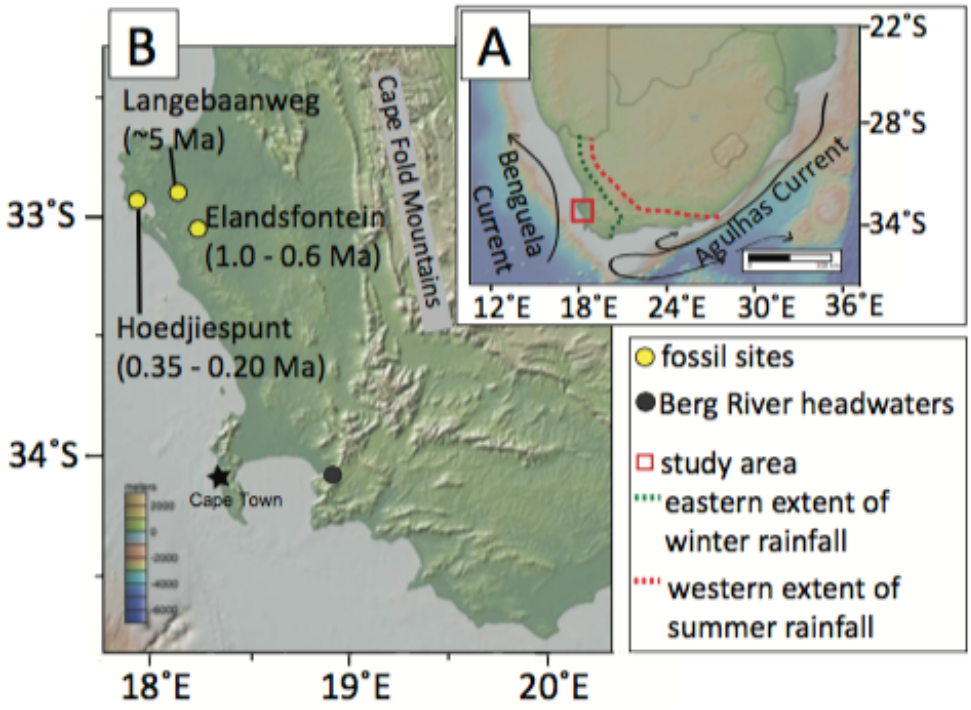

Figure 2.1: Marine currents, climate zones, and southwestern South African fossil sites discussed in text. A) A map of southern Africa indicating the location of the study area with a schematic of the present day extent of the winter and summer rainfall zones and the Benguela and Agulhas Currents and present-day political boundaries (Chase and Meadows, 2007). B) A map of the study area denoting the fossil localities discussed in text (yellow circles), Cape Town, the Cape Fold Mountains, and the headwaters of the Berg River. The color base maps indicating topography were generated using Global Multi Resolution Topography from http://www.geomapapp.org (Ryan et al., 2009).

Rainfall zones in South Africa partition zones of vegetation, which can be seen through the spatial distribution of the frequency of the three main photosynthetic pathways: C_3, C_4, and Crassulacean Acid Metabolism (CAM). The distribution of these pathways is largely determined by environmental factors (Farquhar et al., 1989). C_4 plants thrive in environments with a warm growing season while C_3 plants grow primarily

in cool growing seasons. CAM plants, such as cacti and succulents, are often found in semiarid to arid environments. The distribution of grass type is related to the seasonality of rainfall in South Africa; C_4 grasses mostly grow in regions with summer rainfall, C_3 grasses grow where there is winter rainfall, and both C_3 and C_4 grasses grow in the annual rainfall zone (Vogel et al., 1978; Cowling et al., 2002; Bar-Matthews et al., 2010). Increased upwelling and the latitudinal movement of the Benguela Current may modify the movement of warm waters along the coast of South Africa and this could impact the distribution of the rainfall zones (Chase and Meadows, 2007). The positions of the rainfall and vegetation zones are hypothesized to have shifted during the late Quaternary in response to the position and upwelling intensity of the Benguela Current (Lee-Thorp and Beaumont, 1995), however it is unclear whether they were stable in the Pliocene and mid-Pleistocene.

The paleontological and archaeological sites that are the focus of this paper are within southwestern South Africa, west of the Cape Fold Mountains and stretch across 40 kms of the coastal plain. These sites, Langebaanweg (~5 million years ago (Ma), early Pliocene), Elandsfontein (1.0 – 0.6 Ma, mid-Pleistocene) and Hoedjiespunt (0.35 – 0.20 Ma, late Pleistocene), are within the winter rainfall zone (Fig. 2.1). Regionally the area is known as Strandveld (literally 'beach vegetation') and geomorphologically is dominated by a coastal plain variably covered by marine sands (Mabbutt, 1955; Roberts et al., 2012). Limited outcrops of granite to the south and west interrupt Cenozoic-aged eolian deposits that blanket much of the region. The western portion of the area is underlain by shales of the Malmesbury Group leading up to the Paloezoic sandstones of the Cape Supergroup (Besaans, 1972; Roberts et al., 2009). The contemporary vegetation in the study area is

primarily composed of small-leafed, nutrient-poor taxa of the strandveld and fynbos families. C_3 grasses and trees are scarce in this area because of the nutrient-poor soils. It has generally been presumed that C_4 grasses are limited in the southwestern Cape by the long, hot and dry summers, however C_4 grasses are able to grow in areas that are well watered throughout the year (e.g., Cowling et al., 2002; 2005).

2.2.2. Pliocene and Pleistocene climate and vegetation in western South Africa

2.2.2.1. Marine records

Marine sediment records from cores off the coast of southwestern Africa span the past 4.5 myr and provide information about terrestrial responses to global climate change and the degree of ocean upwelling (Marlow et al., 2000; Dupont, 2005; Etourneau et al., 2009). Charcoal and plant waxes preserved offshore show that there was an increase in aridity, seasonality and fires to the north of the study area during the Miocene and Pliocene (Hoetzel et al., 2013). The drying trend continued across the Pliocene-Pleistocene climatic transition; offshore pollen records indicate a reduction in grass and an increased occurrence of fynbos and semi-desert vegetation (e.g., Dupont et al., 2005).

2.2.2.2. Terrestrial records

In contrast to the high-resolution, marine-based proxy records that extend into the Miocene, there are no terrestrial-based proxy records with a similar time span or resolution. However the numerous archives of eolian and riverine sedimentary sequences on the coastal plains of southwestern South Africa provide some details of late Cenozoic

environments. There have been numerous studies of ancient environments in this region based on these records (e.g., Klein, 1978; 1982; 1983; 1991; Klein and Cruz-Uribe, 1991; February, 1992; Meadows et al., 1996). However, the vast majority of these studies have focused on environments since the Last Interglacial (0.125 Ma). Langebaanweg, Elandsfontein and Hoedjiespunt are paleontological and archeological sites within the study area that date to within the last ~5 myr. These sites are well known for their contribution to our understanding of faunal change and human evolution in South Africa (e.g., Hendey, 1976; Klein, 1978; Berger and Parkington, 1995; Stynder, 1997; Stynder et al., 2001; Klein et al., 2007; Braun et al., 2013). The flora, fauna and sediment records at these sites provide a record of environmental change in the area from the Pliocene and Pleistocene (Luyt et al., 2000; Franz-Odendaal et al., 2002; Stynder, 2009; Roberts et al., 2011; Stynder, 2011; Braun et al., 2013; Hare and Sealy, 2013; Eze and Meadows, 2014). While these sites have been the focus of a variety of paleoecological studies (Table 2.1), currently there is no detailed, integrated record of the hydrological, ecological and climatic changes in southwestern South Africa over the past 5 myr.

2.2.3. Carbon and oxygen isotope composition of herbivore tooth enamel

C_3, C_4 and CAM plants have distinct stable carbon isotope values primarily due to different physiologies of the different photosynthetic pathways (e.g., Farquhar et al., 1989). Carbon isotope data of plants are traditionally presented using δ-notation, where $\delta = \left(\frac{R_{sample}}{R_{standard}} - 1 \right) * 1000$ in per mil (‰) units and R_{sample} and $R_{standard}$ are the ratios of heavy to light isotopes (in this case, ^{13}C and ^{12}C) of the sample and standard, respectively. $\delta^{13}C$

values are reported relative to Vienna Pee Dee Belemnite (VPDB). The $\delta^{13}C$ values of C_3 plants globally range from ~ -31.7‰ to ~ -23.1‰ (Kohn et al., 2010). The $\delta^{13}C$ values C_4 plants range from ~ -14.0‰ and ~ -10.0‰ (Hattersley, 1982). In southwestern South Africa the average $\delta^{13}C$ value of C_4 plants is -12.8 ± 1.3‰ (Radloff, 2008), whereas $\delta^{13}C$ values of CAM plants range from ~ -24‰ to ~ -16‰ (Boom et al., 2014).

Table 2.1: A summary of the terrestrial records of climate, vegetation and depositional environment from southwestern South Africa.

Age	Locality	Depositional environment	Substrate	Vegetation	Climate	Data sets	References
late Pleistocene (0.35 - 0.25 Ma)	Hoedjiespunt	Coastal	Sands	Shrubs and widespread grasslands	Glacial	Taxonomy[a] Stable isotopes[a]	Klein, 1983 Stynder, 1997 Hare and Sealy, 2013
mid-Pleistocene (~1.0 - 0.6 Ma)	Elandsfontein	Spring-fed and eolian	Eolian and marine sands, carbonate-leached sediments, pedogenicaly modified sands	Trees, shrubs, and seasonal grasses	Glacial and/or Interglacial	Taxonomy[a] Stable isotopes[a] Microwear[a] Sediment	Butzer, 1973 Klein, 1978 Luyt et al., 2000 Stynder, 2009 Braun et al., 2013
Pliocene (~5 Ma)	Langebaanweg	Fluvial and deltaic	Floodplain, marsh, and river channel deposits	Trees, shrubs, and seasonal grasses	Warm and wet	Taxonomy[a] Stable isotopes[a] Mesowear[a] Microwear[a] Sediment	Franz-Odendaal et al., 2002 Roberts et al., 2011 Stynder, 2011

[a] Datasets that apply to teeth.

The $\delta^{13}C_{enamel}$ value reflects the proportion of C_3 and C_4 plants in an animal's diet such that the $\delta^{13}C_{enamel}$ values of fossil herbivore teeth can be used to determine the

presence or absence of C_3 and C_4 grasses in the past. There is a +14.1‰ dietary enrichment of $\delta^{13}C$ values between the diet of large herbivorous mammals (> 6 kg) and their enamel (Cerling et al., 1999) and as such the $\delta^{13}C$ value of tooth enamel ($\delta^{13}C_{enamel}$) reflects the isotopic composition of an animal's diet (see Kohn and Cerling, 2002 for review). Here we define large mammals as > 6 kg because the smallest mammal included in this category is the grysbok, which is ~ 10 kg, whereas we refer to the mammals from Elandsfontein with body weights < 6 kg as small mammals, which includes the rodent genera *Bathyergus* and *Otomys*. For fossil sites, in southern Africa, the presence or absence of C_3 and C_4 grasses in mammalian diet has been presumed to reflect the presence or absence of winter and summer rainfall (Luyt et al., 2000; Franz-Odendaal et al., 2002; Hare and Sealy, 2013). Within a C_3-dominated ecosystem, the isotopic composition of tooth enamel from large herbivores can be used to tease apart subtleties in the distribution of vegetation (e.g., Luyt et al., 2000; Franz-Odendaal et al., 2002; Hare and Sealy, 2013). For example, Hare and Sealy (2013) suggest that there was some C_4 grass in C_3-dominated grasslands in southwestern South Africa during the late Pleistocene because the $\delta^{13}C_{enamel}$ values of grazers were more enriched in $\delta^{13}C_{enamel}$ values than what is expected for a grazer consuming purely C_3 vegetation. CAM plants are not considered to have greatly influenced the $\delta^{13}C_{enamel}$ values because they do not comprise a major proportion of large mammalian herbivore diets (Cerling et al., 2003) and therefore they will not be further considered in this study.

The stable oxygen isotope composition of the carbonate component of herbivore tooth enamel is affected by a number of factors including the $\delta^{18}O$ value of ingested

water, which is influenced by the $\delta^{18}O$ values of precipitation, surface and plant water, as well as animal physiology and behavior (as reviewed in Kohn and Cerling, 2002). All of these factors generally contribute to higher $\delta^{18}O$ values of enamel in more arid environments. The comparison of enamel $\delta^{18}O$ values between obligate drinkers and non-obligate drinkers has been specifically used for evaluating relative aridity in terrestrial ecosystems (e.g., Levin et al., 2006).

The oxygen isotopic composition of enamel phosphate has also been used as a proxy for paleoclimate and is considered to be less susceptible to alteration than the oxygen isotope composition of the carbonate component of enamel because oxygen in the phosphate component is more tightly bound than in the carbonate component of enamel (Chenery et al., 2012). The offset between $\delta^{18}O$ values of the carbonate and phosphate components of enamel ranges from 7.2‰ to 10.6‰ in well-preserved teeth and has been used as a means to evaluate diagenetic modification of the $\delta^{18}O$ values of fossil teeth (e.g., Iacumin et al., 1996).

2.3. Materials and Methods

2.3.1. Fossil enamel samples

We sampled mid-Pleistocene fossil teeth from two separate faunal collections at Elandsfontein. The first collection is housed at the Iziko South African Museums in Cape Town, South Africa. This faunal sample, known as Elandsfontein Main (EFTM), was predominantly collected from surface deposits over the course of several decades as

described in Klein et al. (2007). The second collection derives from recent fieldwork conducted by the West Coast Research Project (WCRP) between 2008 and 2014. These materials are archived at the Archaeology Department, University of Cape Town and include both surface samples and excavated teeth. All fossils that we sampled from the WCRP collection derive from the Upper Pedogenic Sand lithological unit that is part of the Langebaan Formation (Braun et al., 2013). We also sampled Pliocene teeth (n = 10) from the Varswater Formation at the Langebaanweg paleontological locality, which were obtained from the West Coast Fossil Park (Roberts et al., 2011). The teeth from Langebaanweg were sampled to provide a point of comparison in the evaluation of the diagenetic alteration of oxygen isotopes in tooth enamel from Elandsfontein. All tooth enamel was sampled with a diamond drill bit along the tooth growth axis. When possible, third molars were sampled. New data were compiled with previously published carbon and oxygen isotope tooth enamel data from the region, including 64 teeth from Langebaanweg (Franz-Odendaal et al., 2002), 18 teeth from Elandsfontein (Luyt et al., 2000), and 39 teeth from Hoedjiespunt (Hare and Sealy, 2013). This compilation does not include the isotope data of the fossil teeth from the "Bone Circle" at Elandsfontein that Luyt et al. (2000) published because we are uncertain of their context and relationship to the other fossils from Elandsfontein (Braun et al., 2013).

2.3.2. Isotopic measurements

We measured $\delta^{13}C_{enamel}$ values and $\delta^{18}O$ values of both the carbonate and phosphate components of fossil tooth enamel. We also measured $\delta^{18}O$ and $\delta^{2}H$ values of

surface and ground waters in the immediate vicinity of Elandsfontein and in the general Langebaan-Hopefield region.

2.3.2.1. Analysis of the enamel carbonate component

Fossil enamel was powdered, treated with 3% H_2O_2 to remove organic material and rinsed three times with deionized water. The resultant powder was rinsed with 0.1 *M* buffered acetic acid to remove secondary carbonate, rinsed three times with deionized water and dried overnight at 60ºC. Approximately 500 to 800 µg of each powdered sample were placed in a silver capsule then digested under vacuum in a common bath of 100% phosphoric acid at 90ºC and the resultant CO_2 was purified using a custom-built automated device (Passey et al., 2010). The CO_2 was analyzed for $^{13}C/^{12}C$ and $^{18}O/^{16}O$ ratios using a dual inlet system on a Thermo MAT253 isotope ratio mass spectrometer in the Department of Earth and Planetary Sciences, Johns Hopkins University. The isotopic composition of the resultant CO_2 was determined with respect to a working CO_2 reference, calibrated using NBS-19, and monitored using working references of calcite and enamel. The precision of the working carbonate enamel standards over the course of the analyses made for this study was 0.4‰ and 0.2‰ for $\delta^{13}C$ and $\delta^{18}O$, respectively. An acid fractionation factor of 1.00725 was used for determining $\delta^{18}O$ values of the carbonate component of fossil enamel digested at 90ºC (Passey et al., 2007). All $\delta^{13}C$ values are reported relative to VPDB (Vienna Pee Dee Belemnite) and $\delta^{18}O$ values are reported relative to VSMOW (Vienna Standard Mean Ocean Water).

2.3.2.2. Analysis of the $\delta^{18}O$ values of enamel phosphate

Forty-eight fossil teeth from Langebaanweg and Elandsfontein were analyzed for the $\delta^{18}O$ values of enamel phosphate, in addition to carbon and oxygen isotope analyses of enamel carbonate mentioned above. Samples were drilled and pretreated in the manner described above (Section 3.2.1). Phosphate-bound oxygen was isolated and extracted from enamel using a modified version of the batch Ag_3PO_4 precipitation method of O'Neil et al. (1994) followed by $\delta^{18}O$ analysis of approximately 400 μg of Ag_3PO_4 via high temperature pyrolysis to CO (TC/EA) on a continuous flow Delta Plus XL isotope ratio mass spectrometer at the Department of Geosciences, Princeton University.

Long-term performance (precision of the isotope ratio mass spectroscopy measurement and wet chemistry conversion from hydroxyapatite to Ag_3PO_4) was confirmed by repeat analysis of NBS120c, a phosphate rock with certified metal oxide abundances and distributed by the National Institute of Standards and Technology and the *de facto* standard for $\delta^{18}O$ in phosphate, with $\delta^{18}O$ values ranging from 21.3 to 22.6‰ VSMOW (e.g., Vennemann et al., 2002; Halas et al., 2011). Although precipitation yield varied using the modified O'Neil et al. (1994) batch precipitation method (52±22 %), repeat analysis of the NBS120c phosphate standard over 18 months averaged 22.36±0.48‰ and showed no dependence of measured $\delta^{18}O$ values on precipitation yield, with the average value aligning well with published $\delta^{18}O$ values.

2.3.2.3. Analysis of the $\delta^{18}O$ values of water

Samples of standing water and ground water (n = 3) were collected from a series of active springs in the vicinity (within a ~3 km to ~17 km radius) of the Quaternary

deposits at Elandsfontein where fossil teeth were collected. Tap water from The Western Cape Fossil Park (which is in the general proximity of the study area) was also collected (n = 1). Samples were passed through a 0.45-μm filter in the field and sealed in a glass bottles with polycone seal lids and wrapped in parafilm to prevent evaporation. Samples were cleaned with activated charcoal to remove organics, filtered again and then analyzed by laser absorption spectroscopy on a Los Gatos Research Liquid-Water Isotope Analyzer at the Department of Earth and Planetary Sciences, Johns Hopkins University. The precision of the working water standard USGS48 over the course of the water analyses was 0.03‰ and 0.1‰ for $\delta^{18}O$ and $\delta^{2}H$ respectively. The $\delta^{18}O$ and $\delta^{2}H$ values of water samples are reported relative to the VSMOW-SLAP scale, where SLAP is Standard Light Antarctic Precipitation.

2.3.3. Interpretation of stable isotope results

2.3.3.1. Influence of $\delta^{13}C$ values of atmospheric CO_2

The $\delta^{13}C$ value of atmospheric CO_2 has decreased over the past 5 myr (Tipple et al., 2010) and this decrease needs to be considered when using $\delta^{13}C_{enamel}$ values to determine the proportion of C_3 and C_4 plants in an animal's diet. The $\delta^{13}C$ value of atmospheric CO_2 will influence the $\delta^{13}C$ values of C_3 and C_4 plants and as a consequence will influence $\delta^{13}C_{enamel}$ values of the tissues of the animals that eat these plants. We calculated the ranges in $\delta^{13}C$ values that we expect for C_3 and C_4 plants at the time periods representative of Langebaanweg (~5 Ma), Elandsfontein (1.0 – 0.6 Ma) and Hoedjiespunt (0.35 – 0.20 Ma) to better determine what herbivore $\delta^{13}C_{enamel}$ values may

indicate about the distribution of C_3 and C_4 plants in the study area, considering the $\delta^{13}C$ values of atmospheric CO_2 reconstructed from benthic foraminifera (Tipple et al., 2010; see Table S2.1 for details). Given changes in the $\delta^{13}C$ value of atmospheric CO_2, the maximum $\delta^{13}C_{enamel}$ values for large mammals with a pure C_3 diet are -7.6‰ for Langebaanweg and -8.4‰ for both Elandsfontein and Hoedjiespunt (Table S2.1). If the $\delta^{13}C_{enamel}$ value of a grazer is higher than the reconstructed maximum $\delta^{13}C_{enamel}$ value for an animal eating a pure C_3 diet, then it implies the presence of C_4 grass in the animal's diet and, in turn, the growth of C_4 plants in the otherwise dry summer months in southwestern South Africa. As mentioned earlier, the presence of C_4 grass in southwestern South Africa is interpreted as the inclusion of rainfall during the summer months in this ecosystem. Alternatively, large mammals may be feeding around permanent water sources such as springs and rivers where C_4 plants may have grown.

2.3.3.2. Analysis of the $\delta^{18}O$ values of enamel phosphate

Low carbonate content of fossils, bones and sediments at Elandsfontein have led to hypotheses that carbonate has been leached from the fossil deposits at the Elandsfontein archeological site since initial deposition and burial (Luyt et al., 2000). This is in contrast to fossils from the sites Langebaanweg and Hoedjiespunt, which have been recovered from carbonate-rich sediments (Stynder, 1997; Roberts et al., 2013). To evaluate the potential influence of leaching on the $\delta^{18}O$ values of the carbonate component of tooth enamel at Elandsfontein and whether or not these $\delta^{18}O$ values can be used as indicators of paleoclimate, we compared the offsets in $\delta^{18}O$ values of the carbonate and phosphate of fossil teeth from Elandsfontein to those from Langebaanweg.

Oxygen in enamel phosphate is more strongly bound and more resistant to diagenetic alteration than in enamel carbonate. There is a consistent enrichment between the $\delta^{18}O$ value in enamel phosphate and carbonate and as such $\delta^{18}O$ values of the oxygen in the phosphate and carbonate component of tooth enamel are strongly correlated for modern and unaltered fossil enamel (Bryant et al., 1996; Iacumin et al., 1996; Martin et al., 2008). This enrichment, or epsilon

(i.e., $\varepsilon\ \delta^{18}O_{A\text{-}B}$ where $\varepsilon\delta^{18}O_{A\text{-}B} = \left[\frac{1000 + \delta^{18}O_A}{1000 + \delta^{18}O_B}\right] \text{x } 1000$ and where in this case A = CO_3 and B = PO_4), ranges from 7.2 to 10.6‰ for enamel that has not experienced significant diagenesis (Bryant et al., 1996; Iacumin et al., 1996; Martin et al., 2008). The $\varepsilon\delta^{18}O_{CO3\text{-}PO4}$ has been used to determine if the oxygen isotopic composition of the carbonate in bioapatite has been diagenetically altered (Iacumin et al., 1996). We compared $\varepsilon\delta^{18}O_{CO3\text{-}PO4}$ values of teeth at Elandsfontein to those from Langebaanweg and from compilations of modern teeth to evaluate the integrity of the $\delta^{18}O$ values of the carbonate component of teeth from Elandsfontein. If the $\varepsilon\delta^{18}O_{CO3\text{-}PO4}$ values at Langebaanweg and Elandsfontein are similar to one another and within the range expected for unaltered teeth, then the $\delta^{18}O$ values of the carbonate component of enamel from Elandsfontein can be used to reconstruct paleoenvironment.

2.3.3.3. Statistical comparison of isotopic values

All comparisons of isotope data from fossil teeth were performed using the JMP 11, a statistical analytical software program developed by the SAS Institute and evaluated

using the Tukey-Kramer HSD test. The ± symbol is used throughout this paper to represent one standard deviation from the mean.

2.4. Results

2.4.1. Isotopic composition of fossil enamel carbonate from Elandsfontein

The compiled dataset for carbon and oxygen isotope data (carbonate component only) for large mammalian teeth from Elandsfontein is comprised of two collections that represent the mid-Pleistocene, EFTM (n = 71; Luyt et al., 2000; this study) and WCRP (n = 123; this study). The EFTM and WCRP collections include fossil teeth from seven herbivore families: Bovidae, Elephantidae, Equidae, Giraffidae, Hippopotamidae, Rhinocerotidae and Suidae, in addition to a single tooth from the primate family, Cercopithecidae (see Table 2.2 and Table S2.2). These samples likely all belong to the same stratigraphic unit, the mid-Pleistocene Upper Pedogenic Sand in the Langebaan Formation (Braun et al., 2013). The main difference between these collections is that fossils in the EFTM collection were collected from surface finds over decades (Klein et al., 2007), whereas the WCRP collection includes a combination of fossils recovered from surface surveys and excavations made with careful attention to stratigraphic context (Braun et al., 2013).

Table 2.2: $\delta^{13}C$ and $\delta^{18}O$ values of fossil tooth enamel from sites in southwestern South Africa, averaged by family and bovid tribe.

Taxon (family or tribe)	Dietary behavior[b]	$\delta^{13}C_{enamel}$ (‰ VPDB±1σ)	$\delta^{18}O_{enamel}$ (‰ VSMOW±1σ)	Number of samples
Hoedjiespunt (0.35 - 0.25 Ma)				
Alcelaphini	grazer	-9.8±1.3	31±1.5	16
Bovini	grazer	-7.1±1.3	32.9±0.6	2
Reduncini	grazer	-10.2±2.3	32.7±2.0	2
Antelopini	mixed feeder	-9.6±1.1	31.2±2.1	5
Neotragini	mixed feeder	-8.4±2.5	32.2±1.3	3
Cephalophini	browser	-10.4±0.6	31.1±1.5	3
Tragelaphini	browser	-9.5±1.3	31.2±1.2	8
All Bovidae	-	-9.5±1.5	31.4±1.5	39
Elandsfontein (~1.0 - 0.6 Ma)				
Alcelaphini	grazer	-10.3±1.2	32.6±1.9	19
Bovini	grazer	-10.3±0.8	33.8±1.6	18
Reduncini	grazer	-9.6±0.7	33.3±2.7	9
Hippotragini	mixed feeder	-10.3±1.3	31.3±1.9	4
Neotragini	browser	-12.3±1.4	32.6±0.7	2
Tragelaphini	browser	-11.8±0.5	34.6±1.4	8
All Bovidae	-	-10.0±1.3	33.2±2.0	123
Elephantidae	grazer	-8.5	30.8	1
Cercopithecidae	-	-10.2	31.2	1
Equidae	grazer	-9.8±0.7	32.7±1.0	32
Giraffidae	browser	-11.0±1.3	32.5±2.0	7
Hippopotamidae	semi-aquatic	-12.3±1.1	29.7±1.5	9
Suidae	grazer	-9.9±1.4	28.0±3.1	8
Rhinocerotidae	grazer and browser	-11.0±0.8	31.6±1.8	13
Langebaanweg (~5 Ma)				
Alcelaphini	browser to grazer	-10.8±1.0	27.5±1.5	7
Reduncini	-	-10.7±0.0	28.0±2.1	2
All Bovidae	-	-10.7±0.8	28.7±2.8	11
Equidae	grazer	-10.7±1.4	28.1±2.4	8
Giraffidae	browser	-11.4±1.2	28.4±2.0	29
Suidae	-	-11.8±1.0	27.7±0.9	4
Rhinocerotidae	grazer	-10.9±0.7	26.2±1.4	4
Hippopotamidae	semi-aquatic	-11.9±1.5	25.4±1.7	18

[a] In addition to the new isotopic data, the isotopic data from previously published papers are included to determine the average $\delta^{13}C_{enamel}$ and $\delta^{18}O_{enamel}$ data for mammalian families and bovid tribes at each fossil site (Luyt et al., 2000; Franz-Odendaal et al., 2002; Hare and Sealy, 2013). See Table S2.2 for the compilation of data from individual teeth and the corresponding references.

[b] References for the classification of dietary behavior are provided in Table S2.2.

There are no differences in either the $\delta^{13}C$ values ($p > 0.9$) or $\delta^{18}O$ values ($p > 0.2$) of enamel carbonate, grouped by taxonomic family, from the EFTM collection data reported by Luyt et al. (2000) and the new EFTM data that we report in this study. When the isotopic data from teeth in the combined EFTM dataset (Luyt et al., 2000; this study) are compared to the isotopic data from fossils in the WCRP collection (this study only), we do not find any differences in $\delta^{13}C$ and $\delta^{18}O$ values of fossil teeth from like families except for $\delta^{18}O$ values (enamel carbonate) of the suids (EFTM, $n = 5$, 26.3±2.6‰; WCRP, $n = 3$, 32.1±0.6‰, $p = 0.004$). We note that the sample size is small for several of the families analyzed at Elandsfontein (see Table 2.2 and Table S2.2). From here on out, we discuss the isotope data from both the EFTM and WCRP collections together and refer to them as all from Elandsfontein, unless otherwise noted.

We classified the dietary behavior (i.e., grazer, browser or mixed feeder) of 104 teeth from the compiled collections for Elandsfontein using a combination of approaches, including mesowear, microwear and taxonomic analogy (Fig. 2.2; Table S2.2; Stynder, 2009; 2011). The individual teeth fall into three groups: browsers ($n = 20$), mixed feeders ($n = 4$) and grazers ($n = 71$). *Theropithecus* at Elandsfontein has not yet been analyzed using mesowear or microwear to determine diet so we do not place it in one of these categories. We consider hippopotamids apart from the other taxa that we sampled and classify it as semi-aquatic because in modern African ecosystems *Hippopotamus amphibious* spends a significant amount of time immersed in water, unlike the other taxa in this dataset (e.g., Bocherens et al., 1996; Cerling et al., 2008). The $\delta^{13}C_{enamel}$ values of browsers, mixed feeders and grazers average -11.6±0.8‰ ($n = 20$), -10.3±1.1‰ ($n = 4$)

and -10.1±1.0‰ (n = 71), respectively. The average $\delta^{13}C_{enamel}$ value of hippopotamids from Elandsfontein is -12.3±1.1‰ (n = 9). The $\delta^{18}O$ values of the carbonate component of enamel of browsers, mixed feeders, grazers and hippopotamids are 33.1±1.9‰, 31.3±1.6‰, 32.4±2.5‰ and 29.7±1.5‰, respectively. Hippopotamid $\delta^{18}O$ values of enamel carbonate are significantly lower than $\delta^{18}O$ values of browsers (p = 0.002) and grazers (p = 0.005).

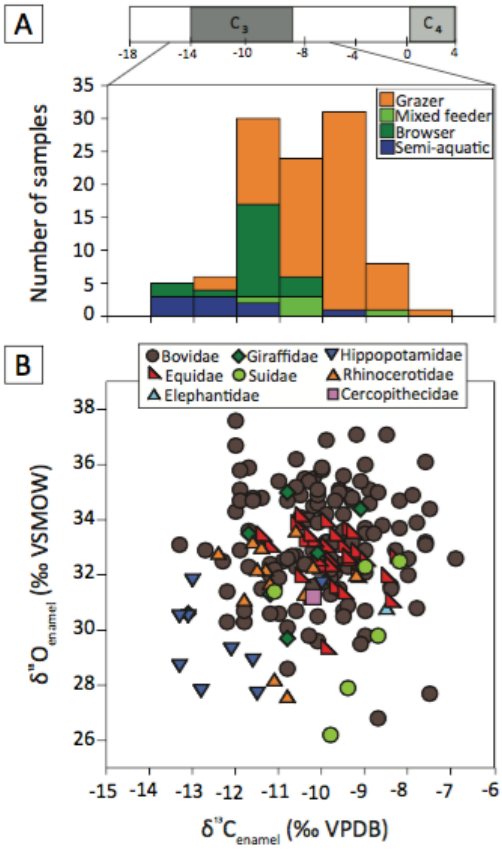

Figure 2.2: The $\delta^{13}C$ and $\delta^{18}O$ values of the carbonate component of fossil mammalian tooth enamel from the Elandsfontein collections EFTM and WCRP (Luyt et al., 2000; this study). A) Histogram of $\delta^{13}C$ values of teeth that can be categorized as browser (n = 20), grazer (n = 71), mixed feeder (n = 4) and semi-aquatic hippopotamid (n = 9) (Table S2.2). The smaller plot above the histogram provides a guide for interpreting $\delta^{13}C$ values in terms of animal diet (pure C_3 and C_4 vegetation, gray bars). B) The $\delta^{13}C$ and $\delta^{18}O$ values of the carbonate component of tooth enamel are plotted for each fossil tooth, grouped by family.

2.4.2. Comparison of oxygen isotopic values between enamel carbonate and enamel phosphate

We analyzed the oxygen isotope composition of both the carbonate and phosphate components of a subset of tooth enamel from Elandsfontein and Langebaanweg to evaluate whether the $\delta^{18}O$ value of the carbonate component of enamel from fossil teeth at Elandsfontein is well enough preserved that it can be used as a proxy for conditions during the animal's life. The average $\varepsilon\delta^{18}O_{CO3\text{-}PO4}$ values of enamel are 9.2±0.7‰ (n = 38) and 8.2±0.7‰ (n = 10) for Elandsfontein and Langebaanweg, respectively; these values fit within the range observed for well-preserved teeth (7.2 – 10.6‰) (Bryant et al., 1996; Iacumin et al., 1996 and Martin et al., 2008; Fig. 2.3; Table S2.3). Based on the similarities in these offsets to what has been measured in well-preserved enamel, we consider the $\delta^{18}O$ values of the carbonate component of tooth enamel from Elandsfontein to be unaltered and to reflect the environmental and physiological conditions experienced by an animal during tooth formation.

Further data to support this conclusion comes from interspecific comparisons of $\delta^{18}O$ values of enamel carbonate. Numerous fossil and modern localities have documented that $\delta^{18}O$ values of hippopotamid enamel carbonate are lower than the $\delta^{18}O$ values of coeval taxa because they would be eating plants close to water and drinking water (e.g., Bocherens et al., 1996; Levin et al., 2006). Similar taxonomic distinctions found between ancient taxa in the Elandsfontein collection indicate that the unaltered biogenic signal of isotopic values is preserved in these specimens (Fig. 2.2b). Henceforth,

we only discuss the $\delta^{18}O$ values from the carbonate component of tooth enamel and refer to them as $\delta^{18}O_{enamel}$ values.

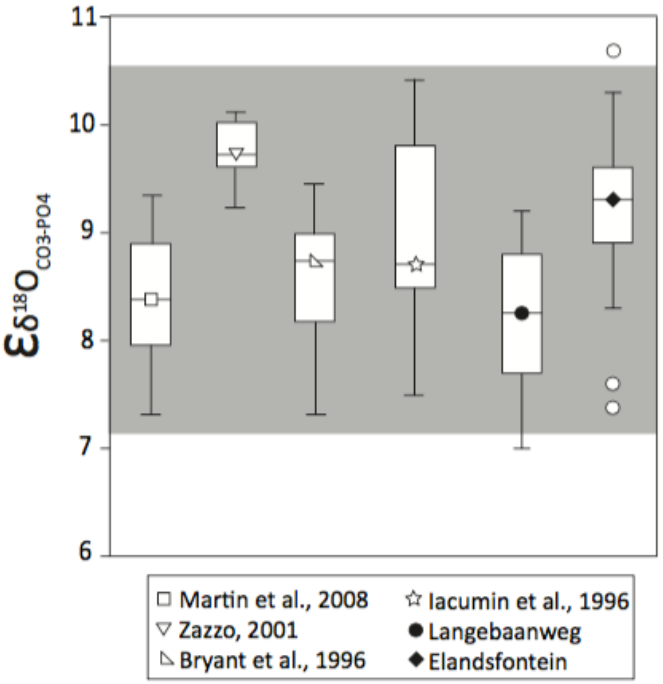

Figure 2.3: Box plot of the offset of $\delta^{18}O$ values of enamel carbonate and enamel phosphate ($\varepsilon\ \delta^{18}O_{CO3\text{-}PO4}$) for fossil enamel from Langebaanweg and Elandsfontein (closed symbols) and modern enamel from published studies (open symbols). The ends of the boxes represent the quartile values and the horizontal line within is the median, horizontal lines outside of the box indicate the range, and the outliers are plotted as circles. The gray bar denotes the maximum and minimum $\varepsilon\ \delta^{18}O_{CO3\text{-}PO4}$ values measured for modern teeth (Bryant et al., 1996; Iacumin et al., 1996; Zazzo, 2001; Martin et al., 2008).

2.4.3. Trends in $\delta^{13}C_{enamel}$ and $\delta^{18}O_{enamel}$ values from southwestern South Africa since 5 Ma

We compiled the new carbon and oxygen isotope data from tooth enamel produced in this study from Elandsfontein and Langebaanweg with the published data from Langebaanweg (Franz-Odendaal et al., 2002), Elandsfontein (Luyt et al., 2000) and Hoedjiespunt (Hare and Sealy, 2013) to examine environmental and climatic changes in

southwestern South Africa over the past ~5 myr. We used mesowear, microwear and taxonomic analogy to classify the dietary behavior of taxa for samples from Langebaanweg and Elandsfontein (Sponheimer et al., 2001; Franz-Odendaal et al., 2004; Stynder, 2009; 2011). Dietary behaviors of Hoedjiespunt bovids are discussed in Hare and Sealy (2013). These data are compiled in Table S2.2.

The $\delta^{13}C_{enamel}$ values of fossil teeth average -11.3±1.3‰ (n = 74) at Langebaanweg, -10.6±1.3‰ (n = 194) at Elandsfontein and -9.5±1.5‰ (n = 39) at Hoedjiespunt. The average $\delta^{13}C_{enamel}$ value of large mammals (> 6 kg) at each site fall within the range of the $\delta^{13}C_{enamel}$ values expected for animals with diets comprised of purely C_3 vegetation (Fig. 2.4).

Comparisons of $\delta^{18}O_{enamel}$ values from each family from Langebaanweg and Elandsfontein indicate significant differences for like taxa ($p < 0.001$), where the $\delta^{18}O_{enamel}$ values for teeth from Elandsfontein are typically ~4.5‰ more positive than those from Langebaanweg (Table 2.2; Table S2.2, Fig. 2.4b). This distinction holds for $\delta^{18}O_{enamel}$ values of all taxa sampled from the two sites except for suids for which there is no difference in $\delta^{18}O_{enamel}$ values for Elandsfontein (28.0±3.1‰) and Langebaanweg (27.7±0.9‰) (Fig. 2.4b). However, we do observe a ~4.4‰ increase in suid $\delta^{18}O_{enamel}$ values between Langebaanweg and Elandsfontein when we only consider the suid $\delta^{18}O_{enamel}$ values from the WCRP collection at Elandsfontein (32.1±0.6‰, n =3) and exclude the suid $\delta^{18}O_{enamel}$ values from EFTM from Luyt et al. (2000). The Hoedjiespunt enamel samples are limited to bovids and the comparison of $\delta^{18}O_{enamel}$ values for fossil bovids from the three fossil sites are distinct from one another ($p < 0.001$). Bovid

$\delta^{18}O_{enamel}$ values average 28.7±2.8‰ at Langebaanweg, 33.2±2.0‰ at Elandsfontein, and 31.4±1.5‰ at Hoedjiespunt.

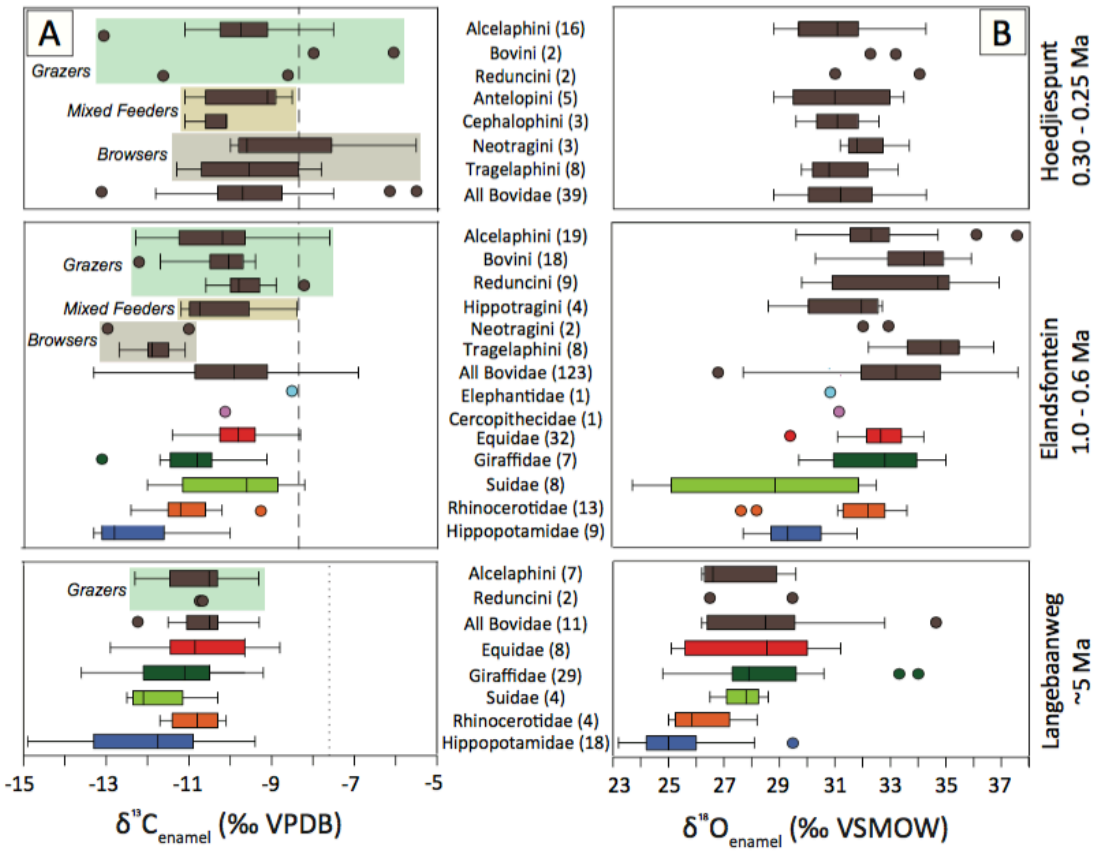

Figure 2.4: Box plot of the compiled $\delta^{13}C$ values (A) and $\delta^{18}O$ values (B) of the carbonate component of tooth enamel data from this study and of published records of Pliocene and Pleistocene fossil teeth from southwestern South Africa (Luyt et al., 2000; Franz Odendaal et al., 2002; Hare and Sealy, 2013; this study). Data are divided by family and bovid tribe. The number of individual analyses for each category is indicated in parentheses and when there are fewer than three isotopic values, analyses are presented as points. The dietary behaviors of bovids are divided into browsers, mixed feeders and grazers. See Table S2.2 for the compilation of isotope data and source for dietary behaviors. A vertical line within the box marks median values. The ends of the boxes represent the quartile values, horizontal lines indicate the range, and the outliers are plotted as circles. The maximum $\delta^{13}C$ value of herbivores with a pure C_3 diet are represented by a vertical dotted black line (Langebaanweg) and a vertical dashed black line (Elandsfontein and Hoedjiespunt). These values are based on reconstructed $\delta^{13}C$ values of CO_2 (Tipple et al., 2010) in Table S2.1.

2.5. Discussion

2.5.1. Vegetation trends in southwestern South Africa

Mammalian faunal and offshore pollen records indicate that the ecosystem of southwestern South Africa was different in the Pliocene and Pleistocene from today and that C_3 grasses were an important component of the physiognomic structure of these ecosystems at times during the last 5 myr (e.g., Dupont et al., 2005; Faith, 2011; Hare and Sealy, 2013). Today the vegetation community is composed of mostly woody, fynbos shrubs. Although rare in southwestern South Africa, grasses are more common inland where they grow on shale substrate, than they are on the marine sands typically found in the study area (Cowling, 1992).

The $\delta^{13}C_{enamel}$ values of large mammals from Langebaanweg, Elandsfontein and Hoedjiespunt show that herbivores had diets composed largely of C_3 vegetation (Luyt et al., 2000; Franz-Odendaal et al., 2002; Hare and Sealy, 2013; this study). Specifically, the $\delta^{13}C_{enamel}$ values of grazers indicate that the majority of the grasses consumed were C_3 grasses. Although the presence of C_4 vegetation cannot be totally discounted at Elandsfontein and Hoedjiespunt (Luyt et al., 2000; Hare and Sealy, 2013; Patterson et al., *in revision*), the $\delta^{13}C_{enamel}$ data presented here indicate that it was a relatively small component of the diets of large herbivores (Fig. 2.4).

The bovids at Elandsfontein are diverse and have a range of dietary behaviors such that the variation in the isotopic composition of bovid teeth may be used to develop a more detailed understanding of the nature of vegetation in the C_3-dominated ecosystem of southwestern South Africa. For this reason, we compared the $\delta^{13}C_{enamel}$ and $\delta^{18}O_{enamel}$

values among different bovid tribes, classifying them as browsers, grazers or mixed feeders (see Table 2.2 and Fig. 2.4).

When split by tribe there are no distinctions among the $\delta^{13}C_{enamel}$ values of bovids from the other grazing and browsing taxa at Langebaanweg ($p > 0.8$). The $\delta^{13}C_{enamel}$ values of all fossil teeth at Langebaanweg (browsers, grazers and mixed feeders) are > 2‰ more negative than the cutoff value for animals with a diet that includes any C_4 vegetation (-7.6‰, refer to Section 2.3.3.1), indicating that all of the animals we sampled had diets composed of solely C_3 vegetation. At Elandsfontein, the $\delta^{13}C_{enamel}$ values of browsing taxa (Tragelaphini, Neotragini and giraffid) are significantly more negative than those of grazing taxa (Alcelaphini, Bovini, Reduncini and equid) ($p = 0.005$). In comparison, at Hoedjiespunt the $\delta^{13}C_{enamel}$ values of browsing and grazing bovids are not statistically different from one another ($p = 0.97$). In addition, we find that $\delta^{13}C_{enamel}$ values of browsing bovid tribes at Hoedjiespunt are ~4‰ more positive than those of the browsers at Elandsfontein (Fig. 2.4), whereas the $\delta^{13}C_{enamel}$ values of grazing bovids at Elandsfontein and Hoedjiespunt are not significantly different from one another in ($p = 0.2$). This might indicate that the browse vegetation at Elandsfontein was different from that at Hoedjiespunt, which could be related to a drier or less dense mosaic landscape (Kohn, 2010) at Hoedjiespunt compared with Elandsfontein. There are no clear trends that distinguish the $\delta^{18}O_{enamel}$ values among different bovid tribes at either Elandsfontein or Hoedjiespunt. There are some indications of C_4 vegetation in the diets of both browsers and grazers at Hoedjiespunt and of grazers at Elandsfontein, however there are no indications of C_4 in the diet among browsers at Elandsfontein and any of the

herbivores at Langebaanweg. There are no distinctions in $\delta^{13}C_{enamel}$ or $\delta^{18}O_{enamel}$ values among the bovids that were sampled and identified to tribe (Acelaphini and Reduncini) at Langebaanweg ($p = 1.0$).

The $\delta^{13}C_{enamel}$ values of grazers at Elandsfontein and Hoedjiespunt that are more positive than what is expected for a pure C_3 diet (-8.4‰, refer to Section 2.3.3.1) could indicate the presence of some C_4 grasses, either in some seasons or on specific points on the landscape, like well-watered areas such as springs which is consistent with results from Patterson et al. (*in revision*). Hare and Sealy (2013) also suggest that the presence of some C_4 vegetation in the diets of grazing bovids from Hoedjiespunt might reflect the ability for C_4 plants to grow within a winter rainfall zone during low pCO_2 conditions that are characteristic of glacial intervals. Although low pCO_2 conditions might account for the presence of some C_4 vegetation in the diets of grazers at Elandsfontein, the dating of the deposits at Elandsfontein precludes us from assigning it to either a glacial or interglacial period (Braun et al., 2013).

The survival of large herbivores in southwestern South Africa would have required access to resources throughout the year. It is possible that there was an extended rainy season and that abundant food resources grew on nutrient-rich calcareous soils, which are no longer present at the fossil sites (Luyt et al., 2000). A year-round supply of palatable browse and graze would have required sufficient surface water and at Elansfontein, this likely included springs (Braun et al., 2013).

2.5.2. Oxygen isotope record

The ~4.5‰ increase in $\delta^{18}O_{enamel}$ values between the Langebaanweg and Elandsfontein fossil localities (from ~5 to 1.0 – 0.6 Ma) occurs across a time of global cooling and aridification (Marlow et al., 2000; Etourneau et al., 2009). $\delta^{18}O_{enamel}$ values can be influenced by a combination of factors including the $\delta^{18}O$ value of surface water, aridity and animal physiology (Kohn and Cerling, 2002). We do not think that physiological changes are responsible for the increase in $\delta^{18}O_{enamel}$ values as we observe it among multiple herbivore families and consider it unlikely that multiple disparately related herbivore families would converge upon identical physiological changes across this time span. Consequently, we must consider the influence of changes in the $\delta^{18}O$ value of surface water and changes in aridity on the observed increase in $\delta^{18}O_{enamel}$ values between the fossil teeth at Langebaanweg and Elandsfontein.

2.5.2.1. Oxygen isotopic composition of reconstructed surface water

In modern ecosystems $\delta^{18}O_{enamel}$ values of hippopotamids closely track the $\delta^{18}O$ values of meteoric water (Bocherens et al., 1996) and as such, fossil hippopotamid $\delta^{18}O_{enamel}$ values can be used to reconstruct the $\delta^{18}O$ values of meteoric waters (Levin et al., 2006). We used hippopotamid $\delta^{18}O_{enamel}$ values from Langebaanweg (n = 18) and Elandsfontein (n = 9) to estimate the $\delta^{18}O$ values of the surface waters in which these hippopotamids lived, which would reflect a combination of the $\delta^{18}O$ value of regional precipitation and the hydrological condition of the local surface waters. We were not able to estimate the $\delta^{18}O$ values of the surface waters at Hoedjiespunt because there are no

hippopotamid teeth preserved at the site (Stynder, 1997). We estimated $\delta^{18}O$ values of local surface waters from the hippopotamid $\delta^{18}O_{enamel}$ values by considering both the 5.4±1.3‰ enrichment in $\delta^{18}O$ between local surface water and hippopotamid body water reported by Levin et al. (2006) for modern hippopotamids and the carbonate-water $^{18}O/^{16}O$ fractionation relationship reported by Kim and O'Neil (2005), assuming that tooth formation formed at typical mammalian body temperatures of 37ºC.

Using this approach, we reconstruct the average $\delta^{18}O$ values of local surface water to -3.9±1.6‰ at Langebaanweg and -0.3±1.5‰ at Elandsfontein. For comparison, spring, tap and standing water nearby modern springs exhibit a mean $\delta^{18}O$ value of -1.7±2.2‰ (n = 4) (Table S2.4). The similarity between the $\delta^{18}O$ values of the reconstructed mid-Pleistocene water and that of modern waters within the Elandsfontein vicinity indicate that hydrological conditions of waters near spring systems in the region may not have not changed greatly since the mid-Pleistocene. However, the 3.6±1.8‰ increase in reconstructed surface water $\delta^{18}O$ values between Langebaanweg and Elandsfontein requires further explanation. The possible explanations for this ~4‰ increase include 1) a change in regional precipitation patterns as a result of changes in global climatic patterns that would affect precipitation $\delta^{18}O$ values and 2) a change in the type of surface waters (rivers vs. springs) that the hippopotamids were living in during the early Pliocene vs. the mid-Pleistocene. Here we review the potential roles of climate change and hydrological setting on the increase in $\delta^{18}O$ values of surface waters in southwestern South African between the early Pliocene and the mid-Pleistocene.

2.5.2.2. Global cooling

Decreased global temperatures and increased ice volume affected $\delta^{18}O$ values of precipitation globally between the Pliocene and Pleistocene with the onset of glacial and interglacial cycles (Zachos et al., 2001) but it is not clear how these oscillations affected $\delta^{18}O$ values of precipitation in southern Africa. A study of $\delta^{18}O$ values from speleothem carbonate from Buffalo Cave in South Africa (Hopley et al., 2007) that dates to the Pliocene/early Pleistocene (1.99 to 1.52 Ma) can provide perspective on the amplitude of change in the $\delta^{18}O$ values of meteoric water that we would expect between glacial and interglacial periods in southern Africa. Hopley et al. (2007) determine that there may be a ~2‰ increase in $\delta^{18}O$ values of regional precipitation between interglacials and glacials based on a combination of temperature and ice-volume effects. Despite some work that attributes the fossils at Elandsfontein to an interglacial interval based on the size of fossil carnivores (Klein et al., 2007), this assignment is less certain from more recent work at Elandsfontein (Braun et al., 2013). Regardless of whether the Elandsfontein fossils represent an interglacial or glacial interval, the maximum amount of change in $\delta^{18}O$ values of precipitation that we would expect between glacials and interglaicals is ~2‰, which is not enough to explain a ~4‰ difference in $\delta^{18}O$ values of surface water between the early Pliocene and mid-Pleistocene.

2.5.2.3. Rainfall amount

The negative correlation between rainfall amount and the $\delta^{18}O$ value of rain is termed the "amount effect" (Dansgaard, 1964). This effect must be considered in the

interpretation of the ~4‰ increase in $\delta^{18}O$ values of reconstructed surface waters. If southwestern South Africa became more arid between the early Pliocene and the mid-Pleistocene, as indicated by offshore archives (e.g., Marlow et al., 2010; Dupont et al., 2013), then we might expect to see indications of less rainfall in the reconstructed surface water $\delta^{18}O$ values. Modern precipitation data from Cape Town indicate that the "amount effect" is limited in southwestern South Africa (Midgley and Scott, 2004; Harris et al., 2010; West et al., 2014); it is equivalent to -10mm/1‰ $\delta^{18}O$ for monthly winter rainfall (based on $\delta^{18}O$ values of monthly rainfall reported in Harris et al. (2010)) and thus very little of the variation in $\delta^{18}O$ values of precipitation in modern southwestern South Africa can be explained by amount rainfall. In comparison, Panama (WGS-84 Lat/Long: 9.00970, -79.60324) has a strong "amount effect" with -35 mm rainfall for every 1‰ increase in the $\delta^{18}O$ value of rainfall (Higgins and MacFadden, 2004).

In addition, we do not expect to observe an "amount effect" in southwestern South Africa because this oxygen isotopic effect mostly occurs where temperatures are > 20ºC and where there is high humidity or significant rainfall (e.g., Rozanski et al., 1993), a pattern seen at collection sites globally (IAEA/WMO, 2001). The majority of rain in this region falls in the winter and it is associated with cold, westerly fronts; it is unlikely that average winter temperatures were > 20ºC. If temperatures during the rainy season were > 20ºC during the Pliocene and Pleistocene, then it could have been warm enough for the growth of C_4 grass. The $\delta^{13}C$ values of fossil enamel from grazers, however, suggest that there was little C_4 grass in this region.

Although a change in the $\delta^{18}O$ values of rainfall related to moisture source may contribute to the increase in the $\delta^{18}O$ values of rainfall, it is unlikely that this would represent a substantial contribution to the full ~4‰ increase documented between the Pliocene and mid-Pleistocene. If there had been a change in the rainfall related moisture source from the east (i.e., contribution of summer rainfall), then we would expect to see the $\delta^{13}C_{enamel}$ values of some large mammalian herbivores to be more positive than what is calculated for a pure C_3 diet because they would be incorporating C_4 grasses that grow during the summer months into their diet. We find that the majority of $\delta^{13}C_{enamel}$ values are within the range expected for animals with pure C_3 diets and no change in $\delta^{13}C_{enamel}$ values between the fossil herbivores at Langebaaweg and Elandsfontein (Fig. 2.4). Furthermore, models of regional climate indicate that the source of atmospheric moisture, Atlantic water off the coast of southwestern South Africa, would have been constrained by relatively stable regional meteorological factors (e.g. ICTZ, Agulhas Current, Subtropical convergence zone and Benguela Current; McClymont et al., 2005) and thus would not have drastically changed between the early Pliocene and mid-Pleistocene.

2.5.2.4. Depositional mode and surface water

A change in the local hydrology and $\delta^{18}O$ value of surface water might be responsible for the increase $\delta^{18}O_{enamel}$ values between Langebaanweg and Elandsfontein. Today much of the coastal plain of southwestern South Africa is fed by ground water and many areas have standing water associated with artesian wells. The depositional environments of the Varswater Formation (i.e., the Langebaanweg fossil site) indicate the

presence of fluvial and estuarine waters (Roberts et al., 2011). Various sedimentological studies indicate that the paleo-Berg River in the early Pliocene had a southerly trajectory and emptied into the embayment which is today the Saldanha Bay as opposed to emptying into the Atlantic Ocean in St. Helena Bay as the Berg River does today (e.g., Roberts et al., 2011; Fig.1). Although a previous study of Elandsfontein suggested the presence of fluvial activity (Butzer, 1973), recent investigations document the complete lack of any sedimentary structures that would support a fluvial explanation for the sediments in which fossils at Elandsfontein have been found (Braun et al., 2013). Geomorphological reviews emphasize that large Cenozoic eolianites as well as granite outcrops act as barriers for any fluvial systems west of the Salt River and south of the Berg River (Mabbutt, 1952). As a result the main source of surface water in the region is provided by springs fed by the large underground Elandsfontyn and Langebaan Road aquifers (Brumfitt et al., 2013). Thus the $\delta^{18}O$ values of the enamel from large, mid-Pleistocene mammals at Elandsfontein likely reflect the $\delta^{18}O$ values of isolated springs distributed around the landscape. The waters from the Berg River headwaters have $\delta^{18}O$ values today that range from -6.0‰ to -4.0‰ (Weaver and Telma, 2005; West et al., 2014), whereas $\delta^{18}O$ values of spring and tap waters surrounding the Elandsfontein vicinity today range from -3.6 to -1.9‰ (Table S2.4; Midgley and Scott, 1994; West et al., 2014; this study). There is a 0.4 to 4.1‰ difference in $\delta^{18}O$ values between surface waters sourced from the Berg River compared with waters from springs near Elandsfontein. Standing spring water at Elandsfontein has been evaporated and yields $\delta^{18}O$ value of 1.5‰. Furthermore, the average $\delta^{18}O$ value of reconstructed surface water

at Elandsfontein (-0.3±1.5‰) sits within the expected range of water near the Elandsfontein locality today. If offsets between $\delta^{18}O$ values of waters from the Berg River and from springs in the study area were consistent over the last 5 myr, then the ~4‰ increase in reconstructed surface water $\delta^{18}O$ values from tooth enamel between Langebaanweg and Elandsfontein fossil sites can be explained solely by a difference in local hydrology. At Langebaanweg, hippopotamids likely spent much of their time in waters that derived from the paleo-Berg River, whereas some four million years later, the hippopotamids from the Elandsfontein fossil deposits likely spent much of their time in water bodies that were fed by springs. The differences in the enamel $\delta^{18}O$ values of these two hippopotamid populations may be best explained by these local differences types of water bodies in which they wallowed.

2.5.2.5. Aridity

Aridity can have an effect on $\delta^{18}O_{enamel}$ values in multiple ways. Aridity can be the result of decreased rainfall amount which will affect $\delta^{18}O_{enamel}$ values due to a change in $\delta^{18}O$ values of precipitation that then contributes to the water that animals ingest. However, the degree of aridity may influence $\delta^{18}O_{enamel}$ values independent of any changes in the $\delta^{18}O$ values of precipitation via the ingestion of leaf water, which becomes greatly enriched in ^{18}O relative to ^{16}O in arid climates (Levin et al., 2006). The $\delta^{18}O_{enamel}$ values of animals that are not obligate drinkers (e.g., giraffes and oryx) are sensitive to aridity in part because a large fraction of their body water may come from leaf water. The strong relationship between aridity and $\delta^{18}O_{enamel}$ values of these Evaporation Sensitive

(ES) animals, taxa whose body water is derived largely from leaf water, today can be used to evaluate aridity in the past by comparing $\delta^{18}O_{enamel}$ values of ES animals to those from Evaporation Insensitive (EI) animals, taxa whose body water is derived largely from ingested surface water (e.g., hippopotamids and elephantids). The $\delta^{18}O_{enamel}$ values of EI taxa do not vary with aridity and can be used to control for changes in meteoric water $\delta^{18}O$ values (Levin et al., 2006). The $\varepsilon_{ES\text{-}EI}$ between $\delta^{18}O_{enamel}$ values of ES and EI taxa is greater in more arid environments than in less arid environments (Levin et al., 2006).

We evaluated whether increased aridity could explain the ~4‰ increase in enamel $\delta^{18}O$ values between the early Pliocene and mid-Pleistocene by comparing the $\varepsilon_{ES\text{-}EI}$ of $\delta^{18}O_{enamel}$ values of individual teeth from Langebaanweg (n = 47) and Elandsfontein (n = 16), where hippopotamids (i.e., *Hippopotamus*) are the representative EI taxa and giraffids (i.e., *Sivatherium*) are the representative ES taxa. Calculated $\varepsilon_{ES\text{-}EI}$ values are +3.0±1.9‰ and +2.7±1.9‰ for Langebaanweg and Elandsfontein, respectively. There is no large difference between the $\varepsilon_{ES\text{-}EI}$ values for the two populations, suggesting no change in aridity between the Pliocene and mid-Pleistocene environments in southwestern South Africa. However, we cannot simply evaluate aridity as outlined above if 1) there were changes in $\delta^{18}O$ values of surface water due to the differences in depositional setting between Langebaanweg and Elandsfontein and 2) if the behavior of EI and ES taxa was different during the Pleistocene and the Pliocene. First, $\delta^{18}O_{enamel}$ values from hippopotamids might not be closely tracking precipitation $\delta^{18}O$ values during the mid-Pleistocene in the same way as in the early Pliocene if hippopotamids from Elandsfontein wallowed in pools of evaporated spring water, whereas hippopotamids

from the Langebaanweg collection spent time immersed in river waters. Our compilation of $\delta^{18}O$ values from modern waters in the region indicates that spring-based water sources have more positive $\delta^{18}O$ values than that of river waters (Table S2.4). Second, it is important to note that in this analysis we use the genus *Sivatherium* rather than *Giraffa* as the ES taxon. Although these two taxa are within the family Giraffidae, isotopic studies from eastern Africa indicate that *Sivatherium* underwent a major transition during the Pliocene and Pleistocene to incorporate more graze into their diet, while *Giraffa* did not (Cerling et al., 2015). Thus, it is feasible that sensitivity to aridity was different between these two taxa such that *Sivatherium* might not be an appropriate ES taxon to use in the $\delta^{18}O_{enamel}$-based aridity index proposed by Levin et al. (2006).

While we cannot rule out the effects of evaporation on surface water $\delta^{18}O$ values, we do not think that aridity is the primary driver of the ~4‰ increase in reconstructed surface water $\delta^{18}O$ values between the early Pliocene and the mid-Pleistocene. It is unlikely that we would observe a uniform increase in the average $\delta^{18}O_{enamel}$ values of herbivore families from Langebaanweg and Elandsfontein because hippopotamids would have remained in the water, somewhat buffered from increased aridity, resulting in a smaller shift for hippopotamids than for other herbivore families. Furthermore, the ~4‰ increase in reconstructed surface water $\delta^{18}O$ values between fossil sites can be explained solely by a shift from riverine water to groundwater-fed springs as discussed in Section 5.2.4. Given the present data, we view this as the simplest way to explain the trends in the fossil $\delta^{18}O_{enamel}$ values we observe.

2.5.3. Theropithecus diet at Elandsfontein

The diet of fossil *Theropithecus* species from southern and eastern Africa have been evaluated to determine the partitioning of resources between primates and other mammalian species as well as to better define the influences that contributed to the success of *Homo* (e.g., Lee-Thorp et al., 1989; Codron et al., 2005; Cerling et al., 2013; Levin et al., 2015). A single *Theropithecus* mandible was excavated from Elandsfontein (WCRP collection) and this specimen has a $\delta^{13}C_{enamel}$ value of -10.2‰, which is indicative of a diet composed of C_3 vegetation (Fig. 2.4; Table S2.2). This is the only $\delta^{13}C_{enamel}$ value of *Theropithecus* from Pleistocene southwestern South Africa. Contemporaneous *Theropithecus* $\delta^{13}C_{enamel}$ values from eastern Africa and in other locations in South Africa indicate that *Theropithecus* consumed C_4 graze (e.g., Codron et al., 2005; Cerling et al., 2013). The addition of carbon isotope data from *Theropithecus* at Elandsfontein shows that *Theropithecus* was able to survive on diets composed C_3 vegetation during the Pleistocene (whether it was browse or graze) if it lived in environments where C_3 vegetation was dominant, as with the modern gelada baboon (Levin et al., 2008).

2.5.4. Hominin paleoenvironment at mid-Pleistocene Elandsfontein

The sedimentary record at Elandsfontein provides unique insights into the ecology of southwestern South Africa during the mid-Pleistocene, which is not well documented elsewhere in southern Africa (Klein et al., 2007; Braun et al., 2013). The archives at Elandsfontein also provide evidence for some of the earliest hominin behavior in a winter rainfall zone in southern Africa. The association of the fossil fauna with Acheulean stone

tools (i.e., hominin technology that indicate behavioral advances intersecting with the biological change) in an excavated context at Elandsfontein allows us to use inferences about paleoclimate from $\delta^{13}C_{enamel}$ and $\delta^{18}O_{enamel}$ values to develop an understanding of hominin ecology. This is especially important because of the age of this locality (1.0 – 0.6 Ma) situates the site around the time of the mid-Pleistocene transition in climate dynamics (McClymont et al., 2005). Large mammalian remains at Elandsfontein indicate that there were both large browsing and grazing herbivore communities, suggesting that the landscape would have had sufficient resources to assure the survival of these animals, in stark contrast to the modern ecosystems in this area. This ancient landscape clearly was a draw for hominins, as indicated by the thousands of stone tools recovered from this locality (Singer and Wymer, 1968; Klein, 1983; Braun et al., 2013) as well as fossil remains of early humans (Drennan, 1953). The springs at Elandsfontein (Braun et al., 2013) would have been a resource-rich environment for early humans, if Elandsfontein had been buffered from the regional aridification during the mid-Pleistocene. This is consistent with studies of Pleistocene archaeological sites where springs and groundwater-fed areas have been considered to be important resource for hominins (e.g., Cuthbert and Ashley, 2014).

2.6. Conclusions

The results of this study add to a growing body of work, from both terrestrial- and marine-based archives, on how climate and vegetation in southwestern South Africa have changed over the last 5 myr (Fig. 2.5). The main conclusions from this study are:

1) The $\delta^{13}C_{enamel}$ values of fossil teeth from southwestern South Africa indicate that both browsing and grazing herbivores had diets dominated by C_3 vegetation, which suggests the dominance of the winter rainfall season during the time intervals of fossil deposition at Langebaanweg, Elandsfontein and Hoedjiespunt. We can not, however, totally discount the presence of C_4 grasses during the mid-Pleistocene and late Pleistocene.
2) There is an increase in reconstructed surface water $\delta^{18}O$ values from southwestern South Africa between the early Pliocene and mid-Pleistocene of ~4‰. We attribute the increase in $\delta^{18}O$ values of surface waters primarily to a shift in hydrology and depositional environments along the coastal plain of southwestern South Africa. The major source of water for animals during the Pliocene appears to have been a fluvial system whereas springs were likely the dominant surface waters in the mid-Pleistocene.
3) While increased aridity in southwestern Africa is indicated both by the marine- and terrestrial-based proxy records compiled in this study, it is not clearly evident in the isotopic record of large mammals presented here. The Elandsfontein archaeological site may have been buffered from regional mid-Pleistocene aridification as a result of the available surface water indicated by ancient spring deposits. If springs were annually active, then water and other resources associated with springs would have been available to mammals, such that the area may have served as an oasis of sorts within a relatively drier landscape.

4) This study highlights the importance of considering depositional environment and the local environmental setting when understanding how specific terrestrial environments responded to regional climate and environmental change.

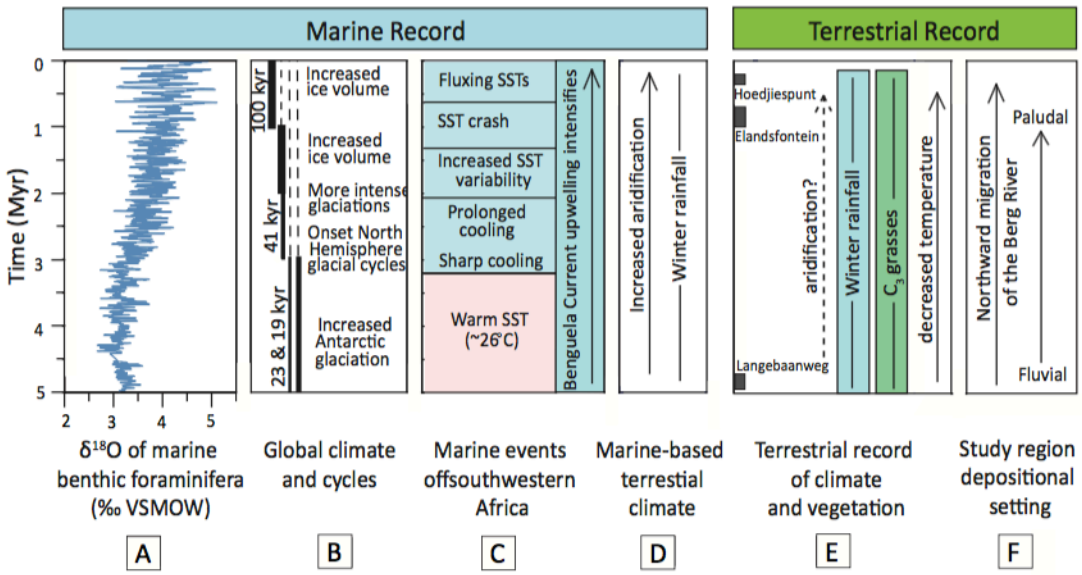

Figure 2.5: A summary of Pliocene and Pleistocene records of global, regional, marine, and terrestrial changes relevant to southwestern Africa. A) The global benthic foraminifera $\delta^{18}O$ curve (Zachos et al., 2001) and B) a summary of major change in global climate (composite record based on data from Ruddiman et al., 1989; Shackleton et al., 1990; 1995). C) Summary of results from mid latitude marine sediment cores off the southwestern Africa (Marlow et al., 2000; Dupont et al., 2005; Etourneau et al., 2009). D) Summary of data from terrestrial records including $\delta^{13}C$ and $\delta^{18}O$ values from fossil teeth and soil geochemistry from southwestern South Africa (Eze and Meadows, 2014; this study). E) Summary of depositional environments based on sedimentological data from Langebaanweg and Elandsfontein (Butzer, 1973; Roberts et al., 2011; Braun et al., 2013).

CHAPTER 3: Environmental and ecological implications of strontium ratios in mid-Pleistocene fossil teeth from Elandsfontein in southwestern South Africa

ABSTRACT

The mid-Pleistocene site of Elandsfontein has yielded fossil fauna and artifacts dating to ca. 0.6 to 1 million years ago, as well as the Saldanha, or Hopefield, hominin calvarium. This site is located within the Greater Cape Floristic Region (GCFR), in an area that is dry and hot, blanketed by marine-derived sand dunes, and primarily vegetated by woody shrubs and sedges of the fynbos biome with minimal amounts of grass growing on nutrient-poor soils. This region does not support communities of large mammalian herbivores. In contrast, the mid-Pleistocene faunal assemblage is rich in mammalian herbivores, suggesting that the environment and ecology at that time could support such communities. However, it is unknown whether browsing and grazing herbivores survived on local vegetation or if they migrated to more distant, nutrient-rich areas to obtain food, such as to shale substrates ~ 20 to 30 km inland from Elandsfontein where palatable grass and shrubs grow today. We measured strontium isotope ratios ($^{87}Sr/^{86}Sr$ ratio) in fossilized teeth from Elandsfontein and compared these ratios to the bioavailable $^{87}Sr/^{86}Sr$ ratios from the major substrates in the region to determine if large mammalian herbivores were able to obtain sufficient resources locally (i.e., if teeth had signature of local $^{87}Sr/^{86}Sr$ ratio) or whether they also ranged across other geological substrates. The bioavailable $^{87}Sr/^{86}Sr$ ratios from marine sands from Elandsfontein range from 0.709380 to 0.711690 and are distinct from the bioavailable $^{87}Sr/^{86}Sr$ ratios for granite, sandstone

and shale substrates in the region. The $^{87}Sr/^{86}Sr$ ratios of fossil teeth of carnivores, large herbivores and rodents from Elandsfontein range from 0.709254 to 0.711171, values within the range of the marine sands $^{87}Sr/^{86}Sr$ ratios. These data suggest that during the mid-Pleistocene the vegetation growing on coastal marine sands in southwestern South Africa was adequate to support large herbivores and that these animals remained within the coastal area, and therefore did not need to migrate away from the coastal area of the reigon for resources. These data, along with the evidence of ancient spring-fed environments suggest that the mid-Pleistocene environment at Elandsfontein, unlike today, provided sufficient resources for rich and diverse communities of large animals. It is possible that this environment is what attracted hominins to Elandsfontein and that it served as a refuge for animals in a region that was becoming increasingly arid.

3.1. Introduction

The southwestern coast of South Africa is located within the Greater Cape Floristic Region (GCFR). The endemic fynbos vegetation constitutes one of the most diverse and variable biomes in the world, dating to before the Pliocene (e.g., Dupont et al., 2011). While the fynbos ecosystem is thought to have drastically evolved since its emplacement, little is actually known about the variability of vegetation in southwestern South Africa or about its faunal associations before the Last Glacial Maximum (LGM), ~21,000 years ago (Stynder, 2009; Rossouw et al., 2009). Terrestrial-based proxies of climate and vegetation are important for evaluating the history and composition of the fynbos biome, however it is uncommon to find an open air site (as opposed to cavernous sites) that preserves artifacts and fossils within the original depositional setting and that dates to before the LGM anywhere within southern Africa (Braun et al., 2013).

Elandsfontein is an open-air archeological and paleontological site that dates to within the mid-Pleistocene (~ 1.0 to 0.6 million years ago; Ma) and where artifacts and fossils co-occur on a buried paleolandscape (e.g., Klein and Cruz-Uribe, 1991; Braun et al., 2013). Sediments and the faunal assemblage at Elandsfontein indicate that the mid-Pleistocene landscape of southwestern South Africa was composed of shrub land and grassland (Luyt et al., 2002; Stynder, 2009; Thesis Chapter 2; Patterson et al., 2016). The regional vegetation during the mid-Pleistocene would have had to have supported a community of large herbivorous mammals, both browsers and grazers, including species within the Bovidae, Rhinocerotidae, Hippopotamidae, Giraffidae, Elephantidae, Equidae and Suidae families (Thesis Chapter 2). The preservation of ancient spring deposits and the presence of Hippopotamidae at Elandsfontein suggest the presence of standing water

and that this location may have been a spring-fed environment (e.g., Braun et al., 2013; Lehmann et al., 2016; Patterson et al., 2016). Stone tools from the Acheulean Industry, the first example of standardized artifact manufacturing and considered to have developed alongside major behavioral and biological changes in human evolution, are found at Elandsfontein and indicate that the environment at this location was utilized by hominins (e.g., Braun et al., 2013).

In contrast to the environment of the mid-Pleistocene, contemporary southwestern South Africa is an arid shrub land and is mostly vegetated by woody, low-nutrient fynbos vegetation growing on marine-derived sands (Rebelo et al., 2006). There is minimal surface water and the minor amounts of grass in the region grows primarily on shale ~ 20 km east of Elandsfontein but the grass is likely not of sufficient quantities to feed large mammalian grazers (Rebelo et al., 2006). The carbon isotopic composition of fossil teeth ($\delta^{13}C$ values) from mid-Pleistocene Elandsfontein indicate that, like today, this area was within a winter rainfall zone, dominated by C_3 vegetation adapted to grow during the cool, wet season (Luyt et al., 2000; Thesis Chapter 2). Large mammalian herbivores from the mid-Pleistocene would have found survival difficult to impossible given the current composition of vegetation and lack of water at Elandsfontein.

Climatic and environmental proxies from marine sediment records and paleosols indicate that this region may have experienced aridification since the Pliocene in association with increased upwelling of the Benguela Current (e.g., Marlow et al., 2000; Eze and Meadows, 2013). While it is known that the environment and faunal composition of southwestern South Africa were different in the mid-Pleistocene than they are today, there is no modern analog for the ancient ecosystems and environments (Braun et al.,

2013). Little is understood about the ecological composition and vegetative diversity of the fynbos in southwestern South Africa during the mid-Pleistocene or about how animals would have survived in the region.

Modern vegetation in southwestern South Africa varies by rock type, where woody fynbos shrubs grow on sandstone and marine-derived sands, the substrate found at Elandsfontein. More palatable shrubs and grasses, representing vegetation suitable for browsers and grazers, grow on shale and on granite (Sealy et al., 1991; Rebelo et al., 2006). Sealy et al. (1991) have shown that the substrates in the region differ in $^{87}Sr/^{86}Sr$ ratio values and that they can be divided into the categories of coastal sands and more inland shales and sandstones (Fig. 3.1; Table 3.1). The $^{87}Sr/^{86}Sr$ ratio of herbivore tissues (e.g., bone and tooth enamel) is the same as the $^{87}Sr/^{86}Sr$ ratio of ingested plants, which in turn is determined by the bioavailable $^{87}Sr/^{86}Sr$ ratio of the soil or rock substrate on which these plants grew (i.e., the $^{87}Sr/^{86}Sr$ ratio of the strontium in a rock or soil that can be taken up by biological organisms) (e.g., Bentley, 1996; Sillen et al., 1998). The $^{87}Sr/^{86}Sr$ ratio range of bioavailable strontium can differ from that of the bulk substrate, because different minerals (with different $^{87}Sr/^{86}Sr$) physically and chemically weather at different rates.

Table 3.1: Summary of the compiled bioavailable $^{87}Sr/^{86}Sr$ ratios for major substrates in southwestern South Africa from Sealy et al. (1991) and this study based on modern bone, enamel and plant samples. See Table S3.1 for details.

Location	$^{87}Sr/^{86}Sr$ ratio		$^{87}Sr/^{86}Sr$ ratio range		*n*[b]
	Average	Stdev[a]	Minimum	Maximum	
Substrate					
Pleistocene marine sands	0.710377	0.000786	0.709380	0.711690	8
Mixed granite and marine sands	0.710617	0.001908	0.709575	0.714741	2
Cape Granite suite	0.717491	0.004166	0.711421	0.723563	12
Table Mountain Sandstone	0.716704	0.001802	0.714092	0.718546	12
Malmesbury shale	0.718064	0.001632	0.715332	0.720390	6

[a] standard deviation is ± 1σ from average

[b] number of individual samples compiled for each substrate and region

Here we utilize and expand upon existing studies on the variation in $^{87}Sr/^{86}Sr$ ratios from the four major substrates in southwestern South Africa to determine whether or not mid-Pleistocene mammals from Elandsfontein traveled to other areas in southwestern South Africa for food or if they found resources in the coastal area and/or around Elandsfontein. In the case of migrating animals, such as large herbivores, there may be situations where vegetation is obtained at one site for part of a year (e.g., season), and in another location during a different part of the year, or season. We investigated this possibility for fossil herbivores preserved at Elandsfontein, by analyzing the $^{87}Sr/^{86}Sr$ ratios along the tooth growth axis of browsing and grazing mammals, since these ratios should change if animals consumed foods from distinct substrates at different stages of tooth formation (Balasse et al., 2002; Copeland et al., 2016). If animals from Elandsfontein did not travel to find food, their enamel $^{87}Sr/^{86}Sr$ ratios should be the same as the bioavailable $^{87}Sr/^{86}Sr$ ratios of the marine sands found at Elandsfontein. In this case it is likely that the environment at Elandsfontein provided sufficient food for the large

mammalian herbivore community that lived in this region during the mid-Pleistocene. If, however, the $^{87}Sr/^{86}Sr$ ratios of enamel indicate that herbivores traveled to other substrates in the region for food, then it is likely that animals could not have survived solely on the vegetation that grew at Elandsfontein during the mid-Pleistocene. By combining existing faunal and sediment records of climate and environment from Elandsfontein with $^{87}Sr/^{86}Sr$ of fossil teeth, we can improve our understanding of how the broader regional vegetation and environment may have changed since the mid-Pleistocene and how animals and hominins may have utilized the southwestern South African region.

The first steps to determining whether animals moved for food are to 1) develop a map of bioavailable $^{87}Sr/^{86}Sr$ for each major substrate in the region and 2) perform a control using fossil and modern enamel to determine whether or not the $^{87}Sr/^{86}Sr$ ratios of mid-Pleistocene teeth are primary or if they have been subjected to diagenesis, as well as to determine the ideal pretreatment needed to remove secondary strontium, if present, for this particular study. Only then can we then considered the movement of herbivore for food during the mid-Pleistocene by comparing their enamel $^{87}Sr/^{86}Sr$ ratios with the bioavailable $^{87}Sr/^{86}Sr$ ratios of substrates in the region. Once we understood if and how herbivores used the land for food, we could then evaluate the distribution of vegetation in the region and the ecological and environmental context of mid-Pleistocene Elandsfontein.

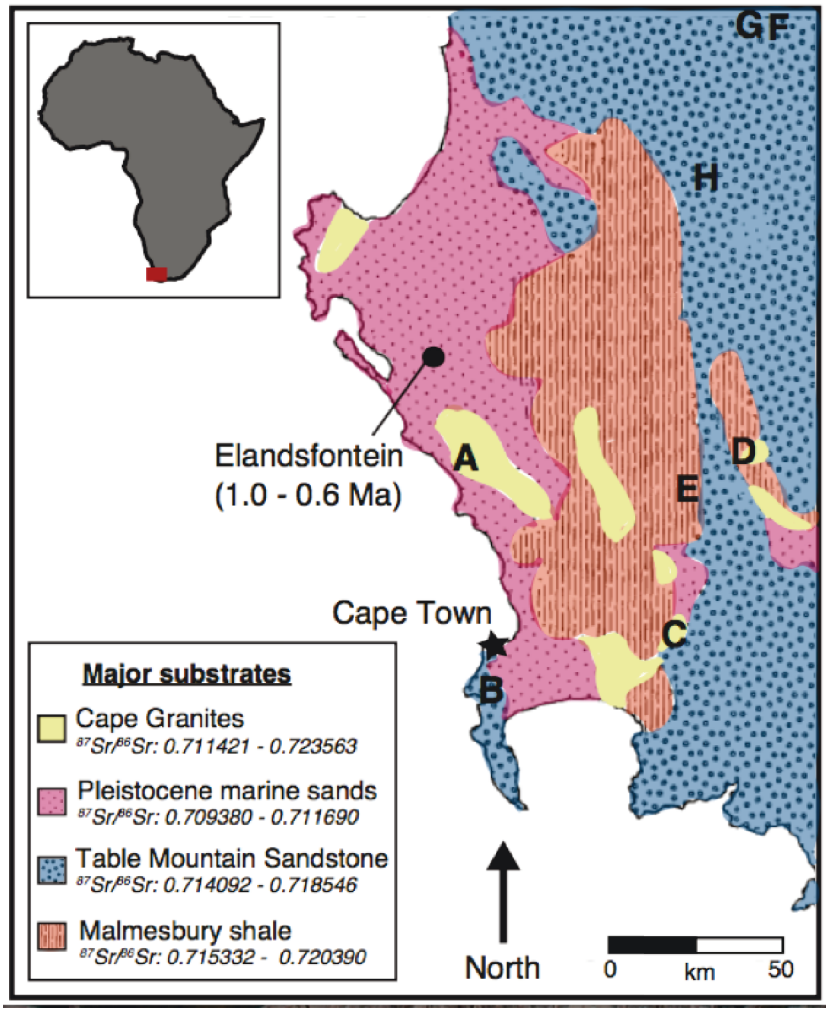

Figure 3.1: Map of southwestern South Africa outlining the locations of the major substrates in the region and indicating the location of Elandsfontein (black circle). Letters A through H denote the sampling locations of plants, modern bone and enamel used to determine the range of bioavailable $^{87}Sr/^{86}Sr$ ratios for each substrate (see Table S3.1 for the corresponding sample location and sample information). The range in bioavailable $^{87}Sr/^{86}Sr$ ratios for each major substrate is reported in the legend and in Table 3.1. These ratios are based on both the newly analyzed bone and teeth (this study) and from the bioavailable $^{87}Sr/^{86}Sr$ ratios of substrates in the region that are reported in Sealy et al. (1991). The location of the study region is denoted by a red rectangle on the continent of Africa. The base map with outlines the major geologic substrates is based on Sealy et al. (1991).

3.2. Background

3.2.1. Study Region

3.2.1.1. Elandsfontein

Initial surveys of fossil and artifacts in the 1950s yielded a hominin calvarium, known as the Saldanha specimen, and excavations in the 1960s recovered stone tools in association with large mammalian fossils (e.g., Drennan, 1953; Singer and Wymer, 1968; Deacon, 1998). It was not until more than 50 years later that in situ materials were found again and it was determined only at this time that large mammalian fossils and artifacts were located on a buried landscape across a > 11 km^2 area of the archeological site Elandsfontein (Braun et al., 2013). Fossils from Elandsfontein have a low carbonate content (Luyt et al., 2000; Thesis Chapter 2) and excavations have shown extensive leaching zones in some sediment profiles that contain fossils and artifacts, though leaching is not homogeneous across the region (Braun et al., 2013).

3.2.1.2. Climate and vegetation

The region of southwestern South Africa is on the western coast of South Africa and within the winter rainfall zone, a climatic zone encompassing ~ 200 km^2 that receives ~ 65% of its annual precipitation between April and September (Chase and Meadows, 2007). This climatic zone is distinct from the climate for the rest of South Africa. East of the study region, rainfall mostly occurs year round or during the summer months (> 66% of mean annual precipitation between October and March). Each climatic zone is associated with distinct vegetation; for example, grasses that grow within southwestern South Africa consist mainly of species that only grow during the wet, winter months,

however, C_4 species can be locally quite abundant and are found, such as on shales (e.g., Cowling and Lombard, 2002).

3.2.1.3. Regional geology

The coastal plain of southwestern South Africa is covered by what were originally marine sands containing shell fragments and which date to the Pliocene and Pleistocene. About 12 granitic plutons outcrop in southwestern South Africa and these are associated with orogenic events related to the convergence of South American and Namibian cratons during the Precambrian (Rozendaal et al., 1999; Belcher and Kisters, 2003). These granites are scattered throughout the study region and form what is called the Cape Granite suite (Fig. 3.1). Granites of the Cape Granite suite can be defined and distinguished from one another by mineralogical and geochemical composition. The most dominant granite types are found in the area surrounding Elandsfontein and along the southwestern South African coast (e.g., the Darling batholith and the Saldania pluton) (Scheepers, 1995). Inland from the marine sands and coastal granites, older substrates dominate. These substrates are the Precambrian to Cambrian Malmesbury shales and Cape Fold Mountain Belt complex sandstones and quartzites (i.e., Table Mountain/ Witteberg/ Bokkeveld series) (Fig. 3.1).

3.2.1.4. Relationship between geology and composition of vegetation

The composition of vegetation in southwestern South Africa varies across the landscape as a function of geological substrate because the mineralogical composition of a substrate dictates the minerals/nutrients available for plants (Cowling, 1997; Cowling et

al., 2002). Today, southwestern South Africa is dominated by nutrient-poor, though diverse fynbos shrub land that grows on coastal sands as well as on sandstones and quartzite (Rebelo et al., 2006). In contrast, where present, shales support more nutrient-rich fynbos species as well as the nutrient-rich renosterveld grasses and evergreen asteracerous shrubs that would be palatable to the large herbivorous mammals that lived in the region during the mid-Pleistocene. These latter plant types are only a minor component of the current regional vegetation and likely can not produce the quantity of vegetation necessary to feed a large community of browsing and grazing herbivores (Rebelo et al., 2006). Granites produce richer soils than marine sands and today the majority of the Western Cape's vineyards are found on granite-derived soils.

Large mammalian herbivore communities existed at Elandsfontein during the mid-Pleistocene (taxa ranged from Hippopotamidae to Bovidae and Giraffidae) would have needed substantial and nutrient-rich vegetation, both browse and graze (Klein et al., 2007; Braun et al., 2013). In the contemporary setting, we expect that these animals would have to travel inland from Elandsfontein to find palatable food resources, such as the grasses that can grow on the soils derived from nutrient-rich shales. However, as stated earlier, grass is a minor component of the current regional ecology, primarily growing in small quantities on shale substrate during the winter months (Rebelo et al., 2006).

3.2.2. $^{87}Sr/^{86}Sr$ isotope ratio of bioapatite and the determination of animal migration and regional vegetation

The $^{87}Sr/^{86}Sr$ ratio in bioapatite, where bioapatite refers to enamel and bone, can be used as a geochemical fingerprint of the substrates on which animals lived, because the $^{87}Sr/^{86}Sr$ ratio from different substrates is preserved in plants and also the teeth and bones of animals eating the plants (e.g., Bentley, 2006; Copeland et al., 2011). The following subsection discusses how the $^{87}Sr/^{86}Sr$ ratios of fossil enamel can be applied to evaluating regional migration for food and how the differences in the bioavailable $^{87}Sr/^{86}Sr$ ratios of substrates and the ecology associated with these substrates (i.e., food resources for herbivores) can be used in tandem to determine 1) the locations of food resources for large mammalian herbivores preserved at Elandsfontein and 2) the ecology and environments of southwestern South Africa and Elandsontein. We also assess the role of diagenesis on the $^{87}Sr/^{86}Sr$ ratios in teeth preserved at Elandsfontein, which is of concern because a number of fossils and sediments at Elandsfontein have been leached, thus some of the original carbonate content has been removed (Luyt et al., 2000; Braun et al., 2013; Thesis Chapter 2).

3.2.2.1. Regional substrate bioavailable $^{87}Sr/^{86}Sr$ ratios

Bioapatite $^{87}Sr/^{86}Sr$ ratios can provide information about the type of vegetation available in a region during that animal's life, which in turn can be useful when evaluating the ecology of an ancient environment (e.g., Copeland et al., 2016). For example, if grazers within an herbivore community have enamel $^{87}Sr/^{86}Sr$ ratios

characteristic of Area A but not of Area B, then we would deduce that the Area A had plentiful grass for the grazers to eat.

Three of the four major substrates in the southwestern South Africa have been approximately characterized in terms of their range in bioavailable $^{87}Sr/^{86}Sr$ ratios through the analysis of modern animal $^{87}Sr/^{86}Sr$ ratios (Sealy et al., 1991). Shales and sandstones (substrates that are older and generally occur further inland than marine-derived sands) have bioavailable $^{87}Sr/^{86}Sr$ ratios that have been reported to range from 0.71777 to 0.71794 (n = 2) and from 0.71543 to 0.71746 (n = 2), respectively. The Pleistocene marine-derived sands in the region have bioavailable $^{87}Sr/^{86}Sr$ ratios that range from 0.70938 to 0.71169 (n = 6) (Sealy et al., 1991; Fig. 3.1). The bioavailable $^{87}Sr/^{86}Sr$ ratios of shales and sandstones that make up this dataset cannot be distinguished with the Sealy et al. (1991) dataset, but they are distinct from those of the marine sand substrate. There are currently no published bioavailable $^{87}Sr/^{86}Sr$ ratios of granites and therefore it is unknown whether or not the bioavailable $^{87}Sr/^{86}Sr$ ratios of granites are distinct from the bioavailable $^{87}Sr/^{86}Sr$ ratio ranges of the other major substrates in this region or if specific granitic outcrops can be distinguished from one another. The new data presented in this paper will expand on the bioavailable $^{87}Sr/^{86}Sr$ ratios of the substrates in the region.

Previous studies show that it is possible to exploit the ranges in the bioavailable $^{87}Sr/^{86}Sr$ ratios from substrates to determine resource- and landscape-use among herbivores in the region (Besaan, 1972; Sealy et al., 1991; Radloff et al., 2010). This is the result of two interconnected aspects to the study region, 1) the bioavailable $^{87}Sr/^{86}Sr$ ratios of coastal marine sands are distinct from that of the shales and sandstones which

are found further inland along the coast and 2) the composition of vegetation in this region varies according to substrate (Rebelo et al., 2006; Cowling and Lombard, 2002).

3.2.2.2. Tooth enamel formation and the factors determining $^{87}Sr/^{86}Sr$ ratio of bioapatite

In determining the movement of an animal for food and in the application of these data to evaluate ecology, it is important to remember that in the case of large mammalian herbivores, the enamel of a single tooth can take > 8 months to fully mineralize (as reviewed in Kohn and Cerling, 2002). As a result, each sampled portion of enamel from a tooth represents a period of time as opposed to a split moment of time, such as a single meal or single day in the life of an animal. Tooth enamel is oldest at the crown and youngest at the cervix and enamel incorporates the $^{87}Sr/^{86}Sr$ ratios of the resources consumed over the period of time it took for the enamel to mineralize. Once formed, enamel is not remodeled or added to. By serial sampling along the tooth growth axis, it is possible to determine if and where animals traveled for food over time.

The primary $^{87}Sr/^{86}Sr$ ratio of a material can be altered after deposition via removal or addition of secondary, diagenetic strontium (e.g., Bentley, 2006). The presence of diagenetic strontium can mask the primary $^{87}Sr/^{86}Sr$ ratio and it is necessary to assess whether or not a material preserves its primary $^{87}Sr/^{86}Sr$ ratio (e.g., Sealy et al., 1991; Hoppe et al., 2003; Bentley, 2006). Secondary structural and nonstructural diagenetic strontium is more heavily substituted in bioapatite than primary, biogenic strontium, therefore diagenetic strontium in bioapatite tends to be more soluble (Sillen, 1986; Tuross et al., 1989). When bioapatite is bathed in a weak acid, the secondary

strontium will dissolve and become part of the supernatant more readily than will the primary, biogenic strontium over a series during rinses, which is called a solubility profile (e.g., Sealy et al., 1991). If the supernatant $^{87}Sr/^{86}Sr$ ratio changes in the course of the solubility profile, and/or is different from the cleaned enamel powder $^{87}Sr/^{86}Sr$ ratio, then the primary $^{87}Sr/^{86}Sr$ ratio of the enamel has been altered (Fig. 3.3.4A; Sealy et al., 1991). This assessment is particularly important when measuring the $^{87}Sr/^{86}Sr$ ratio of buried bone because it is porous and can accumulate material (Lee-Thorp, 2008). On the other hand, enamel is an example of a material that is more resistant to strontium isotope alteration because it is not as porous as bone. While it is important to determine the presence of secondary strontium, diagenetic strontium can often be removed from bioapatite by rinsing a powdered sample in a weak acid and then the rinsed bioapatite can be analyzed for the primary, biogenic $^{87}Sr/^{86}Sr$ ratio (e.g., Sealy et al., 1991). Each sample set, however, needs to be evaluated on an individual basis to determine the number of rinses needed (Sillen and LeGeros, 1982; Sealy et al., 1991). We report on such control studies for the fossil enamel samples studied herein.

3.3. Methods

3.3.1. Sample collection

We collected samples for three different purposes: refining the regional map of bioavailable $^{87}Sr/^{86}Sr$ ratios of the major substrates in southwestern South Africa, assessing diagenetic alteration in fossil enamel from Elandsfontein and evaluating

whether or not mid-Pleistocene herbivores had sufficient resources at Elandsfontein to survive or if they had to travel to other substrates in the region to find food.

We collected plant samples and the bones and teeth of contemporary small herbivores with small ranges (e.g., rodents and tortoises) from each major substrate in our study area. Herbivore tissues provide the best estimate of the bioavailable $^{87}Sr/^{86}Sr$ ratio of a substrate (Bentley, 2006). We avoided cultivated areas because the $^{87}Sr/^{86}Sr$ ratios of fertilizers can mask the primary bioavailable $^{87}Sr/^{86}Sr$ ratio of the substrate, plant, bone and teeth. The bioavailable $^{87}Sr/^{86}Sr$ ratios are shown (Table 3.1; Table S3.1). Granites that comprise the Cape Granite suite are different in age and mineralogical composition and may also differ in $^{87}Sr/^{86}Sr$ ratios (Rozendaal et al., 1999; Belcher and Kisters, 2003). We therefore collected samples from different granitic outcrops. New $^{87}Sr/^{86}Sr$ data from this study were then compiled with previously published data from Sealy et al. (1991) to determine if the major substrates in southwestern South Africa could be distinguished from one another using their bioavailable $^{87}Sr/^{86}Sr$ ratios.

The fossil teeth from Elandsfontein were collected as both surface and excavated finds by members of the West Coast Research Project between 2008 and 2014 (Braun et al., 2013), and are archived at The Archaeology Department, University of Cape Town. We sampled 25 teeth from the mammalian herbivore families Bovidae (n = 18), Equidae (n = 1) and Elephantidae (n = 2), rodent families Bathyergidae (n = 1) and Hystricidae (n = 1), and the carnivore family Hyaenidae (n = 2) (Table 3.2; Table S3.2). We preferred to sample the third molars of browsing and grazing herbivore taxa that were potentially migratory and may have traveled for food (Stynder, 2009; Copeland et al., 2016). We selected teeth that were unworn or lightly worn because they preserve more of the tooth

enamel growth than a worn tooth and are more likely to capture variations in $^{87}Sr/^{86}Sr$ ratios along the length of the tooth growth axis. In addition, we sampled teeth of mid-Pleistocene animals that were likely local to Elandsfontein, such as rodents. These would not have strayed from the Elandsfontein area. Two carnivores, both the brown hyena, could have traveled long distances in search for food (Klein et al., 2007). We also targeted a subset of modern tooth enamel (n = 2) and fossil tooth enamel fragments (n = 8) with a range of preservation states to assess the degree of alteration of the primary $^{87}Sr/^{86}Sr$ ratio of fossil teeth at Elandsfontein.

Table 3.2: Diet and migratory behavior of the mid-Pleistocene mammalian herbivores and carnivores from Elandsfontein analyzed for enamel $^{87}Sr/^{86}Sr$ ratios.

Mammalian family	Taxon	Common name	Dietary behavior	Inclination to migrate
Bovidae	*Tragelaphus strepsiceros*	Greater kudu	Browser	Potentially migratory
Bovidae	Alcelaphini sp. indet.	-	Grazer	Potentially migratory
Bovidae	*Syncerus antiquus*	Giant buffalo	Grazer	Potentially migratory
Bovidae	Bovid indent.	-	-	-
Equidae	*Equus capensis*	Cape zebra	Grazer	Potentially migratory
Elephantidae	*Loxodonta africana*	African elephant	Grazer	Potentially migratory
Bathyergidae	*Bathyergus suillus*	Dune mole rat	Mixed	Not migratory
Hystricidae	*Hystrix africaeaustralis*	Porcupine	Mixed	Not migratory
Hyaenidae	*Hyaena brunnea*	Brown hyena	Carnivore	Can travel long distances

3.3.2. Sample preparation and analysis

3.3.2.1. Sample preparation

Modern enamel, bone and plants used to determine bioavailable $^{87}Sr/^{86}Sr$ were placed in porcelain crucibles with lid and then organic materials were removed by ashing the samples in a muffle furnace (500ºC, overnight) at the Department of Archaeology,

University of Cape Town. Each fossil tooth was cleaned of the outermost, exposed enamel and then serially sampled with a diamond-tip drill bit by taking samples of enamel (~ 10 mg) in a series of approximately horizontal lines from the base of the tooth to the occlusal surface. Care was taken to sample as closely as possible without overlap. We sampled between 40 and 50 mg of each tooth fragment used to determine diagenesis of the primary $^{87}Sr/^{86}Sr$ ratios of fossil teeth.

Enamel samples were either prepared for solution analysis by powdering the enamel or for in situ analysis by clearing the enamel surface. The enamel powder (< 10 mg; both modern and fossil enamel) were prepared and analyzed in the Department of Geological Sciences at the University of Cape Town. Enamel samples were rinsed five times in 1 ml of buffered nitric acid (100 mM, pH 4.5) to remove strontium from the surrounding environment from enamel powder and then dried. Powder was then digested in 2 ml of 2.0 M HNO_3 in a closed Teflon beaker, heated at 140ºC for one hour and dried. The remaining material was then dissolved in 1.5 ml 2.0 M HNO_3 for strontium separation chemistry. Between 25 and 50 mg of plants and soils were digested to make a solution for strontium separation chemistry using the method outlined in Copeland et al. (2016). The strontium separation chemistry for every sample was done following the method of Pin et al. (1994). The strontium fraction of each sample was then dried, dissolved in 2 ml 0.2% HNO_3 and then diluted to a concentration of 200 ppb Sr.

3.3.2.2. Sample analysis

The $^{87}Sr/^{86}Sr$ ratios of modern and fossil samples were analyzed using either laser ablation inductively-coupled plasma mass spectroscopy (LA-ICP-MS) or solution

ICP-MS. There are strengths and limitations to each of these techniques. Briefly, measuring $^{87}Sr/^{86}Sr$ ratios using solution ICP-MS requires that the sample is dissolved and concentrated before analysis. This method is time consuming and is destructive which can be problematic, especially when there are multiple samples needed (e.g., serial sampling a tooth), however it produces data that is ten times more precise than analysis via LA-ICP-MS, 0.000001 and 0.00001, respectively (Copeland et al., 2010). Analysis using LA-ICP-MS is much faster than solution ICP-MS as teeth or enamel fragments are merely abraded at the surface to remove dirt and secondary strontium. LA-ICP-MS allows for in situ analysis of $^{87}Sr/^{86}Sr$ ratios of a material. Materials can be serial sampled using laser ablation, which is particularly useful when determining intra-tooth $^{87}Sr/^{86}Sr$ ratio variation.

The majority of samples were analyzed for their $^{87}Sr/^{86}Sr$ ratio in solution using high-resolution multicollector inductively-coupled plasma mass spectroscopy (HR-MC-ICP-MS) using a Nu Instruments NuPlasma instrument (University of Cape Town). Almost every fossil and modern tooth and tooth fragment was too large to fit into the standard 2.5-cm x 2.5-cm cylinder chamber currently available at the University of Cape Town for LA-ICP-MS. Fossil teeth from Elandsfontein do not all have pristine enamel and some have even been subjected to carbonate leaching. Therefore, even if the fossil teeth did fit within the chamber used for LA-ICP-MS analysis, each fossil sample needed to be pretreated to remove diagenetic material and we were concerned that light abrasion of the tooth surface would not have been sufficient to remove secondary strontium. We considered solution ICP-MS to be the most reliable method for producing $^{87}Sr/^{86}Sr$ data that reflected the primary $^{87}Sr/^{86}Sr$ ratios of the fossil enamel.

The international standard, NIST SRM987 ($^{87}Sr/^{86}Sr$ ratio = 0.710255), was analyzed intermittently between unknown samples. The in-house carbonate standard, NM95, was measured during each run of unknowns and agreed with the long-term average obtained in this laboratory of 0.708907 with two standard deviation (i.e., 2σ) of 0.000031 (n = 24). Unknown samples were analyzed once to determine $^{87}Sr/^{86}Sr$ ratio of a solution and the error is reported as 2σ internal error.

3.3.3. Determining the presence of diagenetic strontium

To determine if the $^{87}Sr/^{86}Sr$ ratio of fossil teeth had been significantly changed by environmental strontium after deposition, we analyzed the $^{87}Sr/^{86}Sr$ ratio of modern enamel and fossil tooth fragments that ranged in quality of preservation (i.e., from well-preserved enamel to enamel that had likely experienced carbonate leaching and alteration of the primary $^{87}Sr/^{86}Sr$ ratio). Enamel samples were ground into a powder using a mortar and pestle. Our method for evaluating the presence of diagenetic strontium in an enamel sample (i.e., $^{87}Sr/^{86}Sr$ ratios that are different from the primary value) and removal of the secondary strontium was based on the evaluation of diagenetic strontium in Sealy et al. (1991), in which solubility profiles, or the $^{87}Sr/^{86}Sr$ ratios from a series of weak acid baths and the remaining, cleaned bone powder were analyzed, to determine the presence and subsequent removal of diagenetic strontium in samples from a specific site. Powdered enamel samples were then rinsed 24 to 26 times in the buffered nitric acid solution (100 mM, pH 4.5) as described in the above in Section 3.3.2.1. Supernatants from every fourth or fifth rinse and the remaining powdered enamel were prepared for solution analysis of $^{87}Sr/^{86}Sr$ ratios using HR-MC-ICP-MS.

3.3.4. Statistical comparison of $^{87}Sr/^{86}Sr$ ratio values

Comparisons of the $^{87}Sr/^{86}Sr$ ratios of materials were performed using JMP 11 software, a statistical analytical program developed by the SAS Institute. We used the Tukey-Kramer HSD test for these comparisons and we use the ± symbol throughout the paper to represent one standard deviation from the mean, unless otherwise noted.

3.4. Results

3.4.1. Mapping of bioavailable $^{87}Sr/^{86}Sr$ ratios

Modern bones (n = 15) and teeth (n = 3) from individual animals and nine plant samples were collected from the dominant substrates in the region. Their $^{87}Sr/^{86}Sr$ ratios were compiled with those of modern bone samples (n = 10) reported in Sealy et al. (1991) (data compiled in Table S3.1 and summarized in Table 3.1). We have included solution and laser ablation-based data; the difference between the $^{87}Sr/^{86}Sr$ ratios of the sample modern enamel samples determined using these two methods is $< \pm 0.000150$ (n = 3).

The bioavailable $^{87}Sr/^{86}Sr$ ratios of Pleistocene marine sands range from 0.709388 to 0.711690 (Fig. 3.2; Table S3.1). The bioavailable $^{87}Sr/^{86}Sr$ ratios of the Table Mountain sandstone complex and the Malmesbury Shale have values that overlap and together these samples range from 0.714092 to 0.720390 (Fig. 3.2; Table 3.1; Table S3.1). The new $^{87}Sr/^{86}Sr$ data presented here have expanded upon the range of $^{87}Sr/^{86}Sr$ ratios for shale and sandstone complexes presented in Sealy et al. (1991) and these data confirm that the two substrates are not distinct in terms of strontium isotope composition.

We have added $^{87}Sr/^{86}Sr$ ratio data for Cape Granites to the map of bioavailable $^{87}Sr/^{86}Sr$ ratios of the major substrates in the region and find that the Cape Granite $^{87}Sr/^{86}Sr$ ratios have a wide spread, ranging from 0.711421 to 0.723563 (Table 3.1; Table S3.1; Fig. 3.1; Fig. 3.2).

3.4.2. Assessment of diagenesis in fossil teeth

We measured the $^{87}Sr/^{86}Sr$ ratios of modern (n = 2) and fossil (n = 8) enamel fragments and that of the weak nitric acid supernatant from a series of enamel rinses to evaluate possible diagenesis of the primary isotopic composition of elemental strontium. Fossil fragments are from Bovidae and Equidae families and also from unidentified large mammalian herbivores. We did not observe differences > 0.0006 in $^{87}Sr/^{86}Sr$ ratios over the series of rinses for any of the sample solubility profiles (Fig. 3.3; Table S3.3). The enamel $^{87}Sr/^{86}Sr$ ratios from the fossil teeth at Elandsfontein (all rinses and the enamel powder remaining at the end of the process) ranged from 0.709366 to 0.710679: these values are within the range of marine-derived sand $^{87}Sr/^{86}Sr$ ratios (Fig. 3.3). The two modern enamel samples have a span of $^{87}Sr/^{86}Sr$ ratios of 0.0004 and 0.0006 (for all rinses and the enamel powder remaining at the end of the process), which overlaps with the span of $^{87}Sr/^{86}Sr$ ratios of fossil enamel and their supernatants over a series of ~ 25 rinses (0.00008 to 0.00050). For both of the modern samples, Rinse 1 had noticeably lower $^{87}Sr/^{86}Sr$ ratios than the rest of the rinses and the residue enamel powder; the fossil samples do not show this pattern. It is possible that there is some labile strontium component that the modern samples are picking up soon after deposition where as fossilized enamel samples are in some way stabilized. Modern samples are collected from

the surface and are from animals that have died and sat out on the surface long enough to be completely cleared of soft tissue and hair.

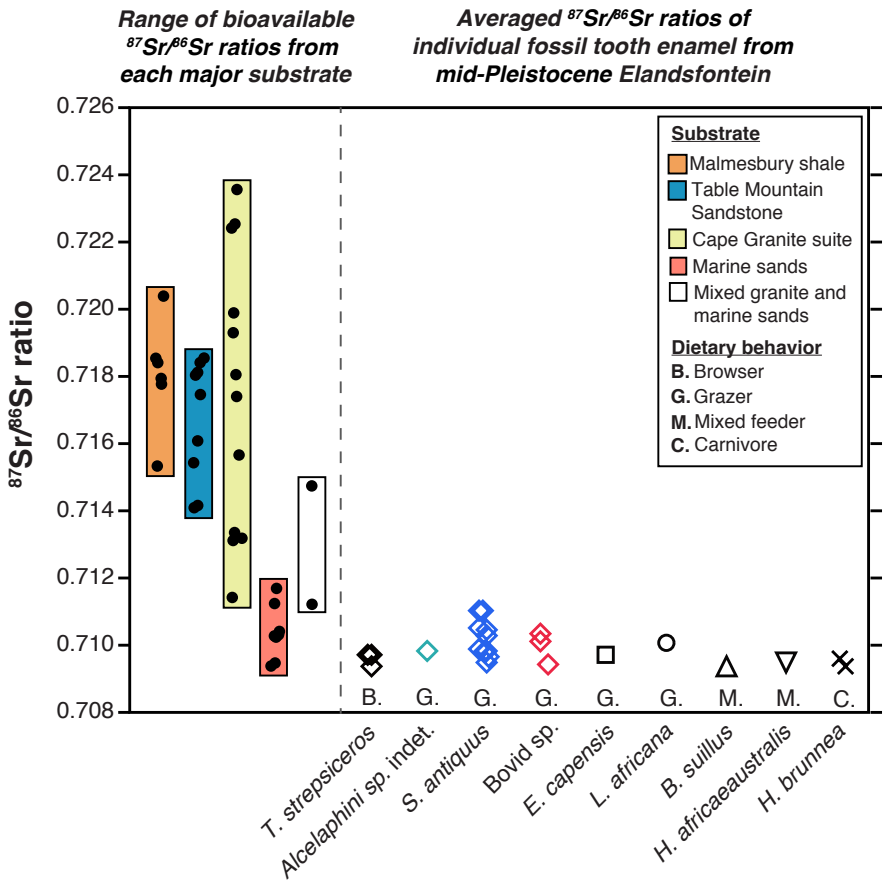

Figure 3.2: Ranges of bioavailable $^{87}Sr/^{86}Sr$ ratios for the major substrates (and mixed marine sands and granite) in southwestern South Africa compared with the average $^{87}Sr/^{86}Sr$ ratio for each mid-Pleistocene mammalian tooth from Elandsfontein. The black dots represent both the new and previously published bioavailable $^{87}Sr/^{86}Sr$ ratios from each major substrate (Sealy et al., 1991; this study). Materials analyzed are bone, enamel and plants (Table S3.1). The range of substrate bioavailable $^{87}Sr/^{86}Sr$ ratios is encompassed within a vertical rectangle. The $^{87}Sr/^{86}Sr$ ratio for each sample used to determine the range of bioavailable $^{87}Sr/^{86}Sr$ ratios of substrates can be found in Table S3.1 and the ranges of these data are presented in Table 3.1. The average $^{87}Sr/^{86}Sr$ ratios of individual fossil teeth are presented by taxon. Fossil enamel samples are from the following mammalian families and represent a single tooth: Bovidae (◇), Equidae (□), Elephantidae (o), the rodent families Bathyergidae (△) and Hystricidae (▽) and feliform family Hyaenidae (×). Probable dietary behavior of animals are indicated by letters and are based on the findings of Stynder (2009) and Klein et al. (2007). Symbols are defined in the legend.

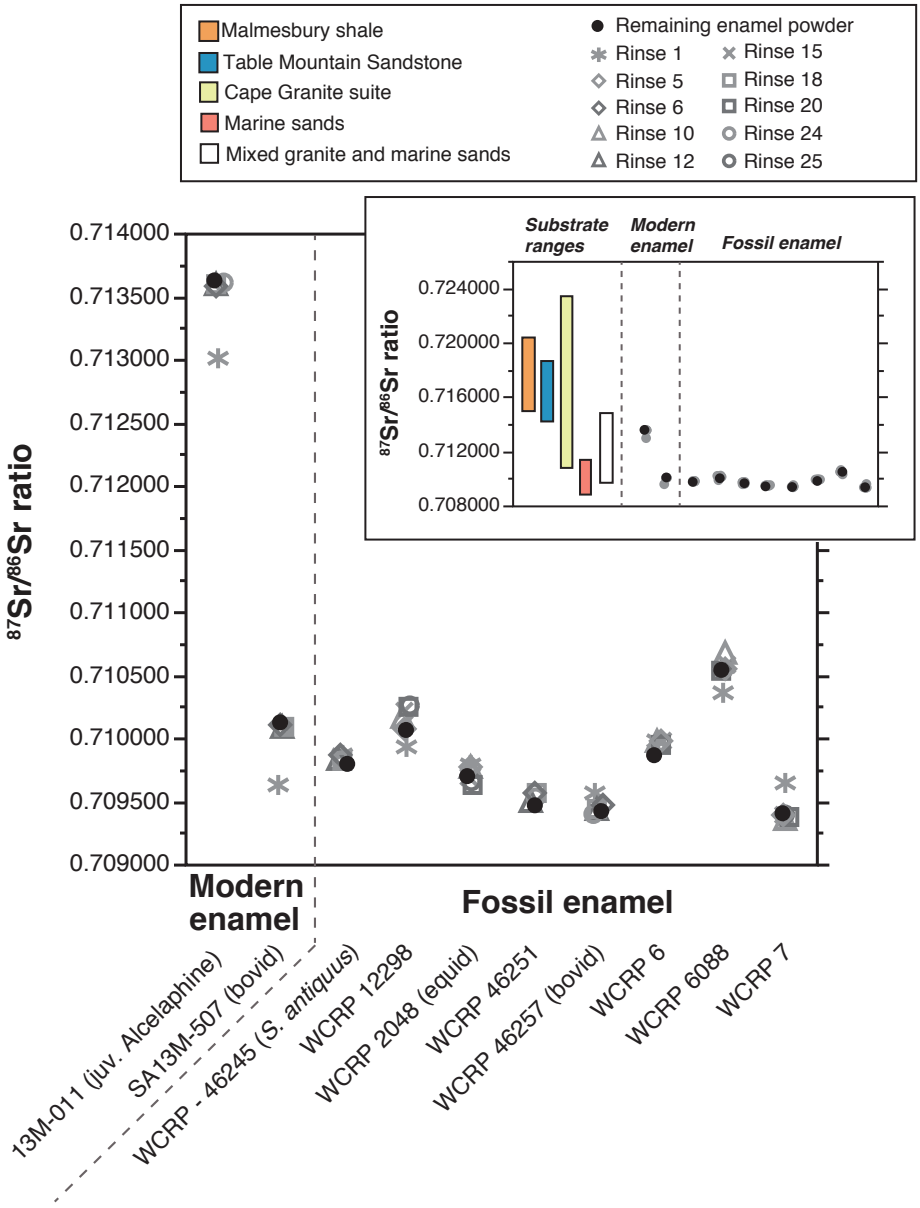

Figure 3.3: $^{87}Sr/^{86}Sr$ ratios of the supernatants from a series of rinses of modern and fossil tooth enamel powder bathed in in weak nitric acid (gray symbols) and the remaining enamel powder (black circle). When taxon is not indicated after the sample ID, it is because the herbivore taxon is unknown. The $^{87}Sr/^{86}Sr$ ratios from modern enamel and the supernatants from their acid baths were analyzed so that any trends in the supernatant $^{87}Sr/^{86}Sr$ ratios of fossil enamel could be compared with that of modern, pristine enamel. The smaller plot in the upper right hand corner of the figure outlines the range of bioavailable strontium $^{87}Sr/^{86}Sr$ ratios of the major substrates in southwestern South Africa in comparison with the range of $^{87}Sr/^{86}Sr$ ratios for the series of supernatants and the remaining powder of enamel samples.

We assessed the presence of diagenetic strontium in fossil samples by comparing the $^{87}Sr/^{86}Sr$ ratios of a powdered enamel sample after pretreating samples and also the supernatant from each rinse in weak nitric acid. We compared the $^{87}Sr/^{86}Sr$ ratios of both modern and fossil enamel with that of the supernatants after powdered enamel samples were bathed in weak acid to see if there were substantial differences between the enamel $^{87}Sr/^{86}Sr$ ratios of pristine, modern enamel and the buried fossil enamel from Elandsfontein (Fig. 3.3). The change in $^{87}Sr/^{86}Sr$ ratios of supernatants over a series of ~ 25 rinses was small (~ 0.0004) relative to the range of $^{87}Sr/^{86}Sr$ ratios for each substrate (> 0.002). The majority of change in supernatant $^{87}Sr/^{86}Sr$ ratio for each enamel fragment occurred within the first five rinses (Fig. 3.3; Table S3.3). Figure 3.4A shows possible scenarios for how the $^{87}Sr/^{86}Sr$ ratio of supernatant of powdered enamel bathed in weak acid could change with successive rinses for the fossil samples at Elandsfontein.

We rinsed each sample of fossil enamel powder five times before analyzing the $^{87}Sr/^{86}Sr$ ratio of the enamel powder because, although the total change was small (< 0.0006), the majority of change in the solubility profile occurred within the first rinse. Regardless of fossil enamel condition, the $^{87}Sr/^{86}Sr$ ratios of the fossil enamel samples and all of the supernatants analyzed to determine strontium diagenesis remained within the range of bioavailable $^{87}Sr/^{86}Sr$ ratios from marine sands, which is the geologic substrate at Elandsfontein.

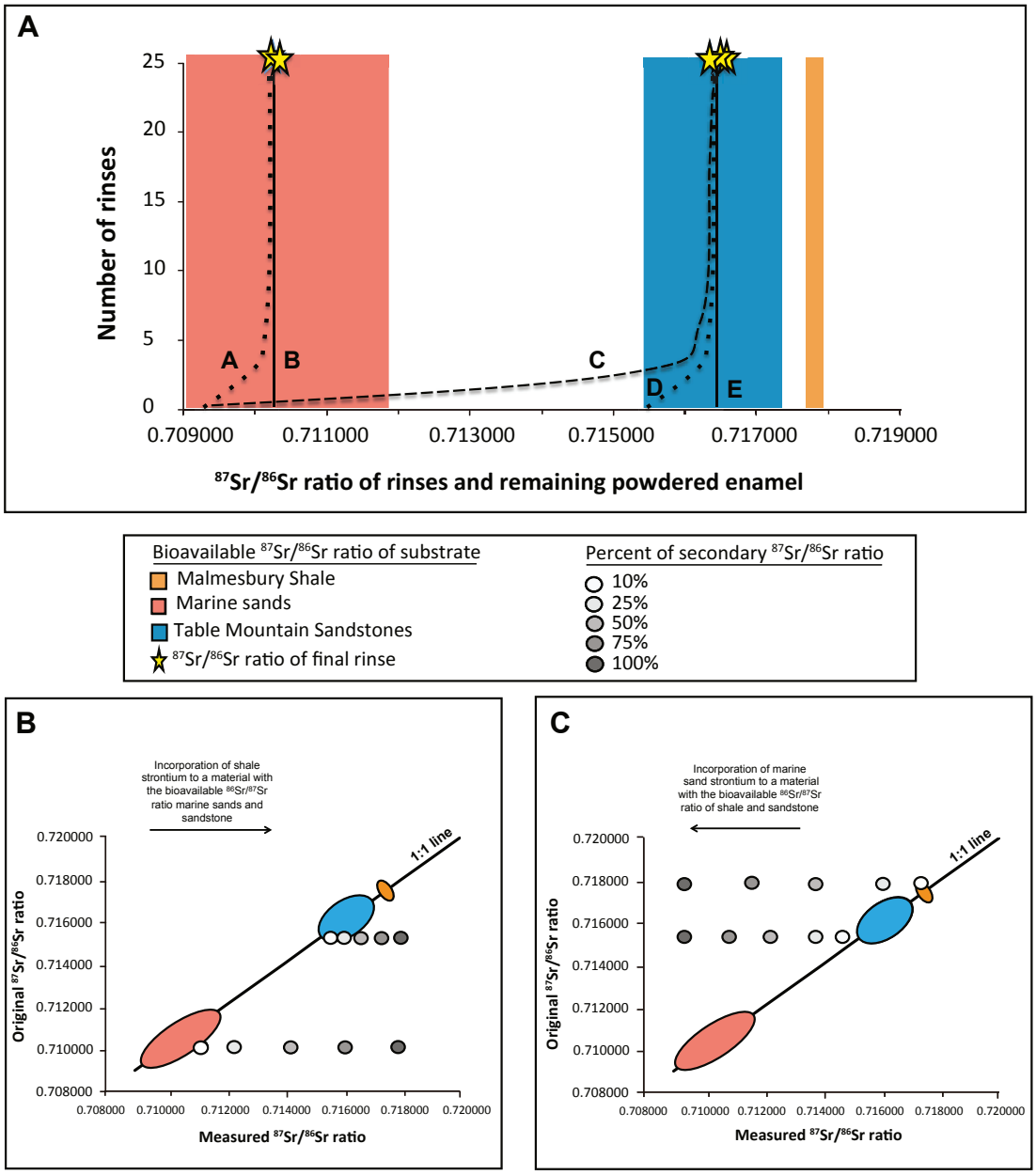

Figure 3.4: Scenarios outlining the expected trends of $^{87}Sr/^{86}Sr$ ratios over a series of supernatants remaining after enamel powder is bathed in weak nitric acid to remove secondary strontium and that of the cleaned enamel (A). Scenarios A and D are the expected trends in $^{87}Sr/^{86}Sr$ ratios over a series of rinses when there has only been minor alteration of the primary $^{87}Sr/^{86}Sr$ ratio of a sample. Scenarios B and E indicate the expected trend in the $^{87}Sr/^{86}Sr$ ratio of supernatants and the remaining enamel when the enamel has not experienced measurable alteration of the primary $^{87}Sr/^{86}Sr$ ratio. Scenario C indicates significant alteration of a primary enamel $^{87}Sr/^{86}Sr$ ratio, by which the primary $^{87}Sr/^{86}Sr$ ratio (which reflects Table Mountain Sandstone) is completely masked by the $^{87}Sr/^{86}Sr$ ratio of the secondary strontium ($^{87}Sr/^{86}Sr$ ratio reflecting marine sands).

We used the linear mixing model described in Copeland et al. (2010) to evaluate how the primary $^{87}Sr/^{86}Sr$ ratio of an enamel sample would change with the addition of secondary strontium, when secondary strontium composed 10%, 25%, 50%, 75% and 100% of the total strontium in a sample (Fig. 3.4B and 4C). Mean values for the bioavailable $^{87}Sr/^{86}Sr$ ratios of the marine sands, shales and sandstones in southwestern South Africa were used in our calculations, as these are three of the four main substrates in the region. We did not include granites in this study since the bioavailable $^{87}Sr/^{86}Sr$ ratios in the suite of Cape Granites must be better defined before the Copeland et al. (2010) model can be applied to them. As expected, when secondary strontium from a substrate that is not the same in $^{87}Sr/^{86}Sr$ ratio as the primary substrate replaces the primary strontium, then the enamel $^{87}Sr/^{86}Sr$ ratio moves further from the primary enamel $^{87}Sr/^{86}Sr$ ratio and closer to that of the secondary strontium (Fig. 3.4B and 4C).

3.4.3. $^{87}Sr/^{86}Sr$ ratios of fossil mammalian teeth from Elandsfontein

Fossil mammalian tooth enamel from mid-Pleistocene Elandsfontein have been serially-sampled along the tooth growth axis whenever possible. The averaged $^{87}Sr/^{86}Sr$ ratio from the serial samples (n = 156) of 22 individual teeth is 0.710013 ± 0.000470 and ranges from 0.709255 to 0.711171. We did not observe any significant differences in the $^{87}Sr/^{86}Sr$ ratios for different herbivore taxa. Carnivores (n = 2) were not distinct from other taxa and were within the range of the bioavailable $^{87}Sr/^{86}Sr$ of marine-derived sands (0.709507 ± 0.000160; Fig. 3.2). All data points from the Elandsfontein fossil teeth have $^{87}Sr/^{86}Sr$ ratios equivalent to bioavailable $^{87}Sr/^{86}Sr$ ratios of marine-derived sands and were not within the ratio range of any other substrate. We found that there were slight

differences in $^{87}Sr/^{86}Sr$ ratios for each serial sample within an individually sampled tooth, where intra-tooth ratios have differences between 0.000049 and 0.001249 (Table S3.2). In addition we observed no behavioral difference between the $^{87}Sr/^{86}Sr$ ratios of enamel along the tooth growth axis of fossil teeth, regardless of the animal species.

3.5. Discussion

3.5.1. Distribution of the $^{87}Sr/^{86}Sr$ ratios of regional substrates and determining herbivore migration for food

Determining the distribution of bioavailable $^{87}Sr/^{86}Sr$ ratios for substrates in southwestern South Africa provided the foundation for understanding how animals utilized their landscape in the mid-Pleistocene. In addition, this has also provided the foundation for future studies of animal and human mobility in this region since deposition of marine sands (i.e., since the Pliocene) in the area.

Values for bioavailable $^{87}Sr/^{86}Sr$ measured in bone and tooth enamel in this study are consistent with those of Sealy et al. (1991), but extend that work substantially by adding data to each of the major substrates (i.e., shale, sandstone and marine sand) (Table S3.1). The sandstone and shale bioavailable $^{87}Sr/^{86}Sr$ ratio ranges are similar to one another but they are distinct from, and are more positive than those of marine sands (Table 3.1; Fig. 3.2). The range of bioavailable $^{87}Sr/^{86}Sr$ ratios of Cape Granites in southwestern South Africa is based on modern animal bones that lived on different Cape Granite outcrops and plants that grew on these granites (Table 1; Table S1). The range in bioavailable $^{87}Sr/^{86}Sr$ ratios from the granites encompasses the $^{87}Sr/^{86}Sr$ ratio range of

sandstone and shale, substrates that are more positive than that of marine sands. This is in agreement with Sealy et al. (1991). The range of bioavailable $^{87}Sr/^{86}Sr$ ratios from marine sands are mostly distinct from that of granites, but the lowermost granite $^{87}Sr/^{86}Sr$ ratio overlaps with the two most positive $^{87}Sr/^{86}Sr$ ratios of marine sands, though this should be studied in more detail (Table 3.1; Fig. 3.2).

The bioavailable $^{87}Sr/^{86}Sr$ ratios from the Cape Granites in southwestern South Africa currently have a wide span and this range overlaps with the other substrate bioavailable $^{87}Sr/^{86}Sr$ ratios. Age and mineralogy are the two primary factors that directly influence the $^{87}Sr/^{86}Sr$ ratio of a rock (e.g., Bentley, 1996). It is possible that these different granitic bodies that are part of the suite of Cape Granites can be distinguished from one another using $^{87}Sr/^{86}Sr$ ratios because, 1) granites within the suite vary in age (within the Precambrian) and 2) they have unique mineralogical compositions (Sheepers, 1995; Rozendaal et al., 1999; Belcher and Kisters, 2003). To better determine if there are differences between the bioavailable $^{87}Sr/^{86}Sr$ ratios of the granitic intrusions that belong to the Cape Granite suite and in turn if animals traveled to specific granitic outcrops for food, multiple plants and or bones and teeth from the distinct granitic bodies would need to be collected and analyzed. In particular, the granites in the area surrounding Elandsfontein should be targeted because these are the most likely (i.e., most convenient) granitic outcrops that herbivores could have traveled to for food.

Given that the bioavailable $^{87}Sr/^{86}Sr$ ratios of the marine sands are distinct from that of sands and shales, we propose the following framework for using $^{87}Sr/^{86}Sr$ ratios of teeth to study resource use by animals that lived in areas within the region (such as animals from Elandsfontein) where marine sands are the main substrate. There are two

basic scenarios for how the $^{87}Sr/^{86}Sr$ data for fossil teeth from Elandsfontein can be interpreted: 1) the animals from Elandsfontein with tooth $^{87}Sr/^{86}Sr$ ratios similar to the bioavailable $^{87}Sr/^{86}Sr$ ratios for marine sands were able to subsist on food found at Elandsfontein and in the surrounding, coastal location, and 2) the animals with tooth $^{87}Sr/^{86}Sr$ ratios similar to the bioavailable $^{87}Sr/^{86}Sr$ ratios of shales and sandstones would have needed to travel inland for food.

3.5.2. Diagenesis of primary $^{87}Sr/^{86}Sr$ ratios and pretreatment procedure

Possible diagenesis of the strontium of fossil tooth enamel was tested by analyzing $^{87}Sr/^{86}Sr$ ratios in solubility profiles (i.e., the supernatants of enamel bathed in weak acid and the enamel after a series of ~25 baths) from several tooth enamel fragments spanning a range of preservations. The $^{87}Sr/^{86}Sr$ ratios along the solubility profile remain within the range of bioavailable $^{87}Sr/^{86}Sr$ ratios of marine sands in the region (See Fig. 3.3 and Fig. 3.4). Based on the consistency of $^{87}Sr/^{86}Sr$ ratios along the solubility profile, there was no significant diagenesis of the enamel in any of the specimens studied.

The finding that the primary $^{87}Sr/^{86}Sr$ ratios of the fossil teeth have been preserved is consistent with a previous study that showed that the oxygen isotopic composition (i.e., $\delta^{18}O$ value) of fossil tooth enamel from Elandsfontein were unaltered. This assessment was based on the fact that, first, the relative oxygen isotopic compositions of different taxa from Elandsfontein are preserved, for example hippopotamids are more negative in their oxygen isotopic composition than are the other

taxa. Second, the offset between the $\delta^{18}O$ value of enamel carbonate and that of enamel phosphate for each sample is as expected from pristine enamel (see Chapter 2).

Based on these results we consider the $^{87}Sr/^{86}Sr$ ratios of fossil teeth at Elandsfontein to be unaltered and representative of the substrate on which the animal ate. Therefore, each enamel sample used to analyze diet and vegetation at Elandsfontein was pretreated in a standard manner (i.e., rinsed five times in weak nitric acid).

3.5.3. Herbivore migration and environment at Elandsfontein during mid-Pleistocene

The $^{87}Sr/^{86}Sr$ ratios of fossil teeth from Elandsfontein lie within the range of $^{87}Sr/^{86}Sr$ ratios expected for animals that obtain their food from the marine sand substrates that are local to Elandsfontein. These data indicate that the browsing and grazing herbivores, rodents and carnivores at Elandsfontein consistently consumed resources on the marine-derived sand substrate (Fig. 3.2; Table 3.3; Table S3.2). We did not observe any patterns in the $^{87}Sr/^{86}Sr$ ratios of the fossil teeth that we sampled serially along the tooth growth axis (Table S3.2).

Table 3.3: Average $^{87}Sr/^{86}Sr$ ratios of fossil mammals from mid-Pleistocene Elandsfontein.

Sample ID	Taxon	Inclination to migrate[a]	Dietary behavior[a]	$^{87}Sr/^{86}Sr$ ratio		$^{87}Sr/^{86}Sr$ ratio		
				Average	Stdev[b]	Min	Max	*n*[c]
Bovidae								
WCRP 20443	*Tragelaphus strepsiceros*	Potentially migratory	Browser	0.709384	0.000031	0.709330	0.709428	9
WCRP 36612	*Tragelaphus strepsiceros*	Potentially migratory	Browser	0.709721	0.000046	0.709671	0.709780	7
WCRP 9386	*Tragelaphus strepsiceros (?)*	Potentially migratory	Browser	0.709689	0.000071	0.709546	0.709754	10
WCRP 1358	Alcelaphini sp. indet.	Potentially migratory	Grazer	0.709843	0.000058	0.709770	0.709980	12
WCRP 36309	*Syncerus*	Potentially	Grazer	0.711010	0.000154	0.710710	0.711120	6

	antiquus	migratory						
WCRP 9043	*Syncerus antiquus*	Potentially migratory	Grazer	0.710293	0.000058	0.710130	0.710570	12
WCRP 1666	*Syncerus antiquus*	Potentially migratory	Grazer	0.709641	0.000241	0.709255	0.710078	9
WCRP 36309	*Syncerus antiquus*	Potentially migratory	Grazer	0.710431	0.000053	0.710351	0.710488	5
WCRP 8787	*Syncerus antiquus*	Potentially migratory	Grazer	0.711047	0.000144	0.710889	0.711171	3
WCRP 9046	*Syncerus antiquus*	Potentially migratory	Grazer	0.710496	0.000142	0.710327	0.710835	21
WCRP 9944	*Syncerus antiquus*	Potentially migratory	Grazer	0.709855	0.000056	0.709771	0.709888	4
WCRP 46245	*Syncerus antiquus*	Potentially migratory	Grazer	0.709876	0.000194	0.709324	0.710141	12
WCRP 46251	*Syncerus antiquus*	Potentially migratory	Grazer	0.709474	-	-	-	1
WCRP 46245	*Syncerus antiquus*	Potentially migratory	Grazer	0.709802	-	-	-	1
WCRP 46225	*Syncerus antiquus*	Potentially migratory	Grazer	0.709640	0.000022	0.709609	0.709658	6
WCRP 32386	Bovid	-	Grazer	0.710320	0.000433	0.709856	0.711105	12
WCRP 46257	Bovid	-	? Grazer	0.709428	-	-	-	1
WCRP 1468	Bovid indent.	-	? Grazer	0.710090	0.000080	0.709976	0.710181	10
Equidea								
WCRP 2048	*Equus capensis*	Potentially migratory	Grazer	0.709705	-	-	-	1
Elephantidae								
WCRP 12298	*Loxodonta africana*	Potentially migratory	Grazer	0.710071	-	-	-	1
WCRP 6088	*Loxodonta africana*	Potentially migratory	Grazer	0.710547	-	-	-	1
Bathyergidae								
WCRP 32007	*Bathyergus suillus*	Not migratory	Mixed feeder	0.709392	0.000083	0.709275	0.709489	6
Hystricidae								
WCRP 32012	*Hystrix africaeaustralis*	Not migratory	Mixed feeder	0.709476	0.000066	0.709423	0.709587	7
Hyaenidae								
WCRP 32121	*Hyaena brunnea*	Potentially migratory	Carnivore	0.709393	-	-	-	1
WCRP 32442	*Hyaena brunnea*	Potentially migratory	Carnivore	0.709620	-	-	-	1

[a] migratory inclination and dietary behavior information from Copeland et al. (2016) and coauthor Deano Stynder in 2014 to 2016

[b] standard deviation is ± 1σ from the average

[c] number of individual serial samples from an individual tooth that have been averaged

Herbivores ate vegetation growing on marine sands. We used the linear mixing model that was used to evaluate mixing of primary and secondary strontium as an approach for determining the percentage of total food an animal could have consumed from shale in the region and still have retained a $^{87}Sr/^{86}Sr$ ratio within the range of bioavailable $^{87}Sr/^{86}Sr$ ratios for marine sands (Fig. 3.4). We find that vegetation growing on shale could have contributed ~10% of the total food consumed by an animal living mainly on the marine sands (Fig. 3.4) without registering a significant change in the enamel $^{87}Sr/^{86}Sr$ ratio (i.e., the $^{87}Sr/^{86}Sr$ ratio remains within the range of bioavailable $^{87}Sr/^{86}Sr$ ratios for the marine sands). Animals would need to eat ~ 25% of their total food from the vegetation growing on shale before their enamel $^{87}Sr/^{86}Sr$ ratios would necessarily become more positive than the range of bioavailable $^{87}Sr/^{86}Sr$ ratios for marine sands. However, there are no fossil enamel $^{87}Sr/^{86}Sr$ ratios that are more positive than the bioavailable $^{87}Sr/^{86}Sr$ ratios for marine sands (Fig. 3.2).

We also produced carbon isotope datasets for serial samples of teeth (one tooth from each taxon) from three large grazing mammals (*Equus capensis*, *Connochaetes gnou* and *Syncerus antiquus*) at Elandsfontein that might have migrated for food (Thesis Chapter 2). Each of these fossil teeth (n = 3) had intra-tooth variation of ≤ 1 ‰ in $\delta^{13}C$. Mean $\delta^{13}C$ values were -9.9 ± 0.6‰ (13 serial samples averaged), -9.4 ± 0.5‰ (12 serial samples averaged) and -9.7 ± 1.0‰ (8 serial samples averaged) for *Equus capensis*, *Connochaetes gnou* and *Syncerus antiquus*, respectively. These data indicate that these grazers consumed diets that consisted overwhelmingly of C_3 grasses characteristic of the winter rainfall zone, and the isotopic composition of their diets did not vary in the early years of their lifetimes when their teeth mineralized. The sum of these data are published

in Lehmann et al. (2016), indicate that the mid Pleistocene environment at Elandsfontein supported large grazing mammals who were able to subsist wholly on the grasses that grew in the coastal regions of the winter rainfall zone where there must have been a year-round supply of grass.

3.5.4. Environments at Elandsfontein and southwestern South Africa during mid-Pleistocene

The $^{87}Sr/^{86}Sr$ ratios of fossil teeth from Elandsfontein suggest that mid-Pleistocene mammals did not need to travel from the coast to find food. Mesowear and microwear records from mid-Pleistocene Bovidae teeth indicate that these animals had access to both browse and graze at Elandsfontein and in the surrounding area and that the presence of grassland in this area would have provided food resources for grazing herbivores during the mid-Pleistocene (Stynder, 2009). Fossil enamel from herbivores at Elandsfontein have carbon isotopic compositions indicating that grazers ate grass adapted to a winter rainfall zone. Southwestern South Africa was within a winter rainfall zone during the mid-Pleistocene, as it is today (Luyt et al., 2000; Hare and Sealy, 2013; Lehmann et al., 2016).

During the mid-Pleistocene herbivores did not spend a significant time outside of the winter rainfall zone nor did they spend a significant amount of time eating on the major regional substrates other than marine-derived sands on the coast of southwestern South Africa. Elandsfontein appears to have provided both palatable browse and graze vegetation during the mid-Pleistocene. Together these data suggest that the fossil herbivores that have been found at Elandsfontein could access enough food and water in

the area around Elandsfontein and also could have acquired their food resources along the coast; suggesting an environment and ecological setting that is nothing like those seen today.

This suggestion of a mid-Pleistocene environment with grasses and adequate vegetation to feed both browsers and grazers has also been suggested by Luyt et al. (2000) and Stynder (2009). Spring sediments preserved at Elandsfontein suggest the presence of surface water during the mid-Pleistocene (e.g., Braun et al., 2013). Standing water could have provided enough water to support the growth of grass year round as well as other vegetation like trees, shrubs and sedges, all within a winter rainfall zone. Overall it would be quite unrecognizable in the current landscape, environment and ecology. At some point between the mid-Pleistocene and today, southwestern South Africa changed from a lush environment with a diverse animal community to an environment that is hot, dry and hostile to the communities that existed during the mid-Pleistocene.

3.6. Conclusion

1) Enamel $^{87}Sr/^{86}Sr$ ratios indicate that herbivores did not migrate from coastal region suggesting that there was enough nutritious vegetation to feed both browsers and grazers on the coast of southwestern South Africa without animals having to move inland.
2) These data indicate the presence of browse and graze on what is now fynbos shrub land suggests the presence of water resources, which supports the idea of

the EFT region having springs during the mid-Pleistocene, and proposes an environment and large mammal community at Elandsfontein and in the study region that is fundamentally different from the low carrying capacity environment that there is today.

3) These results do not support the hypothesis that large herbivores in coastal regions during the Pleistocene undertook long-distance migrations for food or other resources.
4) Tooth enamel from Elandsfontein was shown to retain effectively unaltered biogenic $^{87}Sr/^{86}Sr$ ratios as well as biogenic $^{18}O/^{16}O$ values.

CHAPTER 4: Triple oxygen isotope distributions in tooth enamel of extant mammals and potential geologic applications

ABSTRACT

The fractionation of the heavier oxygen isotope ^{18}O relative to ^{16}O is broadly used to study the hydrological and carbon cycles today and in the Earth's past. The extensive applications of $^{18}O/^{16}O$ ratios stem from its sensitivity to a range of environmental and geographic parameters (e.g., temperature, relative humidity, latitude), however the relationships among these parameters also limit its utility for probing the Earth system. The triple oxygen isotopic composition ($\Delta^{17}O$) of a material, which includes the rare isotope ^{17}O in addition to the more common ^{16}O and ^{18}O, can be used to distinguish processes influenced by mass-dependent fractionation from those influenced by mass-independent fractionation. $\Delta^{17}O$ can also be used to determine the influence of equilibrium and kinetic isotope effects during processes involving mass-dependent fractionation. There is an emerging literature that shows the potential utility of $\Delta^{17}O$ measurements in bones, tooth enamel and eggshells for studies of hydroclimate, pCO_2, pO_2 and diagenesis in the fossil record. However, in order to evaluate the potential of using $\Delta^{17}O$ compositions of fossilized materials, we need a better understanding of the range of $\Delta^{17}O$ values in the modern enamel of animals with a variety of behaviors and from a different environments as to provide a baseline to which fossil datasets can be compared. Here we present the $\Delta^{17}O$ values from 50 teeth of extant large mammalian herbivores. Teeth were obtained from several species with a range of behaviors and from

a broad range of environments and latitudes (0º to 68º). The range of $\Delta^{17}O$ values for tooth enamel is -291 to -137 per meg (161 per meg; 1 per meg is 0.001‰). The range in enamel $\Delta^{17}O$ values appears sensitive to aridity, contrasting the $\delta^{18}O$ values that vary with both latitude and the $\delta^{18}O$ of local meteoric water. Our results provide a baseline for the expected range of $\Delta^{17}O$ values in contemporary bones and teeth that can be applied in studies using fossilized samples. We argue that the $\Delta^{17}O$ values of enamel have strong potential as a tool to evaluate past aridity, in addition to their utility in evaluating oxygen isotope diagenesis of a material and past atmospheric pCO_2.

4.1. Introduction and Background

Oxygen isotopes in marine and terrestrial carbonates have long been used to reconstruct Earth's climate and environmental conditions across geological time (e.g., Rowley and Currie, 2006; Hopley et al., 2007; Zachos et al., 2001). These records which rely on $^{18}O/^{16}O$ ratios of carbonates, or $\delta^{18}O$ values, where $\delta\ ^{18}O = \left(\frac{^{18}O/^{16}O\ \text{sample}}{^{18}O/^{16}O\ \text{standard}} - 1\right) \times 1000$, have defined our current understanding of major aspects of Earth history ranging from the history of mountain uplift, global temperature changes, and aridification. However $\delta^{18}O$-based paleoclimate reconstructions are inherently limited because there are multiple factors that can influence $\delta^{18}O$ values of carbonates and the waters from which they form, which can include geographic location (e.g., elevation), temperature and evaporation. These factors influence $\delta^{18}O$ values of water through processes involving a combination of equilibrium and kinetic isotopic fractionation effects that cannot be distinguished using $\delta^{18}O$ alone. In order to constrain the potential influences on $\delta^{18}O$ values and to use $\delta^{18}O$ carbonate records to reconstruct past climate and environment with more confidence, we need an additional tool that allows us to evaluate the influencing factors on the $\delta^{18}O$ of a carbonate and the water from which it forms.

^{17}O is the least common stable isotope of oxygen as it comprises only 0.038% of the total amount of oxygen. It has long been recognized that $^{18}O/^{16}O$ and $^{17}O/^{16}O$ have different fractionation factors (α), where $^{x}\alpha = {}^{x}R_{sample}/{}^{x}R_{standard}$, where x is either 18 or 17 and indicates if the isotopic ratio, R, is $^{18}O/^{16}O$ or $^{17}O/^{16}O$, respectively (Matsuhisa et

al., 1978; Barkan and Luz, 2005). For the majority of Earth surface processes, oxygen isotope fractionation is largely mass-dependent, such that $^{18}\alpha$ and $^{17}\alpha$ vary in predictable ways relative to one another as a function of their mass; these relationships are characterized by the triple oxygen isotope exponent, θ, where $^{17}\alpha = {}^{18}\alpha^{\theta}$ (e.g., Young et al. 2002). This exponent is generally greater for processes involving equilibrium fractionation (e.g., phase changes) than for processes involving kinetic fractionation (e.g., diffusion), such that we can use the combination of $\delta^{18}O$ and $\delta^{17}O$ values to understand the influences of equilibrium and kinetic processes on the oxygen isotopic composition of materials (Matsuhisa et al. 1978; Young et al., 2002).

The measure of ^{17}O in addition to ^{18}O and ^{16}O, triple oxygen isotopes, is defined as $\Delta^{17}O$, where $\Delta^{17}O = \delta'^{17}O - \lambda_{REF} \times \delta'^{18}O$, and λ is the slope of the reference line (REF) and is dependent upon the reference frame used for the measurements in a given study (Miller, 2002; Pack and Herwartz, 2014). $\delta'^{x}O = \ln(R_{sample}/R_{standard})$ (Hulston and Thode, 1965). The delta prime notation, $\delta'^{x}O$, is used so the relationship between $\delta^{17}O$ and $\delta^{18}O$ values can be viewed linearly and where the slope of plots of $\delta'^{18}O$ and $\delta'^{17}O$ values can be expressed as λ. λ is the mathematical equivalent of as θ, but instead of dealing with one fractionation process, λ is used to describe oxygen isotope fractionation when several processes are combined as is likely processes that involve multiple phases and steps such as carbonate formation (Passey et al., 2014). We present isotopic data using δ-values and δ'-values in units of per mil (‰) and $\Delta^{17}O$ values in units of in per meg, where 1‰ = 1000 per meg.

For the triple oxygen isotope data that we discuss below we define $\Delta^{17}O$ values using λ_{REF} as 0.528, which is the slope that characterizes the distribution of global meteoric waters on a $\delta'^{18}O$-$\delta'^{17}O$ plot and is similar to the theoretical exponent for processes involving equilibrium fractionation (Meijer and Li, 1998; Luz and Barkan, 2010). This reference line has been used in $\Delta^{17}O$ studies of meteoric water, terrestrial carbonates and silica because it is serves as a model for $\delta'^{18}O$ and $\delta'^{17}O$ values if mass-dependent equilibrium processes are the sole drivers of isotopic fractionation in a system (Barkan and Luz, 2005; Luz and Barkan, 2010; Passey et al., 2014; Li et al., 2015; Sharp et al., 2016). Any material that has experienced a kinetic fractionation process (e.g. evaporation of water) will have $\delta'^{18}O$ and $\delta'^{17}O$ values that will have lower $\Delta^{17}O$ values than the initial water (e.g., Young et al., 2002; Barkan and Luz, 2005; Landais et al., 2006).

While there is enormous potential for the use of $\Delta^{17}O$ values of terrestrial materials to better understand factors influencing the water from which a material derived and thereby expand the utility of carbonate $\delta^{18}O$ paleoclimate records, the use of triple oxygen isotopes have primarily been limited to studies of systems where there is a relatively large range in $\Delta^{17}O$ values, such as meteorites, atmospheric chemistry and of Precambrian paleoclimate (e.g., Franchi et al. 1999; Boering et al. 2004; Bao et al. 2008). However, it is now possible to use triple oxygen isotopes to understand processes involving mass-dependent fractionation that are common on the Earth's surface in part because 1) meaningful mass-dependent variation in $\Delta^{17}O$ in Earth surface processes is now recognized and 2) analytical advances make it possible to measure the small

differences in $\Delta^{17}O$ value in materials (e.g., water, carbonate) that are products of these processes.

We consider the evaluation of $\Delta^{17}O$ values in terrestrial carbonates to be a viable way to address the limitations of the $\delta^{18}O$ record. However, before we can address the fossil record we must first understand the modern framework and the primary influences of $\Delta^{17}O$ values of carbonates and the waters from which they derived.

4.1.1. Current understanding of the $\Delta^{17}O$ values of terrestrial materials

In the following paragraphs we briefly review the $\Delta^{17}O$ values of meteoric-derived waters and the water from which bioapatites and biocarbonates (i.e., bones, tooth enamel and eggshells) precipitate. We report the $\Delta^{17}O$ values of animal body water and of bones, teeth and eggshells and then consider the major influences on the $\Delta^{17}O$ values of these materials. We then discuss the potential for using the $\Delta^{17}O$ values of bioapatite and biocarbonate in the fossil record to evaluate paleoclimate and paloenvironment.

Meteoric water that has not experienced significant evaporation on average falls along a slope of 0.528 with an intercept of 33 per meg (Luz and Barkan, 2010). In contrast, precipitation and surface water from dry, continental settings can be subject to extensive evaporation, yielding $\Delta^{17}O$ values as low as -60 per meg (e.g., Li et al., 2015; Surma et al., 2015; Fig 4.1). Plant water is derived from meteoric water and is highly susceptible to kinetic isotopic effects (i.e., diffusion/evaporation). With increased aridity, kinetic isotope effects more strongly influence the oxygen isotopic composition of plant water and there is further deviation from the reference line. Thus, with increasing aridity,

the $\Delta^{17}O$ value of plant water becomes increasingly negative (Landais et al., 2006). Plant water $\Delta^{17}O$ values, specifically leaf water, can be < -300 per meg (Fig. 4.1).

The $\Delta^{17}O$ values of bones, teeth and eggshells are directly related to the $\Delta^{17}O$ values of animal body water from which these minerals have formed and have been measured in several studies. When $\lambda_{REF} = 0.528$, animal body water $\Delta^{17}O$ values vary and can be more negative than ca. -200 per meg (Passey et al., 2014). There is only a ca. 20 per meg overlap of body water $\Delta^{17}O$ values with the meteoric water $\Delta^{17}O$ values (Fig. 4.4.1A). Analyzed eggshells have $\Delta^{17}O$ values that are as negative as ca. -200 per meg (Passey et al., 2014). Enamel $\Delta^{17}O$ values have a similar range in values to that of body water, but can be more negative than -280 per meg (Fig. 4.4.1B; Passey et al., 2014).

The primary factors influencing animal body water $\Delta^{17}O$ values and the $\Delta^{17}O$ values of bioapatites and biocarbonates are 1) the $\Delta^{17}O$ values of ingested water from food and drinking water and 2) the $\Delta^{17}O$ value of inhaled atmospheric O_2 (Pack et al., 2013). Herbivore body water and the minerals that precipitate from body water are thought to have $\Delta^{17}O$ values strongly influenced by the $\Delta^{17}O$ value of ingested leaf water and the $\Delta^{17}O$ value water that they drink. The $\Delta^{17}O$ value of contemporary atmospheric O_2 is depleted in ^{17}O (-500 per meg) relative to meteoric waters and plant waters as the result of mass-independent fractionation from photochemical reactions in the atmosphere and stratosphere (Bao et al., 2008). It is inhaled and incorporated into the animal body water and results in body water and bioapatite and biocarbonate $\Delta^{17}O$ values that are more negative then the global meteoric water line. Inhaled atmospheric O_2 could represent up to 40% of the total oxygen in body water (Kohn, 1996; Gehler et al., 2011; Pack et al., 2013; Passey et al., 2014).

4.1.2. Using $\Delta^{17}O$ values of bioapatite in the fossil record

$\Delta^{17}O$ values of bioapatite and biocarbonate have been proposed as useful in geological studies to understand aridity, pCO_2 (concentration of CO_2 in the atmosphere) and diagenesis (e.g., Pack et al., 2013; Gehler et al., 2011; Passey et al., 2014; Gehler et al., 2016). These applications are based on the different processes of mass-dependent and mass-independent fractionation that influence the $\Delta^{17}O$ value of body water and in turn, the $\Delta^{17}O$ values of biocarbonates and bioapatites (e.g., Hu et al., *in prep*). Part of the utility of these $\Delta^{17}O$-based approaches is that they can be applied to any materials in the fossil record that contain oxygen.

The $\Delta^{17}O$ values of biologically precipitated apatites and carbonates (i.e., bioapatites and biocarbonates) of large herbivore communities could be a proxy for aridity because animals incorporate evaporated leaf water into their diet and thus it is incorporated into bioapatite and carbonate (Hu et al., *in prep*). An animal that gets a large proportion of its water from leaf water (which can have more negative $\Delta^{17}O$ values than that of meteoric water, see Fig 4.1) will have a body water $\Delta^{17}O$ value substantially lower than that of an animal that drinks a large proportion of the water it ingests because the $\Delta^{17}O$ values of leaf water become more negative with increased evaporation (Hu et al., *in prep*). With increased aridity, $\Delta^{17}O$ values of leaf water will be more negative such that the animals that get their water from leaves will have $\Delta^{17}O$ values of bioapatite and biocarbonate that are more negative than they would in more humid environments (reviewed in Passey et al., 2014). However, the range in $\Delta^{17}O$ values of bioapatites and biocarbonates in various environments is unexplored such that we do not know if it would be useful for constraining paleoaridity.

Changes in the $\Delta^{17}O$ value of inhaled atmospheric O_2 can also affect the $\Delta^{17}O$ of bioapatite and biocarbonate as it can be a substantial portion of total balance of oxygen in a mammal's body water as stated above. The $\Delta^{17}O$ value of atmospheric O_2 is in part a function of atmospheric pCO_2 due to mass-independent fractionation of oxygen isotopes within the stratosphere; the $\Delta^{17}O$ of atmospheric O_2 becomes more negative as pCO_2 increases. This relationship has been applied to the study of past pCO_2 using terrestrial materials such as sulfates whose oxygen isotope composition is influenced primarily by the oxygen isotopes of atmospheric O_2, and not water (e.g., Bao et al, 2008). There is potential to use fossil tooth enamel $\Delta^{17}O$ values to determine or constrain past pCO_2 and this has been attempted in studies using fossil rodent tooth enamel (Gehler et al., 2016), however if this method for pCO_2 reconstruction is to gain traction, we need to develop a better understanding for the range in $\Delta^{17}O$ values of bioapatites and biocarbonates that exist when pCO_2 is relatively constant.

Another potential geologic application for $\Delta^{17}O$ in bioapatites and biocarbonates is for assessing the influence of diagenesis on $\delta^{18}O$ carbonate records. The oxygen composition of bioapatite and biocarbonate is prone to diagenesis, however determining whether the material has experienced isotopic alteration is not always straightforward. The $\Delta^{17}O$ of bioapatite has been proposed as a direct chemical proxy for isotopic diagenesis of oxygen (Gehler et al., 2011) based on the premise that bioapatite $\Delta^{17}O$ values are more negative than those of meteoric waters or even of a mixture of meteoric water and plant water (Fig. 4.4.1). The diagenetic fluid that would alter the oxygen isotopic composition of bioapatite and carbonate is meteoric water, with $\Delta^{17}O$ values

more positive than that of animal body water (Gehler et al., 2011). Thus, if the $\Delta^{17}O$ value of a bioapatite was found to be within the realm of the expected range of the $\Delta^{17}O$ values of meteoric waters, then it is likely that the oxygen isotopes in the bioapatite have been altered from their primary composition and that the oxygen isotopes should not be considered in the evaluation of past Earth conditions and processes.

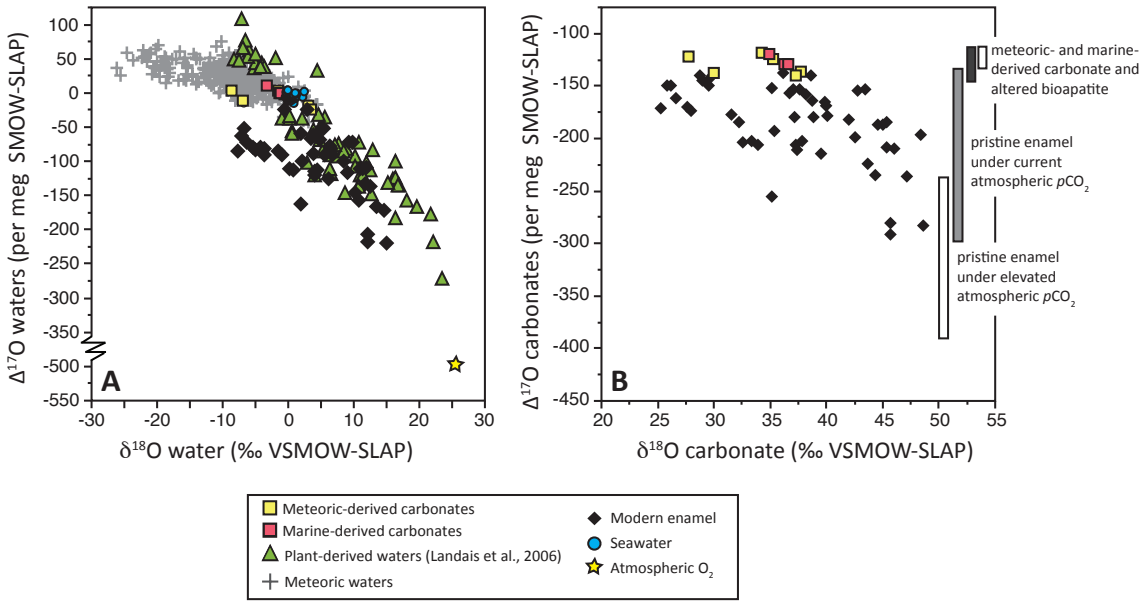

Figure 4.1: $\Delta^{17}O$ and $\delta^{18}O$ values of marine- and meteoric- derived waters, plant water, atmospheric O_2, and reconstructed water and body water (A). Marine- and meteoric derived carbonates and enamel $\Delta^{17}O$ and $\delta^{18}O$ values with vertical bars indicating the range in $\Delta^{17}O$ values for marine- and meteoric-derived carbonates and for tooth enamel carbonate under current atmospheric pCO_2 (B). Data point are from Landais et al. (2006), Bao et al. (2008), Luz and Barkan (2010), Landais et al. (2010), Passey et al. (2014), Li et al. (2015), Hu et al. (*in prep*) and this study. Vertical bars are also used to represent the theoretical range of tooth enamel $\Delta^{17}O$ values for enamel that has experienced alteration of O_2 by diagenetic meteoric- and marine- derived fluids based on carbontes from Passey et al. (2014) and enamel samples from this study (i.e., new data, Passey et al. (2014), Hu et al. (*in prep*), and for enamel from animals that lived during a period of elevated atmospheric pCO_2 (generalized from Pack et al., (2012) and Gehlers et al., (2016)).

There is great potential for using $\Delta^{17}O$ in enamel and other biominerals to address questions about paleoaridity, diagenesis and pCO_2, but we need to understand how $\Delta^{17}O$

values of biominerals vary in modern system before we can begin to apply $\Delta^{17}O$ to the fossil record and to geological and paleoecological questions.

4.1.3. Study layout

We analyzed the triple oxygen isotope composition of pristine, modern tooth enamel from mammalian herbivores that span various taxa, environments, locations and $\delta^{18}O$ values of local water (n = 45, Table 4.1; Table S4.1). In combination with the two published $\Delta^{17}O$ values of enamel from large herbivore teeth (Passey et al. 2014) and three teeth from Hu et al. (*in prep*), we used these data to evaluate the influences on the $\Delta^{17}O$ values of enamel carbonate. We then consider this dataset in terms of its application to the geological record in three ways: 1) as an aridity index, 2) to constrain past pCO_2 and 3) to evaluate the role of diagenesis on the oxygen isotopic composition of enamel.

Table 4.1: Taxa, location, and triple oxygen isotopic values of enamel samples. Measured isotopic compositions of enamel and calculated isotopic compositions of parent waters of the enamel. Values are given in units of per mil (‰) or per meg (‰ x 1000) relative to the VSMOW-SLAP scale of Schoenemann et al. (2013), with reference line $\lambda = 0.528$.

				***Enamel triple oxygen isotopic values*[b]**					***Calculated body water triple oxygen isotopic values*[c]**		
Analytical ID (first # of a series)	**Common name**	**Family**	**Genus and species**	**$\delta^{18}O$ (‰) avg**	**±[e]**	**$\Delta^{17}O$ (per meg)[g] avg**	**±[e]**	***n*[d]**	**$\delta^{18}O$ (‰) avg**	**$\Delta^{17}O$ (per meg)[g] avg**	**Reference**
East Africa											
JHU-17O-2057	Okapi	Bovidae	*Oryx gazella beisa*	44.3	0.3	-235	4	2	10.74	-157	this study
JHU-17O-2059	Elephant	Elephantidae	*Loxodonta africana africana*	45.4	0.0	-184	5	2	11.83	-109	this study
JHU-17O-2154	Elephant	Elephantidae	*Loxodonta africana africana*	45.0	0.5	-187	1	2	11.40	-111	this study
JHU-17O-2156	Elephant	Elephantidae	*Loxodonta africana africana*	40.1	0.3	-178	2	2	6.64	-91	this study

JHU-17O-2055	Giraffe	Giraffidae	*Giraffa camelopardalis*	48.6	0.2	-283	3	2	14.94	-219	Hu et al., *in prep.*
JHU-17O-2158	Hippo	Hippopotamidae	*Hippopotamus amphibius amphibius*	43.4	0.1	-153	3	2	9.85	-73	this study
JHU-17O-2048	Hippo	Hippopotamidae	*Hippopotamus amphibius amphibius*	42.8	0.3	-154	5	2	9.26	-72	Hu et al., *in prep.*
JHU-17O-2160	Okapi	Bovidae	*Oryx gazella beisa*	45.4	0.5	-208	3	2	11.81	-133	this study
JHU-17O-2151	Hippo	Hippopotamidae	*Hippopotamus amphibius amphibius*	39.8	0.0	-165	1	2	6.38	-77	this study
JHU-17O-2077	Giraffe	Giraffidae	*Giraffa camelopardalis*	47.2	0.1	-236	2	2	13.55	-166	Hu et al., *in prep.*
-	Hippo	Hippopotamidae	*Hippopotamus amphibius*	36.2	0.1	-137	6	2	2.91	-25	Passey et al. 2014
JHU-17O-2320	Elephant	Elephantidae	*Loxodonta africana africana*	38.9	0.9	-179	8	2	5.53	-90	this study
JHU-17O-2322	Elephant	Elephantidae	*Loxodonta africana africana*	38.2	0.4	-158	8	2	4.81	-68	this study
JHU-17O-2326	African buffalo	Bovidae	*Syncerus caffer*	42.5	0.7	-199	6	4	8.96	-117	this study
JHU-17O-2071	Giraffe	Giraffidae	*Giraffa camelopardalis*	46.0	0.7	-210	3	2	12.41	-137	this study
JHU-17O-2300	Giraffe	Giraffidae	*Giraffa camelopardalis*	48.4	1.5	-196	11	2	14.68	-172	this study
JHU-17O-2069	Hippo	Hippopotamidae	*Hippopotamus amphibius amphibius*	38.6	0.0	-140	9	2	5.20	-51	this study
JHU-17O-2079	Elephant	Elephantidae	*Loxodonta africana africana*	44.6	-	-187	-	1	11.00	-110	this study
JHU-17O-2075	Giraffe	Giraffidae	*Giraffa camelopardalis*	43.7	0.7	-224	9	2	10.14	-145	this study
JHU-17O-2052	Elephant	Elephantidae	*Loxodonta africana africana*	37.1	0.5	-153	2	3	3.82	-62	this study
JHU-17O-2073	Okapi	Giraffidae	*Okapia johnstoni*	42.0	0.2	-182	1	2	8.53	-99	this study
JHU-17O-2315	Elephant	Elephantidae	*Loxodonta africana africana*	37.6	0.4	-153	2	2	4.25	-63	this study
-	Black rhino	Rhinocerotidae	*Diceros bicornis*	38.7	0.6	-164	5	2	5.36	-52	Passey et al. 2014
South Africa											
JHU-17O-2331	Blue wildebeest	Bovidae	*Connochaetes taurinus taurinus*	45.7	0.7	-280	2	2	12.07	-206	this study
JHU-17O-2339	Giraffe	Giraffidae	*Giraffa camelopardalis*	45.7	2.2	-291	10	2	12.14	-218	this study
JHU-17O-2341	Red hartebeest /Cape hartebeest	Bovidae	*Alcelaphus buselaphus caama*	39.5	1.6	-214	9	2	6.13	-126	this study

JHU-17O-2324	Elephant	Elephantidae	*Loxodonta africana africana*	40.0	0.5	-169	2	2	6.57	-82	this study
Finland											
JHU-17O-2486	Beaver	Castoridae	*Castor fiber*	28.8	1.1	-140	2	2	-4.25	-80	this study
JHU-17O-2482	Reindeer	Cervidae	*Rangifer tarandus*	29.0	1.1	-145	7	2	-4.05	-85	this study
JHU-17O-2484	Reindeer	Cervidae	*Rangifer tarandus*	29.5	0.4	-143	1	2	-3.61	-82	this study
JHU-17O-2480	Moose	Cervidae	*Alces alces*	29.5	0.8	-150	3	2	-3.63	-90	this study
JHU-17O-2488	Moose	Cervidae	*Alces alces*	26.2	0.4	-150	4	2	-6.77	-52	this study
United States											
JHU-17O-2556	Bison	Bovidae	*Bison bison bison*	28.0	0.9	-173	6	2	-5.07	-83	this study
JHU-17O-2537	White-tailed deer	Cervidae	*Odocoileus virginianus virginianus*	33.9	0.7	-206	3	2	0.72	-113	this study
JHU-17O-2542	Bison	Bovidae	*Bison bison bison*	36.7	1.3	-157	1	2	3.39	-66	this study
JHU-17O-2552	Bison	Bovidae	*Bison bison bison*	25.8	0.9	-149	13	2	-7.17	-63	this study
JHU-17O-2554	Bison	Bovidae	*Bison bison bison*	27.6	0.6	-170	2	2	-5.45	-80	this study
JHU-17O-2080	Bison	Bovidae	*Bison bison bison*	31.5	0.9	-177	2	2	-1.62	-85	Hu et al., *in prep.*
JHU-17O-2061	White-tailed deer	Cervidae	*Odocoileus virginianus virginianus*	35.1	0.0	-255	8	2	1.87	-163	Hu et al., *in prep.*
JHU-17O-2539	Caribou	Cervidae	*Rangifer tarandus*	25.3	1.0	-171	0	2	-7.68	-85	this study
JHU-17O-2535	White-tailed deer	Cervidae	*Odocoileus virginianus virginianus*	33.4	1.3	-203	12	2	0.17	-110	this study
JHU-17O-2328	Beaver	Castoridae	*Castor fiber*	35.2	1.6	-152	5	4	1.92	-60	this study
JHU-17O-2347	White-tailed deer	Cervidae	*Odocoileus virginianus virginianus*	37.8	0.4	-203	6	2	4.47	-113	this study
JHU-17O-2343	White-tailed deer	Cervidae	*Odocoileus virginianus virginianus*	37.4	0.6	-211	2	2	4.07	-121	this study
JHU-17O-2524	White-tailed deer	Cervidae	*Odocoileus virginianus virginianus*	37.3	0.5	-206	2	2	4.00	-115	this study
JHU-17O-2520	White-tailed deer	Cervidae	*Odocoileus virginianus virginianus*	37.2	1.1	-180	4	2	3.89	-89	this study
JHU-17O-2522	White-tailed deer	Cervidae	*Odocoileus virginianus virginianus*	35.4	0.6	-193	1	2	2.10	-100	this study

JHU-17O-2345	White-tailed deer	Cervidae	*Odocoileus virginianus virginianus*	32.6	0.2	-204	5	2	-0.54	-25	this study
JHU-17O-2526	White-tailed deer	Cervidae	*Odocoileus virginianus virginianus*	32.2	0.7	-184	7	2	-0.96	-91	this study
JHU-17O-2541	Moose	Cervidae	*Alces alces*	26.6	-	-161	-	1	-6.40	-73	this study

[a] More information about climate can be found in Table S4.1

[b] $\delta^{18}O$, $\delta^{17}O$ and $\Delta^{17}O$ values normalized to VSMOW-SLAP scale, as per Schoenemann et al. (2013), and normalized to known $\delta^{18}O(CO_2/CaCO_3)$ values, as described in the Methods Section, where the reference slope of $\lambda = 0.528$

[c] Where ± is used to indicated standard deviation of 1σ

[d] Number of analyses, where each analysis involves extraction of CO_2 from enamel carbonate, reduction and fluorination of CO_2 to O_2, and analysis on the Thermo MAT 253 mass spectrometer over seven acquisitions of ten cycles each, where each cycle has a 26 s ion counting time (=1820 s total counting time)

[e] Body water triple oxygen isotope values were calculated using an animal body temperature of (T°C = 38°) based on general temperatures from Passey et al. (2014) and the fractionation factor between enamel and water is ($^{18}\alpha = 1.0332$) based on Lécuyer et al. (2010)

[f] Calculated using body water $\Delta^{17}O = \Delta^{17}O_{enamel} + 10^3 \ln^{18}\alpha_{CaCO3–H2O}\ (0.528 - \lambda_{CaCO3–H2O})$, where $^{18}\alpha_{CaCO3–H2O}$ is 1.0332 for tooth enamel samples, and $\lambda_{CaCO3–H2O}$ is 0.5245 for all samples

[g] Where per meg is ‰ x 1000.

4.2. Materials and Methods

4.2.1. Nomenclature and notation

Oxygen isotope measurements are described using δ^xO and $\Delta^{17}O$ notation, where x is 17 or 18. Material type is indicated in subscript after the δ^xO and $\Delta^{17}O$ notation (e.g., $\Delta^{17}O_{enamel}$ and $\Delta^{17}O_{meteoric\ water}$). We also apply this nomenclature when describing fractionation factors between parent waters and the bioapatite and carbonate precipitated from these parent waters.

4.2.2. Sample selection

Sample selection was designed to evaluate the full range in $\Delta^{17}O_{enamel}$ that exists in extant mammalian herbivores and how it varies with geographic and environmental parameters in order to fully explore its utility in geologic applications. The total number of

teeth we analyzed was limited by the long analytical times associated with $\Delta^{17}O$ measurements of bioapatites (> 5 hours/sample for $\Delta^{17}O$ vs. 35 minutes/sample for $\delta^{18}O$).

We used teeth from East Africa and South Africa that had been collected over the past five decades and for which many had been used in previous studies of the stable isotopic composition of teeth (Cerling et al., 1999; 2003; 2004; 2008; 2010; 2015; Passey and Cerling, 2006; Levin et al., 2008; Passey et al., 2007; 2014; Blumenthal et al., *in prep.*). Teeth from Finland were from the Finnish Museum of National History in Helsinki and teeth from the United States were provided by state parks or by individual researchers. We analyzed 50 teeth in total coming from hippopotamids (n = 4), elephantids (n = 9), bovids (n = 9), castorids (n = 2), cervids (n = 15) and giraffids (n = 5). These data have been combined with the isotopic data of a hippopotamid and rhinocerotid from Passey et al. (2014) and hipppotamid, giraffid (n = 2), bovid and cervid from Hu et al. (*in prep.*). The combined isotopic data are presented in Table S4.2. Samples were specifically chosen to span a range of environments, local $\delta^{18}O_{meteoric\ water}$ values, latitudes, taxa and animal water use strategies. Samples represent mainly water-dependent and water-independent taxa from humid to arid regions located at both mid and high latitudes.

4.2.3. Locations and climate

The geographical and climatic information for sample sites are listed in Table S4.1. Geographic information (latitude, longitude and elevation) were obtained from Cerling et al. (2015) for East African samples. The locations of all other samples were determined using Satellite Imagery. Climate parameters for each location are modeled from University of East

Anglia, Climate Research Unit (CRU) data from 1961 to 1990 and is based on mean climate grids of 10-minute latitudinal/longitudinal global land areas (New et al., 2002).

4.2.3.1 Characterization of environmental aridity and relative humidity

We use both relative humidity (RH) and the Aridity Index (MAP:PET) to understand the distribution of $\Delta^{17}O_{enamel}$ values and we have tabulated this information for every site from which we have $\Delta^{17}O$ data in Table 4.1 and Table S4.1. RH helps us connect the $\Delta^{17}O_{enamel}$ to the process influencing the water from which enamel forms (i.e., animal body water) whereas the Aridity Index helps us to connect $\Delta^{17}O$ values to actual environments (i.e., identifying the climate in which animals lived). The Aridity Index is defined here as the ratio of mean annual precipitation and mean annual potential evapotranspiration (MAP:PET) as this definition is widely used way to characterize aridity (e.g., UNESCO, 1979).

Aridity Index values were determined for all sites using precipitation from the CRU dataset model output and PET calculated for each site (Table S4.1). We also compiled RH values (% daily average RH) from the CRU dataset model output and for locations where we have actual measurements of RH, we find that the RH from the CRU dataset is within ± 15% of the measured values.

4.2.4. Preparation of tooth enamel powder for isotopic analysis

Enamel was removed along the tooth growth axis using a diamond saw blade, cleared of dentine and any dirt, and ground into a homogenized powder using a mortar and

pestle. Enamel powder was treated with 3% H_2O_2 to remove any organic material, rinsed three times with deionized water, treated with 0.1 M buffered acetic acid to remove any secondary carbonate and rinsed three times with deionized water before being dried overnight at 60ºC.

4.2.5. Triple oxygen isotope analysis and normalization

4.2.5.1. Triple oxygen isotope analysis

Analysis of triple oxygen isotopes of tooth enamel followed the methods outlined in Passey et al. (2014). For each analysis, 140 - 200 mg of tooth enamel powder was placed in silver capsules and reacted under vacuum in 100% phosphoric acid at 90ºC to extract CO_2, which was then reduced to H_2O in the presence of a catalyst (Fe powder heated to 560ºC) for 20 minutes (Passey et al., 2014). The resulting H_2O was fluorinated at 370ºC using a cobalt trifluoride reactor to produce O_2 that was then analyzed by duel inlet isotope ratio mass spectroscopy on a Thermo Scientific MAT 253 gas-sourced isotope ratio mass spectrometer at the Johns Hopkins University, Department of Earth and Planetary Sciences (Passey et al., 2014; Li et al., 2015). Water standards SLAP2 and VSMOW2 (3 µl) were directly injected into the cobalt trifluoride reactor to produce O_2 gas. All samples were analyzed in duplicate.

We evaluated the performance of the triple oxygen isotope measurements of carbonates external standards, both international standards carbonates (NBS18 and NBS19) and an in-house carbonate (102-GC-AZ01), as well as a CO_2 gas standard (Tank#2 CO_2). The mean external precision (1σ) for the reference carbonates and CO_2 was $\delta^{18}O$ of 0.7‰ and $\Delta^{17}O$ of 10 per meg.

4.2.5.2. Triple oxygen isotope normalization

All unknown and known waters and carbonates were fluorinated to produce O_2 using the in-house fluorination line before being analyzed for the triple oxygen isotope composition. Thus, it was possible to normalize the triple oxygen isotope data from carbonate O_2 directly with the triple oxygen isotope data from the O_2 of international water standards, VSMOW2 and SLAP2. Raw triple oxygen isotope data of known and unknown carbonates were normalized to international water standards VSMOW2 ($\delta^{18}O = 0‰$ and $\delta^{17}O = 0$ per meg) and scaled to SLAP2 ($\delta^{18}O = -55.5‰$). We use the reference frame where $\Delta^{17}O_{SLAP2}$ is set to 0 per meg, thus $\delta^{17}O_{SLAP2} = -29.6986490‰$ when $\delta^{18}O_{SLAP2} = -55.5‰$ and $\lambda = 0.528$ (Schoenemann et al., 2013). The reference line $\lambda = 0.528$ ($\delta^{17}O$-$\delta^{18}O$ meteoric water line) has also been used in the determination of $\Delta^{17}O$ of other natural waters (Landais et al., 2006; Barkan and Luz, 2007; Luz and Barkan, 2010; Li et al., 2015) and for terrestrial materials formed from natural waters, such as organic and inorganic carbonates (Passey et al., 2014).

A secondary normalization step was performed on carbonates to correct for slopes of < 1 for regressions between the measured and known values of $\delta^{18}O$. See Section 2.3 in Passey et al. (2014) for a detailed description of the data normalization of carbonates. We then compared our carbonate standard data to those from Passey et al. (2014) and adjusted the corrected $\Delta^{17}O$ values of carbonate standards and unknown enamels when the offset was $> 0.013‰$. All data and calculations pertaining to each run (i.e., standards, unknown samples and corrections) are detailed in Table S4.5.

4.2.6. Statistical analysis

All comparisons of isotopic data were evaluated using the statistical analytical software JMP 11 produced by the SAS Institute using the Tukey-Kramer HSD test and linear regressions. We use the ± symbol to report one standard deviation from the mean.

4.3. Results

Here we review all of the available triple oxygen isotope data from modern mammal teeth from this study (n = 45) and those published previously (n = 5) (Passey et al. 2014; Hu et al., *in preparation*) (Table 4.1). These data are from seven mammalian families that come from three continents. The sample sites span ~70˚ in latitude and arid to humid environments (aridity index 0.2 to 2.4) (Tables S4.1 and S4.2). The $\delta^{18}O_{enamel}$ values of these teeth yield a mean value of 37.6 ± 6.6‰ and range from 25.3 to 48.6‰ (Fig. 4.2; Table S4.2). The $\Delta^{17}O_{enamel}$ values average -186 ± 37‰ and range from -291 to -137 per meg. In the following sections we explore the variation in these data in terms of the geography (latitude), environment (aridity) and taxonomy (animal type).

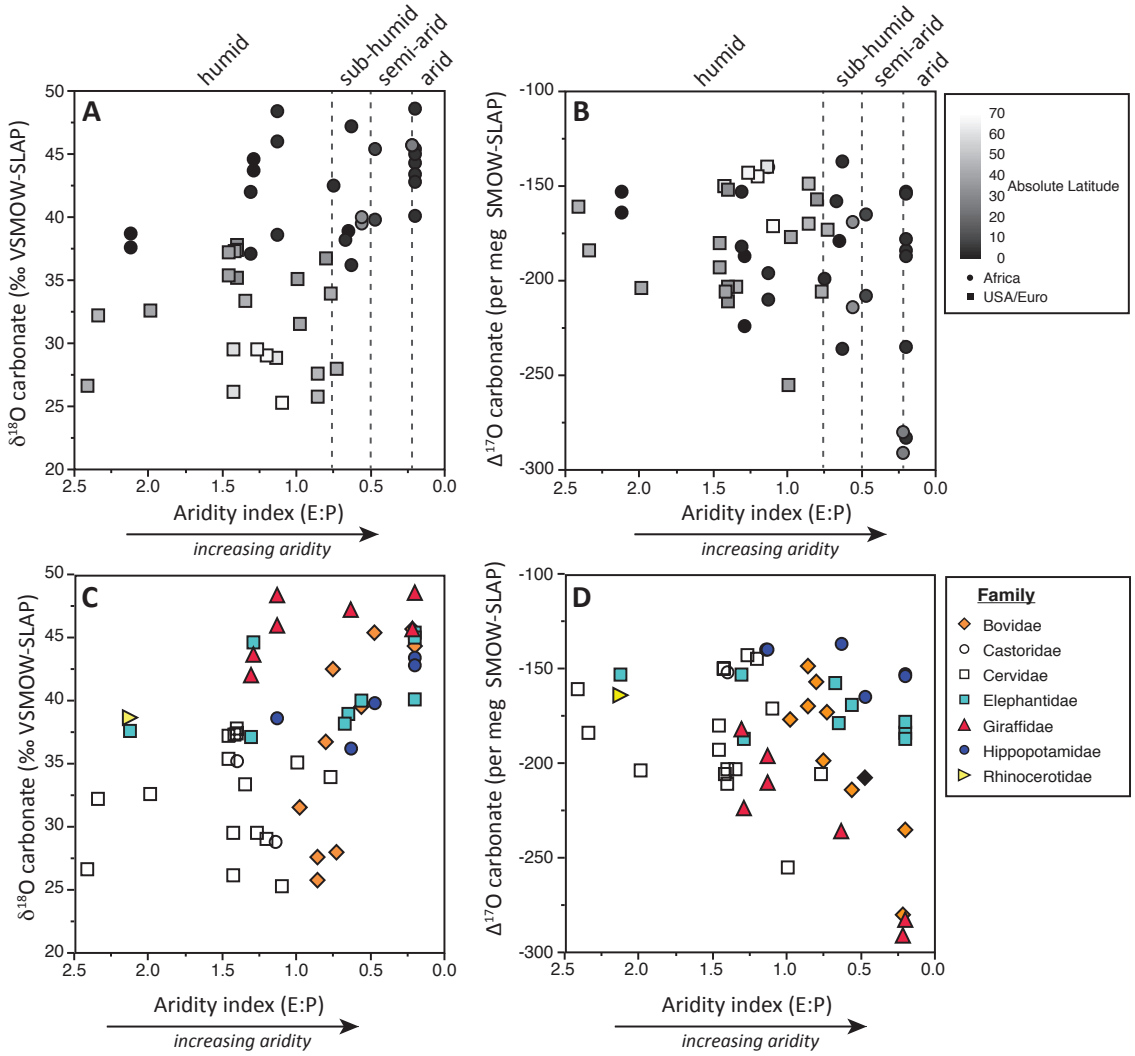

Figure 4.2: $\Delta^{17}O$ and $\delta^{18}O$ values of tooth enamel carbonate across a range of environments and Aridity Index values by absolute latitude and region (A and B) and by mammalian families (C and D). Environmental zones are based on UNESCO (1979) and indicated by vertical dashed lines.

4.3.1. Variation by latitude, aridity and region

4.3.1.1. Latitudinal variation

$\delta^{18}O_{enamel}$ values decrease with increasing absolute latitude ($R^2 = 0.67$) and show distinctions between samples from low latitudes (0 – 24˚, $n = 24$) and those from mid latitudes (24 – 66˚, $n = 21$) and high-latitudes (> 66˚, $n = 3$) ($p < 0.0001$). The lack of

obvious differences in the $\delta^{18}O_{enamel}$ values from mid and high latitudes ($p = 0.09$) may be an artifact of the small number of samples from high latitudes ($n = 3$) (Fig. 4.4.2A-B). In contrast to the $\delta^{18}O_{enamel}$ data, there is no trend in $\Delta^{17}O_{enamel}$ values with latitude ($R^2 = 0.04$); $\Delta^{17}O_{enamel}$ values are similar to each other when sampling locations are binned by low, mid and high latitudes ($p > 0.23$). Notably, the $\Delta^{17}O_{enamel}$ values at low latitudes and mid latitudes have similar ranges, -283 to -137 per meg and -291 to -140 per meg, respectively. The $\Delta^{17}O_{enamel}$ values from high latitude sampling locations in Finland and Alaska overlap with those from low and mid latitudes but have a smaller range, -171 to -143 per meg, which may simply reflect the small sample size ($n = 3$).

4.3.1.2. Environmental variation

The teeth in this dataset come from environments that exhibit a range in Aridity Index values (0.2 to 2.4). These environments include the hot, arid environments in the Turkana and Kgalagadi regions of Kenya and South Africa (Aridity Index 0.20 and 0.22, respectively), mid latitude semi-arid regions of Utah (0.99) and high latitude, cold Alaska (1.1), as well as moist highlands in Kenya (2.12) and cool, humid Finland (> 1.14), where values in parentheses are Aridity Index values for each site.

The teeth for which we have $\Delta^{17}O$ data can be divided into four environmental groups by using the Aridity Index value for each sample location. These environmental groups are humid (> 0.75, $n = 30$), sub-humid (0.5 – 0.75, $n = 9$), semi-arid (0.2 – 0.5, $n = 2$) and arid (< 0.2, $n = 9$) (UNESCO, 1979; Fig. 4.2). The $\delta^{18}O_{enamel}$ values from arid environments are significantly higher than those from humid, sub-humid environments

($p < 0.002$), but there are no distinctions between $\delta^{18}O$ values from semi-arid and humid environments ($p = 0.19$) or between sub-humid climates ($p = 0.34$) (Fig. 4.2). The distribution of $\Delta^{17}O_{enamel}$ values follow a distinct wedge-shaped pattern when plotted with Aridity Index; the range in observed $\Delta^{17}O_{enamel}$ values (from 84 per meg in humid environments to 154 per meg in arid environments) increases with greater aridity (lower Aridity Index values) and the minimum $\Delta^{17}O$ value decreases such that $\Delta^{17}O_{enamel}$ values from arid settings are significantly more variable and lower than those from humid settings ($p < 0.04$) (Fig. 4.3B).

4.3.1.3. Regional variation (Africa compared with North America and Europe)

When considering the teeth from Africa ($n = 27$), we found $\delta^{18}O_{enamel}$ values that ranged from 36.2 to 48.6‰ and averaged 42.4 ± 3.6‰. The $\Delta^{17}O_{enamel}$ values ranged from -291 to -137 per meg with a mean of -193 ± 43 per meg (Fig. 4.2). Samples from North America and Europe ($n = 23$) had $\delta^{18}O_{enamel}$ values that ranged from 25.3 to 37.8‰ and averaged 31.8 ± 4.2‰, with corresponding $\Delta^{17}O_{enamel}$ values ranging from -255 to -140 per meg with a mean of -178 ± 29 per meg (Fig. 4.3). While the $\delta^{18}O_{enamel}$ values from Africa are significantly greater than those from North America and Europe ($p > 0.0001$), the regional $\Delta^{17}O_{enamel}$ values (Africa vs. North America and Europe) cannot be distinguished ($p = 0.14$).

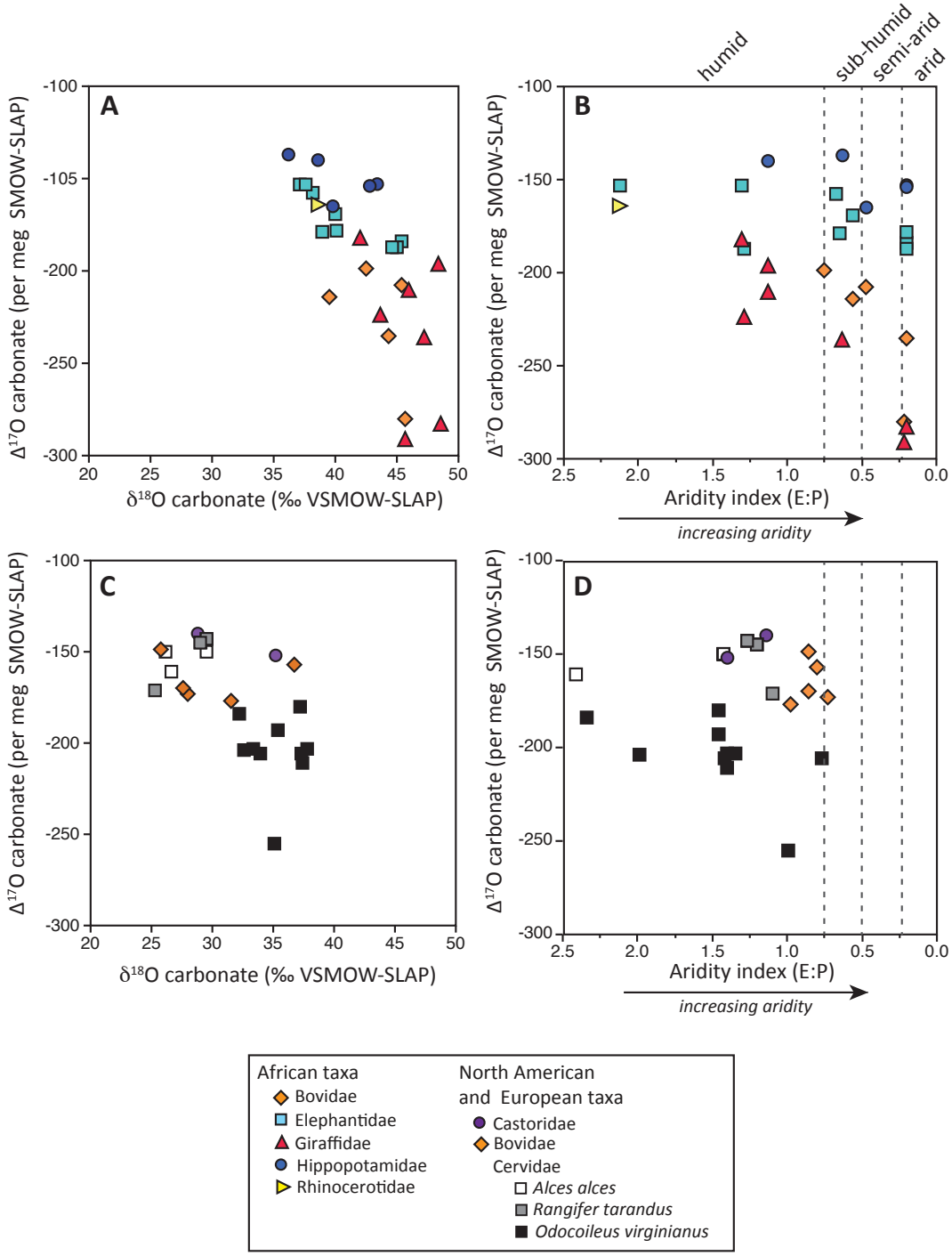

Figure 4.3: $\Delta^{17}O$ and $\delta^{18}O$ values of tooth enamel carbonate and $\Delta^{17}O$ values across a range of environments and Aridity Index values for taxa from Africa (A and B) and North American and Europe (C and D). Environmental zones are based on UNESCO (1979) and indicated by vertical dashed lines.

4.3.2. Variation by taxon

Here we consider the variation in triple oxygen isotope data as a function of the different herbivore families that we sampled. We pool data from regions with similar taxonomic distributions and consider them in two groups, those from Africa and those from North America and Europe.

4.3.2.1. African taxa

The African dataset includes teeth from giraffids (n = 7), bovids (n = 5), a rhinocerotid (n = 1), elephantids (n = 9) and hippopotamids (n = 5) from South Africa, Kenya, Uganda and the Democratic Republic of the Congo (Table 4.2, Fig. 4.3). The distribution of $\delta^{18}O_{enamel}$ values from these taxa mostly overlap with one another except for those from giraffids which are significantly higher than $\delta^{18}O_{enamel}$ values of both hippopotamids and elephantids ($p < 0.02$). The correlations between $\delta^{18}O_{enamel}$ values and aridity for some of the taxa sampled (hippopotamids $R^2 = 0.50$; elephantids $R^2 = 0.23$; bovids $R^2 = 0.35$; giraffids, $R^2 = 0.31$) vary.

The distribution of $\Delta^{17}O_{enamel}$ values varies for each family (Fig. 4.3B). The $\Delta^{17}O_{enamel}$ values of hippopotamids are significantly higher than that of giraffids (p = 0.0004) and bovids (p = 0.0018). Giraffid and bovid $\Delta^{17}O_{enamel}$ values are similar to one another (p = 0.999) and they both exhibit large ranges in $\Delta^{17}O_{enamel}$ (> 100 per meg). In both these groups, there is a strong, negative correlation between $\Delta^{17}O_{enamel}$ and Aridity Index (bovids, $R^2 = 0.65$; giraffids, $R^2 = 0.87$). In contrast, both elephantids and hippopotamids exhibit a narrow range in $\Delta^{17}O_{enamel}$ values (< 35 per meg). Although the

$\Delta^{17}O_{enamel}$ values from the elephantids are lower than those measured for hippopotamids, these differences are not significant ($p = 0.6$).

4.3.2.2. North American and European taxa

The dataset from North America (United States) and Europe (Finland) includes teeth from bovids ($n = 5$), castorids ($n = 2$) and cervids ($n = 16$) (Table 4.2; Fig. 4.3C-D). The distributions of $\delta^{18}O_{enamel}$ values of cervids and bovids are similar to one another ($p = 0.51$), which is notable because the cervids that we sampled originate from a wider range of environments (Aridity Index = 0.77 to 2.41) than the bovids (Aridity Index = 0.73 to 0.98) (Fig 3C). The $\Delta^{17}O_{enamel}$ values of cervids average -185 ± 31 per meg and range from -255 to -143 per meg, whereas bovids and castorids $\Delta^{17}O_{enamel}$ values represent a much tighter range of -177 to -140 per meg, averaging -160 ± 14 per meg.

The cervid teeth span a range of environments and can be further evaluated by considering the three different taxa that we sampled, *Alces alces* ($n = 3$), *Rangifer tarandus* ($n = 3$) and *Odocoileus virginianus* ($n = 10$). We found that the distribution of $\delta^{18}O_{enamel}$ and $\Delta^{17}O_{enamel}$ values of *A. alces* and *R. tarandus* overlapped with one another but were distinct from those values of *O. virginianus*. The latter had higher $\delta^{18}O_{enamel}$ values ($p < 0.01$) and lower $\Delta^{17}O_{enamel}$ values than the *A. alces* and *R. tarandus* teeth ($p < 0.002$). We also noted that the $\Delta^{17}O_{enamel}$ values of *O. virginianus* were significantly lower that the $\Delta^{17}O_{enamel}$ values of all other teeth we sampled from North America and Europe ($p < 0.003$), however there was no equivalent distinction in $\delta^{18}O_{enamel}$ values.

4.4. Discussion

Here we consider the variation of and influences on $\Delta^{17}O_{enamel}$ values, and the utility of $\Delta^{17}O_{enamel}$ data in active fields of study that pertain to the fossil record.

4.4.1. Variation in $\Delta^{17}O_{enamel}$

4.4.1.1. $\Delta^{17}O$ values of enamel and other terrestrial materials

In our survey of $\Delta^{17}O_{enamel}$ values from extant mammals we observe a 161 per meg range in $\Delta^{17}O$ values, which is influenced by a combination of the environmental context and the taxonomy of the teeth sampled. Notably, $\Delta^{17}O_{enamel}$ values are not influenced by latitude, elevation, or geographic region, making them distinct from $\delta^{18}O_{enamel}$ values for which the influences of latitude, elevation and geographic region can obscure the influence of changing aridity, as observed both in this study and others (e.g., Levin et al., 2006; Thesis Chapter 2). When compared to other kinds of terrestrial materials, $\Delta^{17}O_{enamel}$ values are lower than those of meteoric carbonates and meteoric waters, whereas they overlap in distribution of $\Delta^{17}O$ values of plant waters, even though the range in $\Delta^{17}O_{enamel}$ values (-291 to -137 per meg) is smaller than that for plant waters (-271 to +108 per meg) (Fig. 4.1A).

In order to understand the distribution of $\Delta^{17}O_{enamel}$ values in relation to the $\Delta^{17}O$ values of other terrestrial materials, we need to consider all of the influencing factors that contribute to a $\Delta^{17}O_{enamel}$ value (i.e., the environmental and geographic context and the taxonomy of the animals sampled).

4.4.1.2. $\Delta^{17}O$ values of reconstructed body water

The oxygen isotopic composition of animal body water is influenced by an animal's physiology, behavior and environment. Because enamel precipitates from animal body water, enamel is in turn influenced by an animal's physiology, behavior and environment, as reviewed in Kohn and Cerling (2002). In order to understand the $\Delta^{17}O_{enamel}$ dataset and to put it into a framework of the $\Delta^{17}O$ values of other materials (e.g., carbonates, waters, air), we need to be able to relate the measured $\Delta^{17}O_{enamel}$ values to animal physiology and behavior and to their environmental context. Furthermore, to relate the measured $\Delta^{17}O_{enamel}$ values to the aforementioned parameters, it is necessary to understand how the $\Delta^{17}O$ values of the enamel-derived O_2 that is measured in the mass spectrometer relates to the $\Delta^{17}O$ of the tooth enamel itself, and in turn, how the $\Delta^{17}O_{enamel}$ values relate to the $\Delta^{17}O$ values of body water from which the enamel precipitates.

We use the extensive work on $\delta^{18}O_{enamel}$ (e.g., Bocherens et al., 1996; Kohn, 1996 Levin et al., 2006; Hoppe 2006; Cerling et al., 2008) as a framework for understanding fractionation in $\delta^{17}O_{enamel}$ values and thus the variation in $\Delta^{17}O_{enamel}$ values. For any process involving fractionation of $^{18}O/^{16}O$ ratios with a characteristic $^{18}\alpha$, we can calculate the corresponding fractionation $^{17}\alpha$, using an λ that is derived both theoretically or empirically, where $\lambda = \ln(^{17}\alpha)/\ln(^{18}\alpha)$. In reconstructing $\Delta^{17}O_{body\ water}$ values from $\Delta^{17}O_{enamel}$ values, we consider the oxygen isotope fractionation that occurs during the processes of 1) converting tooth enamel to the O_2 that we analyze for $\Delta^{17}O$ values and 2) mineralization of tooth enamel from body water. We determine $\delta^{18}O$, $\delta^{17}O$ and $\Delta^{17}O$ values of body water from tooth enamel by assuming an $^{18}\alpha = 1.0332$ and $\lambda = 0.5245$,

which accounts for the 90˚C phosphoric acid reaction during analysis and 38˚C mammalian body temperature for enamel mineralization (Lécuyer et al., 2010; Passey et al., 2014).

Using this approach, reconstructed $\delta^{18}O_{body\ water}$ and $\Delta^{17}O_{body\ water}$ values range from -7.7‰ to +14.9‰ and from -219 to -25 per meg, respectively (Table 4.1). Reconstructed $\Delta^{17}O_{body\ water}$ values are more negative than $\Delta^{17}O_{meteoric\ water}$ values, but overlap with $\Delta^{17}O_{plant\ water}$ values and are notably higher than $\Delta^{17}O$ of atmospheric O_2 (Fig. 4.1A). Understanding the range in reconstructed $\Delta^{17}O_{body\ water}$ values and how the reconstructed $\Delta^{17}O_{body\ water}$ values vary with environment and taxa are only possible by comparing these data to a model of how we should expect $\Delta^{17}O_{body\ water}$ to vary given different physiological, behavioral and environmental influences.

4.4.1.3. $\Delta^{17}O$ values of modeled and reconstructed body water

To understand the influences on $\Delta^{17}O_{body\ water}$ values, and in turn $\Delta^{17}O_{tooth\ enamel}$ values, we compared our reconstructed $\Delta^{17}O_{body\ water}$ data to the $\Delta^{17}O_{body\ water}$ values predicted by the triple oxygen isotope body water model developed by Hu et al. (*in prep.*). The Hu et al. (*in prep.*) model, where it is described in full, builds on the existing understanding of the fluxes and the fractionation of oxygen isotopes in mammalian body water that have been developed for the $\delta^{18}O$ system (Kohn, 1996) and modifies it for the triple oxygen isotope system. The $\Delta^{17}O$ body water model incorporates the triple oxygen isotopic composition of oxygen influxes and effluxes for an animal (e.g., O_2, water, food, sweat, feces), taking into account animal weight, physiology and environment. The most

important variables in the $\Delta^{17}O$ body water model for extant animals are 1) the RH of the environment, 2) the fraction of evaporated water consumed by an animal, and 3) the water economy index (WEI) of an animal. For fossils of course one has to consider varying $\Delta^{17}O$ values of atmospheric O_2 but we will not consider that in the following, brief overview.

The fraction of evaporated water consumed by an animal is related to the proportion of water received from food, both the amount of free water and the amount of water in a plant relative to the solid leaf material, relative to the proportion of surface water that an animal drinks (Hu et al., *in prep.*). Plant water can be more negative in $\Delta^{17}O$ than the $\Delta^{17}O$ of surface water, because plant water is strongly influenced by evaporation compared to surface water (e.g., as reviewed in Passey et al., 2014). When an animal drinks a large amount of surface water (less negative and more narrow in range than the $\Delta^{17}O$ value of plant water), then body water $\Delta^{17}O$ is heavily influenced by the surface water $\Delta^{17}O$ which dilutes the evaporation-sensitive plant water $\Delta^{17}O$ signal and results in body water $\Delta^{17}O$ that does not reflect the environmental context even in arid environments. In contrast, animals that mostly consume water from plants are more sensitive to changes in RH because a large portion of body water body water $\Delta^{17}O$ is composed of evaporation-sensitive plant water $\Delta^{17}O$. The WEI (in ml water/ kJ Energy) is a measure of the amount of water used by an animal per unit of metabolized energy and is influential in determining the amount of water an animal needs to consume to survive (Nagy and Peterson 1988; Nagy, 2004). Animals with a higher WEI are less efficient in their water use and require a greater intake of water, these animals are more likely to drink a large proportion of water. The WEI is variable according to taxa,

reflecting animal behavior and physiology. In addition, the WEI of a species can vary as a result of different influences including environment and the amount of accessible food and surface water. If an animal can consume its required water intake from food-derived water, then it will not need to drink water, these animals have a relatively low WEI (e.g., giraffes and white-tailed deer). An animal that cannot reach the required amount water from food-derived water will drink water; these animals have a relatively high WEI (e.g., hippopotamids, elephantids, and castorids/beavers).

We chose input values for the $\Delta^{17}O$ body water model for the conditions relevant for the teeth from which we generated $\Delta^{17}O$ data, using contemporary atmospheric $\Delta^{17}O_{O2}$ value (-500 per meg), $\delta^{18}O_{meteoric\ water}$ values representative of sampling locations in North America and Europe (-14‰ to -8‰) and in Africa (-5‰ to +1‰) (input water $\delta^{18}O$ values estimate from Bowen, (2016) are combined in model to produce a single range of input $\delta^{18}O$ values), RH representative of the sampled environments (30%, 50% and 80%; Table 4.1 and Table S4.1) and the minimum and maximum WEI values, 0.60 and 0.05, respectively, that are typical of the taxa we sampled and represent taxa with behaviors that range from animals that receive the majority of their water from food to animals that receive a large proportion of water from drinking surface water (Table S4.4, Table S4.5; Hu et al., *in prep*.). Figure 4 shows the expected $\Delta^{17}O_{body\ water}$ values for these conditions overlain on the reconstructed $\Delta^{17}O_{body\ water}$ from our analyzed samples.

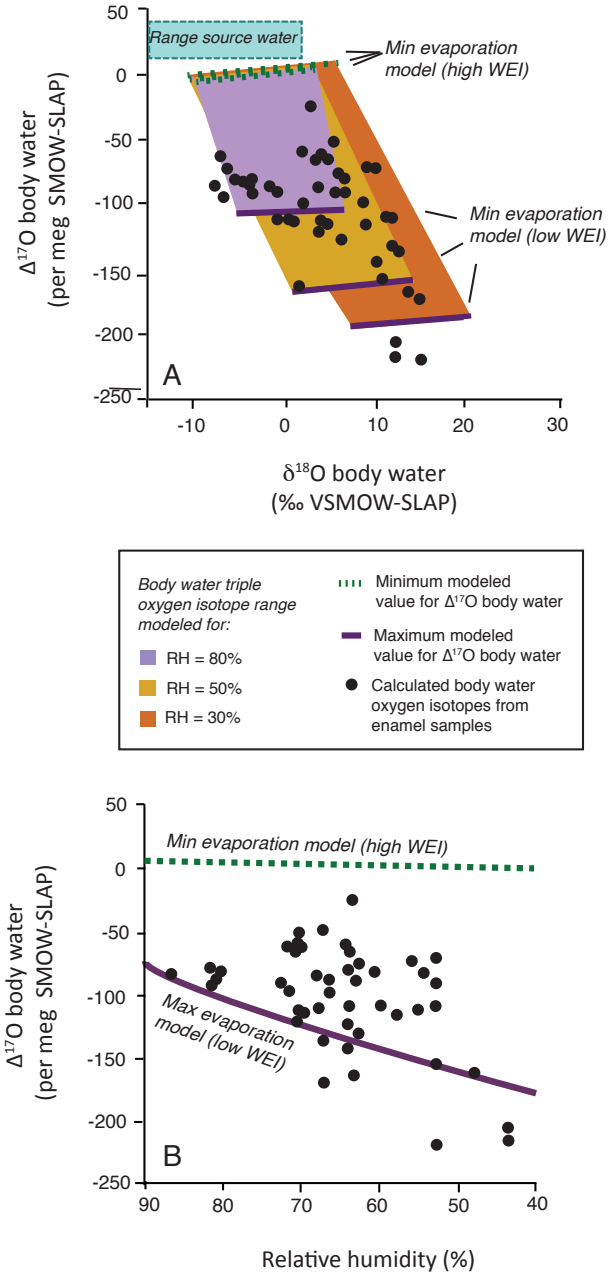

Figure 4.4: The oxygen isotopic composition of reconstructed body water based on the enamel data in this study and the modeled body water ranges at 30%, 50% and 80% relative humidity based on the MIN-EVAP (green dashed lines) and MAX-EVAP (purple solid lines) model outputs based on the parameters in Hu et al. (*in prep.*) (A.). The source water $\delta^{18}O$ range is the combined range of meteoric water from Africa (-5 to +1‰) and the United States and Europe (-14 to -8‰) and $\Delta^{17}O$ values of meteoric water. Body water model output of the minimum and maximum $\Delta^{17}O$ values for a range of relative humidity, where $\Delta^{17}O$ values are based on an animal pair with the highest water economy index (green dashed line) and with the lowest water economy index (purple solid line) and reconstructed body water based on the enamel in this study (B).

Ranges in modeled $\Delta^{17}O_{body\ water}$ for the samples (where the $\delta^{18}O_{meteoric\ water}$ ranges from -14‰ to +1‰, when all locations are combined) differ as a function of the RH used in each model iteration (Fig. 4.4A). There is ~112 per meg range in modeled $\Delta^{17}O_{body\ water}$ values for an environment with 80% RH, ~ 165 per meg range for 50% RH, and ~ 188 per meg range for 30% RH. In the minimum modeled $\Delta^{17}O_{body\ water}$ values, at different RH, are within ~7 per meg of one another for the locations of Africa and North America and Europe (Table S4.4). The minimum modeled $\Delta^{17}O_{body\ water}$ value becomes increasingly more negative with decreasing RH (Fig. 4.4).

In general, the modeled and reconstructed $\Delta^{17}O_{body\ water}$ and $\delta^{18}O_{body\ water}$ data are similar in their distributions (Fig. 4.4). Modeled and reconstructed $\Delta^{17}O_{body\ water}$ values for animals with both low and high WEI which originate from a range of RH, follow the same wedge-shaped pattern, where a greater range in $\Delta^{17}O_{body\ water}$ values correspond with lower RH. The modeled data are compressed and span a smaller range in $\Delta^{17}O$ values relative to what the reconstructed data would predict. For example, reconstructed $\Delta^{17}O_{body\ water}$ values of animals with the most negative $\Delta^{17}O$ values of body water (in this case, giraffids) from the Turkana and Kgalagadi (where RH = ~50% based on modeled CRU data) have $\Delta^{17}O$ values more similar to the predicted minimum $\Delta^{17}O_{body\ water}$ value for an environment with a RH of 30%.

The body water model output results confirm what we observed in the measured $\Delta^{17}O_{enamel}$ values: 1) $\Delta^{17}O_{body\ water}$ does not vary with $\delta^{18}O_{meteoric\ water}$ and is independent of geographic constraints that influence $\delta^{18}O_{enamel}$, 2) there is a strong relationship between $\Delta^{17}O_{body\ water}$ and aridity, where aridity is represented by RH in the model, and 3) the

behavior and physiology of the animals sampled, as represented by a minimum and maximum WEI value in the model, play a strong role in the distribution of $\Delta^{17}O_{body\ water}$ values at a single location and across environments. The model output predicts the general wedge shape of the data on a $\Delta^{17}O_{body\ water}$ vs. RH plot and show that when animals with a range of WEI are sampled, there is a greater range in $\Delta^{17}O$ values in low RH environments than in high RH environments and that these patterns are independent of $\delta^{18}O_{meteoric\ water}$ values (Fig. 4.4). There is some discrepancy between the absolute range in $\Delta^{17}O_{body\ water}$ values of the model outputs and what we measured (Fig. 4.4), and while we need to explore the model more to understand what drives this difference, it is outside the scope of the work that was done for this chapter.

4.4.2. Geological applications using $\Delta^{17}O_{enamel}$ measurements

Our $\Delta^{17}O_{enamel}$ data from extant mammalian herbivores show 1) $\Delta^{17}O_{enamel}$ values are significantly lower than $\Delta^{17}O$ values of meteoric carbonates, 2) $\Delta^{17}O_{enamel}$ values become lower and more varied in more arid environments, 3) animal behavior and physiology is important in determining $\Delta^{17}O_{enamel}$, and 4) the influences of aridity and animal behavior and physiology on $\Delta^{17}O_{enamel}$ values are independent of the $\delta^{18}O$ values of local waters. In the following sections we review how we can use this information in geologic applications. We propose ways in which $\Delta^{17}O_{enamel}$ values from fossils can be used as a proxy for paleoaridity, the use of $\Delta^{17}O$ measurements in identifying the influence of diagenesis in $\delta^{18}O$ records, and the importance of considering data from a

range of taxa when using $\Delta^{17}O_{enamel}$ values to reconstruct concentrations of CO_2 in Earth's ancient atmosphere.

4.4.2.1. Aridity index

The relationship between $\Delta^{17}O_{enamel}$ and aridity, where $\Delta^{17}O$ values become lower and more varied when aridity increases, can be used to evaluate paleoaridity using $\Delta^{17}O$ from fossil teeth. The wedge-shaped distribution in Fig. 4.1B shows that there is a greater range in $\Delta^{17}O$ values in more arid environments than in humid environments. We can use these trends as a template to assess the degree of aridity in fossil environments, and specifically to compare the degree of aridity between fossil sites. This dataset shows that this is a powerful method to assess relative aridity between sites (sites with a greater range in $\Delta^{17}O$ values are more arid than those with a smaller range in $\Delta^{17}O$) but we can also roughly use the distribution of $\Delta^{17}O$ values to designate a fossil site as humid, semi-arid or arid. In general we observe a < 85 per meg range in humid environments (AI = > 0.75, n = 29 out of 30), a ca. 100 per meg range in sub-humid environments (AI = 0.5 - 0.75, n = 9), and > 130 per meg range in arid environments (AI = < 0.2, n = 9), independent of geographic region (Fig. 4.2). These $\Delta^{17}O$ values are from the dataset excluding the sample JHU-17O-2061 (deer from Parowan, Utah) because this location was categorized using the Aridity Index as humid using UNESCO (1979), however this environment is quite dry. We have not analyzed an adequate number of enamel samples from sub-humid to distinguish them from the surrounding environments and to determine

what range we would expect for this environment, however, we would expect a range that is larger than in humid and smaller than in arid environments.

For this method to be useful for determining paleoenvironments, the sampling strategy needs to be designed to capture as much variation in $\Delta^{17}O_{enamel}$ that existed while the animals lived, which means sampling teeth from taxa with a variety of water use strategies. Because it is hard to know water use strategies for fossil animals, the best approach is to sample range of animal types in a fossil assemblage to maximum the potential to sample the full range of $\Delta^{17}O_{enamel}$ values that is reflective of the environment. Given the intensive nature of producing $\Delta^{17}O_{enamel}$ data and the difficulty in generating large datasets, we suggest sampling at least two individuals from at least 3 different taxa with hypothesized differences in physiology and water use strategies from each site that is evaluated (> 6 teeth from each site) to start to assess relative differences in aridity between sites. By sampling teeth from multiple taxa, it will be possible to assess the $\Delta^{17}O$ distributions from a community of animals and increase the potential for capturing the full range of variation in $\Delta^{17}O_{enamel}$ that is indicative of the aridity of the environment in which these animals lived. The relationships between Aridity Index and $\Delta^{17}O_{enamel}$ can be used to place the $\Delta^{17}O_{enamel}$ from a fossil assemblage into a climate classification (e.g., humid, semi-humid, arid) and/or to compare the degree of aridity between sites. The more teeth that are analyzed, the more robust these comparisons will become because additional data will help ensure that the full range in variation in $\Delta^{17}O_{enamel}$ that existed in an environment is represented in the dataset. However this means that any estimate of aridity using this approach is a minimum as additional data

can only increase the observed range in $\Delta^{17}O_{enamel}$ values from a site. The prospects for larger datasets will get better as the analytical throughput is increased and the requirements for sample amounts are minimized.

The main advantages of a paleoaridity proxy using $\Delta^{17}O$ over the existing approaches that use $\delta^{18}O_{enamel}$ values alone are that 1) the $\Delta^{17}O$ approach is not dependent on *a priori* knowledge of the behavior or physiology of the animals sampled and 2) it is independent of the influence of meteoric water $\delta^{18}O$ values. These elements expand the utility of the $\Delta^{17}O$ approach for evaluating paleoaridity to taxonomic assemblages where the behavior and physiology of animals is unknown (i.e., most fossil assemblages, except for very recent fossils for which extant fauna are good analogs). It also makes it possible to compare the paleoaridity between assemblages with different geographic settings where $\delta^{18}O$ of input waters might vary. For these reasons the $\Delta^{17}O$ enamel paleoaridity proxy is versatile and has potential to be applied to a range of geologic settings, going back in time. We should note that if $\Delta^{17}O$ values of teeth are being compared from time periods with different atmospheric CO_2 concentrations, there may be significant differences in absolute $\Delta^{17}O$ values that are not due to changes in aridity but due instead to changes in atmospheric pCO_2. In these cases the range of enamel $\Delta^{17}O$ values (instead of absolute values) from a community of animals at different sites can be compared to assess relative differences in aridity between the sites.

4.4.2.2. Indicator of diagenesis

The differences between $\Delta^{17}O$ values of enamel and meteorically-derived carbonates (Fig. 4.1) be used to identify diagenesis and reprecipitation of mineral with meteoric waters (Gehler et al., 2011). Gehler et al. (2011) first presented the concept for using $\Delta^{17}O$ values of bioapatite of small mammals (< 1 kg) as a tool for assessing diagenesis in the fossil record; we build on this concept here by showing that this works for large mammals (> 1 kg) as well and provide an expanded dataset of $\Delta^{17}O$ values in unaltered teeth. $\Delta^{17}O$ of unaltered enamel can be -291 to -137 per meg which is significantly lower and more varied than the values that have been measured meteoric carbonates which range from -138 to -122 per meg (Passey et al. 2014; Fig 4.1). The restricted range in $\Delta^{17}O$ values of meteoric carbonates that have been measured to date (16 per meg span, see Fig. 4.1 and Passey et al. 2014) is likely due to the small amount of $\Delta^{17}O$ variation in meteoric waters from which carbonates form relative to the variation in $\Delta^{17}O_{enamel}$ values that can be influenced by variation in animal behavior and physiology and fractionation that can occur within the animal and in ingested water sources (e.g. leaves).

The best way to use this distinction between $\Delta^{17}O$ of enamel and meteoric carbonates in the geologic record is to sample both carbonates (meteoric, marine or diagenetic in origin) and bioapatite from a fossil site/location. The $\Delta^{17}O$ values from the fossil teeth should be significantly lower and more varied than the $\Delta^{17}O$ of associated carbonates. If there is significantly overlap in $\Delta^{17}O$ values between the carbonates and enamel and the $\Delta^{17}O$ values of enamel are compressed in distribution ($\Delta^{17}O_{enamel}$ values

< -150 per meg, with < 60 per meg range), then the oxygen isotopes of the system have likely been affected by some post-depositional process and any oxygen isotope data from the enamel should be treated with caution.

4.4.2.3. pCO_2 barometer

As reviewed above, the $\Delta^{17}O$ values of tooth enamel and other forms of bioapatite have been proposed as a CO_2 barometer because these values are strongly influenced by the atmospheric $\Delta^{17}O_{O2}$ value, which in turn is sensitive to concentrations of CO_2 in Earth's atmosphere (e.g., Luz et al., 1999; Bao et al., 2008; Gehler et al., 2016). Measured $\Delta^{17}O$ values of bioapatite and modeled $\Delta^{17}O_{body\ water}$ values indicate that bioapatite can provide constraints to past atmospheric pCO_2 (Pack et al., 2013; Passey et al., 2014; Gehler et al., 2016; Hu et al., *in prep.*). Differences in $\Delta^{17}O_{enamel}$ values of 60 per meg in the fossil record have recently been used to infer changes in pCO_2 across the Paleocene-Eocene Thermal Maximum that range from ca. 400 to 1000 ppmv, depending on the models that are used that relate pCO_2 to atmospheric O_2 $\Delta^{17}O$ and global primary productivity (Gehler et al. 2016). This approach to estimating pCO_2 in Earth's past could be powerful because bioapatite is abundant in the geologic record. However, the successful use of any $\Delta^{17}O_{enamel}$ based CO_2 paleobarometer needs to consider the range of $\Delta^{17}O_{enamel}$ that may exist any one time interval, given that we observe a > 160 per meg range in $\Delta^{17}O_{enamel}$ values in extant mammals that represent a time interval when pCO_2 is relatively steady (and low).

Here we propose that fossil enamel $\Delta^{17}O$ values can be successfully utilized as a pCO_2 barometer when a fossil assemblage is sampled using a community approach at multiple fossil sites. The community approach includes analysis of fossil teeth from any fossil site that represent a range of species, for the purpose of capturing the full range of $\Delta^{17}O_{enamel}$ values that existed. This should then be done at multiple sites to capture the full range in $\Delta^{17}O_{enamel}$ values due to environmental variation within one set of pCO_2 conditions. By sampling teeth at multiple sites using a community approach, one can account for the influences of animal taxonomy and environment on $\Delta^{17}O_{enamel}$ values before using them to infer changes in atmospheric pCO_2. By sampling in this way, we expect to see a wholesale shift in the distribution of minimum and maximum $\Delta^{17}O_{enamel}$ values across multiple sites and taxa if there is a change in pCO_2.

4.5. Conclusion

We find that $\Delta^{17}O_{enamel}$ values from extant mammals range from -291 to -137 per meg and span 161 per meg. The $\Delta^{17}O_{enamel}$ values from extant mammalian herbivores vary as a function of taxonomy and environmental aridity, but they are independent of latitude and $\delta^{18}O$ values of nearby meteoric waters. In addition, because the $\Delta^{17}O_{enamel}$ values are influenced by different variables than those influencing $\delta^{18}O_{enamel}$, $\Delta^{17}O_{enamel}$ adds an additional perspective on geological problems that cannot be reconciled with $\delta^{18}O$ values alone. Measurements of $\Delta^{17}O_{enamel}$ have the potential to expand our understanding of how aridity and pCO_2 has changed through time in any place where fossil teeth are preserved.

We suggest $\Delta^{17}O_{enamel}$ values can be utilized in the following ways:

1) The $\Delta^{17}O_{enamel}$ values obtained for large herbivore communities can be used to provide as an indicator of paleoaridity where $\Delta^{17}O_{enamel}$ values that have a greater range and are more negative point to increasingly arid environments.
2) $\Delta^{17}O$ values can be used to evaluate diagenesis in bioapatite and biocarbonate $\delta^{18}O$ records by directly targeting the oxygen isotopic composition of these materials. It is expected that the $\Delta^{17}O$ values of teeth, bone and eggshells will have a wider range in $\Delta^{17}O$ values than inorganic carbonates because they are influenced by the $\Delta^{17}O$ values of both plant water and atmospheric O_2. Both values are more negative than the $\Delta^{17}O$ values of meteoric waters. Bioapatites or biocarbonates with $\Delta^{17}O$ that are similar to those of associated meteoric-derived carbonates have likely experienced diagenesis.
3) The $\Delta^{17}O_{enamel}$ based paleobarometer for pCO_2 is only valid if the full range in $\Delta^{17}O_{enamel}$ values for any given time interval is considered. Given the large (>160 per meg) range in $\Delta^{17}O_{enamel}$ values for extant mammals that represent conditions with relative steady pCO_2, the most effective way to use the $\Delta^{17}O_{enamel}$ for reconstructing pCO_2 is to sample teeth from multiple taxa from multiple sites to capture the full range in $\Delta^{17}O_{enamel}$ that existed for each time interval of interest.

5. Conclusion

I considered several stable isotope geochemical techniques in this thesis to evaluate past climate and environment. Determining past climate and environment are not always possible using one proxy record and care must be taken to make interpretations using only signals that are specifically related to climate and environment. Other signals, like diagenesis of the primary isotopic composition, can mask the climatic or environmental signal in a material and potentially lead to invalid conclusions.

A powerful way to evaluate past climate and environment is with the isotope geochemical compositions of biominerals. This is because animals interact with their environmental and ecological surrounding, which are directly influenced by regional and global climate. Changes in the isotopic ratios for certain elements in terrestrial biominerals, such as oxygen and carbon, are often used as climate and environmental proxies. The combination of multiple proxy records and analytical techniques can help add detail to the description of vegetation in an environment and enable a more precise evaluation of the manner by which the environment of a region change.

I used the $\delta^{13}C$, $\delta^{18}O$ and $^{87}Sr/^{86}Sr$ values of enamel from modern and fossil herbivores in southwestern South Africa to, 1) evaluate climate and environment in this region since 5 million years ago (Ma) and 2) characterize the distribution of vegetation of this region during the mid-Pleistocene, specifically at archeological site, Elandsfontein. I then presented and characterized the distribution of the $\Delta^{17}O$ of modern herbivore enamel and proposed a method for using $\Delta^{17}O$ values from biominerals to best evaluate aridity, diagenesis and pCO_2 in the fossil record.

In Chapter 2 I presented and discussed the $\delta^{13}C$ and $\delta^{18}O$ values of tooth enamel from fossil sites in southwestern South Africa and form a proxy record of terrestrial environment and vegetation since 5 Ma. The $\delta^{13}C$ values of enamel indicated that large mammalian herbivores ate C_3 vegetation, with little to no C_4 vegetation, across the Pliocene and Pleistocene. Like today, this region was within a winter rainfall zone since 5 Ma. For large mammalian herbivore communities to have had survived in the past, then this region must have been quite different from the dry and hot environment of today. The environment would have supported the growth of substantial amounts of vegetation and the annual growth of C_3 grasses. The $\delta^{18}O$ values of enamel in herbivore families became more enriched by ~ 5‰ between Pliocene fossil site Langebaanweg and mid-Pleistocene Elandsonftein. Regional aridification has been proposed in others studies, but this can not be supported by the $\delta^{18}O$ values of tooth enamel because the depositional environment at these sites are different, making them incomparable using the $\delta^{18}O$ enamel aridity index method presented in Levin et al. (2007). Alternatively, the ~ 5‰ enrichment of enamel $\delta^{18}O$ values can be fully explained by an enrichment of the $\delta^{18}O$ values of source water. The enrichment in the $\delta^{18}O$ values of the source water could have been related to a change from fluvial to spring-fed water (as a change in the depositional environment at the fossil sites indicates). This conclusion is supported by modern $\delta^{18}O$ values from spring waters around Elandsfontein having values ~ 5‰ greater than river waters in the Western Cape of South Africa (Table S2.4). The dataset presented in Chapter 2 of this thesis has combined a number of records from southwestern South Africa and it can be used as a reference paper for researchers studying climate and vegetation in the region.

The dataset in Chapter 2 contains samples from three time periods (~ 5 Ma, ~1 to 0.6 Ma, 0.35 to 0.20 Ma) and there are large gaps between the dataset from each fossil. There is potential to increase the resolution of the stable isotope record of fossil teeth by analyzing teeth from other Pleistocene fossil sites in the study region. Increasing the resolution of the record will help us better understand aridity levels, vegetative composition and seasonality of rainfall and how these features may have changed in response to global climate change and the effects of upwelling of the Benguela Current off the western coast of South Africa. Furthermore, a more detailed analysis of the enamel $\delta^{13}C$ values from known herbivore taxa could potentially provide information about the distribution of vegetation at the fossil sites, but this study was beyond the scope of the thesis.

I was particularly interested in the environment and vegetation at Elandsfontein because this fossil site indicates the presence of hominins. I proposed that Elandsfontein would have attracted hominins and herbivore communities because there was sustainable year round vegetation and standing water (See Chapter 2). However, the importance of Elandsfontein as a location where herbivores and hominins lived within southwestern South Africa needs to be better understood (i.e., did animals stay at Elandsfontein for food because it provided vegetation and water or if they moved around the region and just passed by Elandsfontein). These data could in turn provide information about the distribution of vegetation in southwestern South Africa at ~ 1 Ma and to better evaluate the environment and the vegetative composition of Elandsfontein.

Chapter 3 focused on the $^{87}Sr/^{86}Sr$ ratios in modern teeth from southwestern South Africa and fossil teeth from mid-Pleistocene mammalian herbivores at Elandsfontein. I

tested my hypothesis from Chapter 2 (i.e., that herbivores could find enough vegetation at Elandsfontein) and evaluated the vegetative distribution of southwestern South Africa using enamel $^{87}Sr/^{86}Sr$ ratios of the fossil teeth. The $^{87}Sr/^{86}Sr$ ratios of fossil teeth were compared with the newly updated map of the bioavailable $^{87}Sr/^{86}Sr$ ratios of the major regional substrates in southwestern South Africa (Fig. 3.2). The $^{87}Sr/^{86}Sr$ ratios from herbivore teeth reflected the bioavailable $^{87}Sr/^{86}Sr$ ratios range of marine sands, like those at Elandsfontein.

Overall, the evaluation of $^{87}Sr/^{86}Sr$ ratios of tooth enamel, in addition to that of the $\delta^{13}C$ and $\delta^{18}O$ values of the fossil teeth from Elandsfontein, provided further detail about the ecological and environmental composition of mid-Pleistocene Elandsfontein. These results indicated that herbivores, in particular those that could have migrated around the region for food, did not do so. The landscape at mid-Pleistocene Elandsfontein, which was within a winter rainfall zone, must have had enough vegetation growing throughout the year to support the large, diverse mammalian herbivores. Today the landscape is largely comprised of fynbos shrubs, woody vegetation that is unpalatable and can not support large, herbivorous mammalian communities. This study has also greatly increased the number of data points contributing to the map of bioavailable $^{87}Sr/^{86}Sr$ of southwestern South Africa (Fig. 3.1; Table 3.1); this updated map can be used in future studies of the $^{87}Sr/^{86}Sr$ values in biominerals to determine animal migration and/or past environment and vegetation.

Additional work could add to the understanding of *where* within the coastal region of southwestern South Africa (i.e., on marine sands and or Cape Granites) herbivores found food resources during the mid-Pleistocene. The $^{87}Sr/^{86}Sr$ ratios of fossil

teeth confined the movement of herbivorous animals to the coastal region and quite possibility to the marine sands at Elandsfontein. However, this needs to be studied in further detail by, 1) determining if and how the coastal marines sands and the various granitic bodies that make up the Cape Granite suite separate by their bioavailable $^{87}Sr/^{86}Sr$ ratios, and 2) how these then compare with the fossil tooth enamel $^{87}Sr/^{86}Sr$ ratios from Elandsfontein.

In Chapter 4 I presented $\Delta^{17}O$ data from tooth enamel and outlined the $\Delta^{17}O$ ranges for various modern environments and locations. This was the first report of a detailed dataset of mammalian herbivore tooth enamel $\Delta^{17}O$ values. $\Delta^{17}O$ values of mammalian herbivore communities from arid environments have greater range and include more negative $\Delta^{17}O$ values than samples from humid areas. The $\Delta^{17}O$ value of enamel is not greatly influenced by $\delta^{18}O$ value of local meteoric water or by latitude. Body water $\Delta^{17}O$ values were reconstructed from the enamel $\Delta^{17}O$ values and then compared with modeled body water $\Delta^{17}O$ values determined using the model presented in Hu et al. (*in prep*). In general, the modeled and calculated body water $\Delta^{17}O$ datasets both had larger span and incorporated more negative $\Delta^{17}O$ values with decreasing relative humidity (RH). This comparison allowed us to connect measurable parameters of environment with a proxy record of aridity (i.e., Aridity Index). With decreased Aridity Index, the enamel $\Delta^{17}O$ values of animal communities yielded lower minima and exhibit a greater range of values. I proposed that the most efficient way to use $\Delta^{17}O$ values of fossil teeth, bone and eggshells for understanding paleoclimate and environment is to compare fossil data (series of samples from one fossil community) with the modern dataset presented herein (see Chapter 4). This dataset lays out the ranges in $\Delta^{17}O$ values

that would be expected for materials in different environments and for enamel samples that have not experienced any alteration of their original oxygen isotopic composition.

Adding more samples from different regions and climates, specifically from semi-arid environments, would form a more detailed dataset by which to compare fossil $\Delta^{17}O$ values and in turn to evaluate past environment. The next step in this project is to apply the proposed $\Delta^{17}O$ approaches to the fossil record.

This thesis focused on the isotope geochemistry of fossil tooth enamel to characterize the climate and environment of past terrestrial landscapes. This work highlighted the value of applying various techniques when evaluating past environments. The composition of different isotopes in fossil teeth from one site and time can provide new ways to evaluate past environments, because different isotope systems can capture unique aspects of past climate and environment across local and regional scales. Based on the work presented in this thesis, I advocate for the continued development and use of new isotope geochemical approaches to aid in the evaluation of past climate and environments because they have the potential of adding new dimensions of understanding to geological questions. The continued use of known isotope systems in conjunction with the development and use of new isotope geochemical approaches can provide insight into previously unanswered hypotheses about the past Earth, the puzzles and the unknowns, thereby furthering the understanding of past climate and environments. In addition this aids in the prediction of the changes that we might expect in present and future climates and ecosystems, and importantly, how we as humans have in the past and also might expect to interact with our ever-changing Earth system.

References

Annan, J.D., Hargreaves, J.C., 2013. A new global reconstruction of temperature changes at the Last Glacial Maximum. Climate of the Past. 9, 367-376.

Balasse, M., Ambrose, S.H., Smith, A., Price, T.D., 2002. The seasonal mobility modelfor prehistoric herders in the south-western Cape of South Africa assessed by isotopic analysis of sheep tooth enamel. Journal of Archaeological Science. 29, 917-932.

Bao, H., Lyons, J.R., Zhou, C., 2008. Triple oxygen isotope evidence for elevated CO_2 levels after a Neoproterozoic glaciation. Nature. 453, 504-506.

Bar-Matthews, M., Maren, C.W., Jacobs, Z., Karkanas, P., Fisher, E.C., Herries, A.I.R., Brown, K., Williams, H.M., Bernatchez, J., Ayalon, A., Nilssen, P.J., 2010. A high resolution and continuous isotopic speleothem record of paleoclimate and paleoenvironment from 90 to 53 ka from Pinnacle Point on the south coast of South Africa. Quaternary Science Review. 29, 2131-2145.

Barkan, E., Luz, B., 2005. High precision measurements of $^{17}O/^{16}O$ and $^{18}O/^{16}O$ ratios in H_2O. Rapid Communications of Mass Spectrometry. 19, 3737-3742.

Barkan, E., Luz, B., 2007. Diffusivity fractionations of $H_2{}^{16}O/H_2{}^{17}O$ and $H_2{}^{16}O/H_2{}^{18}O$ in air and their implications for isotope hydrology. Rapid Communications of Mass Spectrometry. 21, 2999-3005.

Belcher, R.W. and Kisters, A.F.M., 2003. Lithostratigraphic correlations in the western branch of the Pan-African Saldania Belt, South Africa: the Malmesbury Group revisited. South African Journal of Geology. 106, 327-342.

Bentley, R.A., 2006. Strontium isotopes from the earth to the archaeological skeleton: a review: Journal of Archaeological Method and Theory. 13, 135-187.

Berger, L.R., Parkington, J.E., 1995. Brief communication: a new Pleistocene hominid-bearing locality at Hoedjiespunt, South Africa. American Journal of Physical Anthropology. 98, 601–609.

Besaans, A.J., 1972. 3217D & 3218 C-st. Helenabaai 3317B & 3318A Saldanhabaai. Geological Survey of South Africa. Department of Mines. Pretoria.

Blumenthal, S.A., Levin, N.E., Cerling, T.E., Brown, F.H., Brugal, J.-P., Chritz, K.L., Harris, J.M., Jehle, G.E., in prep. Aridity and early hominin environments.

Bocherens, H., Koch, P.L., Mariotti, A., Geraads, D., Jaeger, J.-J., 1996. Isotopic biogeochemistry (^{13}C, ^{18}O) of mammalian enamel from African Pleistocene hominid sites. Palaios. 11, 306-318.

Boering, K.A., Jackson, T., Hoag, K.J., Cole, A.S., Perri, M.J., Thiemens, M.H., Atlast, E., 2004. Observations of the anomalous oxygen isotopic composition of carbon dioxide in the lower stratosphere and the flux of the anomaly to the troposphere. Geophysical Research Letters. 31, L03109.

Boom, A., Carr, A.S., Chase, B.M., Grimes, H.L., Meadows, M.E., 2014. Leaf wax n alkanes and $\delta^{13}C$ values of CAM plants from arid southwest Africa. Organic Geochemistry. 67, 99-102.

Bowen, 2016, waterisotopes.org, http://wateriso.utah.edu/waterisotopes/pages/resources/res_main.html, accessed August 1, 2016.

Braun, D.R., Levin, N.E., Stynder, D., Herries, A.I.R., Archer, W., Forrest, F., Roberts, D.L., Bishop, L.C., Matthews, T., Lehmann, S.B., Pickering, R., Fitzsimmons, K.E., 2013. Mid-Pleistocene hominin occupation at Elandsfontein, Western Cape, South Africa. Quaternary Science Reviews. 82, 145-166.

Brumfitt, I., Chinsamy, A., Compton, J., 2013. Depositional environment and bone diagenesis of the Mio/Pliocene Langebaanweg Bonebed, South Africa, South African Journal of Geology 116, 241-258.Bryant, J.D., Koch, P.L., Froelich, P.N., Showers, W.J., Genna, B.J., 1996. Oxygen isotope partitioning between phosphate and carbonate in mammalian apatite. Geochimica et Cosmochimica Acta. 60, 5145-5148.

Butzer, K.W., 1973. Re-evaluation of the geology of the Elandsfontein (Hopefield) Site, South-western Cape, South Africa. South Africa Journal of Science. 69, 234-238.

Cerling, T.E., Andanje, S.A., Blumenthal, S.A., Brown, F.H., Chritz, K.L., Harris, J.M., Hart, J.A., Kirera, F.M., Kaleme, P., Leakey, L.N., Leakey, M.G., Levin, N.E., Manthi, F.K., Passey, B.E., Uno, K.T., 2015. Dietary changes of large herbivores in the Turkana Basin, Kenya from 4 to 1 Ma. Proceedings of the National Academy of Sciences. 112, 11467-11472.

Cerling, T.E., Harris, J.M., 1999. Carbon isotope fractionation between diet and bioapatite in ungulate mammals and implications for ecological and paleoecological studies. Oecologia. 120, 347-363.

Cerling, T.E., Harris, J.M., Hart, J.A., Kaleme, P., Klingel, H., Leakey, M.G., Levin, N.E., Lewison, R.L., Passey, B.H., 2008. Stable isotope ecology of the common hippopotamus. Journal of Zoology. 276, 204-212.

Cerling, T.E., Harris, J.M., Leakey, M.G., 1999. Browsing and grazing in elephants: the isotope record of modern and fossil proboscideans. Oecologia. 120, 364-374.

Cerling, T.E., Harris, J.M., Leakey, M.G., Mudida, N., 2003. Stable isotope ecology of Northern Kenya with emphasis on the Turkana Basin, in: Leakey, M.G., Harris, J.M. (Eds.), Lothagam: The Dawn of Humanity. Columbia University Press, New York, pp. 583-594.

Cerling, T.E., Harris, J.M., Leakey, M.G., Passey, B.H., Levin, N.E., 2010. Stable carbon and oxygen isotopes in East African mammals: modern and fossil, in: Werdelin, L., Sanders, W.J. (Eds.), Cenozoic Mammals of Africa. University of California Press, Berkeley, pp. 949-960.

Cerling, T.E., Harris, J.M., Passey, B.H., 2003. Dietary preferences of East African Bovidae based on stable isotope analysis. Journal of Mammalogy. 84, 456-471.

Cerling, T.E., Hart, J.A., Hart, T.B., 2004. Stable isotope ecology in the Ituri Forest. Oecologia. 138, 5-12.

Cerling, T.E., Manthi, F.K, Mbua, E.N., Leakey, L.N., Leakey, M.G., Leakey, R.E., Brown, F.H., Grine, F.E., Hart, J.A., Kaleme, P., Roche, H., Uno, K.T., Wood, B.A., 2013. Stable isotope-based diet reconstructions of Turkana Basin hominins. Proceedings of the National Academy of Science. 110, 10501-10506.

Chase, B. M. and Meadows, M. E., 2007. Late Quaternary dynamics of southern Africa's winter rainfall zone. Earth-Science Reviews. 84, 103-138.

Chenery, C.A., Pashley, V., Lamb, A.L., Sloane, H.J., Evans, J.A., 2012. The oxygen isotope relationship between the phosphate and structural carbonate fractions of human bioapatite. Rapid Communications in Mass Spectrometry. 26, 309-319.

Codron, D., Luyt, J., Lee-Thorp, J.A., Sponheimer, M., de Ruiter, D., Codron, J., 2005. Utilization of savanna-based resources by Plio-Pleistocene baboons. South African Journal of Science. 101, 245-248.

Copeland, S.R., Cawthra, H.C., Fisher, E.C, Lee-Thorp, J.A., Cowling, R.M., le Roux, P.J., Hodgkins, J., Marean, C.W., 2016. Strontium isotope investigation of ungulate movement patterns on the Pleistocene Paleo-Agulhas Plain of the Greater Cape Floristic Region, South Africa. Quaternary Science Reviews. 141, 65-84.

Copeland, S.R., Sponheimer, M., de Ruiter, D.J., Lee-Thorp, J.A., Codron, D., le Roux, P.J., Grimes, V., and Richards, M.P., 2011. Strontium isotope evidence for landscape use by early hominins. Nature. 474, 76-100.

Copeland, S.R., Sponheimer, M., Lee-Thorp, J.A., le Roux, P.J., de Ruiter, D.J., and Richards, M.P., 2010. Strontium isotope ratios in fossil teeth from South Africa: assessing laser ablation MC ICP-MS analysis and the extent of diagenesis. Journal of Archaeological Science. 37, 1437-1446.

Cowling, R., 1992. Fynbos: South Africa's unique floral kingdom. University of Cape Town Press, Cape Town. 156 pp.

Cowling, R.M., Lombard, A.T., 2002. Heterogeneity, speciation/extinction history and climate: explaining regional plant diversity patterns in the Cape Floristic Region. Diversity and Distributions. 8, 163-179.

Cowling, R.M., Ojeda, F., Lamont, B.B., Rundel, P.W., Lechmere-Oertel, R., 2005. Rainfall reliability, a neglected factor in explaining convergence and divergence of plant traits in fire-prone Mediterranean-climate ecosystems. Global Ecology and Biogeography. 14, 509-519.

Cowling, R.M., Richardson D.M., and Mustart, P.J, 1997. Fynbos: Vegetation of Southern Africa, Cambridge University Press, Cambridge, p. 99-130.

Cuthbert, M.O., Ashley, G.M., 2014. A spring forward for hominin evolution in East Africa. PLoS ONE. 9, 9e107358.

Dansgaard, W., 1964. Stable Isotopes in Precipitation. Tellus. 16, 436-468.

Deacon, H.J., Jury, M.R., and Ellis, F., 1992. Selective regime and time: In, Cowling, R.M. (ed), The Ecology of Fynbos. Nutrients, Fire and Diversity, Oxford University Press, Cape Town, p. 6-22.

deMenocal, P.B., 2004. African climate change and faunal evolution during the Pliocene-Pleistocene. Earth and Planetary Science Letters. 220, 3-24.

Drennan, M.R., 1953. The Saldanha skull and its associations. Nature. 172, 791-793.

Dupont, L., 2011. Orbital scale vegetation change in Africa. Quaternary Science Reviews. 30, 3589-3602.

Dupont, L., Donner, B., Vidal, L., Perez, E., Wefer, G., 2005. Linking desert evolution and coastal upwelling: Pliocene climate change in Namibia. Geology. 33, 461-464.

Dupont, L.M., Rommerskirchen, F., Mollenhauer, G., Schefuß, E., 2013. Miocene to Pliocene changes in South African hydrology and vegetation in relation to the expansion of C_4 plants. Earth Planetary Science Letters. 375, 408-417.

Ericson, J., 1985. Strontium isotope characterization in the study of prehistoric human-ecology. Journal of Human Evolution. 14, 503-514.

Etourneau, J., Martinez, P., Blanz, T., Schneider, R., 2009. Pliocene-Pleistocene variability of upwelling activity, productivity, and nutrient cycling in the Benguela

region. Geology. 37, 871-874.

Eze, P.N. and Meadows, M.E., 2014. Multi-proxy palaeosol evidence for late Quaternary (MIS 4) environmental and climate shifts on the coasts of South Africa. Quaternary International. 343, 159-168.

Faith, J.T., 2011. Ungulate community richness, grazer extinctions, and human subsistence behavior in southern Africa's Cape Floral Region. Palaeogeography, Palaeoclimatology, Palaeoecology. 306, 219-227.

Faith, J.T., Behrensmeyer, A.K. 2013. Climate change and faunal turnover: testing the mechanics of the turnover-pulse hypothesis with South African fossil data: Paleobiology. 39, 609-627.

Farquhar, G.D., Ehleringer, J.R., Hubick, K.T., 1989. Carbon isotope discrimination and photosynthesis. Annual Reviews of Plant Physiology and Molecular Biology. 40, 503-537.

February, E., 1992. Archaeological charcoals as indicators of vegetation change and human fuel choice in the late Holocene at Elands Bay, western Cape Province, South Africa, Journal of Archaeological Science. 19, 347-354.

Franchi, I.A., Wright, I.P., Sexton, A.S., Pillinger, C.T., 1999. The oxygen-isotopic composition of Earth and Mars. Meteoritics and Planetary Science. 34, 657-661.

Franz-Odendaal, T., Chinsamy, A., Lee-Thorp, J.A., 2004. High prevalence of enamel hypoplasia in an early Pliocene giraffid (*Sivatherium hendeyi*) from South Africa. Journal of Vertebrate Paleontology. 24, 235-244.

Franz-Odendaal, T., Lee-Thorp, J., Chinsamy, A., 2002. New evidence for the lack of C_4 grassland expansions during the early Pliocene at Langebaanweg, South Africa. Paleobiology. 28, 378-388.

Gehler, A., Gingerich, P.D., Pack, A., 2016. Temperature and atmospheric CO_2 concentration estimates through the PETM using triple oxygen isotope analysis of mammalian bioapatite. Proceedings of the National Academy of Sciences. 113, 7739-7744.

Gehler, A., Tütken, T., Pack, A., 2011. Triple oxygen isotope analysis of bioapatite as tracer for diagenetic alteration of bones and teeth. Paleogeography, Paleoclimatology, Paleoecology. 310, 84-91.

Halas, S., Skryzpek, G., MeierAugenstein, W., Pelc, A., Kemp, H. F., 2011. Interlaboratory calibration of new silver orthophosphate comparison materials for the stable oxygen isotope analysis of phosphates. Rapid Communications in Mass

Spectrometry. 25, 579-584.

Hare, V., Sealy, J., 2013. Middle Pleistocene dynamics of southern Africa's winter rainfall zone from $\delta^{13}C$ and $\delta^{18}O$ values of Hoedjiespunt faunal enamel. Palaeogeography, Palaeoclimatology, Palaeoecology. 374, 72-80.

Harris, C., Burgers, C., Miller, J., Rawoot, F., 2010. O- and H- isotope record of Cape Town rainfall from 1996 to 2008, and its application to recharge studies of Table Mountain groundwater, South Africa. South African Journal of Geology. 113, 33-56.

Harris, C., Diamond. R., 2013. Oxygen and hydrogen isotopes record of Cape Town rainfall and its application to recharge studies of table mountain groundwater, in: Abiye, T. (Ed.), The Use of Isotope Hydrology to Characterize and Assess Water Resources in Southern(ern) Africa. Water Research Commission, Gezina, South Africa, pp. 38-52.

Harris, C., Oom, B., Diamond, R., 1999. A preliminary investigation of the oxygen and hydrogen isotope hydrology of the greater Cape Town area and an assessment of the potential for using stable isotopes as tracers. Water SA. 25, 15-24.

Hattersley, P.W., 1982. $\delta^{13}C$ values of C_4 types in grasses. Australian Journal of Plant Physiology. 9, 139-154.

Hendey, Q. B., 1976. The Pliocene fossil occurrences in ‘E’ quarry, Langebaanweg, South Africa. Annals of the South African Museum. 69, 215–247.

Higgins, P., MacFadden, B.J., 2004. The “Amount Effect” recorded in oxygen isotopes of Late Glacial horse (*Equus*) and bison (*Bison*) teeth from the Sonoran and Chihuahuan deserts, southwestern United States. Palaeogeography, Palaeoclimatology, Palaeoecology. 206, 337-353.

Hoetzel, S., Dupont, L., Schefuß, E., Rommerskirchen, F., Wefer, G., 2013. The role of fire in Miocene to Pliocene C_4 grassland and ecosystem evolution. Nature Geoscience. 6, 1027–1030.

Hopley, P.J., Weedon, G. P., Marshall, J. D., Herries, A. I. R., Latham, A. G., Kuykendall, K. L., 2007. High- and low- latitude orbital forcing of early hominin habitats in South Africa. Earth and Planetary Science Letters. 256, 419-432.

Hopley, P.J., Weedon, G.P., Marshall, J.D., Herries, A.I.R., Latham, A.G., Kuykendall, K.L., 2007. High- and low-latitude orbital forcing of early hominin habitats in South Africa. Earth and Planetary Science Letters. 256, 419-432.

Hoppe, K.A., 2006. Correlation between the oxygen isotope ratio of North American bison teeth and local waters: Implication for paleoclimatic reconstructions. Earth and Planetary Science Letters. 244, 408 417.

Hu, H., Passey, B.H., Lehmann, S.B., Levin, N.E., Johnson, B.J., in prep. Modeling and interpreting triple oxygen isotope variations in animal body water.

Hulston, J.R., Thode, H.G., 1965. Variations in the S^{33}, $S^{3}4$, and S^{36} contents of meteorites and their relation to chemical and nuclear effects. Journal of Geophysical Research. 70, 3475-3484.

Iacumin, P., Bocherens, H., Mariotti, A., Longinelli, A., 1996. Oxygen isotope analyses of co-existing carbonate and phosphate in biogenic apatite: A way to monitor diagenetic alteration of bone phosphate? Earth and Planetary Science Letters. 142, 1-6.

IAEA/WMO, 2001. Global Network of Isotopes in Precipitation. The GNIP Database (available at: http://isohis.iaea.org.).

Imbrie, J., Boyle, E.A., Clemens, S. C., Duffy, A., Howard, W. R., Kukla, G., Kutzbach, J., Martinson, D. G., McIntyre, A., Mix, A. C., Molfino, B., Morley, J. J., Peterson, L. C., Pisias, N. G., Prell, W. L., Raymo, M. E., Shackleton, N. J., Toggweiler, J. R., 1992. On the Structure and Origin of Major Glaciation Cycles 1. Linear Responses to Milankovitch Forcing. Paleoceanography. 7, 701-738.

Kim, S. and O'Neil, J.R., 2005. An experimental study of oxygen isotope fractionation between inorganically precipitated aragonite and water at low temperatures; discussion. Geochimica et Cosmochimica Acta. 69, 3195-3197.

Klein, R. G., 1978. The fauna and overall interpretation of the 'Cutting 10' Acheulean site at Elandsfontein (Hopefield), southwestern Cape Province, South Africa. Quaternary Research. 10, 69-83.

Klein, R.G., 1982. Patterns of ungulate mortality and ungulate mortality profiles from Langebaanweg (early Pliocene) and Elandsfontein (middle Pleistocene), south-Western Cape Province, South Africa. Annals of the South African Museum. 90, 49-94.

Klein, R.G., 1983. Paleoenvironmental implications of Quaternary large mammals in the Fynbos biome. South African National Progress Reports. 75, 116-138.

Klein, R.G., 1991. Size variation in the Cape Dune Molerat (*Bathyergus suilus*) and Late Quaternary climatic change in the Southwestern Cape Province, South Africa. Quaternary Research. 36, 243-256.

Klein, R.G., Avery, G., Cruz-Uribe, K., Steele, T.E., 2007. The mammalian fauna associated with an archaic hominin skullcap at later Acheulean artifacts at Elandsfontein, Western Cape Province, South Africa. Journal of Human Evolution. 52, 164-186.

Klein, R.G., Cruz-Uribe, K., 1991. The bovids from Elandsfontein, South Africa, and their implications for the age, palaeoenvironment, and origins of the site. The African Archaeological Review. 9, 21-79.

Kohn, M.J., 1996. Predicting animal $\delta^{18}O$: accounting for diet and physiological adaptation. Geochimica et Cosmochimica Acta. 60, 4811-4829.

Kohn, M.J., 2010. Carbon isotope compositions of terrestrial C_3 plants as indicators of (paleo)ecology and (paleo)climate. Proceedings of the National Academy of Sciences. 107, 19691- 19695.

Kohn, M.J., Cerling, T.E., 2002. Stable isotope compositions of biological apatite. In Kohn, M.J., Rakovan, J., Hughes, J.M., (Eds.). Phosphates: Geochemical, Geobiological and Material Importance. Reviews in Mineralogy and Geochemistry. Mineralogical Society of America, Washington, DC. 48, 455-488.

Landais, A., Barkan, E., Yakir, D., Luz, B., 2006. The triple isotopic composition of oxygen in leaf water. Geochimica et Cosmochimica Acta. 70, 4105-4115.

Lécuyer, C., Balter, V., Martineau, F., Fourel, F., Bernard, A., Amiot, R., Gardien, V., Otero, O., Legendre, S., Panczer, G., Simon, L., Martini, R., 2010. Oxygen isotope fractionation between apatite-bound carbonate and water determined from controlled experiments with synthetic apatites precipitated at 10-37˚C. Geochimica et Cosmochimica Acta. 74, 2072-2081.

Lee-Thorp, J., Beaumont, P., 1995. Vegetation and seasonality shifts during the Late Quaternary deduced from $^{13}C/^{12}C$ ratios of grazers at Equus Cave, South Africa. Quaternary Research. 43, 426-432.

Lee-Thorp, J.A., van der Merwe, N.J., Brain, C.K., 1989. Isotopic evidence for dietary differences between two extinct baboon species from Swartkrans. Journal of Human Evolution. 18, 183-189.

Lehmann, S.B., Braun, D.R., Dennis, K.J., Patterson, D.B., Stynder, D.D., Bishop, L.C., Forrest, F., Levin, N.E., 2016. Stable isotopic composition of fossil mammal teeth and environmental change in southwestern South Africa during the Pliocene and Pleistocene. Palaeogeography, Palaeoclimatology, Palaeoecology. 457, 396-408.

Levin, N.E., Cerling, T.E., Passey, B.H., Harris, J.M., Ehleringer, J. R., 2006. A stable isotope aridity index for terrestrial environments. Proceedings of the National Academy of Sciences. 103, 11201-11205.

Levin, N.E., Haile-Selassie, Y., Frost, S.R., Saylor, B.Z., 2015. Dietary change among hominins and cercopithecids in Ethiopia during the early Pliocene. Proceedings of the National Academy of Science. 112, 12304-12309.

Levin, N.E., Simpson, S.W., Quade, J., Cerling, T.E., Frost, S.R., 2008. Herbivore enamel carbon isotopic composition and the environmental context of *Ardipithecus* at Gona, Ethiopia, in: Quade, J., Wynn, J.G. (Eds.), The Geology of Early Humans in the Horn of Africa. Geological Society of America, Boulder, pp. 215-234.

Li, S., Levin, N.E., Chesson, L.A., 2015. Continental scale variation in ^{17}O-excess of meteoric waters in the United States. Geochimica et Cosmochimica Acta. 164, 110-126.

Luyt, J., Lee-Thorp, J., Avery, G., 2000. New light on Middle Pleistocene west coast environments from Elandsfontein, Western Cape Province, South Africa. South African Journal of Science. 96, 399-403.

Luz, B., Barkan, E., 2010. Variations of $^{17}O/^{16}O$ and $^{18}O/^{16}O$ in meteoric waters. Geochimica et Cosmochimica Acta. 74, 6276-6286.

Luz, B., Barkan, E., Bender, M.L., Thiemens, M.H., Boering, K.A., 1999. Triple-isotope composition of atmospheric oxygen as a tracer of biosphere productivity. Nature. 400, 547-550.

Mabbutt, J.A., 1956. The physiography and surface geology of the Hopefield fossil site. Transactions of the Royal Society of South Africa. 35, 21-58.

Marlow, J., Lange, C., Wefer, G., Rosell-Mele, A., 2000. Upwelling intensification as part of the Pliocene-Pleistocene climate transition. Science. 290, 2288-2291.

Martin, C., Bentaleb, I., Kaandorp, R., Iacumin, P., Chatri, K., 2008. Intra-tooth study of modern Rhinoceros enamel $\delta^{18}O$; is the difference between phosphate and carbonate $\delta^{18}O$ a sound diagenetic test? Palaeogeography, Palaeoclimatology, Palaeoecology. 266, 183-189.

Matsuhisa, Y., Goldsmith, J.R., Clayton, R.N., 1978. Mechanisms of hydrothermal crystallization of quartz at 250˚C and 15kbar. Geochimica et Cosmochimica Acta. 42, 173-182.

McClymont, E.L., Rosell-Melé, A., Giraudeau, J., Pierre, C., Lloyd, J.M., 2005. Alkenone and coccolith records of the mid-Pleistocene in the south-east Atlantic: Implications for the index and South African climate. Quaternary Science Reviews. 24, 1559-1572.

Meadows, M.E., Baxter, A.J., Parkington, J., 1996. Late Holocene environments at Verlorenvlei, Western Cape Province, South Africa. Quaternary International. 33, 81-95.

Meijer, H.A.J., Li, W.J., 1998. The use of electrolysis for accurate $\delta^{17}O$ and $\delta^{18}O$ isotope measurements in water. Isotopes in Environmental Health Studies. 34, 349-369.

Midgley, J., Scott, D., 1994. The use of stable isotopes of water (D and ^{18}O) in hydrological studies in the Jonkershoek Valley. Water SA. 20, 151-154.

Miller, M.F., 2002. Isotopic fractionation and the quantification of ^{17}O anomalies in the oxygen three-isotope system: an appraisal and geochemical significance. Geochimica et Cosmochimica Acta. 66, 1881-1889.

National Oceanic and Atmospheric Administration (2014) Basic climate statistics data using NOAA regional climate center applied climate information system, NOAA's Online Weather Date (NOWData).

New, M., Lister, D., Hulme, M., Makin, I., 2002. A high-resolution data set of surface climate over global land areas. Climate Research. 21, 1-25.

O'Neil, J.R., Roe, L.J., Reinhard, E., Blake, R.E.,1994. A rapid and precise method of oxygen isotope analysis of biogenic phosphate. Israel Journal of Earth Sciences. 43, 203-212.

Pack, A., Gehler, A., Süssenberger, A., 2013. Exploring the usability of isotopically anomalous oxygen in bones and teeth as paleo-CO_2-barometer. Geochimica et Cosmochimica Acta..102, 306-317.

Pack, A., Herwartz, D., 2014. The triple oxygen isotope composition of the Earth mantle and understanding variations in terrestrial rocks and minerals. Earth and Planetary Science Letters. 390, 138-145.

Passey, B.H., Cerling, T.E., 2006. In situ stable isotope analysis ($\delta^{13}C$, $\delta^{18}O$) of very small teeth using laser ablation GC/IRMS. Chemical Geology. 235, 238-249.

Passey, B.H., Cerling, T.E., Levin, N.E., 2007. Temperature dependence of oxygen isotope acid fractionation for modern and fossil tooth enamels. Rapid Communications in Mass Spectrometry. 21, 2853-2859.

Passey, B.H., Cerling, T.E., Schuster, G.T., Robinson, T.F., Roeder, B.L., Krueger, S.K., 2005. Inverse methods for estimating primary input signals from time-averaged isotope profiles. Geochimica et Cosmochimica Acta. 69, 4101-4116.

Passey, B.H., Hu, H., Ji, H., Montanari, S., Li, S., Henkes, G.A., Levin, N.E., 2014. Triple oxygen isotopes in biogenic and sedimentary carbonates. Geochimica et Cosmochimica Acta. 141, 1-25.

Passey, B.H., Levin, N.E., Cerling, T.E., Brown, F.H., Eiler, J.M., 2010. High-temperature environments of human evolution in East Africa based on bond ordering in paleosol carbonates. Proceedings of the National Academy of Sciences. 107,

11245-11249.

Patterson, D.B., Lehmann, S.B., Matthews, T., Levin, N.E., Stynder, D., Braun, D.R., 2016. Stable isotope ecology of Cape dune mole-rats (Bathyergus suillus) from Elandsfontein, South Africa: implications for C_4 vegetation and hominin paleoecology in the Cape Floral Region. Palaeogeography, Palaeoclimatology, Palaeoecology. 457, 409-421.

Petit, J.R., Jouzel, J., Raynaud, D., Barkov, N.I., Barnola, J.-M., Basile, I., Bender, M., Chappellaz, J., Davis, M., Delaygue, G., Delmotte, M., Kotlyakov, V.M., Legrand, M. Lipenkov, V.Y., Lorius, C., PÉpin, L., Ritz, C., Saltzman, E., Stievenard, M., 1999. Climate and atmospheric history of the past 420,000 years from the Vostok ice core, Antarctica. Nature. 399, 429-436.

Pin, C., Briot, D., Bassin, C., Poitrasson, F., 1994. Concomitant separation of strontium and samarium-neodymium for isotopic analysis in silicate samples, based on specific extraction chromatography. Analytica Chimica Acta. 298, 209-217.

Radloff, F.G.T., 2008. The ecology of large herbivores native to the coastal lowlands of the Fynbos Biome in the Western Cape, South Africa. Doctoral Dissertation, Department of Botany, University of Stellenbosh, South Africa.

Rebelo, A.G., Boucher, C., Helme, N., Mucina, L., and Rutherford, M.C., 2006, Fynbos biome: The vegetation of South Africa, South African National Biodiversity Institute, p. 53-219.

Roberts, D.L., Bateman, M.D., Murray-Wallace, C.V., Carr, A.S., Holmes, P.J., 2009. West coast dune plumes: climate driven contrasts in dunefield morphogenesis along the western and southern South African coasts. Palaeogeography, Palaeoclimatology, Palaeoecology. 271, 24-38.

Roberts, D.L., Matthews, T., Herries, A.I.R., Boulter, C., Scott, L., Dondo, C., Mtembi, P., Browning, C., Smith, R.M.H., Haarhoff, P., Bateman, M.D., 2011. Regional and global context of the Late Cenozoic Langebaanweg (LBW) palaeontological site: West Coast of South Africa. Earth-Science Reviews. 106, 191-214.

Rossouw, L., Stynder, D., Haarhof, P., 2009. Evidence for opal phytolith preservation in the Langebaanweg 'E' Quarry Varswater Formation and its potential for palaeohabitat reconstruction. South African Journal of Science. 105, 223-227.

Rowley, D.B., Currie, B.S., 2006. Palaeo-altimetry of the late Eocene to Miocene Lunpola basin, central Tibet. Nature. 439, 677-681.

Rozanski, K., Aragua´s-Aragua´s, L., Gonfiantini, R., 1993. Isotopic patterns in modern global precipitation. In: Swart, P.K., Lohmann, K.C., McKenzie, J., Savin, S. (Eds.),

Climate Change in Continental Isotopic Records. American Geophysical Union Geophysical Monograph. American Geophysical Union. Washington, DC. 78, 1-36.

Rozendaal, A., Gresse, P.G., Scheepers, R. and Le Roux, J.P., 1999. Neoproterozoic to early Cambrian Crustal Evolution of the Pan-African Saldania Belt, South Africa. Precambrian Research. 97, 303-323.

Ruddiman, W.F., Raymo, M.E., Martinson, D.G., Clement, B.M., Backman, J., 1989. Pleistocene evolution: Northern Hemisphere ice sheets and North Atlantic Ocean. Paleoceanography. 4, 353- 412.

Ruxton, G.D., Wilkinson, D.M., 2011. Thermoregulation and endurance running in extinct hominins: Wheeler's models revisited. Journal of Human Evolution. 61, 169-175.

Ryan, W.B.F., Carbotte, S.M., Coplan, J.O., O'Hara, S., Melkonian, A., Arko, R., Weissel, R.A., Ferrini, V., Goodwillie, A., Nitsche, F., Bonczkowski, J., Zemsky, R., Global multi-resolution topography synthesis. Geochemistry Geophysics Geosystems. 10, Q03014.

Scheepers, R., 1995. Geology, Geochemistry and petrogenesis of Late Precambrian S-, I- and A type granitoids in the Saldania Belt, Western Cape Province South Africa. Journal of African Earth Sciences. 2, 35-58.

Schoenemann, S.W., Schauer, A.J., Steig, E.J., 2013. Measurement of SLAP2 and GISP $\delta^{17}O$ and proposed VSMOW-SLAP normalization for $\delta^{17}O$ and $\delta^{18}O$. Rapid Communications in Mass Spectrometry. 27, 582-590.

Sealy, J., van der Merwe, N., Sillen, A., Kruger, F., and Krueger, H., 1991. $^{87}Sr/^{86}Sr$ as a dietary indicator in modern and archaeological bone. Journal of Archaeological Science. 18, 399-416.

Shackleton, N.J., Berger, A., Peltier, W.R., 1900. An alternative astronomical calibration of the lower Pleistocene timescale based on ODP Site 677. Transactions of the Royal Society of Edinburgh. 81, 251-261.

Shackleton, N.J., Crowhurst, S., Hagelberg, T., Pisias, N.G., Schneider, D.A., 1995. A new late Neogene time scale: application to Leg 138 sites. Proceedings of Ocean Drilling Program Scientific Results. 138, 73-101.

Sharp, Z.D., Gibbons, J.A., Maltsev, O., Atudorei, V., Pack, A., Sengupta, S., Shock, E.L., Knauth, L.P., 2016. A calibration of the triple oxygen isotope fractionation in the SiO2–H2O system and applications to natural samples. Geochimica et Cosmochimica Acta. 186, 105-119.

Sillen, A., 1986. Biogenic and Diagenetic Sr/Ca in Plio-Pleistocene fossils of the Omo Shungura Formation. Paleobiology. 12, 311-323.

Singer, R., Wymer, J., 1968. Archaeological investigations at the Saldanha skull site in South Africa. South African Archaeological Bulletin. 23, 63-74.

Sponheimer, M., Reed, K., Lee-Thorp, J.A., 2001. Isotopic palaeoecology of Makapansgat Limeworks Perissodactyla. South African Journal of Sciences. 97, 327-327.

Stynder, D.D., 1997. The use of faunal evidence to reconstruct site history at Hoedjiespunt 1 (HDP1). Western Cape. Masters Thesis. Department of Archaeology. University of Cape Town.

Stynder, D.D., 2009. The diets of ungulates from the hominid fossil-bearing site of Elandsfontein, Western Cape, South Africa. Quaternary Research. 71, 62-70.

Stynder, D.D., 2011. Fossil bovid diets indicate a scarcity of grass in the Langebaanweg E Quarry (South Africa) late Miocene/early Pliocene environment. Paleobiology. 37, 126-139.

Stynder, D.D., Moggi-Cecchi, J., Berger, L.R., Parkington, J.E., 2001. Human mandibular incisors from the late Middle Pleistocene locality of Hoedjiespunt 1, South Africa. Journal of Human Evolution. 41, 369–383.

Surma, J., Assonov, S., Bolourchi, M.J., Staubwasser, M., 2015. Triple oxygen isotope signatures in evaporated water bodies from the Sistan Oasis, Iran. Geophysical Research Letters. 42, 8456-8462.

Tipple, B. J., Meyers, S.R., Pagani, M., 2010. Carbon isotope ratio of Cenozoic CO_2; a comparative evaluation of available geochemical proxies. Paleoceanography. 25, PA3202.

UNESCO, 1979. Map of the world distributions of arid regions, explanatory note, MAB Technical Notes, Paris.

Vennemann, T., Fricke, H., Blake, R., O'Neil, J., Colman, A., 2002. Oxygen isotope analysis of phosphates: a comparison of techniques for analysis of Ag_3PO_4. Chemical Geology. 185, 321-336.

Vogel, J.C., Fuls, A., Ellis, R.P., 1978. The geographical distribution of Kranz grasses in South Africa. South African Journal of Science. 74, 209-215.

Weaver, J.M.C., Talma, A.S., 2005. Cumulative rainfall collectors - A tool for assessing groundwater recharge. Water SA. 31, 283-290.

West, A.G., February, E. C., Bowen, G.J., 2014. Spatial analysis of hydrogen and oxygen stable isotopes ('isoscapes') in ground water and tap water across South Africa. Journal of Geochemical Exploration. 145, 213-222.

Young, E.D., Galy, A., Nagahara, H., 2002. Kinetic and equilibrium mass-dependent isotope fractionation laws in nature and their geochemical and cosmochemical significance. Geochimica et Cosmochimica Acta. 66, 1095-1104.

Zachos, J., Pagani, M., Sloan, L., Thomas, E., Billups, K., 2001. Trends, rhythms, and aberrations in global climate 65 Ma to present. Science. 292, 686-693.

Zazzo, A., 2001. Validation méthodologique de l'utilisation des compositions isotopiques (^{13}C, ^{18}O) des bioapatites fossiles pour les reconstitutions des paléoenvironnement continentaux. Thèse de doctorat de l'université Pierre et Marie Curie, Paris 6.

Appendix I
(CHAPTER 2 Supplementary Tables)

Table S2.1: Estimated $\delta^{13}C$ values for atmospheric CO_2, vegetation and herbivore tooth enamel for the time intervals discussed in the text.

	Time Interval (Ma)			
	Present $\delta^{13}C$ (‰ VPDB)	**Hoedjiespunt $\delta^{13}C$ (‰ VPDB) (0.35 - 0.25 Ma)**	**Elandsfontein $\delta^{13}C$ (‰ VPDB) (~1.0 - 0.6 Ma)**	**Langebaanweg $\delta^{13}C$ (‰ VPDB) (~5 Ma)[a]**
Time span from benthic foraminifera record (Ma)	n/a	0.35 - 0.25	1.0 - 0.6	5.7 - 3.33
$\delta^{13}C$ CO_2 [b]	-8.0	-7.1	-7.1	-6.3
$\delta^{13}C$ of vegetation (‰ VPDB)[c]				
C_3 (average)	-26.1	-25.3	-25.3	-24.5
C_3 minimum	-31.7	-30.8	-30.8	-30.0
C_3 maximum	-23.1	-22.2	-22.2	-21.4
C_4 (average)	-11.0	-10.1	-10.1	-9.3
C_4 minimum (mesic)	-10.0	-9.1	-9.1	-8.3
C_4 maximum (xeric)	-14.0	-13.2	-13.2	-12.4
$\delta^{13}C_{enamel}$ (‰ VPDB)[d]				
C_3 diet (average)	-12.6	-11.5	-11.5	-10.7
C_3 diet minimum	-18.2	-17.1	-17.1	-16.4
C_3 diet maximum	-9.5	-8.4	-8.4	-7.6
C_4 diet (average)	2.9	3.8	3.8	4.6
C_4 diet minimum (mesic)	3.9	4.9	4.9	5.7
C_4 diet maximum (xeric)	-0.2	0.8	0.8	1.6

[a] Paleo-CO_2 record is based on the mean benthic foraminifera record with two data points for the Langebaanweg time period that date to 5.7 Ma and 3.33 Ma (-6.19‰ and -6.35‰, respectively).

[b] Foraminifera isotopic data are used to estimate the $\delta^{13}C$ value of atmospheric CO_2 (Tipple et al., 2010).

[c] The $\varepsilon_{atmosphere\text{-}plant}$ values were calculated from the modern $\delta^{13}C$ values of CO_2 and the average, minimum and maximum $\delta^{13}C$ values of C_4 (Hattersley, 1982) and C_3 plants (Kohn, 2010). The $\varepsilon_{atmosphere\text{-}plant}$ values and the average reconstructed $\delta^{13}C$ values of CO_2 for each time period (Tipple et al., 2010) were used to estimate the $\delta^{13}C$ values of C_3 and C_4 vegetation in the past.

[d] The $\delta^{13}C$ values of enamel for herbivores with a diet of C_3 and C_4 vegetation were calculated using an $\varepsilon_{plant\text{-}enamel}$ of +14.1‰ (Cerling et al., 1999) and the calculated plant $\delta^{13}C$ values at each time period denoted in this table.

Table S2.2: Compilation of new and published $\delta^{13}C$ and $\delta^{18}O$ values of the carbonate component of tooth enamel from Pliocene and Pleistocene sites in southwestern South Africa.

Sample ID	Family	Tribe	Genus	Species	Locality	Collection, horizon[b]	Bay[c]	Behavior[d]	$\delta^{13}C_{enamel}$ (‰ VPDB)	1σ	$\delta^{18}O_{enamel}$ (‰ VSMOW)[e]	1σ	n[f]	Tooth element[g]	Reference
-	Bovidae	Alcelaphini	*Connochaetes/Alcelaphus*	-	Hoedjiespunt	Hoedjiespunt 1, HOMS	-	Grazer	-9.2	-	31.2	-	-	Third molar when possible	Hare and Sealy, 2013
-	Bovidae	Alcelaphini	*Connochaetes/Alcelaphus*	-	Hoedjiespunt	Old Hoedjiespunt	-	Grazer	-9.8	-	31.9	-	-	Third molar when possible	Hare and Sealy, 2013
-	Bovidae	Alcelaphini	*Connochaetes/Alcelaphus*	-	Hoedjiespunt	Hoedjiespunt 1, HOMS	-	Grazer	-10.0	-	32.0	-	-	Third molar when possible	Hare and Sealy, 2013
-	Bovidae	Alcelaphini	*Connochaetes/Alcelaphus*	-	Hoedjiespunt	Hoedjiespunt 1, HOMS	-	Grazer	-9.7	-	29.5	-	-	Third molar when possible	Hare and Sealy, 2013
-	Bovidae	Alcelaphini	*Connochaetes/Alcelaphus*	-	Hoedjiespunt	Hoedjiespunt 1, HOMS	-	Grazer	-9.6	-	31.3	-	-	Third molar when possible	Hare and Sealy, 2013
-	Bovidae	Alcelaphini	*Connochaetes/Alcelaphus*	-	Hoedjiespunt	Hoedjiespunt 1, HOMS	-	Grazer	-8.1	-	31.0	-	-	Third molar when possible	Hare and Sealy, 2013
-	Bovidae	Alcelaphini	*Connochaetes/Alcelaphus*	-	Hoedjiespunt	Hoedjiespunt 1, HOMS	-	Grazer	-10.2	-	31.7	-	-	Third molar when possible	Hare and Sealy, 2013
-	Bovidae	Alcelaphini	*Connochaetes/Alcelaphus*	-	Hoedjiespunt	Old Hoedjiespunt	-	Grazer	-10.3	-	29.7	-	-	Third molar when possible	Hare and Sealy, 2013
-	Bovidae	Alcelaphini	*Connochaetes/Alcelaphus*	-	Hoedjiespunt	Old Hoedjiespunt	-	Grazer	-9.0	-	30.4	-	-	Third molar when possible	Hare and Sealy, 2013
-	Bovidae	Alcelaphini	*Connochaetes/Alcelaphus*	-	Hoedjiespunt	Old Hoedjiespunt	-	Grazer	-9.0	-	29.7	-	-	Third molar when possible	Hare and Sealy, 2013
-	Bovidae	Alcelaphini	*Connochaetes/Alcelaphus*	-	Hoedjiespunt	Old Hoedjiespunt	-	Grazer	-10.2	-	30.1	-	-	Third molar when possible	Hare and Sealy, 2013
-	Bovidae	Alcelaphini	*Connochaetes/Alcelaphus*	-	Hoedjiespunt	Old Hoedjiespunt	-	Grazer	-7.5	-	29.7	-	-	Third molar when possible	Hare and Sealy, 2013
-	Bovidae	Alcelaphini	*Damaliscus*	*pygargus pygargus*	Hoedjiespunt	Hoedjiespunt 1, HOMS	-	Grazer	-9.3	-	28.8	-	-	Third molar when possible	Hare and Sealy, 2013
-	Bovidae	Alcelaphini	*Damaliscus*	*pygargus pygargus*	Hoedjiespunt	Hoedjiespunt 1, HOMS	-	Grazer	-13.1	-	31.8	-	-	Third molar when possible	Hare and Sealy, 2013
-	Bovidae	Alcelaphini	*Damaliscus*	*pygargus pygargus*	Hoedjiespunt	Hoedjiespunt 1, LCSS	-	Grazer	-11.1	-	34.3	-	-	Third molar when possible	Hare and Sealy, 2013
-	Bovidae	Alcelaphini	*Damaliscus*	*pygargus pygargus*	Hoedjiespunt	Hoedjiespunt 1, HOMS	-	Grazer	-10.4	-	33.3	-	-	Third molar when possible	Hare and Sealy, 2013
-	Bovidae	Antelopini	*Antidorcas*	*australis*	Hoedjiespunt	Hoedjiespunt 1, ROOF	-	Mixed feeder	-8.9	-	29.5	-	-	Third molar when possible	Hare and Sealy, 2013
-	Bovidae	Antelopini	*Antidorcas*	*australis*	Hoedjiespunt	Hoedjiespunt 1, LCSS	-	Mixed feeder	-11.1	-	28.8	-	-	Third molar when possible	Hare and Sealy, 2013
-	Bovidae	Antelopini	*Antidorcas*	*australis*	Hoedjiespunt	Hoedjiespunt 1, LCSS	-	Mixed feeder	-10.6	-	31.0	-	-	Third molar when possible	Hare and Sealy, 2013
-	Bovidae	Antelopini	*Antidorcas*	*australis*	Hoedjiespunt	Hoedjiespunt 1, HOMS	-	Mixed feeder	-8.5	-	33.5	-	-	Third molar when possible	Hare and Sealy, 2013
-	Bovidae	Antelopini	*Antidorcas*	*australis*	Hoedjiespunt	Hoedjiespunt 1, HOMS	-	Mixed feeder	-9.1	-	33.0	-	-	Third molar when possible	Hare and Sealy, 2013
-	Bovidae	Bovini	*Bovini*	-	Hoedjiespunt	Hoedjiespunt 1, HOMS	-	Grazer	-8.0	-	33.3	-	-	Third molar when possible	Hare and Sealy, 2013
-	Bovidae	Bovini	*Bovini*	-	Hoedjiespunt	Hoedjiespunt 1, HOMS	-	Grazer	-6.1	-	32.4	-	-	Third molar when possible	Hare and Sealy, 2013
-	Bovidae	Cephalophini	*Sylvicapra*	*grimmia*	Hoedjiespunt	Hoedjiespunt 1, LCSS	-	Browser	-10.1	-	31.1	-	-	Third molar when possible	Hare and Sealy, 2013
-	Bovidae	Cephalophini	*Sylvicapra*	*grimmia*	Hoedjiespunt	Hoedjiespunt 1, LCSS	-	Browser	-10.1	-	32.6	-	-	Third molar when possible	Hare and Sealy, 2013
-	Bovidae	Cephalophini	*Sylvicapra*	*grimmia*	Hoedjiespunt	Hoedjiespunt 1, LCSS	-	Browser	-11.1	-	29.6	-	-	Third molar when possible	Hare and Sealy, 2013
-	Bovidae	Neotragini	*Raphicerus*	-	Hoedjiespunt	Hoedjiespunt 1, ROOF	-	Mixed feeder	-10.0	-	33.7	-	-	Third molar when possible	Hare and Sealy, 2013
-	Bovidae	Neotragini	*Raphicerus*	-	Hoedjiespunt	Hoedjiespunt 1, HOMS	-	Mixed feeder	-9.6	-	31.2	-	-	Third molar when possible	Hare and Sealy, 2013
-	Bovidae	Neotragini	*Raphicerus*	-	Hoedjiespunt	Old Hoedjiespunt	-	Mixed feeder	-5.5	-	31.8	-	-	Third molar when possible	Hare and Sealy, 2013
-	Bovidae	Reduncini	*Redunca*	*arundinum*	Hoedjiespunt	Hoedjiespunt 1, LCSS	-	Grazer	-11.8	-	34.1	-	-	Third molar when possible	Hare and Sealy, 2013
-	Bovidae	Reduncini	*Redunca*	*arundinum*	Hoedjiespunt	Old Hoedjiespunt	-	Grazer	-8.6	-	31.3	-	-	Third molar when possible	Hare and Sealy, 2013
-	Bovidae	Tragelaphini	*Tragelaphus*	*strepsiceros*	Hoedjiespunt	Hoedjiespunt 1, HOMS	-	Browser	-11.3	-	32.1	-	-	Third molar when possible	Hare and Sealy, 2013
-	Bovidae	Tragelaphini	*Tragelaphus*	*strepsiceros*	Hoedjiespunt	Old Hoedjiespunt	-	Browser	-9.0	-	29.8	-	-	Third molar when possible	Hare and Sealy, 2013
-	Bovidae	Tragelaphini	*Tragelaphus*	*strepsiceros*	Hoedjiespunt	Hoedjiespunt 1, GUFI	-	Browser	-10.3	-	30.9	-	-	Third molar when possible	Hare and Sealy, 2013
-	Bovidae	Tragelaphini	*Tragelaphus*	*strepsiceros*	Hoedjiespunt	Hoedjiespunt 1, HOMS	-	Browser	-10.1	-	33.3	-	-	Third molar when possible	Hare and Sealy, 2013
-	Bovidae	Tragelaphini	*Tragelaphus*	*strepsiceros*	Hoedjiespunt	Old Hoedjiespunt	-	Browser	-8.5	-	30.7	-	-	Third molar when possible	Hare and Sealy, 2013
-	Bovidae	Tragelaphini	*Tragelaphus*	*strepsiceros*	Hoedjiespunt	Old Hoedjiespunt	-	Browser	-11.1	-	30.0	-	-	Third molar when possible	Hare and Sealy, 2013
-	Bovidae	Tragelaphini	*Tragelaphus*	*strepsiceros*	Hoedjiespunt	Hoedjiespunt 1, ROOF	-	Browser	-8.2	-	30.4	-	-	Third molar when possible	Hare and Sealy, 2013
-	Bovidae	Tragelaphini	*Tragelaphus*	*oryx*	Hoedjiespunt	Hoedjiespunt 1, HOMS	-	Mixed feeder	-7.8	-	32.3	-	-	Third molar when possible	Hare and Sealy, 2013
-	Bovidae	Alcelaphini	*Connochaetes*	*gnou*	Elandsfontein	EFTM	-	Grazer	-11.8	-	30.3	-	-	Second or third molar when possible	Luyt et al., 2000
EFTM 11281	Bovidae	Alcelaphini	*Connochaetes*	*gnou*	Elandsfontein	EFTM	-	Grazer	-12.0	-	37.6	-	-	M2 or M3	This study
EFTM 1656	Bovidae	Alcelaphini	*Connochaetes*	*gnou*	Elandsfontein	EFTM	-	Grazer	-9.9	-	33.2	-	-	rm2	This study
EFTM 20858	Bovidae	Alcelaphini	*Connochaetes*	*gnou*	Elandsfontein	EFTM	-	Grazer	-10.1	-	29.6	-	-	lm3 or lmM2	This study
EFTM 20996	Bovidae	Alcelaphini	*Connochaetes*	*gnou*	Elandsfontein	EFTM	-	Grazer	-11.1	-	31.5	-	-	lm3	This study
EFTM 6177[a]	Bovidae	Alcelaphini	*Connochaetes*	*gnou*	Elandsfontein	EFTM	-	Grazer	-9.7	1.0	32.1	1.0	8	rm3	This study
EFTM 8953	Bovidae	Alcelaphini	*Connochaetes*	*gnou*	Elandsfontein	EFTM	-	Grazer	-10.2	-	31.6	-	-	rm2	This study
EFTM 8958A	Bovidae	Alcelaphini	*Connochaetes*	*gnou*	Elandsfontein	EFTM	-	Grazer	-10.6	-	32.7	-	-	rm3	This study
WCRP 1669	Bovidae	Alcelaphini	*Megalotragus*	-	Elandsfontein	WCRP	0609	Grazer	-10.5	-	34.1	-	-	Molar fragment	This study
WCRP 2168	Bovidae	Alcelaphini	*Megalotragus*	-	Elandsfontein	WCRP	0609	Grazer	-12.3	-	32.5	-	-	Molar fragment	This study
WCRP 1352	Bovidae	Aepyceros	genus indet.	-	Elandsfontein	WCRP	0209	Grazer	-7.6	-	36.1	-	-	Molar	This study
WCRP 17324	Bovidae	Aepyceros	genus indet.	-	Elandsfontein	WCRP	0609	Grazer	-8.4	-	31.6	-	-	Molar or premolar fragment	This study
WCRP 18010	Bovidae	Aepyceros	genus indet.	-	Elandsfontein	WCRP	0609	Grazer	-9.2	-	32.5	-	-	Molar or premolar fragment	This study
WCRP 32340	Bovidae	Aepyceros	genus indet.	-	Elandsfontein	WCRP	0313	Grazer	-11.4	-	31.5	-	-	Molar fragment	This study
WCRP 36612	Bovidae	Aepyceros	genus indet.	-	Elandsfontein	WCRP	0909	Grazer	-9.3	-	34.7	-	-	Molar or premolar fragment	This study
WCRP 3698	Bovidae	Aepyceros	genus indet.	-	Elandsfontein	WCRP	0209	Grazer	-9.6	-	32.4	-	-	Molar	This study
WCRP 46257	Bovidae	Aepyceros	genus indet.	-	Elandsfontein	WCRP	0313	Grazer	-11.8	-	30.7	-	-	Fragment	This study
WCRP 7505	Bovidae	Aepyceros	genus indet.	-	Elandsfontein	WCRP	0609	Grazer	-9.9	-	31.7	-	-	Second or third molar	This study
WCRP 9060	Bovidae	Aepyceros	genus indet.	-	Elandsfontein	WCRP	0610	Grazer	-10.6	-	32.3	-	-	Molar fragment	This study
EFTM 11908	Bovidae	Bovini	*Syncerus*	*antiquus*	Elandsfontein	EFTM	-	Grazer	-9.5	-	30.7	-	-	lm3	This study
EFTM 1694	Bovidae	Bovini	*Syncerus*	*antiquus*	Elandsfontein	EFTM	-	Grazer	-10.2	-	35.5	-	-	lm3	This study
EFTM 1746	Bovidae	Bovini	*Syncerus*	*antiquus*	Elandsfontein	EFTM	-	Grazer	-9.8	-	31.9	-	-	lm3	This study
EFTM 1755	Bovidae	Bovini	*Syncerus*	*antiquus*	Elandsfontein	EFTM	-	Grazer	-9.9	-	33.2	-	-	lm3	This study
EFTM 1759+1742	Bovidae	Bovini	*Syncerus*	*antiquus*	Elandsfontein	EFTM	-	Grazer	-10.9	-	32.5	-	-	lm3	This study
EFTM 5063	Bovidae	Bovini	*Syncerus*	*antiquus*	Elandsfontein	EFTM	-	Grazer	-9.7	-	33.2	-	-	lm3	This study
EFTM 5113[a]	Bovidae	Bovini	*Syncerus*	*antiquus*	Elandsfontein	EFTM	-	Grazer	-9.4	0.5	34.9	0.5	12	lm3	This study
EFTM IZ 7892	Bovidae	Bovini	*Syncerus*	*antiquus*	Elandsfontein	EFTM	-	Grazer	-10.21	-	32.9	-	-	lm3	This study
WCRP 32064	Bovidae	Bovini	*Syncerus*	*antiquus*	Elandsfontein	WCRP	0313	Grazer	-10.2	-	34.5	-	-	Premolar or first molar	This study

Table S2.2: Compilation of new and published $\delta^{13}C$ and $\delta^{18}O$ values of the carbonate component of tooth enamel from Pliocene and Pleistocene sites in southwestern South Africa.

Sample ID	Family	Tribe	Genus	Species	Locality	Collection, horizon[b]	Bay[c]	Behavior[d]	$\delta^{13}C_{enamel}$ (‰ VPDB)	1σ	$\delta^{18}O_{enamel}$ (‰ VSMOW)[e]	1σ	n[f]	Tooth element[g]	Reference
WCRP 32119	Bovidae	Bovini	*Syncerus*	*antiquus*	Elandsfontein	WCRP	0313	Grazer	-10.1	-	34.6	-	-	Third molar	This study
WCRP 32265	Bovidae	Bovini	*Syncerus*	*antiquus*	Elandsfontein	WCRP	0313	Grazer	-9.6	-	35.1	-	-	Molar or premolar fragment	This study
WCRP 32289	Bovidae	Bovini	*Syncerus*	*antiquus*	Elandsfontein	WCRP	0313	Grazer	-9.5	-	34.2	-	-	Molar fragment	This study
WCRP 32386	Bovidae	Bovini	*Syncerus*	*antiquus*	Elandsfontein	WCRP	0313	Grazer	-9.9	-	34.2	-	-	Molar	This study
WCRP 34441	Bovidae	Bovini	*Syncerus*	*antiquus*	Elandsfontein	WCRP	0710	Grazer	-10.0	-	35.8	-	-	Fragment	This study
WCRP 46245	Bovidae	Bovini	*Syncerus*	*antiquus*	Elandsfontein	WCRP	0313	Grazer	-11.7	-	35.9	-	-	Molar fragment	This study
WCRP 46251	Bovidae	Bovini	*Syncerus*	*antiquus*	Elandsfontein	WCRP	0313	Grazer	-10.5	-	34.9	-	-	Fragment	This study
WCRP 46256	Bovidae	Bovini	*Syncerus*	*antiquus*	Elandsfontein	WCRP	0313	Grazer	-12.2	-	30.3	-	-	Fragment	This study
WCRP 9380	Bovidae	Bovini	*Syncerus*	*antiquus*	Elandsfontein	WCRP	0309	Grazer	-11.7	0.0	33.6	0.5	2	Molar fragment	This study
-	Bovidae	Hippotragini	*Hippotragus*	*gigas*	Elandsfontein	EFTM	-	Mixed feeder	-10.8	-	28.6	-	-	Second or third molar when possible	Luyt et al., 2000
-	Bovidae	Hippotragini	*Hippotragus*	*gigas*	Elandsfontein	EFTM	-	Mixed feeder	-8.4	-	31.5	-	-	Second or third molar when possible	Luyt et al., 2000
WCRP 1666	Bovidae	Hippotragini	*Hippotragus*	*gigas*	Elandsfontein	WCRP	0609	Mixed feeder	-10.7	-	32.7	-	-	rm3	This study
WCRP 5387	Bovidae	Hippotragini	*Hippotragus*	*gigas*	Elandsfontein	WCRP	0609	Mixed feeder	-11.2	-	32.4	-	-	Molar fragment	This study
WCRP 5656	Bovidae	Neotragini	*Raphicerus*	*melanotis*	Elandsfontein	WCRP	0609	Browser	-13.3	0.5	33.1	0.5	4	rm1	This study
WCRP 5675	Bovidae	Neotragini	*Raphicerus*	*melanotis*	Elandsfontein	WCRP	0609	Browser	-11.2	2.2	32.0	1.3	2	rm1	This study
EFTM 1575	Bovidae	Reduncini	*Redunca*	*arundinum*	Elandsfontein	EFTM	-	Grazer	-8.9	0.5	35.1	1.2	2	lm3	This study
EFTM 1587	Bovidae	Reduncini	*Redunca*	*arundinum*	Elandsfontein	EFTM	-	Grazer	-8.2	-	34.7	-	-	lm3	This study
EFTM 2834	Bovidae	Reduncini	*Redunca*	*arundinum*	Elandsfontein	EFTM	-	Grazer	-9.8	-	31.3	-	-	lm3	This study
EFTM 3514	Bovidae	Reduncini	*Redunca*	*arundinum*	Elandsfontein	EFTM	-	Grazer	-9.9	-	36.9	-	-	Molar fragment	This study
EFTM 6700	Bovidae	Reduncini	*Redunca*	*arundinum*	Elandsfontein	EFTM	-	Grazer	-10.6	-	30.7	-	-	rm3	This study
EFTM 8568	Bovidae	Reduncini	*Redunca*	*arundinum*	Elandsfontein	EFTM	-	Grazer	-10.0	-	35.9	-	-	lm2 and lm3	This study
EFTM 8657	Bovidae	Reduncini	*Redunca*	*arundinum*	Elandsfontein	EFTM	-	Grazer	-9.3	-	34.8	-	-	lm3	This study
EFTM 1585	Bovidae	Reduncini	*Redunca*	*arundinum*	Elandsfontein	EFTM	-	Grazer	-10.3	-	29.8	-	-	Molar fragment	This study
WCRP 8399	Bovidae	Reduncini	*Redunca*	*arundinum*	Elandsfontein	WCRP	0909	Grazer	-9.4	-	30.9	-	-	RM3	This study
EFTM 2296	Bovidae	Tragelaphini	*Tragelaphus*	*strepsiceros*	Elandsfontein	EFTM	-	Browser	-11.4	-	34.8	-	-	rm3	This study
EFTM 2719	Bovidae	Tragelaphini	*Tragelaphus*	*strepsiceros*	Elandsfontein	EFTM	-	Browser	-11.9	-	35.1	-	-	rm3	This study
EFTM 2728	Bovidae	Tragelaphini	*Tragelaphus*	*strepsiceros*	Elandsfontein	EFTM	-	Browser	-12.0	-	36.7	-	-	rm3	This study
EFTM 2733	Bovidae	Tragelaphini	*Tragelaphus*	*strepsiceros*	Elandsfontein	EFTM	-	Browser	-11.9	-	35.8	-	-	rm3	This study
EFTM 2736[a]	Bovidae	Tragelaphini	*Tragelaphus*	*strepsiceros*	Elandsfontein	EFTM	-	Browser	-11.1	1.4	32.2	2.8	2	rm3	This study
EFTM 2738	Bovidae	Tragelaphini	*Tragelaphus*	*strepsiceros*	Elandsfontein	EFTM	-	Browser	-11.6	0.3	34.8	0.8	2	rm3	This study
EFTM 8273	Bovidae	Tragelaphini	*Tragelaphus*	*strepsiceros*	Elandsfontein	EFTM	-	Browser	-12.7	0.4	32.9	1.4	2	rm3	This study
WCRP 5043	Bovidae	Tragelaphini	*Taurotragus*	*oryx*	Elandsfontein	WCRP	0609	Browser	-12.0	-	34.3	-	-	Second molar	This study
WCRP 13288	Bovidae	Bovidae indet.	-	-	Elandsfontein	WCRP	0209	-	-9.0	-	33.7	-	-	Fragment	This study
WCRP 13461	Bovidae	Bovidae indet.	-	-	Elandsfontein	WCRP	0609	-	-8.9	-	34.6	-	-	Fragment	This study
WCRP 13642	Bovidae	Bovidae indet.	-	-	Elandsfontein	WCRP	0609	-	-9.0	-	32.1	-	-	Fragment	This study
WCRP 1467	Bovidae	Bovidae indet.	-	-	Elandsfontein	WCRP	0509	-	-9.0	-	33.5	-	-	Fragment	This study
WCRP 1468	Bovidae	Bovidae indet.	-	-	Elandsfontein	WCRP	0509	-	-10.6	-	36.2	-	-	Lower Molar	This study
WCRP 1654	Bovidae	Bovidae indet.	-	-	Elandsfontein	WCRP	0609	-	-9.6	-	35.0	-	-	Fragment	This study
WCRP 17201[a]	Bovidae	Bovidae indet.	-	-	Elandsfontein	WCRP	0609	-	-9.0	0.1	29.8	0.3	2	Molar or premolar fragment	This study
WCRP 18432	Bovidae	Bovidae indet.	-	-	Elandsfontein	WCRP	0609	-	-9.6	-	31.5	-	-	Fragment	This study
WCRP 18838	Bovidae	Bovidae indet.	-	-	Elandsfontein	WCRP	0609	-	-10.8	-	32.6	-	-	Fragment	This study
WCRP 19349	Bovidae	Bovidae indet.	-	-	Elandsfontein	WCRP	0609	-	-11.4	-	33.2	-	-	Molar	This study
WCRP 19429	Bovidae	Bovidae indet.	-	-	Elandsfontein	WCRP	0209	-	-9.8	-	32.6	-	-	Fragment	This study
WCRP 20443	Bovidae	Bovidae indet.	-	-	Elandsfontein	WCRP	0710	-	-10.3	-	34.0	-	-	rm3	This study
WCRP 2105	Bovidae	Bovidae indet.	-	-	Elandsfontein	WCRP	0609	-	-9.1	-	32.3	-	-	Fragment	This study
WCRP 2158	Bovidae	Bovidae indet.	-	-	Elandsfontein	WCRP	0609	-	-10.1	-	32.5	-	-	Fragment	This study
WCRP 2189	Bovidae	Bovidae indet.	-	-	Elandsfontein	WCRP	0609	-	-10.8	-	34.7	-	-	Molar	This study
WCRP 23212	Bovidae	Bovidae indet.	-	-	Elandsfontein	WCRP	0209	-	-10.1	-	30.5	-	-	Fragment	This study
WCRP 2395	Bovidae	Bovidae indet.	-	-	Elandsfontein	WCRP	0609	-	-9.2	-	37.1	-	-	Fragment	This study
WCRP 2689	Bovidae	Bovidae indet.	-	-	Elandsfontein	WCRP	0609	-	-8.7	-	26.8	-	-	Third molar	This study
WCRP 27624	Bovidae	Bovidae indet.	-	-	Elandsfontein	WCRP	0110	-	-11.0	-	35.4	-	-	Fragment	This study
WCRP 2891	Bovidae	Bovidae indet.	-	-	Elandsfontein	WCRP	0609	-	-8.2	-	33.7	-	-	Premolar or incisor	This study
WCRP 29026	Bovidae	Bovidae indet.	-	-	Elandsfontein	WCRP	0910	-	-9.1	-	29.5	-	-	Molar	This study
WCRP 32213	Bovidae	Bovidae indet.	-	-	Elandsfontein	WCRP	0313	-	-10.1	-	33.9	-	-	Molar	This study
WCRP 32391	Bovidae	Bovidae indet.	-	-	Elandsfontein	WCRP	0313	-	-11.9	-	34.7	-	-	Fragment	This study
WCRP 34057	Bovidae	Bovidae indet.	-	-	Elandsfontein	WCRP	0110	-	-9.1	-	35.4	-	-	Fragment	This study
WCRP 34690	Bovidae	Bovidae indet.	-	-	Elandsfontein	WCRP	0609 or 0710	-	-9.7	-	34.7	-	-	Molar	This study
WCRP 34695	Bovidae	Bovidae indet.	-	-	Elandsfontein	WCRP	0609 or 0710	-	-8.6	-	33.8	-	-	Molar	This study
WCRP 39321[a]	Bovidae	Bovidae indet.	-	-	Elandsfontein	WCRP	0112	-	-7.5	0.8	34.4	0.1	2	Fragment	This study
WCRP 39322	Bovidae	Bovidae indet.	-	-	Elandsfontein	WCRP	0112	-	-8.0	-	32.6	-	-	Fragment	This study
WCRP 46258	Bovidae	Bovidae indet.	-	-	Elandsfontein	WCRP	0313	-	-12.2	-	31.4	-	-	Fragment	This study
WCRP 46259	Bovidae	Bovidae indet.	-	-	Elandsfontein	WCRP	0313	-	-11.0	-	30.6	-	-	Fragment	This study
WCRP 46260	Bovidae	Bovidae indet.	-	-	Elandsfontein	WCRP	0313	-	-9.8	-	32.2	-	-	Fragment	This study
WCRP 5266	Bovidae	Bovidae indet.	-	-	Elandsfontein	WCRP	0609	-	-9.0	-	36.0	-	-	Fragment	This study
WCRP 5565	Bovidae	Bovidae indet.	-	-	Elandsfontein	WCRP	0609	-	-7.6	-	33.2	-	-	Fragment	This study
WCRP 5636	Bovidae	Bovidae indet.	-	-	Elandsfontein	WCRP	0609	-	-10.4	-	35.5	-	-	Fisrt molar	This study
WCRP 5654	Bovidae	Bovidae indet.	-	-	Elandsfontein	WCRP	0609	-	-9.4	-	32.3	-	-	rm3	This study
WCRP 5655	Bovidae	Bovidae indet.	-	-	Elandsfontein	WCRP	0609	-	-6.9	-	32.6	-	-	Molar	This study

Table S2.2: Compilation of new and published $\delta^{13}C$ and $\delta^{18}O$ values of the carbonate component of tooth enamel from Pliocene and Pleistocene sites in southwestern South Africa.

Sample ID	Family	Tribe	Genus	Species	Locality	Collection, horizon[b]	Bay[c]	Behavior[d]	$\delta^{13}C_{enamel}$ (‰ VPDB)	1σ	$\delta^{18}O_{enamel}$ (‰ VSMOW)[e]	1σ	n[f]	Tooth element[g]	Reference
WCRP 5659	Bovidae	Bovidae indet.	-	-	Elandsfontein	WCRP	0609	-	-7.6	-	33.1	-	-	Second molar	This study
WCRP 5660	Bovidae	Bovidae indet.	-	-	Elandsfontein	WCRP	0609	-	-8.7	-	35.0	-	-	Fisrt molar	This study
WCRP 5823	Bovidae	Bovidae indet.	-	-	Elandsfontein	WCRP	0609	-	-10.3	-	35.4	-	-	M2 or M3	This study
WCRP 5825	Bovidae	Bovidae indet.	-	-	Elandsfontein	WCRP	0609	-	-10.6	-	35.2	-	-	Molar	This study
WCRP 5843[a]	Bovidae	Bovidae indet.	-	-	Elandsfontein	WCRP	0609	-	-11.0	0.2	31.9	0.5	2	Fragment	This study
WCRP 6185	Bovidae	Bovidae indet.	-	-	Elandsfontein	WCRP	0309	-	-7.8	-	33.9	-	-	Molar fragment	This study
WCRP 6243	Bovidae	Bovidae indet.	-	-	Elandsfontein	WCRP	0309	-	-9.3	-	33.2	-	-	Molar fragment	This study
WCRP 6695	Bovidae	Bovidae indet.	-	-	Elandsfontein	WCRP	0610	-	-10.1	-	34.9	-	-	Molar	This study
WCRP 6703	Bovidae	Bovidae indet.	-	-	Elandsfontein	WCRP	0610	-	-11.7	-	32.3	-	-	Premolar	This study
WCRP 6717	Bovidae	Bovidae indet.	-	-	Elandsfontein	WCRP	0610	-	-11.2	-	30.6	-	-	Premolar or first molar	This study
WCRP 6802	Bovidae	Bovidae indet.	-	-	Elandsfontein	WCRP	0610	-	-7.8	-	30.8	-	-	Molar	This study
WCRP 6806	Bovidae	Bovidae indet.	-	-	Elandsfontein	WCRP	0610	-	-9.5	-	35.6	-	-	Second molar	This study
WCRP 6975[a]	Bovidae	Bovidae indet.	-	-	Elandsfontein	WCRP	0109	-	-9.5	0.2	33.6	0.2	2	Second molar	This study
WCRP 7169	Bovidae	Bovidae indet.	-	-	Elandsfontein	WCRP	0109	-	-7.5	0.2	27.7	0.5	2	Fragment	This study
WCRP 7589	Bovidae	Bovidae indet.	-	-	Elandsfontein	WCRP	0109	-	-10.8	-	30.1	-	-	Molar	This study
WCRP 7611	Bovidae	Bovidae indet.	-	-	Elandsfontein	WCRP	0109	-	-9.0	-	30.7	-	-	Molar or premolar fragment	This study
WCRP 7639	Bovidae	Bovidae indet.	-	-	Elandsfontein	WCRP	0109	-	-9.5	-	30.5	-	-	Molar	This study
WCRP 7832	Bovidae	Bovidae indet.	-	-	Elandsfontein	WCRP	0109	-	-11.9	-	32.9	-	-	Molar	This study
WCRP 9043[a]	Bovidae	Bovidae indet.	-	-	Elandsfontein	WCRP	0609	-	-10.1	1.1	35.1	0.3	2	Fragment	This study
WCRP 9050	Bovidae	Bovidae indet.	-	-	Elandsfontein	WCRP	0609	-	-8.5	-	37.1	-	-	Molar fragment	This study
WCRP 9053	Bovidae	Bovidae indet.	-	-	Elandsfontein	WCRP	West Site	-	-8.3	-	32.9	-	-	Fragment	This study
WCRP 9079	Bovidae	Bovidae indet.	-	-	Elandsfontein	WCRP	0510	-	-8.0	-	32.0	-	-	Molar	This study
WCRP 9085	Bovidae	Bovidae indet.	-	-	Elandsfontein	WCRP	0610	-	-9.0	-	32.9	-	-	Molar	This study
WCRP 9377	Bovidae	Bovidae indet.	-	-	Elandsfontein	WCRP	0809	-	-10.4	-	32.4	-	-	Fragment	This study
WCRP 9378	Bovidae	Bovidae indet.	-	-	Elandsfontein	WCRP	ND	-	-7.9	-	34.9	-	-	Third molar	This study
WCRP 9386	Bovidae	Bovidae indet.	-	-	Elandsfontein	WCRP	0609	-	-8.8	-	33.5	-	-	Third molar	This study
WCRP 9944	Bovidae	Bovidae indet.	-	-	Elandsfontein	WCRP	0609	-	-11.6	-	34.7	-	-	Molar fragment	This study
WCRP 32232	Cercopithecidae	-	*Theropithecus*	-	Elandsfontein	WCRP	0313	-	-10.2	0.3	31.2	1.9	2	lm3	This study
WCRP 17199	Elephantidae	Elephantidae indet.	-	-	Elandsfontein	WCRP	0609	Grazer	-8.5	-	30.8	-	-	Fragment	This study
-	Equidae	-	*Equus*	*capensis*	Elandsfontein	EFTM	-	Grazer	-10.3	-	31.2	-	-	Second or third molar when possible	Luyt et al., 2000
-	Equidae	-	*Equus*	*capensis*	Elandsfontein	EFTM	-	Grazer	-9.9	-	29.4	-	-	Second or third molar when possible	Luyt et al., 2000
-	Equidae	-	*Equus*	*capensis*	Elandsfontein	EFTM	-	Grazer	-9.4	-	32.6	-	-	Second or third molar when possible	Luyt et al., 2000
EFTM 2619	Equidae	-	*Equus*	*capensis*	Elandsfontein	EFTM	-	Grazer	-9.7	-	31.6	-	-	rm3	This study
EFTM 13873[a]	Equidae	-	*Equus*	*capensis*	Elandsfontein	EFTM	-	Grazer	-9.9	0.6	33.1	0.6	13	rm3	This study
EFTM 16660	Equidae	-	*Equus*	*capensis*	Elandsfontein	EFTM	-	Grazer	-9.2	-	32.0	-	-	rm3	This study
EFTM 1952	Equidae	-	*Equus*	*capensis*	Elandsfontein	EFTM	-	Grazer	-11.2	-	33.1	-	-	rm3	This study
EFTM 2112	Equidae	-	*Equus*	*capensis*	Elandsfontein	EFTM	-	Grazer	-10.6	-	33.9	-	-	rm3	This study
EFTM 5065	Equidae	-	*Equus*	*capensis*	Elandsfontein	EFTM	-	Grazer	-9.5	-	33.1	-	-	rm3	This study
EFTM 6727[a]	Equidae	-	*Equus*	*capensis*	Elandsfontein	EFTM	-	Grazer	-8.5	0.4	32.0	0.1	2	rm3	This study
WCRP 2103	Equidae	-	*Equus*	*capensis*	Elandsfontein	WCRP	0609	Grazer	-10.1	-	32.3	-	-	lm3	This study
WCRP 6242	Equidae	-	*Equus*	*capensis*	Elandsfontein	WCRP	0309	Grazer	-10.0	-	32.4	-	-	RM3	This study
WCRP 9384	Equidae	-	*Equus*	*capensis*	Elandsfontein	WCRP	0609	Grazer	-9.8	0.3	32.6	0.3	3	Fragment	This study
WCRP 1007	Equidae	Equidae indet.	-	-	Elandsfontein	WCRP	0109	-	-9.2	-	32.9	-	-	Fragment	This study
WCRP 12965	Equidae	Equidae indet.	-	-	Elandsfontein	WCRP	0609	-	-8.3	-	32.7	-	-	Fragment	This study
WCRP 13314	Equidae	Equidae indet.	-	-	Elandsfontein	WCRP	0109	-	-9.8	-	32.6	-	-	Fragment	This study
WCRP 17333	Equidae	Equidae indet.	-	-	Elandsfontein	WCRP	0609	-	-9.4	-	33.7	-	-	Fragment	This study
WCRP 2049	Equidae	Equidae indet.	-	-	Elandsfontein	WCRP	0609	-	-10.4	-	33.3	-	-	Molar	This study
WCRP 2101	Equidae	Equidae indet.	-	-	Elandsfontein	WCRP	0609	-	-10.2	-	33.3	-	-	Molar	This study
WCRP 2102	Equidae	Equidae indet.	-	-	Elandsfontein	WCRP	0609	-	-10.5	-	32.0	-	-	Molar	This study
WCRP 2106	Equidae	Equidae indet.	-	-	Elandsfontein	WCRP	0609	-	-9.3	-	33.6	-	-	Fragment	This study
WCRP 2110	Equidae	Equidae indet.	-	-	Elandsfontein	WCRP	0609	-	-8.4	-	31.1	-	-	Molar	This study
WCRP 2182	Equidae	Equidae indet.	-	-	Elandsfontein	WCRP	0609	-	-10.5	-	34.2	-	-	Fragment	This study
WCRP 29223	Equidae	Equidae indet.	-	-	Elandsfontein	WCRP	0110	-	-11.4	-	33.5	-	-	Fragment	This study
WCRP 36806	Equidae	Equidae indet.	-	-	Elandsfontein	WCRP	0909	-	-9.4	-	32.7	-	-	Fragment	This study
WCRP 3815	Equidae	Equidae indet.	-	-	Elandsfontein	WCRP	0209	-	-9.0	-	32.6	-	-	Fragment	This study
WCRP 5056	Equidae	Equidae indet.	-	-	Elandsfontein	WCRP	0609	-	-9.7	-	33.5	-	-	Fragment	This study
WCRP 9041[a]	Equidae	Equidae indet.	-	-	Elandsfontein	WCRP	ND	-	-9.9	0.5	34.0	0.3	2	Fragment	This study
WCRP 9045	Equidae	Equidae indet.	-	-	Elandsfontein	WCRP	0610	-	-9.8	-	32.4	-	-	Molar	This study
WCRP 9054	Equidae	Equidae indet.	-	-	Elandsfontein	WCRP	West Site	-	-10.3	-	33.5	-	-	Molar	This study
WCRP 9140	Equidae	Equidae indet.	-	-	Elandsfontein	WCRP	0609	-	-10.1	-	32.6	-	-	Molar	This study
WCRP 9357[a]	Equidae	Equidae indet.	-	-	Elandsfontein	WCRP	0609	-	-9.5	0.1	31.4	0.2	2	Fragment	This study
-	Giraffidae	-	*Sivatherium*	*maurusium*	Elandsfontein	EFTM	-	Browser	-11.2	-	31.3	-	-	Second or third molar when possible	Luyt et al., 2000
-	Giraffidae	-	*Sivatherium*	*maurusium*	Elandsfontein	EFTM	-	Browser	-13.1	-	30.6	-	-	Second or third molar when possible	Luyt et al., 2000
-	Giraffidae	-	*Sivatherium*	*maurusium*	Elandsfontein	EFTM	-	Browser	-10.8	-	29.7	-	-	Second or third molar when possible	Luyt et al., 2000
EFTM 4028	Giraffidae	-	*Sivatherium*	*maurusium*	Elandsfontein	EFTM	-	Browser	-10.8	-	35.0	-	-	Second molar?	This study
EFTM 4031	Giraffidae	-	*Sivatherium*	*maurusium*	Elandsfontein	EFTM	-	Browser	-11.7	0.5	33.5	0.6	2	lm3	This study
WCRP 8031	Giraffidae	-	*Sivatherium*	*maurusium*	Elandsfontein	WCRP	0709	Browser	-10.1	-	32.8	-	-	rm3	This study

Table S2.2: Compilation of new and published $\delta^{13}C$ and $\delta^{18}O$ values of the carbonate component of tooth enamel from Pliocene and Pleistocene sites in southwestern South Africa.

Sample ID	Family	Tribe	Genus	Species	Locality	Collection, horizon[b]	Bay[c]	Behavior[d]	$\delta^{13}C_{enamel}$ (‰ VPDB)	1σ	$\delta^{18}O_{enamel}$ (‰ VSMOW)[e]	1σ	n[f]	Tooth element[g]	Reference
WCRP 8682	Giraffidae	Giraffidae indet.	-	-	Elandsfontein	WCRP	1009	-	-9.1	-	34.4	-	-	Fragment	This study
-	Hippopotamidae	-	*Hippopotamus*	*amphibius*	Elandsfontein	EFTM	-	Semi-aquatic	-12.8	-	27.8	-	-	Second or third molar when possible	Luyt et al., 2000
-	Hippopotamidae	-	*Hippopotamus*	*amphibius*	Elandsfontein	EFTM	-	Semi-aquatic	-11.5	-	27.7	-	-	Second or third molar when possible	Luyt et al., 2000
EFTM 4030	Hippopotamidae	-	*Hippopotamus*	*amphibius*	Elandsfontein	EFTM	-	Semi-aquatic	-13.1	-	30.5	-	-	Molar fragment	This study
EFTM 4042	Hippopotamidae	-	*Hippopotamus*	*amphibius*	Elandsfontein	EFTM	-	Semi-aquatic	-13.0	-	31.8	-	-	Tusk fragment	This study
EFTM 4088	Hippopotamidae	-	*Hippopotamus*	*amphibius*	Elandsfontein	EFTM	-	Semi-aquatic	-12.1	-	29.3	-	-	Molar	This study
EFTM 5015	Hippopotamidae	-	*Hippopotamus*	*amphibius*	Elandsfontein	EFTM	-	Semi-aquatic	-13.3	-	30.5	-	-	Molar	This study
EFTM 66908	Hippopotamidae	-	*Hippopotamus*	*amphibius*	Elandsfontein	EFTM	-	Semi-aquatic	-11.6	-	28.9	-	-	Tusk fragment	This study
EFTM M5121094	Hippopotamidae	-	*Hippopotamus*	*amphibius*	Elandsfontein	EFTM	-	Semi-aquatic	-13.3	-	28.7	-	-	Molar fragment	This study
WCRP 49364	Hippopotamidae	-	*Hippopotamus*	*amphibius*	Elandsfontein	WCRP	0909	Semi-aquatic	-10.0	1.6	31.7	1.6	2	Canine	This study
EFTM 3410	Rhinocerotidae	-	*Ceratotherium*	*simum*	Elandsfontein	EFTM	-	Grazer	-10.2	-	32.3	-	-	Molar	This study
EFTM 3440	Rhinocerotidae	-	*Ceratotherium*	*simum*	Elandsfontein	EFTM	-	Grazer	-11.6	-	33.2	-	-	Fragment	This study
EFTM 8610B	Rhinocerotidae	-	*Ceratotherium*	*simum*	Elandsfontein	EFTM	-	Grazer	-11.3	-	32.2	-	-	Fragment	This study
EFTM 93998	Rhinocerotidae	-	*Ceratotherium*	*simum*	Elandsfontein	EFTM	-	Grazer	-10.4	-	31.3	-	-	Molar	This study
EFTM 16617	Rhinocerotidae	-	*Diceros*	*bicornis*	Elandsfontein	EFTM	-	Browser	-11.2	-	31.7	-	-	RM3	This study
EFTM 20939	Rhinocerotidae	-	*Diceros*	*bicornis*	Elandsfontein	EFTM	-	Browser	-11.5	-	32.2	-	-	Fragment	This study
EFTM 20982	Rhinocerotidae	-	*Diceros*	*bicornis*	Elandsfontein	EFTM	-	Browser	-11.4	-	33.0	-	-	Molar fragment	This study
EFTM 8700K[a]	Rhinocerotidae	-	*Diceros*	*bicornis*	Elandsfontein	EFTM	-	Browser	-11.8	0.1	31.1	0.3	2	Molar	This study
-	Rhinocerotidae	Rhinocerotidae indet.	-	-	Elandsfontein	EFTM	-	-	-10.8	-	27.6	-	-	Second or third molar when possible	Luyt et al., 2000
-	Rhinocerotidae	Rhinocerotidae indet.	-	-	Elandsfontein	EFTM	-	-	-11.1	-	28.2	-	-	Second or third molar when possible	Luyt et al., 2000
0313 Rhino-Lot 2744	Rhinocerotidae	Rhinocerotidae indet.	-	-	Elandsfontein	WCRP	0313	-	-12.4	0.3	32.8	0.7	3	Premolar	This study
WCRP 18531	Rhinocerotidae	Rhinocerotidae indet.	-	-	Elandsfontein	WCRP	0609	-	-9.2	-	32.0	-	-	Fragment	This study
WCRP 9055	Rhinocerotidae	Rhinocerotidae indet.	-	-	Elandsfontein	WCRP	West Site	-	-10.6	-	33.6	-	-	Fragment	This study
-	Suidae	-	*Kolpochoerus*	*paiceae*	Elandsfontein	EFTM	-	Grazer	-8.7	-	29.8	-	-	Second or third molar when possible	Luyt et al., 2000
-	Suidae	-	*Kolpochoerus*	*paiceae*	Elandsfontein	EFTM	-	Grazer	-9.8	-	26.2	-	-	Second or third molar when possible	Luyt et al., 2000
-	Suidae	-	*Kolpochoerus*	*paiceae*	Elandsfontein	EFTM	-	Grazer	-12.0	-	23.7	-	-	Second or third molar when possible	Luyt et al., 2000
WCRP 12156	Suidae	-	*Kolpochoerus*	*paiceae*	Elandsfontein	WCRP	0209	Grazer	-9.0	-	32.3	-	-	rm3	This study
WCRP 12284	Suidae	-	*Kolpochoerus*	*paiceae*	Elandsfontein	WCRP	0209	Grazer	-8.2	-	32.5	-	-	lm3	This study
WCRP 6438	Suidae	-	*Kolpochoerus*	*paiceae*	Elandsfontein	WCRP	0610	Grazer	-11.1	-	31.4	-	-	lm3	This study
-	Suidae	-	*Metridiochoerus*	*andrewsi*	Elandsfontein	EFTM	-	Grazer	-11.2	-	24.0	-	-	Second or third molar when possible	Luyt et al., 2000
-	Suidae	-	*Metridiochoerus*	*andrewsi*	Elandsfontein	EFTM	-	Grazer	-9.4	-	27.9	-	-	Second or third molar when possible	Luyt et al., 2000
-	Bovidae	Alcelaphini	*Damalacra sp.*	-	Langebaanweg	Varswater Formation, PPM, Bed 3aN	-	Grazer to Browser	-11.4	-	26.3	-	-	Molar fragments when possible	Franz-Odendaal et al., 2002
-	Bovidae	Alcelaphini	*Damalacra sp.*	-	Langebaanweg	Varswater Formation, PPM, Bed 3aN	-	Grazer to Browser	-12.3	-	26.2	-	-	Molar fragments when possible	Franz-Odendaal et al., 2002
-	Bovidae	Alcelaphini	*Damalacra sp.*	-	Langebaanweg	Varswater Formation, PPM, Bed 3aN	-	Grazer to Browser	-9.3	-	28.5	-	-	Molar fragments when possible	Franz-Odendaal et al., 2002
-	Bovidae	Alcelaphini	*Damalacra sp.*	-	Langebaanweg	Varswater Formation, PPM, Bed 3aN	-	Grazer to Browser	-10.5	-	29.3	-	-	Molar fragments when possible	Franz-Odendaal et al., 2002
-	Bovidae	Alcelaphini	*Damalacra sp.*	-	Langebaanweg	Varswater Formation, PPM, Bed 3aN	-	Grazer to Browser	-10.3	-	26.6	-	-	Molar fragments when possible	Franz-Odendaal et al., 2002
-	Bovidae	Alcelaphini	*Damalacra sp.*	-	Langebaanweg	Varswater Formation, PPM, Bed 3aN	-	Grazer to Browser	-10.3	-	29.6	-	-	Molar fragments when possible	Franz-Odendaal et al., 2002
-	Bovidae	Alcelaphini	*Damalacra sp.*	-	Langebaanweg	Varswater Formation, PPM	-	Grazer to Browser	-11.5	-	26.3	-	-	Molar fragments when possible	Franz-Odendaal et al., 2002
-	Bovidae	Reduncini	*Kobus sp.*	-	Langebaanweg	Varswater Formation, PPM	-	-	-10.7	-	26.5	-	-	Molar fragments when possible	Franz-Odendaal et al., 2002
-	Bovidae	Reduncini	*Kobus sp.*	-	Langebaanweg	Varswater Formation, PPM	-	-	-10.7	-	29.5	-	-	Molar fragments when possible	Franz-Odendaal et al., 2002
LBW13G-001	Bovidae	Bovidae indet.	-	-	Langebaanweg	Varswater Formation, PPM	-	-	-10.0	-	34.6	-	-	Molar	This study
LBW13G-002	Bovidae	Bovidae indet.	-	-	Langebaanweg	Varswater Formation, PPM	-	-	-10.4	-	32.8	-	-	Molar	This study
-	Equidae	-	*Hipparion cf.*	*baardi*	Langebaanweg	Varswater Formation, PPM, Bed 3aN	-	Grazer	-11.7	-	25.1	-	-	Molar fragments when possible	Franz-Odendaal et al., 2002
-	Equidae	-	*Hipparion cf.*	*baardi*	Langebaanweg	Varswater Formation, PPM, Bed 3aN	-	Grazer	-12.9	-	25.1	-	-	Molar fragments when possible	Franz-Odendaal et al., 2002
-	Equidae	-	*Hipparion cf.*	*baardi*	Langebaanweg	Varswater Formation, PPM	-	Grazer	-11.0	-	26.1	-	-	Molar fragments when possible	Franz-Odendaal et al., 2002
-	Equidae	-	*Hipparion cf.*	*baardi*	Langebaanweg	Varswater Formation, PPM, Bed 3aN	-	Grazer	-11.2	-	28.6	-	-	Molar fragments when possible	Franz-Odendaal et al., 2002
-	Equidae	-	*Hipparion cf.*	*baardi*	Langebaanweg	Varswater Formation, PPM, Bed 3aN	-	Grazer	-10.7	-	29.6	-	-	Molar fragments when possible	Franz-Odendaal et al., 2002
-	Equidae	-	*Hipparion cf.*	*baardi*	Langebaanweg	Varswater Formation, PPM	-	Grazer	-10.4	-	28.5	-	-	Molar fragments when possible	Franz-Odendaal et al., 2002
LBW13G-003	Equidae	Equidae indet.	-	-	Langebaanweg	Varswater Formation, PPM	-	-	-8.9	-	30.4	-	-	Molar	This study
LBW13G-004	Equidae	Equidae indet.	-	-	Langebaanweg	Varswater Formation, PPM	-	-	-8.8	-	31.2	-	-	Incisor	This study
-	Giraffidae	-	*Sivatherium*	*hendeyi*	Langebaanweg	Varswater Formation, PPM, Bed 3aN	-	Mixed feeder	-12.0	-	27.7	-	-	Molar fragments when possible	Franz-Odendaal et al., 2002
-	Giraffidae	-	*Sivatherium*	*hendeyi*	Langebaanweg	Varswater Formation, PPM, Bed 3aN	-	Mixed feeder	-13.5	-	24.8	-	-	Molar fragments when possible	Franz-Odendaal et al., 2002
-	Giraffidae	-	*Sivatherium*	*hendeyi*	Langebaanweg	Varswater Formation, PPM, Bed 3aN	-	Mixed feeder	-13.2	-	28.5	-	-	Molar fragments when possible	Franz-Odendaal et al., 2002
-	Giraffidae	-	*Sivatherium*	*hendeyi*	Langebaanweg	Varswater Formation, PPM, Bed 3aN	-	Mixed feeder	-13.6	-	26.8	-	-	Molar fragments when possible	Franz-Odendaal et al., 2002
-	Giraffidae	-	*Sivatherium*	*hendeyi*	Langebaanweg	Varswater Formation, PPM, Bed 3aN	-	Mixed feeder	-10.5	-	29.6	-	-	Molar fragments when possible	Franz-Odendaal et al., 2002
-	Giraffidae	-	*Sivatherium*	*hendeyi*	Langebaanweg	Varswater Formation, PPM	-	Mixed feeder	-10.4	-	28.8	-	-	Molar fragments when possible	Franz-Odendaal et al., 2002
-	Giraffidae	-	*Sivatherium*	*hendeyi*	Langebaanweg	Varswater Formation, PPM, Bed 3aN	-	Mixed feeder	-10.7	-	27.9	-	-	Molar fragments when possible	Franz-Odendaal et al., 2002
-	Giraffidae	-	*Sivatherium*	*hendeyi*	Langebaanweg	Varswater Formation, PPM, Bed 3aN	-	Mixed feeder	-10.5	-	27.9	-	-	Molar fragments when possible	Franz-Odendaal et al., 2002
-	Giraffidae	-	*Sivatherium*	*hendeyi*	Langebaanweg	Varswater Formation, PPM, Bed 3aN	-	Mixed feeder	-10.7	-	30.2	-	-	Molar fragments when possible	Franz-Odendaal et al., 2002
-	Giraffidae	-	*Sivatherium*	*hendeyi*	Langebaanweg	Varswater Formation, PPM, Bed 3aN	-	Mixed feeder	-10.3	-	27.2	-	-	Molar fragments when possible	Franz-Odendaal et al., 2002
-	Giraffidae	-	*Sivatherium*	*hendeyi*	Langebaanweg	Varswater Formation, PPM, Bed 3aN	-	Mixed feeder	-11.1	-	27.5	-	-	Molar fragments when possible	Franz-Odendaal et al., 2002
-	Giraffidae	-	*Sivatherium*	*hendeyi*	Langebaanweg	Varswater Formation, PPM, Bed 3aN	-	Mixed feeder	-9.9	-	29.0	-	-	Molar fragments when possible	Franz-Odendaal et al., 2002
-	Giraffidae	-	*Sivatherium*	*hendeyi*	Langebaanweg	Varswater Formation, PPM, Bed 3aN	-	Mixed feeder	-11.1	-	30.6	-	-	Molar fragments when possible	Franz-Odendaal et al., 2002
-	Giraffidae	-	*Sivatherium*	*hendeyi*	Langebaanweg	Varswater Formation, PPM, Bed 3aN	-	Mixed feeder	-12.0	-	27.8	-	-	Molar fragments when possible	Franz-Odendaal et al., 2002
-	Giraffidae	-	*Sivatherium*	*hendeyi*	Langebaanweg	Varswater Formation, PPM, Bed 3aN	-	Mixed feeder	-11.9	-	27.7	-	-	Molar fragments when possible	Franz-Odendaal et al., 2002
-	Giraffidae	-	*Sivatherium*	*hendeyi*	Langebaanweg	Varswater Formation, PPM, Bed 3aN	-	Mixed feeder	-11.6	-	27.4	-	-	Molar fragments when possible	Franz-Odendaal et al., 2002
-	Giraffidae	-	*Sivatherium*	*hendeyi*	Langebaanweg	Varswater Formation, PPM, Bed 3aN	-	Mixed feeder	-12.1	-	26.8	-	-	Molar fragments when possible	Franz-Odendaal et al., 2002

Table S2.2: Compilation of new and published $\delta^{13}C$ and $\delta^{18}O$ values of the carbonate component of tooth enamel from Pliocene and Pleistocene sites in southwestern South Africa.

Sample ID	Family	Tribe	Genus	Species	Locality	Collection, horizon[b]	Bay[c]	Behavior[d]	$\delta^{13}C_{enamel}$ (‰ VPDB)	1σ	$\delta^{18}O_{enamel}$ (‰ VSMOW)[e]	1σ	n[f]	Tooth element[g]	Reference
-	Giraffidae	-	*Sivatherium*	*hendeyi*	Langebaanweg	Varswater Formation, PPM, Bed 3aN	-	Mixed feeder	-10.3	-	27.0	-	-	Molar fragments when possible	Franz-Odendaal et al., 2002
-	Giraffidae	-	*Sivatherium*	*hendeyi*	Langebaanweg	Varswater Formation, PPM, Bed 3aN	-	Mixed feeder	-12.5	-	29.7	-	-	Molar fragments when possible	Franz-Odendaal et al., 2002
-	Giraffidae	-	*Sivatherium*	*hendeyi*	Langebaanweg	Varswater Formation, PPM, Bed 3aN	-	Mixed feeder	-10.4	-	27.9	-	-	Molar fragments when possible	Franz-Odendaal et al., 2002
-	Giraffidae	-	*Sivatherium*	*hendeyi*	Langebaanweg	Varswater Formation, PPM, Bed 3aN	-	Mixed feeder	-10.8	-	28.5	-	-	Molar fragments when possible	Franz-Odendaal et al., 2002
-	Giraffidae	-	*Sivatherium*	*hendeyi*	Langebaanweg	Varswater Formation, PPM, Bed 3aN	-	Mixed feeder	-11.1	-	27.3	-	-	Molar fragments when possible	Franz-Odendaal et al., 2002
-	Giraffidae	-	*Sivatherium*	*hendeyi*	Langebaanweg	Varswater Formation, PPM, Bed 3aN	-	Mixed feeder	-12.3	-	29.7	-	-	Molar fragments when possible	Franz-Odendaal et al., 2002
-	Giraffidae	-	*Sivatherium*	*hendeyi*	Langebaanweg	Varswater Formation, PPM, Bed 3aN	-	Mixed feeder	-11.1	-	27.0	-	-	Molar fragments when possible	Franz-Odendaal et al., 2002
-	Giraffidae	-	*Sivatherium*	*hendeyi*	Langebaanweg	Varswater Formation, PPM, Bed 3aN	-	Mixed feeder	-13.5	-	27.4	-	-	Molar fragments when possible	Franz-Odendaal et al., 2002
-	Giraffidae	-	*Sivatherium*	*hendeyi*	Langebaanweg	Varswater Formation, PPM, Bed 3aN	-	Mixed feeder	-13.0	-	25.4	-	-	Molar fragments when possible	Franz-Odendaal et al., 2002
LBW13G-009	Giraffidae	Giraffidae indet.	-	-	Langebaanweg	Varswater Formation, PPM	-	-	-12.0	-	34.0	-	-	Molar	This study
LBW13G-010	Giraffidae	Giraffidae indet.	-	-	Langebaanweg	Varswater Formation, PPM	-	-	-9.3	-	33.3	-	-	Fragment	This study
LBW13G-011	Giraffidae	Giraffidae indet.	-	-	Langebaanweg	Varswater Formation, PPM	-	-	-9.2	-	30.3	-	-	Molar	This study
-	Hippopotamidae	Hippopotamidae indet.	-	-	Langebaanweg	Varswater Formation, PPM, Bed 3aN	-	Semi-aquatic	-10.9	-	27.0	-	-	Molar fragments when possible	Franz-Odendaal et al., 2002
-	Hippopotamidae	Hippopotamidae indet.	-	-	Langebaanweg	Varswater Formation, PPM, Bed 3aN	-	Semi-aquatic	-13.3	-	23.2	-	-	Molar fragments when possible	Franz-Odendaal et al., 2002
-	Hippopotamidae	Hippopotamidae indet.	-	-	Langebaanweg	Varswater Formation, PPM, Bed 3aN	-	Semi-aquatic	-11.6	-	26.0	-	-	Molar fragments when possible	Franz-Odendaal et al., 2002
-	Hippopotamidae	Hippopotamidae indet.	-	-	Langebaanweg	Varswater Formation, PPM, Bed 3aN	-	Semi-aquatic	-12.7	-	25.3	-	-	Molar fragments when possible	Franz-Odendaal et al., 2002
-	Hippopotamidae	Hippopotamidae indet.	-	-	Langebaanweg	Varswater Formation, PPM, Bed 3aN	-	Semi-aquatic	-14.9	-	24.2	-	-	Molar fragments when possible	Franz-Odendaal et al., 2002
-	Hippopotamidae	Hippopotamidae indet.	-	-	Langebaanweg	Varswater Formation, PPM, Bed 3aN	-	Semi-aquatic	-12.0	-	23.2	-	-	Molar fragments when possible	Franz-Odendaal et al., 2002
-	Hippopotamidae	Hippopotamidae indet.	-	-	Langebaanweg	Varswater Formation, PPM, Bed 3aN	-	Semi-aquatic	-11.8	-	24.2	-	-	Molar fragments when possible	Franz-Odendaal et al., 2002
-	Hippopotamidae	Hippopotamidae indet.	-	-	Langebaanweg	Varswater Formation, PPM, Bed 3aN	-	Semi-aquatic	-9.4	-	24.4	-	-	Molar fragments when possible	Franz-Odendaal et al., 2002
-	Hippopotamidae	Hippopotamidae indet.	-	-	Langebaanweg	Varswater Formation, PPM, Bed 3aN	-	Semi-aquatic	-12.1	-	25.7	-	-	Molar fragments when possible	Franz-Odendaal et al., 2002
-	Hippopotamidae	Hippopotamidae indet.	-	-	Langebaanweg	Varswater Formation, PPM, Bed 3aN	-	Semi-aquatic	-11.5	-	25.9	-	-	Molar fragments when possible	Franz-Odendaal et al., 2002
-	Hippopotamidae	Hippopotamidae indet.	-	-	Langebaanweg	Varswater Formation, PPM, Bed 3aN	-	Semi-aquatic	-13.6	-	24.5	-	-	Molar fragments when possible	Franz-Odendaal et al., 2002
-	Hippopotamidae	Hippopotamidae indet.	-	-	Langebaanweg	Varswater Formation, PPM, Bed 3aN	-	Semi-aquatic	-10.0	-	25.0	-	-	Molar fragments when possible	Franz-Odendaal et al., 2002
-	Hippopotamidae	Hippopotamidae indet.	-	-	Langebaanweg	Varswater Formation, PPM, Bed 3aN	-	Semi-aquatic	-13.8	-	24.3	-	-	Molar fragments when possible	Franz-Odendaal et al., 2002
-	Hippopotamidae	Hippopotamidae indet.	-	-	Langebaanweg	Varswater Formation, PPM, Bed 3aN	-	Semi-aquatic	-11.7	-	23.7	-	-	Molar fragments when possible	Franz-Odendaal et al., 2002
-	Hippopotamidae	Hippopotamidae indet.	-	-	Langebaanweg	Varswater Formation, PPM, Bed 3aN	-	Semi-aquatic	-10.3	-	25.0	-	-	Molar fragments when possible	Franz-Odendaal et al., 2002
LBW13G-006	Hippopotamidae	Hippopotamidae indet.	-	-	Langebaanweg	Varswater Formation, PPM	-	Semi-aquatic	-13.3	-	28.1	-	-	Tusk fragment	This study
LBW13G-007	Hippopotamidae	Hippopotamidae indet.	-	-	Langebaanweg	Varswater Formation, PPM	-	Semi-aquatic	-10.9	-	27.1	-	-	Molar	This study
LBW13G-008[a]	Hippopotamidae	Hippopotamidae indet.	-	-	Langebaanweg	Varswater Formation, PPM	-	Semi-aquatic	-10.2	0.2	29.5	0.9	2	Premolar	This study
-	Rhinocerotidae	-	*Ceratotherium*	*praecox*	Langebaanweg	Varswater Formation, PPM, Bed 3aN	-	Browser	-11.1	-	25.5	-	-	Molar fragments when possible	Franz-Odendaal et al., 2002
-	Rhinocerotidae	-	*Ceratotherium*	*praecox*	Langebaanweg	Varswater Formation, PPM, Bed 3aN	-	Browser	-10.1	-	28.2	-	-	Molar fragments when possible	Franz-Odendaal et al., 2002
-	Rhinocerotidae	-	*Ceratotherium*	*praecox*	Langebaanweg	Varswater Formation, PPM, Bed 3aN	-	Browser	-10.5	-	25.0	-	-	Molar fragments when possible	Franz-Odendaal et al., 2002
-	Rhinocerotidae	-	*Ceratotherium*	*praecox*	Langebaanweg	Varswater Formation, PPM, Bed 3aN	-	Browser	-11.7	-	26.2	-	-	Molar fragments when possible	Franz-Odendaal et al., 2002
-	Suidae	-	*Nyanzachoerus cf.*	*jaegeri*	Langebaanweg	Varswater Formation, PPM	-	-	-12.2	-	27.9	-	-	Molar fragments when possible	Franz-Odendaal et al., 2002
-	Suidae	-	*Nyanzachoerus cf.*	*jaegeri*	Langebaanweg	Varswater Formation, PPM	-	-	-10.3	-	26.5	-	-	Molar fragments when possible	Franz-Odendaal et al., 2002
-	Suidae	-	*Nyanzachoerus cf.*	*jaegeri*	Langebaanweg	Varswater Formation, PPM	-	-	-12.5	-	27.7	-	-	Molar fragments when possible	Franz-Odendaal et al., 2002
-	Suidae	-	*Nyanzachoerus cf.*	*jaegeri*	Langebaanweg	Varswater Formation, PPM	-	-	-12.0	-	28.6	-	-	Molar fragments when possible	Franz-Odendaal et al., 2002

[a] Averaged enamel samples from one specimen.

[b] Teeth are from EFTM (Elandsfontein Main) or WCRP (West Coast Research Project, collected as part of this study). Information for Langebaanweg and Hoedjiespunt are about the collections and geological context.

[c] Location of teeth of WCRP collection is givin by bay number (see Braun et al., 2013).

[d] Taxa were considered semi-aquatic, grazer, mixed feeder and browser when possible (Sponheimer et al., 2001; Franz-Odendaal et al., 2004; Stynder 2009; 2011; Hare and Sealy, 2013).

[e] Original data were reported relative to VPDB and were converted to the VSMOW notation using the equation $\delta^{18}O_{VSMOW} = 1.3086 \times \delta^{18}O_{VPDB} + 30.86$.

[f] Number of analyses averaged.

[g] Abbreviations for tooth position and elements are as follows: R, right; L, left; M, molar. Uppercase and lowercase letters refer to the maxillar and mandibular teeth, respectively. Molar position is indicated by 1, 2 or 3, when known. Tooth element and position information for previsouly published samples are reported from the original studies.

Table S2.3: The $\delta^{18}O$ values of the phosphate and carbonate component of tooth enamel from Elandsfontein and Langebaanweg.

Sample ID	Family	$\delta^{18}O_{enamel\text{-}phosphate}$			$\delta^{18}O_{enamel\text{-}carbonate}$			$\varepsilon_{CO3\text{-}PO4}$	
		(‰ VSMOW)	*1σ*	*n*	(‰ VSMOW)	*1σ*	*n*	avg (‰ VSMOW)	1σ [a]
Elandsfontein									
WCRP-1669	Bovidae	23.7	0.3	3	34.1	0.6	1	10.2	1.0
EFTM-6177.8	Bovidae	23.5	0.5	2	32.6	0.6	1	8.9	1.1
EFTM-8953	Bovidae	23.0	0.3	4	31.6	0.6	1	8.4	0.9
WCRP-5043	Bovidae	24.1	0.2	4	34.3	0.6	1	10.0	0.9
EFTM-11908	Bovidae	21.6	0.2	4	30.7	0.6	1	8.9	0.9
EFTM-5063	Bovidae	24.0	0.3	4	33.2	0.6	1	9.0	1.0
IZ-7892E	Bovidae	23.2	0.1	4	32.9	0.6	1	9.5	0.9
EFTM-5113.6	Bovidae	24.2	0.4	7	34.4	0.6	1	10.0	1.0
EFTM-1746	Bovidae	22.6	0.2	3	31.9	0.6	1	9.2	0.9
EFTM-1694	Bovidae	25.6	0.2	4	35.5	0.6	1	9.6	0.9
EFTM-8657	Bovidae	24.4	0.3	3	34.8	0.6	1	10.1	0.9
EFTM-2728	Bovidae	25.7	0.2	4	36.7	0.6	1	10.7	0.9
EFTM-2738	Bovidae	25.1	0.4	4	34.8	0.6	1	9.4	1.0
WCRP-1666	Bovidae	23.0	0.1	3	32.7	0.6	1	9.5	0.8
EFTM-4088	Hippopotamidae	20.3	0.2	4	29.3	0.6	1	8.8	0.9
EFTM-4030	Hippopotamidae	21.2	0.2	3	30.5	0.6	1	9.1	0.9
EFTM-MSI2699	Hippopotamidae	19.9	0.4	4	28.7	0.6	1	8.6	1.0
EFTM-6727	Equidae	22.1	0.2	4	32.0	0.6	1	9.7	0.9
EFTM-16660	Equidae	22.8	0.4	6	32.0	0.6	1	9.0	1.0
EFTM-2112	Equidae	23.5	0.1	3	33.9	0.6	1	10.2	0.9
EFTM-5065	Equidae	23.7	0.1	4	33.1	0.6	1	9.1	0.9
EFTM-8958A	Equidae	22.8	0.3	3	32.7	0.6	1	9.7	1.0
WCRP-2103	Equidae	23.1	0.4	6	32.3	0.6	1	8.9	1.0
EFTM-2619	Equidae	22.3	0.2	2	31.6	0.6	1	9.0	0.9
EFTM-1952	Equidae	23.3	0.3	4	33.1	0.6	1	9.6	0.9
EFTM-4028A	Giraffidae	24.4	0.0	3	35.0	0.6	1	10.3	0.8
EFTM-4031	Giraffidae	23.6	0.3	2	33.5	0.6	2	9.6	0.9
WCRP-8031	Giraffidae	23.1	0.3	4	32.8	0.6	1	9.5	0.9
EFTM-20939	Rhinocerotidae	23.6	0.2	2	32.2	0.6	1	8.5	0.9
EFTM-20982D	Rhinocerotidae	23.3	0.2	4	33.0	0.6	1	9.4	0.9
EFTM-16617A	Rhinocerotidae	24.0	0.4	4	31.7	0.6	1	7.4	1.0
EFTM-8700K	Rhinocerotidae	23.3	0.2	4	31.1	0.3	2	7.6	0.7
EFTM-3410A	Rhinocerotidae	23.8	0.1	2	32.3	0.6	1	8.3	0.9
EFTM-8610B	Rhinocerotidae	22.9	0.2	3	32.2	0.6	1	9.0	0.9
EFTM-93998	Rhinocerotidae	22.5	0.2	3	31.3	0.6	1	8.6	0.9
WCRP-12156	Suidae	22.5	0.3	3	32.3	0.6	1	9.6	1.0
WCRP-12284	Suidae	22.7	0.3	4	32.5	0.6	1	9.6	1.0
WCRP-6438	Suidae	22.8	0.3	1	31.4	0.6	1	8.4	1.0
Langebaanweg									
LBW13G-001	Bovidae	25.2	0.2	4	34.6	0.6	1	9.2	0.9
LBW13G-004	Equidae	22.8	0.4	6	31.2	0.6	1	8.2	1.0
LBW13G-006	Hippopotamidae	20.3	0.1	4	28.1	0.6	1	7.7	0.9
LBW13G-007	Hippopotamidae	19.9	0.2	4	27.1	0.6	1	7.0	0.9
LBW13G-008A	Hippopotamidae	21.3	0.7	2	30.3	0.6	1	8.8	1.2
LBW13G-008B	Hippopotamidae	21.2	0.6	2	28.7	0.6	1	7.4	1.1
LBW13G-008 (A & B)	Hippopotamidae	21.3	0.6	4	29.5	1.1	2	8.1	1.3
LBW13G-009	Giraffidae	25.2	0.1	4	34.0	0.6	1	8.6	0.9
LBW13G-010	Giraffidae	24.0	0.4	4	33.3	0.6	1	9.1	1.0
LBW13G-011	Giraffidae	21.9	0.2	4	30.3	0.6	1	8.3	0.9

[a] propagated error

$$\varepsilon_{carbonate\text{-}phosphate} = \sqrt{(\text{standard deviation } \delta^{18}O_{enamel\text{-}phosphate}) + (\text{standard deviation } \delta^{18}O_{enamel\text{-}carbonate})}$$

Table S2.4: Oxygen and hydrogen isotope composition of waters from southwestern South Africa.

Location	Sample source	Year(s) of collection[a]	$\delta^{18}O$ of water avg[b] ‰ VSMOW	$\delta^{2}H$ of water avg[b] ‰ VSMOW	Rainfall zone	References
Cape Town	Springs	1996, 1997, 2010 - 2012	-3.3±0.5 (*n* = 87)	-10.7±2.0 (*n* = 69)	Winter	Harris et al., 2000; Harris and Diamond, 2013
Cape Town	Water treatment plants	1996, 1997	-3.0±1.5 (*n* = 16)	-10.3±8.5 (*n* = 16)	Winter	Harris et al., 1999
Cape Town	Aquifers	1996, 1997	-3.0±0.6 (*n* = 29)	-12.1±4.7 (*n* = 29)	Winter	Harris et al., 1999
Western Cape (primarily surrounding Cape Town)	Rivers	1996, 1997, 2010 - 2012	-3.5±1.2 (*n* = 68)	-16.1±10.0 (*n* = 70)	Winter	Harris et al., 1999; Harris and Diamond, 2013
University of Cape Town	Precipitation (monthly)	1996 - 2008	-2.8±1.7 (*n* = 163)	-9.5±2.8 (*n* = 163)	Winter	Harris et al., 2010
University of Cape Town	Precipitation (daily)	1996 - 2008	-2.67±2.1 (*n* = 109)	-7.1±14.2 (*n* = 109)	Winter	Harris et al., 2010
Western Cape (primarily surrounding Cape Town)	Precipitation	2010 - 2012	-2.9 (*n* = ND)[c]	-9.2 (*n* = ND)[c]	Winter	Harris and Diamond, 2013
Table Mountain Cableway, Cape Town	Precipitation	2010 - 2012	-3.6±1.1, -3.7 (*n* = 18)[c]	-12.4±5.8, 14.4 (*n* = 17)[c]	Winter	Harris and Diamond, 2013
Jonkershoek Valley (closest major city is	Catchment waters	1992	-4.0±0.2 (*n* = 24)	ND	Winter	Midgley and Scott, 1994
Western Cape, West Coast	Groundwater and precipitation	1999 - 2000	-3.9±1.4 (*n* = 19)	ND	Winter	Weaver and Telma, 2005
Western Cape, South Coast	Groundwater and precipitation	1999 - 2000	-5.2±1.3 (*n* = 5)	ND	Annual	Weaver and Telma, 2005
Hopefield, Western Cape	Precipitation (annually cumulative)	1999 - 2000	-3.2 (*n* = 1)	ND	Winter	Weaver and Telma, 2005
Langebaan Road Wellfield, Western Cape	Precipitation (annually cumulative)	1999 - 2000	-2.8 (*n* = 1)	ND	Winter	Weaver and Telma, 2005
Langebaan Road Wellfield, Western Cape	Aquifer	1999 - 2000	-3.6±0.1 (*n* = 4)	ND	Winter	Weaver and Telma, 2005
Cape Fold Belt	Precipitation	2010 - 2012	-4.3±1.8 (*n* = 226)	-17.1±9.8 (*n* = 232)	Winter and Annual	Harris and Diamond, 2013
Jonkershoek Valley area	Groundwater, tapwater, modeled isoscape	2006, 2007, 2009, 2010	-5.2 to -2.9 (model based on 770 water samples)	-29.0 to -10.0	Winter	West et al., 2014

Table S2.4: Oxygen and hydrogen isotope composition of waters from southwestern South Africa.

Location	Sample source	Year(s) of collection[a]	$\delta^{18}O$ of water avg[b] ‰ VSMOW	$\delta^{2}H$ of water avg[b] ‰ VSMOW	Rainfall zone	References
Elandsfontein area	Groundwater, tapwater, modeled isoscape	2006, 2007, 2009, 2010	-2.8 to -0.5 (model based on 770 water samples)	-19.0 to 0.0	Winter	West et al., 2014
Elandsfontein[d]	Standing water	2010	1.5 (n = 1)	6.2 (n = 1)	Winter	This study (sample SA10W400) WGS-84 Lat/Long: -33.1250, 18.23667
Elandsfontein[d]	Spring water	2010	-3.2 (n = 1)	-13.8 (n = 1)	Winter	This study (sample SA10W401) WGS-84 Lat/Long: -33.10744, 18.20932
Western Cape Fossil Park[d]	Tap water	2010	-1.9 (n = 1)	-9.2 (n = 1)	Winter	This study (sample SA10W402) WGS-84 Lat/Long: -32.95659, 18.11633
Brakfontein, near Elandsfontein[d]	Spring water	2010	-3.3 (n = 1)	-14.4 (n = 1)	Winter	This study (sample SA10W403) WGS-84 Lat/Long: -32.95215, 18.24296

[a] Only months with both precipitation amount and $\delta^{18}O$ of precipitation were used for this study. Samples were not collected over continous time periods for every site.

[b] Isotope data are reported as averages with thier standard deviation (1σ). The number of samples are given in parentheses.

[c] Weighted mean of rainfall as reported in Harris and Diamond (2013).

[d] GPS coordinates for the samples collected and their sample ID are provided in the refernce column.
'ND' is used to indicate no data.

Appendix II
(CHAPTER 3 Supplementary Tables)

Table S3.1: Bioavailable $^{87}Sr/^{86}Sr$ ratios for major substrates in southwestern South Africa from this study and Sealy et al. (1991).

Sample ID	Geological subtrate	Site[a]	Location	$^{87}Sr/^{86}Sr$ ratio		Material	Common name	Species	Reference
				Average	Stdev[b]				
RND 130919	Cape Granite suite	A	Rondeberg	0.715661	0.000012	Bone	Dassie	*Petromus typicus*	This study
RND130914	Cape Granite suite	A	Rondeberg	0.713183	0.000015	Bone	Dassie	*Petromus typicus*	This study
RND130915	Cape Granite suite	A	Rondeberg	0.713116	0.000011	Bone	Dassie	*Petromus typicus*	This study
RND130916	Cape Granite suite	A	Rondeberg	0.713353	0.000010	Bone	Dassie	*Petromus typicus*	This study
SA14M-500	Cape Granite suite	A	Rondeberg	0.711421	0.000013	Bone	Geometric tortoise	*Psammobates geometricus*	This study
Silvertree upper (granite location)	Cape Granite suite	B	Vlakkenberg, Constantia Valley	0.719891	0.000009	Plant	Silver tree plant	*Leucadendron argenteum*	This study
P1	Cape Granite suite	C	Paarl Rock	0.719300	0.000015	Plant	Fern/bracken	*Pteridium* sp.	This study
P2	Cape Granite suite	C	Paarl Rock	0.717402	0.000016	Plant	Lance-leafed Waxberry	*Morella serrata*	This study
P3	Cape Granite suite	C	Paarl Rock	0.718053	0.000013	Plant	Sumac	*Rhus* sp.	This study
P4	Cape Granite suite	C	Paarl Rock	0.722416	0.000013	Plant	Daisy	*Eriocephalus* sp.	This study
P5	Cape Granite suite	C	Paarl Rock	0.723563	0.000011	Plant	Hopbush	*Dodonea* sp.	This study
P6	Cape Granite suite	C	Paarl Rock	0.722537	0.000018	Plant	Protea	*Protea* sp.	This study
UCT 2274	Malmesbury shale	D	Botmaskloof Pass, near Riebeeck Kasteel	0.715332	0.000014	Bone	Porcupine	*Hystrix africaeaustralis*	This study
UCT 3389	Malmesbury shale	E	Elandsberg	0.718540	0.000014	Bone	Geometric tortoise	*Psammobates geometricus*	This study
UCT 3390	Malmesbury shale	E	Elandsberg	0.720390	0.000013	Bone	Geometric tortoise	*Psammobates geometricus*	This study
UCT 3392	Malmesbury shale	E	Elandsberg	0.718410	0.000011	Bone	Geometric tortoise	*Psammobates geometricus*	This study
UCT 2247	Malmesbury shale	-	Terrestrial area	0.717770	0.000040	Bone	Bat-eared fox	*Otocyon megalotis*	Sealy et al. (1991)
UCT 2801	Malmesbury shale	-	Terrestrial area	0.717940	0.000030	Bone	Elephant shrew	*Macroscelides/Elephantulus* sp.	Sealy et al. (1991)
SA14M-103	Marine sands	Elandsfontein	Elandsfontein	0.710276	0.000010	Enamel (incisor)	Small rodent	-	This study
SA14M-106	Marine sands	Elandsfontein	Elandsfontein	0.710310	0.000014	Enamel (incisor)	Small rodent	-	This study
UCT 876	Marine sands	-	Coastal area	0.711240	0.000030	Bone	Steenbok	*Raphicerus campestris*	Sealy et al. (1991)
UCT 1074	Marine sands	-	Coastal area	0.711690	0.000030	Bone	Steenbok	*Raphicerus campestris*	Sealy et al. (1991)
UCT 1192	Marine sands	-	Coastal area	0.710410	0.000040	Bone	Grey duiker	*Sylvicapra grimmia*	Sealy et al. (1991)
UCT 732	Marine sands	-	Coastal area	0.710240	0.000040	Bone	Steenbok	*Raphicerus campestris*	Sealy et al. (1991)
UCT 821	Marine sands	-	Coastal area	0.709470	0.000030	Bone	Springbok	*Antidorcas marsupialis*	Sealy et al. (1991)
UCT 2061	Marine sands	-	Coastal area	0.709380	0.000030	Bone	Bontebok	*Damaliscus dorcas dorcas*	Sealy et al. (1991)
Fern (granite location)	Mixed granite and marine sands	B	Vlakkenberg, Constantia Valley	0.714741	0.000010	Plant	Fern	*Pteridium* sp.	This study
Silvertree lower (granite locaiton)	Mixed granite and marine sands	B	Vlakkenberg, Constantia Valley	0.711217	0.000011	Plant	Silver tree	*Leucadendron argenteum*	This study
UCT 130921	Table Mountain Sandstone	F	Mertenhof	0.718119	0.000013	Bone	Dassie	*Petromus typicus*	This study
UCT 14347E	Table Mountain Sandstone	F	Mertenhof	0.718546	0.000013	Bone	Dassie	*Petromus typicus*	This study
UCT 14347	Table Mountain Sandstone	F	Mertenhof	0.718411	0.000012	Bone	Dassie	*Petromus typicus*	This study
UCT 14335	Table Mountain Sandstone	G	Heuningvlei, Biedouw Valley	0.714159	0.000011	Bone	Dassie	*Petromus typicus*	This study
UCT 14335E	Table Mountain Sandstone	G	Heuningvlei, Biedouw Valley	0.714092	0.000013	Bone	Dassie	*Petromus typicus*	This study
UCT 4082	Table Mountain Sandstone	H	Boontjieskloof (Sevilla, Boontjieskloof)	0.718039	0.000013	Enamel (third molar)	Porcupine	*Hystrix africaeaustralis*	This study
UCT 2544	Table Mountain Sandstone	H	Boontjieskloof	0.716081	0.000014	Bone	Aardvark	*Orycteropus afer*	This study
UCT 2074	Table Mountain Sandstone	-	Terrestrial area	0.715430	0.000030	Bone	Grey duiker	*Sylvicapra grimmia*	Sealy et al. (1991)
UCT 2081	Table Mountain Sandstone	-	Terrestrial area	0.717460	0.000030	Bone	Chacma baboon	*Papio ursinus*	Sealy et al. (1991)

[a] see Figure 1 for site locations on map of southwestern South Africa
[b] standard deviation is ± 2σ of the internal standard

Table S3.2: $^{87}Sr/^{86}Sr$ ratios of the fossil mammals from mid-Pleistocene Elandsfontein.

Sample ID (top to bottom of the tooth)	$^{87}Sr/^{86}Sr$ ratio	
	Average	Stdev[a]
Bovidae		
Bovid sp., third molar, solution analysis on ICP-MS		
1468 1.5	0.710167	0.000014
1468 2.5	0.710181	0.000014
1468 3.5	0.710069	0.000012
1468 4.5	0.710084	0.000017
1468 5.5	0.710169	0.000017
1468 6.5	0.710181	0.000013
1468 7.5	0.710039	0.000014
1468 8.5	0.710049	0.000012
1468 9.5	0.709976	0.000011
1468 10.5	0.709982	0.000013
Alcelaphini sp. indet., potentially migratory, grazer, molar, laser ablation serial sampling on ICP-MS		
WCRP-1358A_4	0.709810	0.000080
WCRP-1358A_3	0.709770	0.000080
WCRP-1358A_2	0.709820	0.000090
WCRP-1358A_1	0.709900	0.000080
WCRP-1358B_4	0.709860	0.000090
WCRP-1358B_3	0.709860	0.000100
WCRP-1358B_2	0.709790	0.000110
WCRP-1358B_1bottom	0.709880	0.000100
WCRP-1358C_4	0.709790	0.000070
WCRP-1358C_3	0.709830	0.000100
WCRP-1358C_2	0.709980	0.000100
WCRP-1358C_1worn	0.709820	0.000090
Syncerus antiquus, Giant buffalo (extinct), potentially migratory, grazer, third molar, laser ablation serial sampling		
WCRP-36309_1root	0.711120	0.003000
WCRP-36309_2	0.710710	0.000150
WCRP-36309_3	0.711060	0.000120
WCRP-36309_4	0.711050	0.000100
WCRP-36309_5	0.711000	0.000090
WCRP-36309_6	0.711120	0.000090
WCRP-9043_01root	0.710140	0.000040
WCRP-9043_02	0.710140	0.000040
WCRP-9043_03	0.710160	0.000040
WCRP-9043_04	0.710130	0.000030
WCRP-9043_05	0.710240	0.000040
WCRP-9043_06	0.710270	0.000050
WCRP-9043_07	0.710260	0.000040
WCRP-9043_08	0.710340	0.000040
WCRP-9043_09	0.710390	0.000040
WCRP-9043_10	0.710460	0.000050
WCRP-9043_11	0.710420	0.000060
WCRP-9043_12	0.710570	0.000040
Syncerus antiquus, Giant buffalo (extinct), potentially migratory, grazer, third molar, solution analysis on ICP-MS		
46225.01	0.709656	0.000058
46225.02	0.709658	0.000084
46225.03	0.709657	0.000118
46225.04	0.709640	0.000142
46225.05	0.709617	0.000048
46225.06	0.709609	0.000070

Table S3.2: $^{87}Sr/^{86}Sr$ ratios of the fossil mammals from mid-Pleistocene Elandsfontein.

Sample ID (top to bottom of the tooth)	$^{87}Sr/^{86}Sr$ ratio	
	Average	Stdev[a]
46245.01	0.709324	0.000192
46245.02	0.709832	0.000142
46245.03	0.709905	0.000162
46245.04	0.709847	0.000154
46245.05	0.709873	0.000112
46245.06	0.709939	0.000114
46245.07	0.710002	0.000084
46245.08	0.710141	0.000114
46245.09	0.709952	0.000114
46245.10	0.709921	0.000116
46245.11	0.709953	0.000118
46245.12	0.709826	0.000112
1666 1.5	0.709521	0.000020
1666 2.5	0.709528	0.000013
1666 3.5	0.709711	0.000019
1666 4.5	0.709457	0.000023
1666 5.5	0.710078	0.000020
1666 6.5	0.709689	0.000022
1666 7.5	0.709879	0.000019
1666 8.5	0.709656	0.000015
1666 9.5	0.709255	0.000012
36309 1.5	0.710462	0.000025
36309 2.5	0.710442	0.000014
36309 3.5	0.710351	0.000014
36309 4.5	0.710412	0.000016
36309 5.5	0.710488	0.000023
8787 1.5	0.711171	0.000015
8787 2.5	0.711079	0.000020
8787 3.5	0.710889	0.000014
9046.1 A.5	0.710693	0.000015
9046.1 B.5	0.710636	0.000016
9046.1 C.5	0.710574	0.000026
9046.1 D.5	0.710554	0.000016
9046.1 E.5	0.710526	0.000015
9046.1 F.5	0.710457	0.000014
9046.2 G.1	0.710428	0.000015
9046.2 H.5	0.710420	0.000015
9046.2 I.5	0.710382	0.000017
9046.2 J.5	0.710407	0.000020
9046.3 K.5	0.710700	0.000016
9046.3 L.5	0.710340	0.000013
9046.3 M.5	0.710327	0.000015
9046.3 N.5	0.710351	0.000015
9046.3 O.5	0.710380	0.000019
9046.3 P.5	0.710360	0.000015
9046.4 Q.5	0.710363	0.000017
9046.4 R.5	0.710492	0.000015
9046.4 S.5	0.710570	0.000014
9046.4 T.5	0.710622	0.000027
9046.4 U.5	0.710835	0.000023

Table S3.2: $^{87}Sr/^{86}Sr$ ratios of the fossil mammals from mid-Pleistocene Elandsfontein.

Sample ID (top to bottom of the tooth)	$^{87}Sr/^{86}Sr$ ratio	
	Average	Stdev[a]
9944.2 A.5	0.709771	0.000028
9944.2 B.5	0.709888	0.000039
9944.2 C.5	0.709883	0.000032
9944.2 D.5	0.709877	0.000136
Tragelaphus strepsiceros, Greater kudu, potentially migratory, browser, third molar, solution analysis on ICP-MS		
9386 1.5	0.709546	0.000017
9386 2.5	0.709607	0.000013
9386 3.5	0.709648	0.000023
9386 4.5	0.709653	0.000021
9386 5.5	0.709749	0.000021
9386 6.5	0.709754	0.000019
9386 7.5	0.709723	0.000011
9386 8.5	0.709738	0.000015
9386 9.5	0.709741	0.000014
9386 10.5	0.709727	0.000014
36612 1.5	0.709775	0.000012
36612 2.5	0.709780	0.000015
36612 3.5	0.709750	0.000014
36612 4.5	0.709693	0.000020
36612 5.5	0.709685	0.000014
36612 6.5	0.709671	0.000011
36612 7.5	0.709694	0.000012
20443 1.5	0.709414	0.000018
20443 2.5	0.709354	0.000010
20443 3.5	0.709367	0.000013
20443 4.5	0.709376	0.000013
20443 5.5	0.709382	0.000015
20443 6.5	0.709400	0.000013
20443 7.5	0.709406	0.000013
20443 8.5	0.709428	0.000012
20443 9.5	0.709330	0.000025
Bovid sp., potentially migratory, grazer, molar, solution analysis ICP-MS		
32386 1.5	0.710356	0.000012
32386 2.5	0.710495	0.000014
32386 3.5	0.710588	0.000015
32386 4.5	0.711105	0.000011
32386 5.5	0.710982	0.000017
32386 6.5	0.710441	0.000061
32386 7.5	0.710369	0.000013
32386 8.5	0.709993	0.000014
32386 9.5	0.709873	0.000011
32386 10.5	0.709856	0.000017
32386 11.5	0.709863	0.000012
32386 12.5	0.709920	0.000010
Bovid sp., solution analysis ICP-MS		
1468 1.5	0.710167	0.000014
1468 2.5	0.710181	0.000014
1468 3.5	0.710069	0.000012

Table S3.2: $^{87}Sr/^{86}Sr$ ratios of the fossil mammals from mid-Pleistocene Elandsfontein.

Sample ID (top to bottom of the tooth)	$^{87}Sr/^{86}Sr$ ratio	
	Average	Stdev[a]
1468 4.5	0.710084	0.000017
1468 5.5	0.710169	0.000017
1468 6.5	0.710181	0.000013
1468 7.5	0.710039	0.000014
1468 8.5	0.710049	0.000012
1468 9.5	0.709976	0.000011
1468 10.5	0.709982	0.000013
Elephantidae		
Loxodonta africana, African elephant, potentially migratory, grazer, molar fragment, solution analysis ICP-MS		
WCRP 6088	0.710547	0.000017
WCRP 12298	0.710071	0.000014
Equidae		
Equus capensis, Cape zebra, potentially migratory, grazer, third molar, solution analysis ICP-MS		
WCRP 2048	0.709705	0.000016
Hystricidae		
Hystrix africaeaustralis, Porcupine, not migratory, mixed feeder, third molar, laser ablation serial sampling on ICP-MS		
32012.01	0.709587	0.000320
32012.01	0.709428	0.000162
32012.02	0.709552	0.000084
32012.03	0.709470	0.000124
32012.04	0.709446	0.000114
32012.05	0.709423	0.000120
32012.06	0.709429	0.000112
Bathyergidae		
Bathyergus suillus, Dune mole rate, not migratory, mixed diet, incisor, laser ablation serieal sampling on ICP-MS		
32007.01	0.709348	0.000166
32007.02	0.709275	0.000192
32007.03	0.709349	0.000112
32007.04	0.709489	0.000182
32007.05	0.709414	0.000130
32007.06	0.709476	0.000130
Hyaenidae		
Hyaena brunnea, Brown hyena, potentially migratory, carnivore, third molar, solution analysis ICP-MS		
WCRP 32121	0.709393	0.000018
WCRP 32442	0.709620	0.000024

[a] standard deviation is ± 2σ from the internal standard

Table S.3.3: Profiles for mid-Pleistocene and modern enamel fragments from Elandsfontein using the $^{87}Sr/^{86}Sr$ ratio of rinses and enamel powder after series of rinses.

Sample ID	Sample description (enamel or rinse #)	mid-Pleistocene or modern enamel	$^{87}Sr/^{86}Sr$ ratio Average	Stdev[a]
WCRP 46257 (bovid)				
rinse 1	supernatant	mid-Pleistocene	0.709570	0.000018
rinse 6	supernatant	mid-Pleistocene	0.709481	0.000014
rinse 12	supernatant	mid-Pleistocene	0.709448	0.000012
rinse 18	supernatant	mid-Pleistocene	0.709449	0.000016
rinse 24	supernatant	mid-Pleistocene	0.709405	0.000015
enamel residue	enamel powder risidue	mid-Pleistocene	0.709428	0.000014
		avg ± stdev	*0.709463 ± 0.000058*	
		range	*0.709405 to 0.709570*	
		span	*0.000165*	
WCRP 46251				
rinse 1	supernatant	mid-Pleistocene	0.709814	0.000014
rinse 6	supernatant	mid-Pleistocene	0.709569	0.000019
rinse 12	supernatant	mid-Pleistocene	0.709507	0.000018
rinse 18	supernatant	mid-Pleistocene	0.709576	0.000016
rinse 24	supernatant	mid-Pleistocene	0.709535	0.000015
enamel residue	enamel powder risidue	mid-Pleistocene	0.709474	0.000012
		avg ± stdev	*0.709579 ± 0.000121*	
		range	*0.709474 to 0.709814*	
		span	*0.000340*	
WCRP - 46245 (Syncerus antiquus)				
rinse 1	supernatant	mid-Pleistocene	0.709879	0.000011
rinse 6	supernatant	mid-Pleistocene	0.709871	0.000021
rinse 12	supernatant	mid-Pleistocene	0.709849	0.000019
rinse 18	supernatant	mid-Pleistocene	0.709824	0.000021
rinse 24	supernatant	mid-Pleistocene	0.709829	0.000029
enamel residue	enamel powder risidue	mid-Pleistocene	0.709802	0.000016
		avg ± stdev	*0.709842 ± 0.000029*	
		range	*0.709802 to 0.709879*	
		span	*0.000077*	
6				
rinse 1	supernatant		0.709982	0.000012
rinse 5	supernatant		0.709980	0.000016
rinse 10	supernatant		0.709990	0.000017
rinse 15	supernatant		0.709977	0.000015
rinse 20	supernatant		0.709945	0.000014
rinse 25	supernatant		0.709969	0.000013
enamel residue	enamel powder risidue		0.709871	0.000011
		avg ± stdev	*0.709955 ± 0.000044*	
		range	*0.709871 to 0.70999*	
		span	*0.000119*	
7				
rinse 1	supernatant		0.709649	0.000014
rinse 5	supernatant		0.709400	0.000015
rinse 10	supernatant		0.709366	0.000013
rinse 15	supernatant		0.709402	0.000021
rinse 20	supernatant		0.709383	0.000021
rinse 25	supernatant		0.709401	0.000020
enamel residue	enamel powder risidue		0.709411	0.000014
		avg ± stdev	*0.709394 ± 0.000016*	
		range	*0.709366 to 0.709411*	
		span	*0.000045*	
WCRP 2048 (equid)				
rinse 1	supernatant	mid-Pleistocene	0.709799	0.000008
rinse 5	supernatant	mid-Pleistocene	0.709784	0.000021
rinse 10	supernatant	mid-Pleistocene	0.709772	0.000021
rinse 15	supernatant	mid-Pleistocene	0.709696	0.000014
rinse 20	supernatant	mid-Pleistocene	0.709631	0.000017
rinse 25	supernatant	mid-Pleistocene	0.709664	0.000019
enamel residue	enamel powder risidue	mid-Pleistocene	0.709705	0.000016

Table S.3.3: Profiles for mid-Pleistocene and modern enamel fragments from Elandsfontein using the $^{87}Sr/^{86}Sr$ ratio of rinses and enamel powder after series of rinses.

Sample ID	Sample description (enamel or rinse #)	mid-Pleistocene or modern enamel	$^{87}Sr/^{86}Sr$ ratio Average	Stdev[a]
		avg ± stdev	*0.709709 ± 0.000060*	
		range	*0.709631 to 0.709784*	
		span	*0.000153*	
WCRP 6088				
rinse 1	supernatant	mid-Pleistocene	0.710358	0.000013
rinse 5	supernatant	mid-Pleistocene	0.710556	0.000011
rinse 10	supernatant	mid-Pleistocene	0.710679	0.000028
rinse 15	supernatant	mid-Pleistocene	0.710588	0.000017
rinse 20	supernatant	mid-Pleistocene	0.710542	0.000034
rinse 25	supernatant	mid-Pleistocene	0.710545	0.000023
enamel residue	enamel powder risidue	mid-Pleistocene	0.710547	0.000017
		avg ± stdev	*0.710576 ± 0.000053*	
		range	*0.710542 to 0.710679*	
		span	*0.000137*	
WCRP 12298				
rinse 1	supernatant	mid-Pleistocene	0.709930	0.000013
rinse 5	supernatant	mid-Pleistocene	0.710085	0.000012
rinse 10	supernatant	mid-Pleistocene	0.710171	0.000013
rinse 15	supernatant	mid-Pleistocene	0.710228	0.000013
rinse 20	supernatant	mid-Pleistocene	0.710247	0.000043
rinse 25	supernatant	mid-Pleistocene	0.710265	0.000015
enamel residue	enamel powder risidue	mid-Pleistocene	0.710071	0.000014
		avg ± stdev	*0.710178 ± 0.000084*	
		range	*0.710071 to 0.710265*	
		span	*0.000194*	
SA13M-507 (bovid)				
rinse 1	supernatant	mid-Pleistocene	0.709631	0.000014
rinse 6	supernatant	mid-Pleistocene	0.710104	0.000012
rinse 12	supernatant	mid-Pleistocene	0.710091	0.000016
rinse 18	supernatant	mid-Pleistocene	0.710092	0.000019
rinse 24	supernatant	mid-Pleistocene	0.710099	0.000024
enamel residue	enamel powder risidue	mid-Pleistocene	0.710131	0.000013
		avg ± stdev	*0.710025 ± 0.000193*	
		range	*0.709631 to 0.710131*	
		span	*0.000499*	
SA13M-011 (juv. Alcelaphine)				
rinse 1	supernatant	modern	0.713023	0.000013
rinse 6	supernatant	modern	0.713592	0.000016
rinse 12	supernatant	modern	0.713603	0.000012
rinse 18	supernatant	modern	0.713606	0.000013
rinse 24	supernatant	modern	0.713616	0.000012
enamel residue	enamel powder risidue	modern	0.713633	0.000012
		avg ± stdev	*0.713512 ± 0.000240*	
		range	*0.713023 to 0.713633*	
		span	*0.000610*	

[a] standard deviation is ± 2σ from the internal standard

Appendix III
(CHAPTER 4 Supplementary Tables)

Table S4.1: Sample site location and climate information.[a]

Sample location	Latitude	Longitude	MAT (Celsius)[b]	MAP (mm)[c]	Mean RH (%)[d]	PET (mm)[e]	Aridity Index[f]	Climate classification (UNESCO 1979)[g]
East Africa								
Turkana, Kenya	4.2 N	36.3 E	27.9	364.0	52.9	1840.6	0.20	Arid
Awash, Ethiopia	8.9 N	40.0 E	25.1	625.1	62.6	1320.4	0.47	Semiarid to arid
Tsavo, Kenya	3.4 S	38.6 E	23.8	726.3	63.3	1154.7	0.63	Dry subhumid
Meru National Park, Kenya	0.1 N	38.2 E	25.6	894.9	63.2	1372.8	0.65	Dry subhumid
Shimba Hills, Kenya	4.1 S	39.2 E	25.5	914.9	70.9	1374.9	0.67	Dry subhumid
Kidepo, Uganda	3.9 N	33.8 E	23.2	809.7	57.9	1079.3	0.75	Dry subhumid
Garamba, DRC	4.1 N	29.5 E	24.8	1423.5	67.1	1258.9	1.13	Moist subhumid
Laikipia, Kenya	0.3 N	36.9 E	17.3	952.2	63.9	740.7	1.29	Dry subhumid
Ituri Forest, DRC	1.8 N	29.9 E	21.9	1277.8	71.6	974.5	1.31	Humid
Aberdares, Kenya	0.4 S	36.8 E	14.0	1381.5	70.2	652.9	2.12	Moist subhumid to humid
South Africa								
Kgalagadi National Park	26.3 S	20.4 E	20.2	212.2	43.8	981.0	0.22	Arid
Addo Naitonal Park	33.3 S	25.5 E	17.7	444.3	64.2	790.4	0.56	Semiarid
Finland								
Norrmark	61.4 N	21.5 E	4.3	542.2	81.6	475.0	1.14	Humid
Karessuando (Lapland)	68.3 N	22.3 E	-2.7	442.3	86.5	367.1	1.20	Humid
Rovaniemi	66.3 N	25.4 E	0.3	514.9	80.0	405.7	1.27	Humid
Pernaja	60.3 N	26.0 E	4.2	662.3	81.1	463.3	1.43	Humid
Aunus, Nurmoila	60.3 N	23.6 E	3.9	645.7	81.8	450.2	1.43	Humid
United States								
Badlands National Park, SD	43.5 N	102.2 W	8.3	417.9	60.5	569.9	0.73	Semiarid to dry subhumid
Edness Kimball Wilkins State National Park, WY	42.5 N	106.1 W	5.4	327.1	55.3	422.3	0.77	Semiarid
Wichita Mountains Federal Wildlife Refuge, OK	34.5 N	98.4 W	16.6	696.0	63.7	871.9	0.80	Dry subhumid to semiarid
Theodore Roosevelt National Park, ND	46.6 N	103.3 W	5.6	392.2	63.9	454.0	0.86	Dry subhumid
Antelope Island, UT	40.5 N	112.1 W	8.3	538.3	54.3	550.1	0.98	Dry subhumid
Parowan, UT	37.5 N	112.5 W	5.3	404.2	48.1	407.6	0.99	Semiarid
Arctic National Wildlife Refuge, AK	68.3 N	143.4 W	-12.3	131.3	67.9	119.3	1.10	Dry subhumid/cold climate
Middle Fork, Selman River, ID	44.6 N	114.6 W	3.8	488.0	59.9	362.4	1.35	Dry subhumid
Piedmont National Wildlife Refuge, GA	33.1 N	83.5 W	17.0	1181.9	70.2	844.9	1.40	Humid
Berkley Springs, WV	39.4 N	78.1 W	11.7	961.0	69.6	676.5	1.42	Humid

Baltimore, MD	39.2 N	76.4 W	13.4	1076.1	66.6	736.3	1.46	Humid
Westchester County, NY	41.1 N	73.5 W	10.3	1247.5	67.7	626.8	1.99	Humid
Dairymens Country Club, WI	46.1 N	89.4 W	3.6	814.6	72.6	347.9	2.34	Humid
Yellowstone National Park, WY	44.3 N	110.4 W	0.3	542.7	55.7	225.6	2.41	Humid

[a] Climate information for each sample sites is the output for a model produced by University of East Anglia, Climate Research Unit (CRU). These modeled data are based on measured data from 1961 to 1990 and estimated data are produced for mean climate grids of 10-minute latitudinal/longitudinal global land areas (New et al., 2000).

[b] Mean annual temperature (MAT)

[c] Mean annaul precipitation (MAP)

[d] Mean daily relative humidity (RH) is modeled from measurments of the monthly average of daily averages (24 hour) RH values or calculated from vapor pressure measurments and not based on RH at any specific time.

[e] Mean Potential Evapotranspiration (PET) is calculated using the Thronwaite equation PET calculation

$$PET = \sum_{i=1}^{12} 16 * K * (10 * \frac{t}{I})^{a}$$

where K is a factor for the duration of sunlight during each month and varies by latitude, *a* is a coefficient, *t* is temperature and *I* is an annual heat index.

[f] Aridity Index is used as a proxy for aridity and calculated using [MAP:PET]. Where PET is calculated using the Thronwaite PET calculation.

[g] Climate classifications taken from UNSECO Aridity maps of Africa and of the continents (www.unesco.org).

Table S4.2: Triple oxygen isotope data for enamel samples listed by Analytical ID.

Analytical ID	Sample ID	Session ID	$\delta^{17}O$ (‰)	$\delta^{18}O$ (‰)	Additional CO_3 adjustment amount for $\Delta^{17}O$ (‰)	$\Delta^{17}O$ (‰)	$\Delta^{17}O$ per meg	Reference
JHU-17O-2539	AK Caribou #1	Nov 2015	13.47	26.00	-	-0.171	-171	this study
JHU-17O-2540	AK Caribou #1	Nov 2015	12.71	24.53	-	-0.170	-170	this study
JHU-17O-2535	ID deer	Nov 2015	16.80	32.44	-	-0.195	-195	this study
JHU-17O-2536	ID deer	Nov 2015	17.76	34.31	-	-0.212	-212	this study
JHU-17O-2520	MD deer #1	Nov 2015	18.91	36.46	-	-0.177	-177	this study
JHU-17O-2521	MD deer #1	Nov 2015	19.69	37.98	-	-0.183	-183	this study
JHU-17O-2522	MD deer #2	Nov 2015	18.12	34.97	-	-0.193	-193	this study
JHU-17O-2523	MD deer #2	Nov 2015	18.53	35.77	-	-0.192	-192	this study
JHU-17O-2552	ND bison #1	Nov 2015	13.06	25.15	-	-0.140	-140	this study
JHU-17O-2553	ND bison #1	Nov 2015	13.71	26.44	-	-0.158	-158	this study
JHU-17O-2554	ND bison #2	Nov 2015	14.50	27.97	-	-0.168	-168	this study
JHU-17O-2555	ND bison #2	Nov 2015	14.08	27.17	-	-0.171	-171	this study
JHU-17O-2542	OK Bison #1	Nov 2015	18.57	35.76	-	-0.157	-157	this study
JHU-17O-2543	OK Bison #1	Nov 2015	19.54	37.65	-	-0.158	-158	this study
JHU-17O-2556	SD bison #1	Nov 2015	14.17	27.36	-	-0.177	-177	this study
JHU-17O-2557	SD bison #1	Nov 2015	14.81	28.57	-	-0.168	-168	this study
JHU-17O-2526	WI deer	Nov 2015	16.95	32.71	-	-0.189	-189	this study
JHU-17O-2527	WI deer	Nov 2015	16.43	31.70	-	-0.179	-179	this study
JHU-17O-2524	WV deer	Nov 2015	19.16	37.00	-	-0.207	-207	this study
JHU-17O-2525	WV deer	Nov 2015	19.51	37.67	-	-0.204	-204	this study
JHU-17O-2537	WY deer	Nov 2015	17.84	34.47	-	-0.208	-208	this study
JHU-17O-2538	WY deer	Nov 2015	17.30	33.42	-	-0.203	-203	this study
JHU-17O-2541	WY Yellowstone Moose #1	Nov 2015	13.79	26.59	-	-0.161	-161	this study
JHU-17O-2080	AIJB-B3-T4-DP4	Nov 2014	16.67	32.16	-	-0.179	-179	Hu et al., *in prep.*
JHU-17O-2081	AIJB-B3-T4-DP4	Nov 2014	16.01	30.89	-	-0.176	-176	Hu et al., *in prep.*
JHU-17O-2052	CME	Nov 2014	19.01	36.62	-	-0.155	-155	this study
JHU-17O-2053	CME	Nov 2014	19.34	37.24	-	-0.152	-152	this study
JHU-17O-2054	CME	Nov 2014	19.51	37.57	-	-0.151	-151	this study
JHU-17O-2050	ET03-71	Nov 2014	17.74	34.12	-	-0.129	-129	Hu et al., *in prep.*
JHU-17O-2051	ET03-71	Nov 2014	17.64	33.93	-	-0.130	-130	Hu et al., *in prep.*
JHU-17O-2059	ET05-MAGO-19	Nov 2014	23.53	45.39	-	-0.181	-181	this study
JHU-17O-2060	ET05-MAGO-19	Nov 2014	23.56	45.46	-	-0.188	-188	this study
JHU-17O-2071	GNP-giraffe2	Nov 2014	23.57	45.52	-	-0.212	-212	this study
JHU-17O-2072	GNP-giraffe2	Nov 2014	24.09	46.53	-	-0.208	-208	this study
JHU-17O-2069	GNP-Hippo	Nov 2014	20.02	38.54	-	-0.146	-146	this study
JHU-17O-2070	GNP-Hippo	Nov 2014	20.06	38.60	-	-0.134	-134	this study
JHU-17O-2073	Ituri Giraffe	Nov 2014	21.84	42.13	-	-0.183	-183	this study
JHU-17O-2074	Ituri Giraffe	Nov 2014	21.72	41.90	-	-0.182	-182	this study
JHU-17O-2077	K00-TSV-113	Nov 2014	24.38	47.15	-	-0.237	-237	this study
JHU-17O-2078	K00-TSV-113	Nov 2014	24.43	47.24	-	-0.234	-234	this study
JHU-17O-2075	K98-Lai-310	Nov 2014	22.85	44.18	-	-0.230	-230	this study
JHU-17O-2076	K98-Lai-310	Nov 2014	22.35	43.18	-	-0.218	-218	this study
JHU-17O-2048	KN07-112	Nov 2014	22.07	42.53	-	-0.157	-157	Hu et al., *in prep.*
JHU-17O-2049	KN07-112	Nov 2014	22.33	43.01	-	-0.150	-150	Hu et al., *in prep.*
JHU-17O-2079	MGL-93-16	Nov 2014	23.10	44.57	-	-0.187	-187	this study
JHU-17O-2057	TMO	Nov 2014	22.79	44.08	-	-0.238	-238	this study
JHU-17O-2058	TMO	Nov 2014	23.02	44.52	-	-0.232	-232	this study
JHU-17O-2061	UT-deer	Nov 2014	18.14	35.13	-	-0.249	-249	Hu et al., *in prep.*
JHU-17O-2062	UT-deer	Nov 2014	18.13	35.13	-	-0.261	-261	Hu et al., *in prep.*
JHU-17O-2055	KN07-108	Nov 2014	25.03	48.50	-	-0.285	-285	Hu et al., *in prep.*
JHU-17O-2056	KN07-108	Nov 2014	25.18	48.78	-	-0.281	-281	Hu et al., *in prep.*
JHU-17O-2160	ET05-AWSH-04	June 2015	23.33	45.06	-	-0.206	-206	this study
JHU-17O-2161	ET05-AWSH-04	June 2015	23.68	45.74	-	-0.209	-209	this study
JHU-17O-2151	ET05-AWSH-29 (HIPPO)	June 2015	20.66	39.81	-	-0.166	-166	this study
JHU-17O-2152	ET05-AWSH-29 (HIPPO)	June 2015	20.64	39.77	-	-0.164	-164	this study
JHU-17O-2154	ET05-MAG0-10 HIPPO	June 2015	23.12	44.61	-	-0.188	-188	this study
JHU-17O-2155	ET05-MAG0-10 HIPPO	June 2015	23.50	45.35	-	-0.186	-186	this study
JHU-17O-2158	KN07-111	June 2015	22.53	43.41	-	-0.156	-156	this study
JHU-17O-2159	KN07-111	June 2015	22.50	43.34	-	-0.151	-151	this study
JHU-17O-2156	MGL-93-06	June 2015	20.88	40.25	-	-0.177	-177	this study
JHU-17O-2157	MGL-93-06	June 2015	20.67	39.87	-	-0.180	-180	this study
JHU-17O-2328	GA Beaver	Aug 2015_1	19.38	37.34	-	-0.158	-158	this study
JHU-17O-2329	GA Beaver	Aug 2015_1	18.41	35.45	-	-0.152	-152	this study
JHU-17O-2354	GA Beaver	Aug 2015_1	17.55	33.79	-	-0.150	-150	this study

Table S4.2: Triple oxygen isotope data for enamel samples listed by Analytical ID.

Analytical ID	Sample ID	Session ID	$\delta^{17}O$ (‰)	$\delta^{18}O$ (‰)	Additional CO_3 adjustment amount for $\Delta^{17}O$ (‰)	$\Delta^{17}O$ (‰)	$\Delta^{17}O$ per meg	Reference
JHU-17O-2355	GA Beaver	Aug 2015_1	17.74	34.15	-	-0.147	-147	this study
JHU-17O-2347	GA deer 1	Aug 2015_1	19.43	37.53	-	-0.207	-207	this study
JHU-17O-2348	GA deer 1	Aug 2015_1	19.74	38.11	-	-0.199	-199	this study
JHU-17O-2343	GA deer 2	Aug 2015_1	19.58	37.81	-	-0.210	-210	this study
JHU-17O-2344	GA deer 2	Aug 2015_1	19.15	36.99	-	-0.213	-213	this study
JHU-17O-2326	Kidepo buffalo	Aug 2015_1	21.50	41.49	-	-0.195	-195	this study
JHU-17O-2327	Kidepo buffalo	Aug 2015_1	22.34	43.12	-	-0.197	-197	this study
JHU-17O-2349	Kidepo buffalo	Aug 2015_1	21.94	42.36	-	-0.197	-197	this study
JHU-17O-2350	Kidepo buffao	Aug 2015_1	22.19	42.85	-	-0.209	-209	this study
JHU-17O-2322	MGL-93-10 Shimba Hills elephant	Aug 2015_1	19.96	38.47	-	-0.163	-163	this study
JHU-17O-2323	MGL-93-10 Shimba Hills elephant	Aug 2015_1	19.67	37.87	-	-0.152	-152	this study
JHU-17O-2320	MGL-93-17 Meru elephant	Aug 2015_1	19.84	38.24	-	-0.173	-173	this study
JHU-17O-2321	MGL-93-17 Meru elephant	Aug 2015_1	20.52	39.58	-	-0.184	-184	this study
JHU-17O-2315	MGL-93-7 Aberdares elephant	Aug 2015_1	19.37	37.30	-	-0.152	-152	this study
JHU-17O-2316	MGL-93-7 Aberdares elephant	Aug 2015_1	19.67	37.88	-	-0.154	-154	this study
JHU-17O-2345	NY deer 1	Aug 2015_1	16.95	32.75	-	-0.208	-208	this study
JHU-17O-2346	NY deer 1	Aug 2015_1	16.84	32.52	-	-0.200	-200	this study
JHU-17O-2339	UCT 14223 Kgalagadi giraffe#1	Aug 2015_1	22.81	44.20	-	-0.285	-285	this study
JHU-17O-2340	UCT 14223 Kgalagadi giraffe#1	Aug 2015_1	24.38	47.27	-	-0.298	-298	this study
JHU-17O-2331	UCT 14224 Kalagadi Wildebeest	Aug 2015_1	23.85	46.20	-	-0.279	-279	this study
JHU-17O-2332	UCT 14224 Kalagadi Wildebeest	Aug 2015_1	23.30	45.14	-	-0.281	-281	this study
JHU-17O-2341	UCT 14285 Addo hartebeest	Aug 2015_1	21.04	40.66	-	-0.220	-220	this study
JHU-17O-2342	UCT 14285 Addo hartebeest	Aug 2015_1	19.89	38.41	-	-0.208	-208	this study
JHU-17O-2324	UCT 1697 Addo elephant	Aug 2015_1	20.56	39.62	-	-0.168	-168	this study
JHU-17O-2325	UCT 1697 Addo elephant	Aug 2015_1	20.94	40.36	-	-0.170	-170	this study
JHU-17O-2480	AA1 Finland Moose #1	Aug 2015_2	15.56	30.02	+0.031	-0.147	-147	this study
JHU-17O-2481	AA1 Finland Moose #1	Aug 2015_2	14.97	28.89	+0.031	-0.152	-152	this study
JHU-17O-2488	AA2 Finland Moose#2	Aug 2015_2	13.41	25.91	+0.031	-0.153	-153	this study
JHU-17O-2489	AA2 Finland Moose#2	Aug 2015_2	13.73	26.51	+0.031	-0.147	-147	this study
JHU-17O-2486	CF2 Finland Beaver#2	Aug 2015_2	14.52	28.00	+0.031	-0.139	-139	this study
JHU-17O-2487	CF2 Finland Beaver#2	Aug 2015_2	15.35	29.62	+0.031	-0.141	-141	this study
JHU-17O-2482	FT1 Finland deer#1	Aug 2015_2	14.65	28.27	+0.031	-0.140	-140	this study
JHU-17O-2483	FT1 Finland deer#1	Aug 2015_2	15.43	29.77	+0.031	-0.150	-150	this study
JHU-17O-2484	RT1 Finland deer#3	Aug 2015_2	15.14	29.20	+0.031	-0.143	-143	this study
JHU-17O-2485	RT1 Finland deer#3	Aug 2015_2	15.42	29.74	+0.031	-0.142	-142	this study
JHU-17O-2300	GNP giraffe #1	July 2015	24.46	47.28	+0.04	-0.188	-188	this study
JHU-17O-2301	GNP giraffe #1	July 2015	25.56	49.45	+0.04	-0.204	-204	this study

Table S4.3: Modeled body water $\delta^{18}O$ and $\Delta^{17}O$ values at RH of 80%, 50% and 30% for animals with a minimum and maximum WEI resulting from a representative range of $\delta^{18}O$ values of meteoric water from The United States and Finland and from Africa.[a]

United States and Finland meteoric water $\delta^{18}O$ range: -14‰ to -8‰

	MIN-EVAP model RH = 80%		MAX-EVAP model RH = 80%		MIN-EVAP model RH = 50%		MAX-EVAP model RH = 50%		MIN-EVAP model RH = 30%		MAX-EVAP model RH = 30%	
$\delta^{18}O_{mw}$ (‰)[b]	$\delta^{18}O_{bw}$ (‰)[c]	$\Delta^{17}O_{bw}$ (‰)[c]	$\delta^{18}O_{bw}$ (‰)[c]	$\Delta^{17}O_{bw}$ (‰)[c]	$\delta^{18}O_{bw}$ (‰)[c]	$\Delta^{17}O_{bw}$ (‰)[c]	$\delta^{18}O_{bw}$ (‰)[c]	$\Delta^{17}O_{bw}$ (‰)[c]	$\delta^{18}O_{bw}$ (‰)[c]	$\Delta^{17}O_{bw}$ (‰)[c]	$\delta^{18}O_{bw}$ (‰)[c]	$\Delta^{17}O_{bw}$ (‰)[c]
-14	-10.2	-0.001	-5.0	-0.110	-9.7	-0.005	2.7	-0.166	-9.3	-0.008	8.0	-0.189
-13.9	-10.1	-0.001	-5.0	-0.110	-9.6	-0.005	2.8	-0.165	-9.2	-0.008	8.1	-0.189
-13.8	-10.0	-0.001	-4.9	-0.110	-9.5	-0.005	2.9	-0.165	-9.1	-0.008	8.2	-0.188
-13.7	-9.9	-0.001	-4.8	-0.110	-9.4	-0.005	3.0	-0.165	-9.0	-0.008	8.3	-0.188
-13.6	-9.8	-0.001	-4.7	-0.110	-9.3	-0.004	3.0	-0.165	-9.0	-0.007	8.3	-0.188
-13.5	-9.7	0.000	-4.7	-0.110	-9.2	-0.004	3.1	-0.165	-8.9	-0.007	8.4	-0.188
-13.4	-9.7	0.000	-4.6	-0.109	-9.1	-0.004	3.2	-0.165	-8.8	-0.007	8.5	-0.188
-13.3	-9.6	0.000	-4.5	-0.109	-9.0	-0.004	3.3	-0.165	-8.7	-0.007	8.6	-0.188
-13.2	-9.5	0.000	-4.4	-0.109	-8.9	-0.004	3.3	-0.165	-8.6	-0.007	8.6	-0.188
-13.1	-9.4	0.000	-4.4	-0.109	-8.9	-0.004	3.4	-0.165	-8.5	-0.007	8.7	-0.188
-13	-9.3	0.000	-4.3	-0.109	-8.8	-0.004	3.5	-0.165	-8.4	-0.007	8.8	-0.188
-12.9	-9.2	0.000	-4.2	-0.109	-8.7	-0.004	3.6	-0.165	-8.3	-0.007	8.9	-0.188
-12.8	-9.1	0.000	-4.1	-0.109	-8.6	-0.004	3.6	-0.165	-8.2	-0.007	9.0	-0.188
-12.7	-9.0	0.000	-4.1	-0.109	-8.5	-0.004	3.7	-0.165	-8.2	-0.007	9.0	-0.188
-12.6	-8.9	0.000	-4.0	-0.109	-8.4	-0.004	3.8	-0.165	-8.1	-0.007	9.1	-0.188
-12.5	-8.9	0.000	-3.9	-0.109	-8.3	-0.004	3.9	-0.165	-8.0	-0.007	9.2	-0.188
-12.4	-8.8	0.000	-3.8	-0.108	-8.2	-0.004	3.9	-0.165	-7.9	-0.007	9.3	-0.188
-12.3	-8.7	0.000	-3.8	-0.108	-8.2	-0.004	4.0	-0.165	-7.8	-0.006	9.3	-0.188
-12.2	-8.6	0.001	-3.7	-0.108	-8.1	-0.003	4.1	-0.165	-7.7	-0.006	9.4	-0.188
-12.1	-8.5	0.001	-3.6	-0.108	-8.0	-0.003	4.2	-0.165	-7.6	-0.006	9.5	-0.188
-12	-8.4	0.001	-3.5	-0.108	-7.9	-0.003	4.2	-0.165	-7.5	-0.006	9.6	-0.188
-11.9	-8.3	0.001	-3.5	-0.108	-7.8	-0.003	4.3	-0.164	-7.4	-0.006	9.6	-0.188
-11.8	-8.2	0.001	-3.4	-0.108	-7.7	-0.003	4.4	-0.164	-7.4	-0.006	9.7	-0.188
-11.7	-8.1	0.001	-3.3	-0.108	-7.6	-0.003	4.5	-0.164	-7.3	-0.006	9.8	-0.188
-11.6	-8.1	0.001	-3.2	-0.108	-7.5	-0.003	4.5	-0.164	-7.2	-0.006	9.9	-0.188
-11.5	-8.0	0.001	-3.2	-0.108	-7.4	-0.003	4.6	-0.164	-7.1	-0.006	9.9	-0.188
-11.4	-7.9	0.001	-3.1	-0.107	-7.4	-0.003	4.7	-0.164	-7.0	-0.006	10.0	-0.188
-11.3	-7.8	0.001	-3.0	-0.107	-7.3	-0.003	4.8	-0.164	-6.9	-0.006	10.1	-0.188
-11.2	-7.7	0.001	-2.9	-0.107	-7.2	-0.003	4.8	-0.164	-6.8	-0.006	10.2	-0.188
-11.1	-7.6	0.001	-2.9	-0.107	-7.1	-0.003	4.9	-0.164	-6.7	-0.006	10.2	-0.188
-11	-7.5	0.001	-2.8	-0.107	-7.0	-0.003	5.0	-0.164	-6.7	-0.006	10.3	-0.188
-10.9	-7.4	0.001	-2.7	-0.107	-6.9	-0.002	5.1	-0.164	-6.6	-0.005	10.4	-0.188
-10.8	-7.4	0.002	-2.6	-0.107	-6.8	-0.002	5.2	-0.164	-6.5	-0.005	10.5	-0.188
-10.7	-7.3	0.002	-2.6	-0.107	-6.7	-0.002	5.2	-0.164	-6.4	-0.005	10.5	-0.188
-10.6	-7.2	0.002	-2.5	-0.107	-6.6	-0.002	5.3	-0.164	-6.3	-0.005	10.6	-0.188
-10.5	-7.1	0.002	-2.4	-0.107	-6.6	-0.002	5.4	-0.164	-6.2	-0.005	10.7	-0.188
-10.4	-7.0	0.002	-2.3	-0.107	-6.5	-0.002	5.5	-0.164	-6.1	-0.005	10.8	-0.188
-10.3	-6.9	0.002	-2.3	-0.106	-6.4	-0.002	5.5	-0.164	-6.0	-0.005	10.8	-0.188
-10.2	-6.8	0.002	-2.2	-0.106	-6.3	-0.002	5.6	-0.164	-5.9	-0.005	10.9	-0.188
-10.1	-6.7	0.002	-2.1	-0.106	-6.2	-0.002	5.7	-0.164	-5.9	-0.005	11.0	-0.188
-10	-6.6	0.002	-2.0	-0.106	-6.1	-0.002	5.8	-0.164	-5.8	-0.005	11.1	-0.188
-9.9	-6.6	0.002	-2.0	-0.106	-6.0	-0.002	5.8	-0.164	-5.7	-0.005	11.2	-0.188
-9.8	-6.5	0.002	-1.9	-0.106	-5.9	-0.002	5.9	-0.164	-5.6	-0.005	11.2	-0.188
-9.7	-6.4	0.002	-1.8	-0.106	-5.9	-0.002	6.0	-0.164	-5.5	-0.005	11.3	-0.188
-9.6	-6.3	0.002	-1.7	-0.106	-5.8	-0.002	6.1	-0.164	-5.4	-0.005	11.4	-0.188
-9.5	-6.2	0.002	-1.7	-0.106	-5.7	-0.002	6.1	-0.163	-5.3	-0.005	11.5	-0.188
-9.4	-6.1	0.003	-1.6	-0.106	-5.6	-0.001	6.2	-0.163	-5.2	-0.004	11.5	-0.188
-9.3	-6.0	0.003	-1.5	-0.106	-5.5	-0.001	6.3	-0.163	-5.1	-0.004	11.6	-0.188
-9.2	-5.9	0.003	-1.4	-0.106	-5.4	-0.001	6.4	-0.163	-5.1	-0.004	11.7	-0.188
-9.1	-5.8	0.003	-1.4	-0.105	-5.3	-0.001	6.4	-0.163	-5.0	-0.004	11.8	-0.188
-9	-5.8	0.003	-1.3	-0.105	-5.2	-0.001	6.5	-0.163	-4.9	-0.004	11.8	-0.188
-8.9	-5.7	0.003	-1.2	-0.105	-5.1	-0.001	6.6	-0.163	-4.8	-0.004	11.9	-0.188
-8.8	-5.6	0.003	-1.1	-0.105	-5.1	-0.001	6.7	-0.163	-4.7	-0.004	12.0	-0.188
-8.7	-5.5	0.003	-1.1	-0.105	-5.0	-0.001	6.7	-0.163	-4.6	-0.004	12.1	-0.188
-8.6	-5.4	0.003	-1.0	-0.105	-4.9	-0.001	6.8	-0.163	-4.5	-0.004	12.1	-0.188
-8.5	-5.3	0.003	-0.9	-0.105	-4.8	-0.001	6.9	-0.163	-4.4	-0.004	12.2	-0.188
-8.4	-5.2	0.003	-0.8	-0.105	-4.7	-0.001	7.0	-0.163	-4.4	-0.004	12.3	-0.188
-8.3	-5.1	0.003	-0.8	-0.105	-4.6	-0.001	7.0	-0.163	-4.3	-0.004	12.4	-0.188
-8.2	-5.1	0.003	-0.7	-0.105	-4.5	-0.001	7.1	-0.163	-4.2	-0.004	12.4	-0.188
-8.1	-5.0	0.003	-0.6	-0.105	-4.4	-0.001	7.2	-0.163	-4.1	-0.004	12.5	-0.188
-8	-4.9	0.003	-0.5	-0.105	-4.3	-0.001	7.3	-0.163	-4.0	-0.004	12.6	-0.188

Africa meteoric water $\delta^{18}O$ range: -5‰ to +1‰

	MIN-EVAP model RH = 80%		MAX-EVAP model RH = 80%		MIN-EVAP model RH = 50%		MAX-EVAP model RH = 50%		MIN-EVAP model RH = 30%		MAX-EVAP model RH = 30%	
$\delta^{18}O_{mw}$ (‰)[b]	$\delta^{18}O_{bw}$ (‰)[c]	$\Delta^{17}O_{bw}$ (‰)[c]	$\delta^{18}O_{bw}$ (‰)[c]	$\Delta^{17}O_{bw}$ (‰)[c]	$\delta^{18}O_{bw}$ (‰)[c]	$\Delta^{17}O_{bw}$ (‰)[c]	$\delta^{18}O_{bw}$ (‰)[c]	$\Delta^{17}O_{bw}$ (‰)[c]	$\delta^{18}O_{bw}$ (‰)[c]	$\Delta^{17}O_{bw}$ (‰)[c]	$\delta^{18}O_{bw}$ (‰)[c]	$\Delta^{17}O_{bw}$ (‰)[c]
-5	-2.2	0.005	1.7	-0.102	-1.7	0.001	9.5	-0.162	-1.3	-0.002	14.9	-0.188
-4.9	-2.1	0.005	1.8	-0.102	-1.6	0.001	9.6	-0.162	-1.3	-0.002	15.0	-0.189
-4.8	-2.0	0.005	1.9	-0.102	-1.5	0.001	9.7	-0.162	-1.2	-0.002	15.0	-0.189
-4.7	-2.0	0.005	2.0	-0.102	-1.4	0.001	9.8	-0.162	-1.1	-0.002	15.1	-0.189
-4.6	-1.9	0.005	2.0	-0.102	-1.3	0.001	9.8	-0.162	-1.0	-0.002	15.2	-0.189
-4.5	-1.8	0.006	2.1	-0.102	-1.3	0.001	9.9	-0.162	-0.9	-0.002	15.3	-0.189
-4.4	-1.7	0.006	2.2	-0.102	-1.2	0.002	10.0	-0.162	-0.8	-0.002	15.3	-0.189
-4.3	-1.6	0.006	2.3	-0.102	-1.1	0.002	10.1	-0.162	-0.7	-0.001	15.4	-0.189
-4.2	-1.5	0.006	2.3	-0.102	-1.0	0.002	10.1	-0.162	-0.6	-0.001	15.5	-0.189
-4.1	-1.4	0.006	2.4	-0.102	-0.9	0.002	10.2	-0.162	-0.5	-0.001	15.6	-0.189
-4	-1.3	0.006	2.5	-0.102	-0.8	0.002	10.3	-0.162	-0.5	-0.001	15.6	-0.189
-3.9	-1.3	0.006	2.6	-0.102	-0.7	0.002	10.4	-0.162	-0.4	-0.001	15.7	-0.189
-3.8	-1.2	0.006	2.6	-0.102	-0.6	0.002	10.4	-0.162	-0.3	-0.001	15.8	-0.189
-3.7	-1.1	0.006	2.7	-0.102	-0.5	0.002	10.5	-0.162	-0.2	-0.001	15.9	-0.189
-3.6	-1.0	0.006	2.8	-0.102	-0.5	0.002	10.6	-0.162	-0.1	-0.001	15.9	-0.189
-3.5	-0.9	0.006	2.9	-0.102	-0.4	0.002	10.7	-0.162	0.0	-0.001	16.0	-0.189
-3.4	-0.8	0.006	2.9	-0.101	-0.3	0.002	10.8	-0.162	0.1	-0.001	16.1	-0.189
-3.3	-0.7	0.006	3.0	-0.101	-0.2	0.002	10.8	-0.162	0.2	-0.001	16.2	-0.189
-3.2	-0.6	0.006	3.1	-0.101	-0.1	0.002	10.9	-0.162	0.3	-0.001	16.2	-0.189
-3.1	-0.5	0.006	3.2	-0.101	0.0	0.002	11.0	-0.162	0.3	-0.001	16.3	-0.189
-3	-0.5	0.006	3.2	-0.101	0.1	0.002	11.1	-0.162	0.4	-0.001	16.4	-0.189
-2.9	-0.4	0.006	3.3	-0.101	0.2	0.002	11.1	-0.162	0.5	-0.001	16.5	-0.189
-2.8	-0.3	0.006	3.4	-0.101	0.3	0.002	11.2	-0.162	0.6	-0.001	16.5	-0.189

Table S4.3: Modeled body water $\delta^{18}O$ and $\Delta^{17}O$ values at RH of 80%, 50% and 30% for animals with a minimum and maximum WEI resulting from a representative range of $\delta^{18}O$ values of meteoric water from The United States and Finland and from Africa.[a]

-2.7	-0.2	0.006	3.5	-0.101	0.3	0.002	11.3	-0.162	0.7	-0.001	16.6	-0.189
-2.6	-0.1	0.007	3.5	-0.101	0.4	0.002	11.4	-0.162	0.8	-0.001	16.7	-0.189
-2.5	0.0	0.007	3.6	-0.101	0.5	0.002	11.4	-0.162	0.9	-0.001	16.8	-0.189
-2.4	0.1	0.007	3.7	-0.101	0.6	0.003	11.5	-0.162	1.0	-0.001	16.9	-0.189
-2.3	0.2	0.007	3.8	-0.101	0.7	0.003	11.6	-0.162	1.0	0.000	16.9	-0.189
-2.2	0.3	0.007	3.8	-0.101	0.8	0.003	11.7	-0.162	1.1	0.000	17.0	-0.189
-2.1	0.3	0.007	3.9	-0.101	0.9	0.003	11.7	-0.162	1.2	0.000	17.1	-0.189
-2	0.4	0.007	4.0	-0.101	1.0	0.003	11.8	-0.162	1.3	0.000	17.2	-0.189
-1.9	0.5	0.007	4.1	-0.101	1.0	0.003	11.9	-0.162	1.4	0.000	17.2	-0.189
-1.8	0.6	0.007	4.1	-0.101	1.1	0.003	12.0	-0.162	1.5	0.000	17.3	-0.189
-1.7	0.7	0.007	4.2	-0.101	1.2	0.003	12.0	-0.162	1.6	0.000	17.4	-0.189
-1.6	0.8	0.007	4.3	-0.101	1.3	0.003	12.1	-0.162	1.7	0.000	17.5	-0.189
-1.5	0.9	0.007	4.4	-0.101	1.4	0.003	12.2	-0.162	1.8	0.000	17.5	-0.190
-1.4	1.0	0.007	4.4	-0.100	1.5	0.003	12.3	-0.162	1.8	0.000	17.6	-0.190
-1.3	1.0	0.007	4.5	-0.100	1.6	0.003	12.3	-0.162	1.9	0.000	17.7	-0.190
-1.2	1.1	0.007	4.6	-0.100	1.7	0.003	12.4	-0.162	2.0	0.000	17.8	-0.190
-1.1	1.2	0.007	4.7	-0.100	1.8	0.003	12.5	-0.162	2.1	0.000	17.8	-0.190
-1	1.3	0.007	4.7	-0.100	1.8	0.003	12.6	-0.162	2.2	0.000	17.9	-0.190
-0.9	1.4	0.007	4.8	-0.100	1.9	0.003	12.6	-0.162	2.3	0.000	18.0	-0.190
-0.8	1.5	0.007	4.9	-0.100	2.0	0.003	12.7	-0.162	2.4	0.000	18.1	-0.190
-0.7	1.6	0.007	5.0	-0.100	2.1	0.003	12.8	-0.162	2.5	0.000	18.1	-0.190
-0.6	1.7	0.007	5.0	-0.100	2.2	0.003	12.9	-0.162	2.6	0.000	18.2	-0.190
-0.5	1.8	0.007	5.1	-0.100	2.3	0.003	12.9	-0.162	2.6	0.000	18.3	-0.190
-0.4	1.8	0.008	5.2	-0.100	2.4	0.003	13.0	-0.162	2.7	0.000	18.4	-0.190
-0.3	1.9	0.008	5.3	-0.100	2.5	0.003	13.1	-0.162	2.8	0.000	18.4	-0.190
-0.2	2.0	0.008	5.3	-0.100	2.6	0.003	13.2	-0.162	2.9	0.000	18.5	-0.190
-0.1	2.1	0.008	5.4	-0.100	2.6	0.004	13.3	-0.162	3.0	0.000	18.6	-0.190
0	2.2	0.008	5.5	-0.100	2.7	0.004	13.3	-0.162	3.1	0.001	18.7	-0.190
0.1	2.3	0.008	5.6	-0.100	2.8	0.004	13.4	-0.162	3.2	0.001	18.8	-0.190
0.2	2.4	0.008	5.6	-0.100	2.9	0.004	13.5	-0.162	3.3	0.001	18.8	-0.190
0.3	2.5	0.008	5.7	-0.100	3.0	0.004	13.6	-0.162	3.3	0.001	18.9	-0.190
0.4	2.5	0.008	5.8	-0.100	3.1	0.004	13.6	-0.162	3.4	0.001	19.0	-0.190
0.5	2.6	0.008	5.9	-0.100	3.2	0.004	13.7	-0.162	3.5	0.001	19.1	-0.190
0.6	2.7	0.008	5.9	-0.100	3.3	0.004	13.8	-0.162	3.6	0.001	19.1	-0.190
0.7	2.8	0.008	6.0	-0.100	3.3	0.004	13.9	-0.162	3.7	0.001	19.2	-0.190
0.8	2.9	0.008	6.1	-0.100	3.4	0.004	13.9	-0.162	3.8	0.001	19.3	-0.190
0.9	3.0	0.008	6.2	-0.100	3.5	0.004	14.0	-0.162	3.9	0.001	19.4	-0.191
1	3.1	0.008	6.3	-0.099	3.6	0.004	14.1	-0.162	4.0	0.001	19.4	-0.191

[a] Model outputs for the maximum and minimum animalbody water triple oxygen isotopes are also represented in the Fig. 4 and based on the model parameters from Hu et al. *In Prep*

[b] Where mw is meteoric water

[c] Where bw is body water

Table S4.4: Minimum evaporation modeled data for the $\Delta^{17}O$ values of animals with minimum and maximum WEI index with increasing Relative Humidity (RH).[a]

	***Minimum WEI animal*[b]**		***Maximum WEI animal*[c]**	
	Model source water input		**Model source water input**	
	$\delta^{18}O$ (‰ SMOW)	**$\Delta^{17}O$ (‰ SMOW)**	**$\delta^{18}O$ (‰ SMOW)**	**$\Delta^{17}O$ (‰ SMOW)**
	-7.0	0.035	-7.0	-0.010
	Model source body water output		**Model source body water output**	
RH (%)	**$\delta^{18}O$ (‰ SMOW)**	**$\Delta^{17}O$ (‰ SMOW)**	**$\delta^{18}O$ (‰ SMOW)**	**$\Delta^{17}O$ (‰ SMOW)**
0	-2.5	-0.007	21.6	-0.204
1	-2.5	-0.007	21.3	-0.204
2	-2.6	-0.007	21.0	-0.204
3	-2.6	-0.007	20.7	-0.204
4	-2.6	-0.007	20.4	-0.204
5	-2.6	-0.006	20.2	-0.203
6	-2.6	-0.006	19.9	-0.203
7	-2.6	-0.006	19.6	-0.203
8	-2.7	-0.006	19.3	-0.203
9	-2.7	-0.006	19.1	-0.202
10	-2.7	-0.006	18.8	-0.202
11	-2.7	-0.005	18.5	-0.201
12	-2.7	-0.005	18.2	-0.201
13	-2.8	-0.005	18.0	-0.201
14	-2.8	-0.005	17.7	-0.200
15	-2.8	-0.005	17.4	-0.200
16	-2.8	-0.005	17.2	-0.199
17	-2.8	-0.004	16.9	-0.198
18	-2.8	-0.004	16.6	-0.198
19	-2.9	-0.004	16.3	-0.197
20	-2.9	-0.004	16.1	-0.196
21	-2.9	-0.004	15.8	-0.196
22	-2.9	-0.004	15.5	-0.195
23	-2.9	-0.004	15.2	-0.194
24	-2.9	-0.003	15.0	-0.194
25	-3.0	-0.003	14.7	-0.193
26	-3.0	-0.003	14.4	-0.192
27	-3.0	-0.003	14.2	-0.191
28	-3.0	-0.003	13.9	-0.190
29	-3.0	-0.003	13.6	-0.189
30	-3.0	-0.002	13.4	-0.188
31	-3.1	-0.002	13.1	-0.187
32	-3.1	-0.002	12.8	-0.186
33	-3.1	-0.002	12.6	-0.185
34	-3.1	-0.002	12.3	-0.184
35	-3.1	-0.002	12.0	-0.183
36	-3.1	-0.002	11.7	-0.182
37	-3.2	-0.001	11.5	-0.181
38	-3.2	-0.001	11.2	-0.179
39	-3.2	-0.001	10.9	-0.178
40	-3.2	-0.001	10.7	-0.177
41	-3.2	-0.001	10.4	-0.176
42	-3.3	-0.001	10.1	-0.174
43	-3.3	0.000	9.9	-0.173
44	-3.3	0.000	9.6	-0.172
45	-3.3	0.000	9.3	-0.170
46	-3.3	0.000	9.1	-0.169
47	-3.3	0.000	8.8	-0.167
48	-3.4	0.000	8.6	-0.166
49	-3.4	0.000	8.3	-0.164
50	-3.4	0.001	8.0	-0.163
51	-3.4	0.001	7.8	-0.161
52	-3.4	0.001	7.5	-0.160
53	-3.4	0.001	7.2	-0.158
54	-3.5	0.001	7.0	-0.156
55	-3.5	0.001	6.7	-0.155
56	-3.5	0.001	6.4	-0.153
57	-3.5	0.001	6.2	-0.151
58	-3.5	0.002	5.9	-0.149
59	-3.5	0.002	5.7	-0.148
60	-3.6	0.002	5.4	-0.146
61	-3.6	0.002	5.1	-0.144
62	-3.6	0.002	4.9	-0.142
63	-3.6	0.002	4.6	-0.140
64	-3.6	0.002	4.4	-0.138
65	-3.6	0.003	4.1	-0.136
66	-3.7	0.003	3.8	-0.134
67	-3.7	0.003	3.6	-0.132

Table S4.4: Minimum evaporation modeled data for the $\Delta^{17}O$ values of animals with minimum and maximum WEI index with increasing Relative Humidity (RH).[a]

	Minimum WEI animal[b]		***Maximum WEI animal***[c]	
	Model source water input		**Model source water input**	
	$\delta^{18}O$ (‰ SMOW)	**$\Delta^{17}O$ (‰ SMOW)**	**$\delta^{18}O$ (‰ SMOW)**	**$\Delta^{17}O$ (‰ SMOW)**
	-7.0	0.035	-7.0	-0.010
	Model source body water output		**Model source body water output**	
RH (%)	**$\delta^{18}O$ (‰ SMOW)**	**$\Delta^{17}O$ (‰ SMOW)**	**$\delta^{18}O$ (‰ SMOW)**	**$\Delta^{17}O$ (‰ SMOW)**
68	-3.7	0.003	3.3	-0.130
69	-3.7	0.003	3.1	-0.128
70	-3.7	0.003	2.8	-0.126
71	-3.7	0.003	2.5	-0.124
72	-3.8	0.003	2.3	-0.122
73	-3.8	0.004	2.0	-0.120
74	-3.8	0.004	1.8	-0.118
75	-3.8	0.004	1.5	-0.115
76	-3.8	0.004	1.3	-0.113
77	-3.9	0.004	1.0	-0.111
78	-3.9	0.004	0.7	-0.108
79	-3.9	0.004	0.5	-0.106
80	-3.9	0.004	0.2	-0.104
81	-3.9	0.005	0.0	-0.101
82	-3.9	0.005	-0.3	-0.099
83	-4.0	0.005	-0.5	-0.097
84	-4.0	0.005	-0.8	-0.094
85	-4.0	0.005	-1.0	-0.092
86	-4.0	0.005	-1.3	-0.089
87	-4.0	0.005	-1.6	-0.087
88	-4.0	0.005	-1.8	-0.084
89	-4.1	0.005	-2.1	-0.081
90	-4.1	0.006	-2.3	-0.079
91	-4.1	0.006	-2.6	-0.076
92	-4.1	0.006	-2.8	-0.073
93	-4.1	0.006	-3.1	-0.071
94	-4.1	0.006	-3.3	-0.068
95	-4.2	0.006	-3.6	-0.065
96	-4.2	0.006	-3.8	-0.063
97	-4.2	0.006	-4.1	-0.060
98	-4.2	0.006	-4.3	-0.057
99	-4.2	0.007	-4.6	-0.054
100	-4.2	0.007	-4.8	-0.051

[a] Model outputs for the maximum and minimum animalbody water triple oxygen isotopes are also represented in the Fig. 4 and based on the model parameters from Hu et al. (*in prep).*

[b] Where an animal with a minimum WEI (water economy index) is one that must consume a lot of water in different environments.

[c] Where an animal with a maximum WEI (water economy index) is one that need not consume a lot of water in different environments.

Table S4.5: Analytical run data for sessions containing the newly analyzed enamel samples.[a]

							Voltage mismatch corrected data		Corrected carbonate data				
							d33 vs ref.	d34 vs ref.	$\Delta^{17}O$ (‰)	$\delta^{17}O$ (‰)	$\delta^{18}O$ (‰)	$\Delta^{17}O$ (‰)	
Date	**Rank in run**	**Analytical ID**	**Sample ID**	**Sample Description**	**Original Phase**	**Exclude?**	**R^2 > 0.6**	**R^2 > 0.6**				**(when CO_3 adjusted)**	**Session ID**
10/27/10	1	JHU-17O-2042	VSMOW2-052013-2B	International Std.	H2O	Exclude	-17.89	-34.25					Nov 2014
10/27/10	2	JHU-17O-2043	VSMOW2-052013-2B	International Std.	H2O		-17.91	-34.27					Nov 2014
10/27/10	3	JHU-17O-2044	VSMOW2-052013-2B	International Std.	H2O		-17.88	-34.14					Nov 2014
10/28/10	4	JHU-17O-2045	NBS-19	International Std.	CO3	Exclude	-1.19	-2.52	-0.138	18.64	35.88	-0.136	Nov 2014
10/28/10	5	JHU-17O-2046	NBS-19	International Std.	CO3		-0.76	-1.71	-0.136	19.12	36.80	-0.134	Nov 2014
10/28/10	6	JHU-17O-2047	NBS-19	International Std.	CO3		-0.59	-1.39	-0.131	19.32	37.16	-0.129	Nov 2014
10/28/10	7	JHU-17O-2048	KN07-112	Hippo enamel	Modern enamel		1.86	3.30	-0.157	22.07	42.53	-0.155	Nov 2014
10/28/10	8	JHU-17O-2049	KN07-112	Hippo enamel	Modern enamel		2.09	3.72	-0.150	22.33	43.01	-0.148	Nov 2014
10/28/10	9	JHU-17O-2050	ET03-71	Hippo enamel	Fossil enamel		-1.99	-4.05	-0.129	17.74	34.12	-0.127	Nov 2014
10/29/10	10	JHU-17O-2051	ET03-71	Hippo enamel	Fossil enamel		-2.08	-4.23	-0.130	17.64	33.93	-0.128	Nov 2014
10/29/10	11	JHU-17O-2052	CME	Congo modern elephant	modern enamel		-0.86	-1.87	-0.155	19.01	36.62	-0.153	Nov 2014
10/29/10	12	JHU-17O-2053	CME	Congo modern elephant	modern enamel		-0.57	-1.33	-0.152	19.34	37.24	-0.150	Nov 2014
10/29/10	13	JHU-17O-2054	CME	Congo modern elephant	modern enamel		-0.42	-1.04	-0.151	19.51	37.57	-0.150	Nov 2014
10/29/10	14	JHU-17O-2055	KN07-108	Modern Giraffe	modern enamel		4.48	8.52	-0.285	25.03	48.50	-0.283	Nov 2014
10/30/10	15	JHU-17O-2056	KN07-108	Modern Giraffe	modern enamel		4.61	8.76	-0.281	25.18	48.78	-0.279	Nov 2014
10/30/10	16	JHU-17O-2057	TMO	modern oryx	modern enamel		2.50	4.65	-0.238	22.79	44.08	-0.236	Nov 2014
10/30/10	17	JHU-17O-2058	TMO	modern oryx	modern enamel		2.70	5.04	-0.232	23.02	44.52	-0.230	Nov 2014
10/30/10	18	JHU-17O-2059	ET05-MAGO-19	Modern Elephant	modern enamel		3.16	5.80	-0.181	23.53	45.39	-0.179	Nov 2014
10/30/10	19	JHU-17O-2060	ET05-MAGO-19	Modern Elephant	modern enamel		3.18	5.86	-0.188	23.56	45.46	-0.186	Nov 2014
10/30/10	20	JHU-17O-2061	UT-deer	Modern Deer	modern enamel		-1.64	-3.18	-0.249	18.14	35.13	-0.247	Nov 2014
10/31/10	21	JHU-17O-2062	UT-deer	Modern Deer	modern enamel		-1.65	-3.17	-0.261	18.13	35.13	-0.259	Nov 2014
10/31/10	22	JHU-17O-2063	SLAP2-051613-1a	water	water std	Exclude	-45.75	-85.44					Nov 2014
10/31/10	23	JHU-17O-2064	SLAP2-051613-1a	water	water std		-45.76	-85.48					Nov 2014
10/31/10	24	JHU-17O-2065	SLAP2-051613-1a	water	water std		-45.86	-85.67					Nov 2014
10/31/10	25	JHU-17O-2066	NBS-18	International Std.	Carbonates	Exclude	-10.75	-20.62	-0.108	7.89	15.21	-0.106	Nov 2014
10/31/10	26	JHU-17O-2067	NBS-18	International Std.	Carbonates		-10.80	-20.70	-0.119	7.83	15.12	-0.117	Nov 2014
10/31/10	27	JHU-17O-2068	NBS-18	International Std.	Carbonates		-10.79	-20.69	-0.112	7.85	15.13	-0.110	Nov 2014
11/1/10	28	JHU-17O-2069	GNP-Hippo	modern enamel	enamel/CO3		0.03	-0.19	-0.146	20.02	38.54	-0.144	Nov 2014
11/1/10	29	JHU-17O-2070	GNP-Hippo	modern enamel	enamel/CO3		0.08	-0.13	-0.134	20.06	38.60	-0.132	Nov 2014
11/1/10	30	JHU-17O-2071	GNP-giraffe2	modern enamel	enamel/CO3		3.19	5.92	-0.212	23.57	45.52	-0.210	Nov 2014
11/1/10	31	JHU-17O-2072	GNP-giraffe2	modern enamel	enamel/CO3		3.65	6.80	-0.208	24.09	46.53	-0.206	Nov 2014
11/1/10	32	JHU-17O-2073	Ituri Giraffe	modern enamel	enamel/CO3		1.65	2.95	-0.183	21.84	42.13	-0.181	Nov 2014
11/1/10	33	JHU-17O-2074	Ituri Giraffe	modern enamel	enamel/CO3		1.55	2.75	-0.182	21.72	41.90	-0.180	Nov 2014
11/2/10	34	JHU-17O-2075	K98-Lai-310	modern giraffe, Mpala	enamel/CO3		2.55	4.74	-0.230	22.85	44.18	-0.228	Nov 2014
11/2/10	35	JHU-17O-2076	K98-Lai-310	modern giraffe, Mpala	enamel/CO3		2.10	3.87	-0.218	22.35	43.18	-0.216	Nov 2014
11/2/10	36	JHU-17O-2077	K00-TSV-113	modern giraffe, Tsavo	enamel/CO3		3.91	7.34	-0.237	24.38	47.15	-0.235	Nov 2014
11/2/10	37	JHU-17O-2078	K00-TSV-113	modern giraffe, Tsavo	enamel/CO3		3.95	7.42	-0.234	24.43	47.24	-0.232	Nov 2014
11/2/10	38	JHU-17O-2079	MGL-93-16	modern Elephant	enamel/CO3		2.77	5.08	-0.187	23.10	44.57	-0.185	Nov 2014
11/2/10	39	JHU-17O-2080	AIJB-B3-T4-DP4	modern juv. Bison	enamel/CO3		-2.94	-5.77	-0.179	16.67	32.16	-0.177	Nov 2014
11/3/10	40	JHU-17O-2081	AIJB-B3-T4-DP4	modern juv. Bison	enamel/CO3		-3.53	-6.89	-0.176	16.01	30.89	-0.174	Nov 2014
11/3/10	41	JHU-17O-2082	VSMOW2-2-052013-2b	international standard	H2O)	Exclude	-17.43	-33.31					Nov 2014
11/3/10	42	JHU-17O-2083	VSMOW2-2-052013-2b	international standard	H2O)		-17.96	-34.30					Nov 2014
11/3/10	43	JHU-17O-2084	VSMOW2-2-052013-2b	international standard	H2O		-18.07	-34.50					Nov 2014
11/4/10	44	JHU-17O-2085	VSMOW2-2-052013-2b	international standard	H2O		-18.03	-34.44					Nov 2014
11/4/10	45	JHU-17O-2086	A12-897/A12-898	air sample	CO2	Exclude	-2.22	-4.44	-0.160	17.49	33.69	-0.158	Nov 2014
11/4/10	46	JHU-17O-2087	B13-239/A13-152	air sample	CO2		1.35	2.28	-0.132	21.50	41.37	-0.130	Nov 2014
11/4/10	47	JHU-17O-2088	A11-608-A11-609	air sample	CO2		1.45	2.47	-0.128	21.61	41.58	-0.126	Nov 2014
11/4/10	48	JHU-17O-2089	A12-462/A12-463	air sample	CO2		1.31	2.20	-0.127	21.46	41.28	-0.125	Nov 2014
11/4/10	49	JHU-17O-2090	A11-806/A11-807	air sample	CO2		1.33	2.23	-0.123	21.48	41.31	-0.121	Nov 2014
11/5/10	50	JHU-17O-2091	A13-107/A13-108	air sample	CO2		0.81	1.26	-0.132	20.89	40.20	-0.130	Nov 2014
11/5/10	51	JHU-17O-2092	B13-129/B13-130	air sample	CO2		1.43	2.44	-0.130	21.59	41.54	-0.128	Nov 2014
11/5/10	52	JHU-17O-2093	A11-166-A11-165	air sample	CO2		1.29	2.18	-0.133	21.43	41.24	-0.131	Nov 2014
11/5/10	53	JHU-17O-2094	A12-242-A12-243	air sample	CO2		1.28	2.15	-0.127	21.42	41.21	-0.125	Nov 2014
11/5/10	54	JHU-17O-2095	A12-237/A12-236	air sample	CO2		1.48	2.53	-0.134	21.64	41.65	-0.132	Nov 2014
11/6/10	55	JHU-17O-2096	B13-038/B13-037	air sample	CO2		1.20	1.97	-0.124	21.32	41.01	-0.122	Nov 2014
11/6/10	56	JHU-17O-2097	SLAP2-051613-1a	International Std	water	Exclude	-45.80	-85.55					Nov 2014
11/6/10	57	JHU-17O-2098	SLAP2-051613-1a	International Std	water		-46.01	-85.93					Nov 2014
11/6/10	58	JHU-17O-2099	SLAP2-051613-1a	International Std	water		-46.15	-86.19					Nov 2014
11/6/10	59	JHU-17O-2100	Tank #2 CO2	Lab std.	CO2	Exclude	-3.40	-6.77	-0.106	16.15	31.02	-0.104	Nov 2014
11/6/10	60	JHU-17O-2101	Tank #2 CO2	Lab std.	CO2		-3.17	-6.32	-0.112	16.41	31.53	-0.110	Nov 2014
11/6/10	61	JHU-17O-2102	Tank #2 CO2	Lab std.	CO2		-2.82	-5.66	-0.110	16.81	32.29	-0.108	Nov 2014
11/7/10	62	JHU-17O-2103	B13-032/B13-033	atm CO2	CO2		0.24	0.17	-0.127	20.25	38.95	-0.125	Nov 2014

Table S4.5: Analytical run data for sessions containing the newly analyzed enamel samples.[a]

							Voltage mismatch corrected data		Corrected carbonate data				
							d33 vs ref.	d34 vs ref.	$\Delta'^{17}O$ (‰)	$\delta'^{17}O$ (‰)	$\delta'^{18}O$ (‰)	$\Delta'^{17}O$ (‰)	
Date	**Rank in run**	**Analytical ID**	**Sample ID**	**Sample Description**	**Original Phase**	**Exclude?**	**R^2 > 0.6**	**R^2 > 0.6**				**(when CO_3 adjusted)**	**Session ID**
11/7/10	63	JHU-17O-2104	A11-827/A11-828	atm CO2	CO2		0.28	0.23	-0.124	20.29	39.02	-0.122	Nov 2014
11/7/10	64	JHU-17O-2105	A12-036/A12-037	atm CO2	CO2		0.91	1.47	-0.140	21.01	40.43	-0.138	Nov 2014
11/8/10	65	JHU-17O-2106	A12-575/A12-576	atm CO2	CO2		-0.51	-1.28	-0.114	19.40	37.29	-0.112	Nov 2014
11/8/10	66	JHU-17O-2107	A12-759/A12-758	atm CO2	CO2		-0.53	-1.31	-0.120	19.38	37.26	-0.118	Nov 2014
11/8/10	67	JHU-17O-2108	A12-958/A12-959	atm CO2	CO2		-5.97	-10.40	-0.781	13.31	26.87	-0.779	Nov 2014
11/9/10	68	JHU-17O-2109	Tank #2 CO2	Lab std.	CO2		-3.01	-6.02	-0.113	16.59	31.88	-0.111	Nov 2014
11/9/10	69	JHU-17O-2111	1.109.9	Cret. Belemnite	CaCO3		0.16	0.01	-0.123	20.16	38.77	-0.121	Nov 2014
11/9/10	70	JHU-17O-2112	1.109.9	Cret. Belemnite	CaCO3		1.17	1.93	-0.130	21.29	40.97	-0.128	Nov 2014
11/9/10	71	JHU-17O-2113	TGIIF-CO2-23-2	Tao's CO2	CO2		-2.92	-5.86	-0.109	16.69	32.06	-0.108	Nov 2014
11/9/10	72	JHU-17O-2114	LGR-CO2-2	LGR CO2	CO2		-13.95	-26.80	-0.006	4.29	8.15	-0.004	Nov 2014
11/10/10	73	JHU-17O-2115	LGR-CO2-3	LGR CO2	CO2		-14.74	-28.33	0.021	3.40	6.40	0.023	Nov 2014
6/5/15	1	JHU-17O-2116	VSMOW2-052013-2a	International Std.	H2O	Exclude	-18.05	-34.54					June 2015
6/5/15	2	JHU-17O-2117	VSMOW2-052013-2a	International Std.	H2O		-17.97	-34.37					June 2015
6/6/15	3	JHU-17O-2118	VSMOW2-052013-2a	International Std.	H2O		-17.97	-34.36					June 2015
6/6/15	4	JHU-17O-2119	VSMOW2-052013-2a	International Std.	H2O		-18.06	-34.52					June 2015
6/6/15	5	JHU-17O-2120	SLAP2-051613-1b	International Std.	H2O	Exclude	-45.68	-85.34					June 2015
6/6/15	6	JHU-17O-2121	SLAP2-051613-1b	International Std.	H2O		-45.66	-85.32					June 2015
6/7/15	7	JHU-17O-2122	SLAP2-051613-1b	International Std.	H2O		-45.83	-85.63					June 2015
6/7/15	8	JHU-17O-2123	Tank #2 CO2	Lab Standard	CO2	Exclude	-4.83	-9.42	-0.144	15.05	28.98	-0.137	June 2015
6/8/15	9	JHU-17O-2124	Tank #2 CO2	Lab Standard	CO2	Exclude	-3.12	-6.23	-0.120	16.90	32.49	-0.113	June 2015
6/9/15	10	JHU-17O-2125	Tank #2 CO2	Lab Standard	CO2		-3.28	-6.54	-0.127	16.72	32.15	-0.120	June 2015
6/9/15	11	JHU-17O-2126	Tank #2 CO2	Lab Standard	CO2		-3.16	-6.31	-0.124	16.85	32.40	-0.117	June 2015
6/9/15	12	JHU-17O-2127	USABAL-Bird-2	Sample	Eggshell	Exclude	-2.07	-4.11	-0.195	18.03	34.81	-0.188	June 2015
6/9/15	13	JHU-17O-2128	USABAL-Bird-2	Sample	Eggshell		-1.87	-3.76	-0.180	18.25	35.19	-0.173	June 2015
6/9/15	14	JHU-17O-2129	USABAL-Bird-2	Sample	Eggshell		-1.45	-2.97	-0.177	18.70	36.06	-0.170	June 2015
6/10/15	15	JHU-17O-2130	USABAL-Bird-3	Sample	Eggshell		-2.24	-4.50	-0.156	17.85	34.38	-0.149	June 2015
6/10/15	16	JHU-17O-2131	USABAL-Bird-3	Sample	Eggshell		-1.80	-3.67	-0.158	18.32	35.30	-0.151	June 2015
6/10/15	17	JHU-17O-2132	USABAL-Bird-4	Sample	Eggshell		-1.12	-2.34	-0.181	19.06	36.76	-0.174	June 2015
6/10/15	18	JHU-17O-2133	USABAL-Bird-4	Sample	Eggshell	Exclude	-1.90	-3.84	-0.174	18.21	35.11	-0.167	June 2015
6/10/15	19	JHU-17O-2134	USABAL-Bird-5	Sample	Eggshell		-2.19	-4.39	-0.167	17.90	34.50	-0.160	June 2015
6/11/15	20	JHU-17O-2135	USABAL-Bird-5	Sample	Eggshell	Exclude	-2.82	-5.61	-0.157	17.22	33.16	-0.150	June 2015
6/11/15	21	JHU-17O-2136	USABAL-Bird-6	Sample	Eggshell		-1.42	-2.91	-0.174	18.74	36.12	-0.168	June 2015
6/11/15	22	JHU-17O-2137	USABAL-Bird-6	Sample	Eggshell		-1.02	-2.16	-0.174	19.16	36.95	-0.167	June 2015
6/11/15	23	JHU-17O-2138	USABAL-Bird-7	Sample	Eggshell		-1.16	-2.35	-0.218	19.01	36.74	-0.212	June 2015
6/12/15	24	JHU-17O-2139	USABAL-Bird-7	Sample	Eggshell		-1.65	-3.31	-0.202	18.48	35.69	-0.195	June 2015
6/12/15	25	JHU-17O-2140	USABAL-Bird-8	Sample	Eggshell		-2.55	-5.03	-0.193	17.51	33.80	-0.186	June 2015
6/12/15	26	JHU-17O-2141	USABAL-Bird-8	Sample	Eggshell		-2.53	-4.98	-0.198	17.53	33.86	-0.192	June 2015
6/12/15	27	JHU-17O-2142	NBS-18	International Std.	Carbonates	Exclude	-10.72	-20.58	-0.113	8.68	16.73	-0.106	June 2015
6/12/15	28	JHU-17O-2143	NBS-18	International Std.	Carbonates		-11.19	-21.48	-0.101	8.18	15.73	-0.094	June 2015
6/13/15	29	JHU-17O-2144	NBS-18	International Std.	Carbonates		-11.54	-22.14	-0.095	7.80	15.01	-0.089	June 2015
6/13/15	30	JHU-17O-2145	VSMOW2-052013-2a	International Std.	H2O	Exclude	-17.99	-34.36					June 2015
6/13/15	31	JHU-17O-2146	VSMOW2-052013-2a	International Std.	H2O		-18.21	-34.79					June 2015
6/13/15	32	JHU-17O-2147	VSMOW2-052013-2a	International Std.	H2O		-18.15	-34.69					June 2015
6/15/15	33	JHU-17O-2148	VSMOW2-052013-2a	International Std.	H2O		-18.25	-34.87					June 2015
6/15/15	34	JHU-17O-2149	L-TURKANA EYILE SPRING	SAMPLE	H2O		-15.68	-30.03					June 2015
6/15/15	35	JHU-17O-2150	L-TURKANA EYILE SPRING	SAMPLE	H2O		-15.74	-30.15					June 2015
6/15/15	36	JHU-17O-2151	ET05-AWSH-29 (HIPPO)	SAMPLE	MODERN ENAMEL		0.36	0.44	-0.166	20.66	39.81	-0.159	June 2015
6/16/15	37	JHU-17O-2152	ET05-AWSH-29 (HIPPO)	SAMPLE	MODERN ENAMEL		0.34	0.40	-0.164	20.64	39.77	-0.157	June 2015
6/16/15	38	JHU-17O-2153	ET05-MAG0-10 HIPPO	SAMPLE	MODERN ENAMEL		2.65	4.92	-0.235	23.13	44.73	-0.228	June 2015
6/16/15	39	JHU-17O-2154	ET05-MAG0-10 HIPPO	SAMPLE	MODERN ENAMEL		2.64	4.81	-0.188	23.12	44.61	-0.181	June 2015
6/16/15	40	JHU-17O-2155	ET05-MAG0-10 HIPPO	SAMPLE	MODERN ENAMEL		2.99	5.48	-0.186	23.50	45.35	-0.179	June 2015
6/16/15	41	JHU-17O-2156	MGL-93-06	SAMPLE	MODERN ENAMEL		0.56	0.85	-0.177	20.88	40.25	-0.170	June 2015
6/17/15	42	JHU-17O-2157	MGL-93-06	SAMPLE	MODERN ENAMEL		0.38	0.50	-0.180	20.67	39.87	-0.173	June 2015
6/17/15	43	JHU-17O-2158	KN07-111	SAMPLE	MODERN ENAMEL		2.10	3.72	-0.156	22.53	43.41	-0.149	June 2015
6/17/15	44	JHU-17O-2159	KN07-111	SAMPLE	MODERN ENAMEL		2.06	3.65	-0.151	22.50	43.34	-0.144	June 2015
6/17/15	45	JHU-17O-2160	ET05-AWSH-04	SAMPLE	MODERN ENAMEL		2.84	5.22	-0.206	23.33	45.06	-0.199	June 2015
6/17/15	46	JHU-17O-2161	ET05-AWSH-04	SAMPLE	MODERN ENAMEL		3.16	5.84	-0.209	23.68	45.74	-0.203	June 2015
6/18/15	47	JHU-17O-2162	102 GC AZ01	STANDARD	CARBONATE	Exclude	-7.50	-14.53	-0.105	12.16	23.37	-0.098	June 2015
6/18/15	48	JHU-17O-2163	102 GC AZ01	STANDARD	CARBONATE		-7.13	-13.86	-0.097	12.56	24.11	-0.090	June 2015
6/18/15	49	JHU-17O-2164	OSI-001	SAMPLE	EGGSHELL		4.22	7.92	-0.243	24.83	48.02	-0.236	June 2015
6/18/15	50	JHU-17O-2165	OSI-001	SAMPLE	EGGSHELL		4.31	8.09	-0.243	24.92	48.21	-0.236	June 2015
6/19/15	51	JHU-17O-2167	OSI-002	SAMPLE	EGGSHELL		6.82	7.92	2.468	27.61	48.02	2.475	June 2015

Table S4.5: Analytical run data for sessions containing the newly analyzed enamel samples.[a]

							Voltage mismatch corrected data		Corrected carbonate data				
							d33 vs ref.	d34 vs ref.	$\Delta^{17}O$ (‰)	$\delta^{17}O$ (‰)	$\delta^{18}O$ (‰)	$\Delta^{17}O$ (‰)	
Date	**Rank in run**	**Analytical ID**	**Sample ID**	**Sample Description**	**Original Phase**	**Exclude?**	**R^2 > 0.6**	**R^2 > 0.6**				**(when CO_3 adjusted)**	**Session ID**
6/19/15	52	JHU-17O-2168	SLAP2-051613-1b	STANDARD	International Std	Exclude	-46.04	-86.01					June 2015
6/19/15	53	JHU-17O-2169	SLAP2-051613-1b	STANDARD	International Std		-46.16	-86.22					June 2015
6/19/15	54	JHU-17O-2170	CHA-2013	SAMPLE	EGGSHELL		-4.86	-9.51	-0.130	15.01	28.88	-0.123	June 2015
6/19/15	55	JHU-17O-2171	CHA-2013	SAMPLE	EGGSHELL		-3.52	-6.96	-0.131	16.47	31.68	-0.124	June 2015
6/19/15	56	JHU-17O-2172	CHA-2013	SAMPLE	EGGSHELL		-3.35	-6.64	-0.132	16.65	32.03	-0.125	June 2015
6/20/15	57	JHU-17O-2173	OSI-002	SAMPLE	EGGSHELL		3.03	5.66	-0.238	23.55	45.54	-0.231	June 2015
6/20/15	58	JHU-17O-2174	OSI-002	SAMPLE	EGGSHELL		3.77	7.05	-0.233	24.34	47.07	-0.227	June 2015
6/20/15	59	JHU-17O-2175	OSI-002	SAMPLE	EGGSHELL		3.99	7.48	-0.241	24.58	47.54	-0.235	June 2015
6/20/15	60	JHU-17O-2176	NBS-19	STANDARD	STANDARD	Exclude	-0.72	-1.64	-0.143	19.49	37.52	-0.137	June 2015
6/20/15	61	JHU-17O-2177	NBS-19	STANDARD	STANDARD		-1.03	-2.21	-0.154	19.16	36.90	-0.147	June 2015
6/21/15	62	JHU-17O-2178	OSI-003	SAMPLE	EGGSHELL		2.66	4.92	-0.221	23.15	44.73	-0.214	June 2015
6/21/15	63	JHU-17O-2179	OSI-003	SAMPLE	EGGSHELL		2.38	4.38	-0.216	22.84	44.13	-0.209	June 2015
6/21/15	64	JHU-17O-2180	OSI-003	SAMPLE	EGGSHELL		2.76	5.11	-0.218	23.25	44.93	-0.212	June 2015
6/21/15	65	JHU-17O-2181	OSI-004	SAMPLE	EGGSHELL		6.57	12.46	-0.266	27.37	53.01	-0.260	June 2015
6/21/15	66	JHU-17O-2182	OSI-004	SAMPLE	EGGSHELL		6.56	12.45	-0.278	27.36	53.00	-0.272	June 2015
6/21/15	67	JHU-17O-2183	OSI-004	SAMPLE	EGGSHELL		6.83	12.96	-0.278	27.64	53.56	-0.271	June 2015
6/21/15	68	JHU-17O-2184	OSI-005	SAMPLE	EGGSHELL		0.96	1.65	-0.209	21.30	41.14	-0.202	June 2015
6/21/15	69	JHU-17O-2185	OSI-005	SAMPLE	EGGSHELL		0.85	1.43	-0.202	21.18	40.90	-0.195	June 2015
6/21/15	70	JHU-17O-2186	OSI-005	SAMPLE	EGGSHELL		1.03	1.76	-0.190	21.38	41.26	-0.183	June 2015
6/22/15	71	JHU-17O-2187	TANK #2 CO2	STANDARD	STANDARD	Exclude	-2.89	-5.78	-0.133	17.14	32.97	-0.126	June 2015
6/23/15	72	JHU-17O-2188	TANK #2 CO2	STANDARD	STANDARD		-3.08	-6.14	-0.134	16.94	32.59	-0.127	June 2015
6/23/15	73	JHU-17O-2189	OSI-006	SAMPLE	EGGSHELL		2.48	4.61	-0.241	22.95	44.39	-0.234	June 2015
6/23/15	74	JHU-17O-2190	OSI-006	SAMPLE	EGGSHELL		2.41	4.48	-0.243	22.87	44.24	-0.236	June 2015
6/23/15	75	JHU-17O-2191	OSI-006	SAMPLE	EGGSHELL		2.70	5.03	-0.240	23.19	44.85	-0.233	June 2015
6/23/15	76	JHU-17O-2192	VSMOW-052013-2a	INTERNATIONAL STANDARD	Water	Exclude	-17.65	-33.73					June 2015
6/23/15	77	JHU-17O-2193	VSMOW-052013-2a	INTERNATIONAL STANDARD	Water		-17.61	-33.63					June 2015
6/24/15	78	JHU-17O-2194	OSI-007	SAMPLE	EGGSHELL		0.86	1.49	-0.221	21.20	40.96	-0.215	June 2015
6/24/15	79	JHU-17O-2195	OSI-007	SAMPLE	EGGSHELL		1.54	2.76	-0.212	21.93	42.36	-0.205	June 2015
6/24/15	80	JHU-17O-2196	OSI-007	SAMPLE	EGGSHELL		1.75	3.17	-0.216	22.16	42.81	-0.209	June 2015
6/24/15	81	JHU-17O-2197	OSI-008	SAMPLE	EGGSHELL		3.45	6.46	-0.247	23.99	46.42	-0.241	June 2015
6/24/15	82	JHU-17O-2198	OSI-008	SAMPLE	EGGSHELL		3.22	6.03	-0.255	23.74	45.95	-0.248	June 2015
6/24/15	83	JHU-17O-2199	OSI-008	SAMPLE	EGGSHELL		3.38	6.33	-0.247	23.92	46.28	-0.240	June 2015
6/25/15	84	JHU-17O-2200	OSI-009	SAMPLE	EGGSHELL		3.34	6.28	-0.264	23.87	46.22	-0.258	June 2015
6/25/15	85	JHU-17O-2201	OSI-009	SAMPLE	EGGSHELL		3.92	7.38	-0.261	24.50	47.43	-0.254	June 2015
6/25/15	86	JHU-17O-2202	OSI-009	SAMPLE	EGGSHELL		4.80	9.06	-0.262	25.46	49.28	-0.255	June 2015
6/25/15	87	JHU-17O-2203	NBS-18	STANDARD	CARBONATE	Exclude	-10.65	-20.44	-0.113	8.76	16.88	-0.107	June 2015
6/25/15	88	JHU-17O-2204	NBS-18	STANDARD	CARBONATE		-11.18	-21.44	-0.109	8.19	15.78	-0.102	June 2015
6/26/15	89	JHU-17O-2205	OSI-010	SAMPLE	CARBONATE		3.70	6.97	-0.260	24.27	46.97	-0.253	June 2015
6/26/15	90	JHU-17O-2206	OSI-010	SAMPLE	CARBONATE		3.88	7.31	-0.265	24.46	47.35	-0.258	June 2015
6/26/15	91	JHU-17O-2207	OSI-010	SAMPLE	CARBONATE		4.03	7.61	-0.275	24.62	47.68	-0.268	June 2015
6/26/15	92	JHU-17O-2208	OSI-011	SAMPLE	CARBONATE		5.22	9.86	-0.261	25.91	50.16	-0.255	June 2015
6/26/15	93	JHU-17O-2209	OSI-011	SAMPLE	CARBONATE		5.29	10.03	-0.275	25.99	50.34	-0.268	June 2015
6/26/15	94	JHU-17O-2210	OSI-011	SAMPLE	CARBONATE		5.43	10.29	-0.276	26.13	50.62	-0.270	June 2015
6/27/15	95	JHU-17O-2211	OSI-012	SAMPLE	CARBONATE		7.28	13.86	-0.290	28.14	54.54	-0.283	June 2015
6/27/15	96	JHU-17O-2212	OSI-012	SAMPLE	CARBONATE		6.43	12.21	-0.283	27.22	52.74	-0.276	June 2015
6/27/15	97	JHU-17O-2213	OSI-012	SAMPLE	CARBONATE		7.23	13.74	-0.281	28.09	54.42	-0.274	June 2015
6/27/15	98	JHU-17O-2214	SLAP2-051613-1B	STANDARD	STANDARD	Exclude	-44.88	-83.84					June 2015
6/27/15	99	JHU-17O-2215	SLAP2-051613-1B	STANDARD	STANDARD		-45.22	-84.47					June 2015
6/27/15	100	JHU-17O-2216	102GC-AZ-01	STANDARD	CARBONATE	Exclude	-9.89	-18.94	-0.150	9.59	18.52	-0.143	June 2015
6/28/15	101	JHU-17O-2217	102GC-AZ-01	STANDARD	CARBONATE		-7.30	-14.12	-0.130	12.38	23.82	-0.123	June 2015
6/28/15	102	JHU-17O-2218	102GC-AZ-01	STANDARD	CARBONATE		-8.09	-15.65	-0.101	11.53	22.14	-0.094	June 2015
6/28/15	103	JHU-17O-2219	OSI-013	SAMPLE	CARBONATE		2.25	4.14	-0.227	22.69	43.87	-0.221	June 2015
6/28/15	104	JHU-17O-2220	OSI-013	SAMPLE	CARBONATE		3.26	6.08	-0.235	23.79	46.00	-0.228	June 2015
6/28/15	105	JHU-17O-2221	OSI-013	SAMPLE	CARBONATE		3.52	6.60	-0.241	24.08	46.57	-0.235	June 2015
6/28/15	106	JHU-17O-2222	VSMOW-052013-2a	International Standard	Water	Exclude	-17.58	-33.62					June 2015
6/29/15	107	JHU-17O-2223	VSMOW-052013-2a	International Standard	Water		-17.73	-33.91					June 2015
6/29/15	108	JHU-17O-2224	VSMOW-052013-2a	International Standard	Water	Exclude	-17.83	-34.15					June 2015
6/29/15	109	JHU-17O-2225	DIWater_evap_0.2	Evaporating Water	Water		-9.59	-18.39					June 2015
6/29/15	110	JHU-17O-2226	CaCl2_evap_0.2	Evaporating Water	Water		-12.15	-23.20					June 2015
6/30/15	111	JHU-17O-2227	2015NaCl-evap-0.26	Evaporating Water	Water		-10.08	-19.31					June 2015
6/30/15	112	JHU-17O-2228	2015DIWater-evap-0.38	Evaporating Water	Water		-13.31	-25.49					June 2015
6/30/15	113	JHU-17O-2229	2015CaCl2-evap-0.3	Evaporating Water	Water		-13.02	-24.95					June 2015
6/30/15	114	JHU-17O-2230	2015CaCl2-evap-0.54	Evaporating Water	Water		-16.19	-30.98					June 2015

Table S4.5: Analytical run data for sessions containing the newly analyzed enamel samples.[a]

							Voltage mismatch corrected data		Corrected carbonate data				
							d33 vs ref.	d34 vs ref.	$\Delta^{17}O$ (‰)	$\delta^{17}O$ (‰)	$\delta^{18}O$ (‰)	$\Delta^{17}O$ (‰)	
Date	**Rank in run**	**Analytical ID**	**Sample ID**	**Sample Description**	**Original Phase**	**Exclude?**	**R^2 > 0.6**	**R^2 > 0.6**				**(when CO_3 adjusted)**	**Session ID**
6/30/15	115	JHU-17O-2231	2015NaCl-evap-0.46	Evaporating Water	Water		-14.60	-27.97					June 2015
7/1/15	116	JHU-17O-2232	2015KCl-evap-0.37	Evaporating Water	Water		-12.61	-24.16					June 2015
7/1/15	117	JHU-17O-2233	SLAP2-051613-1b	International Standard	Water	Exclude	-45.67	-85.33					June 2015
7/1/15	118	JHU-17O-2234	SLAP2-051613-1b	International Standard	Water		-46.29	-86.47					June 2015
7/2/15	1	JHU-17O-2235	VSMOW-052013-2a	International Standard	Water	Exclude	-17.83	-34.10					July 2015
7/2/15	2	JHU-17O-2236	VSMOW-052013-2a	International Standard	Water		-18.38	-35.12					July 2015
7/3/15	3	JHU-17O-2237	VSMOW-052013-2a	International Standard	Water		-18.09	-34.58					July 2015
7/3/15	4	JHU-17O-2238	DIWATER-EVAP-1	SAMPLE	Water		-22.32	-42.51					July 2015
7/3/15	5	JHU-17O-2239	DIWATER-EVAP-0.45	SAMPLE	Water		-13.76	-26.38					July 2015
7/3/15	6	JHU-17O-2240	VSMOW-052013-2a	STANDARD	Water	Exclude	-17.73	-33.89					July 2015
7/3/15	7	JHU-17O-2241	VSMOW-052013-2a	STANDARD	Water		-18.60	-35.52					July 2015
7/4/15	8	JHU-17O-2242	2015NACl-Evap-0.40	SAMPLE	Water		-13.21	-25.32					July 2015
7/4/15	9	JHU-17O-2243	2015MgCl2-Evap-0.36	SAMPLE	Water		-14.20	-27.19					July 2015
7/5/15	10	JHU-17O-2244	2015KCl-Evap-0.73	SAMPLE	Water		-18.16	-34.71					July 2015
7/5/15	11	JHU-17O-2245	2015MgCl2-Evap-0.73	SAMPLE	Water		-18.91	-36.17					July 2015
7/5/15	12	JHU-17O-2246	2015MgCl2-Evap-0.56	SAMPLE	Water		-16.81	-32.17					July 2015
7/5/15	13	JHU-17O-2247	2015CaCl2-Evap-0.14	SAMPLE	Water		-18.85	-35.88					July 2015
7/6/15	14	JHU-17O-2248	USGS45-140815-1	SAMPLE	Water		-21.10	-40.27					July 2015
7/6/15	15	JHU-17O-2249	NBS-19	standard	carbonate	Exclude	-2.70	-5.33	-0.199	17.91	34.58	-0.159	July 2015
7/6/15	16	JHU-17O-2250	NBS-19	standard	carbonate		-2.31	-4.59	-0.199	18.46	35.63	-0.158	July 2015
7/7/15	17	JHU-17O-2251	NBS-19	standard	carbonate		-2.02	-4.06	-0.189	18.87	36.41	-0.149	July 2015
7/8/15	18	JHU-17O-2252	44K3SC1	Sample	carbonate		3.60	6.81	-0.299	26.86	52.07	-0.259	July 2015
7/8/15	19	JHU-17O-2253	44K3SC1	Sample	carbonate		4.25	8.04	-0.289	27.78	53.85	-0.249	July 2015
7/8/15	20	JHU-17O-2254	44K3SC1	Sample	carbonate		5.36	10.15	-0.287	29.35	56.89	-0.247	July 2015
7/8/15	21	JHU-17O-2255	SLAP2-051613-1b	standard	water	Exclude	-46.09	-86.08					July 2015
7/9/15	22	JHU-17O-2256	SLAP2-051613-1b	standard	water		-46.32	-86.51					July 2015
7/9/15	23	JHU-17O-2257	USGS45-140815-1	standard	water		-19.71	-37.59					July 2015
7/9/15	24	JHU-17O-2258	USGS45-140815-1	standard	water		-19.93	-38.03					July 2015
7/9/15	25	JHU-17O-2259	2015KCl_evap_0.73	evaporating water	water		-18.51	-35.37					July 2015
7/9/15	26	JHU-17O-2260	2015MgCl2_evap_0.73	evaporating water	water		-17.49	-33.42					July 2015
7/9/15	27	JHU-17O-2261	2015MgCl2_evap_0.73	evaporating water	water		-18.79	-35.89					July 2015
7/10/15	28	JHU-17O-2262	2015MgCl2_evap_0.56	evaporating water	water		-16.37	-31.38					July 2015
7/10/15	29	JHU-17O-2263	2015CaCl2_evap_0.14	evaporating water	water		-19.64	-37.34					July 2015
7/10/15	30	JHU-17O-2264	VSMOW2-052013-2a	international standard	water	Exclude	-19.81	-37.86					July 2015
7/10/15	31	JHU-17O-2265	VSMOW2-052013-2a	international standard	water		-19.52	-37.25					July 2015
7/10/15	32	JHU-17O-2266	VSMOW2-052013-2a	international standard	water		-18.89	-36.04					July 2015
7/10/15	33	JHU-17O-2267	VSMOW2-052013-2a	international standard	water		-19.87	-37.93					July 2015
7/11/15	34	JHU-17O-2268	VSMOW2-052013-2a	international standard	water		-19.84	-37.84					July 2015
7/11/15	35	JHU-17O-2269	2015NaCl-evap-1	evaporating water	water		-22.78	-43.35					July 2015
7/11/15	36	JHU-17O-2270	2015KCl-evap-1	evaporating water	water		-22.84	-43.49					July 2015
7/11/15	37	JHU-17O-2271	2015MgCl2-evap-1	evaporating water	water		-22.92	-43.67					July 2015
7/11/15	38	JHU-17O-2272	2015CaCl2-evap-1	evaporating water	water		-21.75	-41.44					July 2015
7/11/15	39	JHU-17O-2273	2015NaCl-evap-0.77	evaporating water	water		-18.43	-35.21					July 2015
7/12/15	40	JHU-17O-2274	2015KCl-evap-0.64	evaporating water	water		-17.58	-33.60					July 2015
7/12/15	41	JHU-17O-2275	2015MgCl2-evap-0.26	evaporating water	water		-12.96	-24.84					July 2015
7/12/15	42	JHU-17O-2276	USGS45-140815-1	standard	water		-19.05	-36.35					July 2015
7/12/15	43	JHU-17O-2277	USGS45-140815-1	standard	water		-18.84	-35.95					July 2015
7/12/15	44	JHU-17O-2278	SLAP2-051613-1b	international standard	water	Exclude	-45.39	-84.79					July 2015
7/12/15	45	JHU-17O-2279	SLAP2-051613-1b	international standard	water		-46.12	-86.14					July 2015
7/12/15	46	JHU-17O-2280	SLAP2-051613-1b	international standard	water	Exclude	-45.69	-86.02					July 2015
7/14/15	47	JHU-17O-2281	SLAP2-051613-1b	international standard	water	Exclude	-46.38	-86.67					July 2015
7/14/15	48	JHU-17O-2282	2015DIWater_evap_0.77	evaporating water	water		-19.53	-37.25					July 2015
7/14/15	49	JHU-17O-2283	2015DIWater_evap_0.64	evaporating water	water		-17.79	-34.00					July 2015
7/14/15	50	JHU-17O-2284	2015CaCl2_evap_0.72	evaporating water	water		-17.77	-33.96					July 2015
7/14/15	51	JHU-17O-2285	2015NaCl_evap_0.64	evaporating water	water		-16.89	-32.32					July 2015
7/15/15	52	JHU-17O-2286	2015KCl_evap_0.37	evaporating water	water		-13.78	-26.36					July 2015
7/15/15	53	JHU-17O-2287	2015CaCl2_evap_0.3	evaporating water	water		-13.12	-25.13					July 2015
7/15/15	54	JHU-17O-2288	2015MgCl2_evap_0.3	evaporating water	water		-12.70	-24.34					July 2015
7/15/15	55	JHU-17O-2289	2015KCl_evap_0.3	evaporating water	water		-11.76	-22.50					July 2015
7/15/15	56	JHU-17O-2290	VSMOW-052013-2a	international standard	water	Exclude	-17.69	-33.80					July 2015
7/16/15	57	JHU-17O-2293	VSMOW-052013-2a	international standard	water		-18.06	-34.49					July 2015
7/17/15	58	JHU-17O-2294	VSMOW-052013-2a	international standard	water		-18.46	-35.25					July 2015

Table S4.5: Analytical run data for sessions containing the newly analyzed enamel samples.[a]

							Voltage mismatch corrected data		Corrected carbonate data				
							d33 vs ref.	d34 vs ref.	$\Delta^{17}O$ (‰)	$\delta^{17}O$ (‰)	$\delta^{18}O$ (‰)	$\Delta^{17}O$ (‰)	
Date	**Rank in run**	**Analytical ID**	**Sample ID**	**Sample Description**	**Original Phase**	**Exclude?**	**R^2 > 0.6**	**R^2 > 0.6**				**(when CO_3 adjusted)**	**Session ID**
7/17/15	59	JHU-17O-2295	NBS-19	international standard	carbonate	Exclude	-3.66	-7.18	-0.174	16.55	31.91	-0.134	July 2015
7/17/15	60	JHU-17O-2296	NBS-19	international standard	carbonate		-1.64	-3.37	-0.172	19.40	37.39	-0.132	July 2015
7/17/15	61	JHU-17O-2297	NBS-19	international standard	carbonate		-1.14	-2.44	-0.160	20.10	38.73	-0.120	July 2015
7/17/15	62	JHU-17O-2298	RCW/WALD 129-140D	sample	carbonate		-1.60	-3.32	-0.154	19.45	37.46	-0.114	July 2015
7/18/15	63	JHU-17O-2299	RCW/WALD 129-140D	sample	carbonate		-1.75	-3.60	-0.156	19.24	37.06	-0.116	July 2015
7/18/15	64	JHU-17O-2300	GNP giraffe #1	enamel sample	carbonate		1.92	3.49	-0.228	24.46	47.28	-0.188	July 2015
7/18/15	65	JHU-17O-2301	GNP giraffe #1	enamel sample	carbonate		2.69	4.99	-0.245	25.56	49.45	-0.204	July 2015
7/19/15	66	JHU-17O-2302	102GCAZ01	international standard sample	carbonate	Exclude	-6.64	-12.87	-0.139	12.32	23.73	-0.099	July 2015
7/19/15	67	JHU-17O-2303	102GCAZ01	international standard sample	carbonate		-6.28	-12.21	-0.126	12.83	24.68	-0.086	July 2015
7/19/15	68	JHU-17O-2304	102GCAZ01	international standard sample	carbonate		-6.63	-12.88	-0.123	12.33	23.72	-0.083	July 2015
7/20/15	69	JHU-17O-2305	SLAP2-051613-1b	international standard sample	water	Exclude	-43.38	-81.08					July 2015
7/20/15	70	JHU-17O-2306	SLAP2-051613-1b	international standard sample	water		-44.35	-82.85					July 2015
7/20/15	71	JHU-17O-2307	SLAP2-051613-1b	international standard sample	water		-44.82	-83.72					July 2015
7/22/15	1	JHU-17O-2308	VSMOW-2-052013-2a	international standard sample	water	Exlude	-18.23	-34.85					Aug 2015_1
7/22/15	2	JHU-17O-2309	VSMOW-2-052013-2a	international standard sample	water		-18.18	-34.74					Aug 2015_1
7/22/15	3	JHU-17O-2310	VSMOW-2-052013-2a	international standard sample	water		-18.16	-34.71					Aug 2015_1
7/23/15	4	JHU-17O-2311	VSMOW-2-052013-2a	international standard sample	water		-18.28	-34.91					Aug 2015_1
7/23/15	5	JHU-17O-2312	CO2 Tank #2	CO2 Tank standard	CO_2 gas	Exclude	-5.59	-11.10	-0.011	14.28	27.25	0.003	Aug 2015_1
7/23/15	6	JHU-17O-2313	CO2 Tank #2	CO2 Tank standard	CO_2 gas	Exclude	-3.73	-7.50	-0.052	16.13	30.87	-0.038	Aug 2015_1
7/23/15	7	JHU-17O-2314	CO2 Tank #2	CO2 Tank standard	CO_2 gas	Exclude	-3.73	-7.44	-0.087	16.13	30.94	-0.074	Aug 2015_1
7/24/15	8	JHU-17O-2315	MGL-93-7 Aberdares elephant	elephant enamel	enamel		-0.46	-1.12	-0.152	19.37	37.30	-0.138	Aug 2015_1
7/24/15	9	JHU-17O-2316	MGL-93-7 Aberdares elephant	elephant enamel	enamel		-0.15	-0.54	-0.154	19.67	37.88	-0.141	Aug 2015_1
7/24/15	10	JHU-17O-2317	NBS-19	International Std	CO_3 international standard	Exclude	-0.26	-0.76	-0.145	19.56	37.66	-0.132	Aug 2015_1
7/24/15	11	JHU-17O-2318	NBS-19	International Std	CO_3 international standard		-1.01	-2.18	-0.143	18.82	36.23	-0.130	Aug 2015_1
7/24/15	12	JHU-17O-2319	NBS-19	International Std	CO_3 international standard		-0.41	-1.05	-0.145	19.41	37.37	-0.132	Aug 2015_1
7/25/15	13	JHU-17O-2320	MGL-93-17 Meru elephant	modern elephant enamel	enamel		0.02	-0.19	-0.173	19.84	38.24	-0.160	Aug 2015_1
7/25/15	14	JHU-17O-2321	MGL-93-17 Meru elephant	modern elephant enamel	enamel		0.71	1.15	-0.184	20.52	39.58	-0.171	Aug 2015_1
7/25/15	15	JHU-17O-2322	MGL-93-10 Shimba Hills elephant	modern elephant enamel	enamel		0.15	0.04	-0.163	19.96	38.47	-0.150	Aug 2015_1
7/25/15	16	JHU-17O-2323	MGL-93-10 Shimba Hills elephant	modern elephant enamel	enamel		-0.16	-0.55	-0.152	19.67	37.87	-0.138	Aug 2015_1
7/25/15	17	JHU-17O-2324	UCT 1697 Addo elephant	modern elephant enamel	enamel		0.74	1.18	-0.168	20.56	39.62	-0.155	Aug 2015_1
7/25/15	18	JHU-17O-2325	UCT 1697 Addo elephant	modern elephant enamel	enamel		1.13	1.92	-0.170	20.94	40.36	-0.157	Aug 2015_1
7/26/15	19	JHU-17O-2326	Kidepo buffalo	modern buffalo enamel	enamel		1.69	3.04	-0.195	21.50	41.49	-0.181	Aug 2015_1
7/26/15	20	JHU-17O-2327	Kidepo buffalo	modern buffalo enamel	enamel		2.55	4.66	-0.197	22.34	43.12	-0.184	Aug 2015_1
7/26/15	21	JHU-17O-2328	GA Beaver	modern beaver molar enamel	enamel		-0.44	-1.08	-0.158	19.38	37.34	-0.145	Aug 2015_1
7/26/15	22	JHU-17O-2329	GA Beaver	modern beaver molar enamel	enamel		-1.42	-2.96	-0.152	18.41	35.45	-0.139	Aug 2015_1
7/26/15	23	JHU-17O-2330	UCT 14224 Kalagadi Wildebeest	modern wildebeest enamel	enamel		3.19	6.00	-0.262	22.97	44.47	-0.249	Aug 2015_1
7/26/15	24	JHU-17O-2331	UCT 14224 Kalagadi Wildebeest	modern wildebeest enamel	enamel		4.08	7.72	-0.279	23.85	46.20	-0.265	Aug 2015_1
7/27/15	25	JHU-17O-2332	UCT 14224 Kalagadi Wildebeest	modern wildebeest enamel	enamel		3.52	6.67	-0.281	23.30	45.14	-0.268	Aug 2015_1
7/27/15	26	JHU-17O-2333	SLAP2-051613-1b	international water standard	water standard	Exclude	-43.61	-81.47					Aug 2015_1
7/27/15	27	JHU-17O-2334	SLAP2-051613-1b	international water standard	water standard		-45.31	-84.64					Aug 2015_1
7/27/15	28	JHU-17O-2335	SLAP2-051613-1b	international water standard	water standard		-45.62	-85.22					Aug 2015_1
7/27/15	29	JHU-17O-2336	102-GC-AZ01	CO_3 standard	CO_3 standard	Exclude	-13.55	-25.74	-0.188	6.38	12.49	-0.175	Aug 2015_1
7/27/15	30	JHU-17O-2337	102-GC-AZ01	CO_3 standard	CO_3 standard	Exclude	-8.78	-16.88	-0.130	11.12	21.42	-0.117	Aug 2015_1
7/28/15	31	JHU-17O-2338	102-GC-AZ01	CO_3 standard	CO_3 standard		-7.35	-14.21	-0.119	12.54	24.11	-0.106	Aug 2015_1
7/28/15	32	JHU-17O-2339	UCT 14223 Kgalagadi giraffe#1	modern giraffe enamel	modern giraffe enamel		3.03	5.74	-0.285	22.81	44.20	-0.271	Aug 2015_1
7/28/15	33	JHU-17O-2340	UCT 14223 Kgalagadi giraffe#1	modern giraffe enamel	modern giraffe enamel		4.62	8.79	-0.298	24.38	47.27	-0.285	Aug 2015_1
7/28/15	34	JHU-17O-2341	UCT 14285 Addo hartebeest	modern hartebeest enamel	0		1.24	2.22	-0.220	21.04	40.66	-0.207	Aug 2015_1
7/28/15	35	JHU-17O-2342	UCT 14285 Addo hartebeest	modern hartebeest enamel	0		0.07	-0.02	-0.208	19.89	38.41	-0.194	Aug 2015_1
7/28/15	36	JHU-17O-2343	GA deer 2	GA deer enamel	GA deer enamel		-0.24	-0.61	-0.210	19.58	37.81	-0.196	Aug 2015_1
7/28/15	37	JHU-17O-2344	GA deer 2	GA deer enamel	GA deer enamel		-0.67	-1.43	-0.213	19.15	36.99	-0.199	Aug 2015_1
7/29/15	38	JHU-17O-2345	NY deer 1	NY deer enamel	NY deer enamel		-2.89	-5.63	-0.208	16.95	32.75	-0.194	Aug 2015_1
7/29/15	39	JHU-17O-2346	NY deer 1	NY deer enamel	NY deer enamel		-3.00	-5.86	-0.200	16.84	32.52	-0.187	Aug 2015_1
7/29/15	40	JHU-17O-2347	GA deer 1	GA deer enamel	GA deer enamel		-0.39	-0.89	-0.207	19.43	37.53	-0.194	Aug 2015_1
7/29/15	41	JHU-17O-2348	GA deer 1	GA deer enamel	GA deer enamel		-0.07	-0.31	-0.199	19.74	38.11	-0.185	Aug 2015_1
7/29/15	42	JHU-17O-2349	Kidepo buffalo	Kidepo buffalo enamel	Kidepo buffalo enamel		2.15	3.90	-0.197	21.94	42.36	-0.183	Aug 2015_1
7/30/15	43	JHU-17O-2350	Kidepo buffao	Kidepo buffalo enamel	Kidepo buffalo enamel		2.40	4.40	-0.209	22.19	42.85	-0.195	Aug 2015_1
7/30/15	44	JHU-17O-2351	NBS-19	International Std	CO_3 international standard	Exclude	-0.06	-0.39	-0.141	19.76	38.03	-0.128	Aug 2015_1
7/30/15	45	JHU-17O-2352	NBS-19	International Std	CO_3 international standard		-0.38	-1.00	-0.138	19.45	37.42	-0.125	Aug 2015_1
7/30/15	46	JHU-17O-2353	NBS-19	International Std	CO_3 international standard		-0.28	-0.79	-0.149	19.55	37.63	-0.136	Aug 2015_1
7/31/15	47	JHU-17O-2354	GA Beaver	tooth enamel	Sample		-2.29	-4.61	-0.150	17.55	33.79	-0.137	Aug 2015_1
7/31/15	48	JHU-17O-2355	GA Beaver	tooth enamel	Sample		-2.10	-4.25	-0.147	17.74	34.15	-0.133	Aug 2015_1
7/31/15	49	JHU-17O-2356	VSMOW2-052013-2a	water	international standard	Exclude	-17.03	-32.53					Aug 2015_1

Table S4.5: Analytical run data for sessions containing the newly analyzed enamel samples.[a]

							Voltage mismatch corrected data		Corrected carbonate data				
							d33 vs ref.	d34 vs ref.	$\Delta^{17}O$ (‰)	$\delta^{17}O$ (‰)	$\delta^{18}O$ (‰)	$\Delta^{17}O$ (‰)	
Date	**Rank in run**	**Analytical ID**	**Sample ID**	**Sample Description**	**Original Phase**	**Exclude?**	**R^2 > 0.6**	**R^2 > 0.6**				**(when CO_3 adjusted)**	**Session ID**
7/31/15	50	JHU-17O-2357	VSMOW2-052013-2a	water	international standard		-17.50	-33.42					Aug 2015_1
7/31/15	51	JHU-17O-2358	VSMOW2-052013-2a	water	international standard		-17.58	-33.60					Aug 2015_1
8/1/15	52	JHU-17O-2359	BUR MH 30Buff	soil carbonates	carbonate		-3.17	-6.31	-0.124	16.68	32.07	-0.111	Aug 2015_1
8/1/15	53	JHU-17O-2360	BUR MH 30Buff	soil carbonates	carbonate		-1.53	-3.21	-0.124	18.30	35.19	-0.110	Aug 2015_1
8/1/15	54	JHU-17O-2361	SHP 80 XTLN	soil carbonates	carbonate		-1.28	-2.75	-0.122	18.55	35.66	-0.108	Aug 2015_1
8/1/15	55	JHU-17O-2362	SHP 80 XTLN	soil carbonates	carbonate		-1.18	-2.54	-0.126	18.65	35.87	-0.112	Aug 2015_1
8/2/15	56	JHU-17O-2363	RCWMA LD 129-140A	soil carbonates	carbonate		-2.28	-4.62	-0.135	17.56	33.78	-0.122	Aug 2015_1
8/2/15	57	JHU-17O-2364	RCWMA LD 129-140A	soil carbonates	carbonate		-2.29	-4.63	-0.136	17.55	33.76	-0.123	Aug 2015_1
8/2/15	58	JHU-17O-2365	RCWMA LD 129-140E	soil carbonates	carbonate		-2.04	-4.16	-0.132	17.80	34.24	-0.118	Aug 2015_1
8/2/15	59	JHU-17O-2366	RCWMA LD 129-140E	soil carbonates	carbonate		-1.68	-3.52	-0.106	18.16	34.88	-0.093	Aug 2015_1
8/2/15	60	JHU-17O-2367	2015MgCl2_evap_1	evaporating water	water		-20.53	-39.13	0.014	-0.53	-1.03	0.028	Aug 2015_1
8/2/15	61	JHU-17O-2368	2015MgCl2_evap_0.73	evaporating water	water		-17.85	-34.13	0.015	2.14	4.02	0.029	Aug 2015_1
Begin getting low O2 yields for water injections starting with JHU-17O-2369													Aug 2015_1
8/2/15	62	JHU-17O-2369	2015MgCl2_evap_0.56	evaporating water	water		-17.48	-33.45	0.016	2.50	4.71		Aug 2015_1
8/4/15	63	JHU-17O-2371	SLAP2-051613-1b	water standard	water	Exclude	-43.94	-82.08					Aug 2015_1
8/4/15	64	JHU-17O-2372	SLAP2-A2-1202	water standard	water		-45.74	-85.43					Aug 2015_1
8/4/15	65	JHU-17O-2373	SLAP2-A2-1202	water standard	water	Exclude	-46.98	-87.72					Aug 2015_1
8/4/15	66	JHU-17O-2374	102-GC-AZ01	CO3 standard	carbonate standard	Exclude	-8.88	-17.04	-0.146	11.02	21.26	-0.132	Aug 2015_1
8/5/15	67	JHU-17O-2375	102-GC-AZ01	CO3 standard	CO3 standard		-8.08	-15.57	-0.130	11.81	22.74	-0.116	Aug 2015_1
8/5/15	68	JHU-17O-2376	102-GC-AZ01	CO3 standard	CO3 standard		-7.71	-14.90	-0.117	12.18	23.41	-0.103	Aug 2015_1
8/5/15	69	JHU-17O-2377	Lake Junin pp409	Lake Junin carbonate	carbonate		-4.04	-7.94	-0.137	15.81	30.43	-0.124	Aug 2015_1
Changed tubing/connections between GC and T3 on F-line between JHU-17O-2377 and JHU-17O-2378. Changed to stainless steel tubing instead of nickel. Observed very low Nitrogen peak after this change.													Aug 2015_1
8/5/15	70	JHU-17O-2378	Lake Junin pp409	Lake Junin carbonate	carbonate		-3.82	-7.53	-0.130	16.04	30.85	-0.117	Aug 2015_1
8/5/15	71	JHU-17O-2379	Lake Junin pp399	Lake Junin carbonate	carbonate		-4.96	-9.69	-0.128	14.91	28.67	-0.114	Aug 2015_1
8/5/15	72	JHU-17O-2380	Lake Junin pp399	Lake Junin carbonate	carbonate		-4.74	-9.29	-0.121	15.12	29.07	-0.107	Aug 2015_1
8/6/15	73	JHU-17O-2381	Lake Junin pp445	Lake Junin carbonate	carbonate		-4.54	-8.90	-0.126	15.32	29.47	-0.112	Aug 2015_1
8/6/15	74	JHU-17O-2382	Lake Junin pp445	Lake Junin carbonate	carbonate		-5.16	-10.07	-0.134	14.70	28.29	-0.121	Aug 2015_1
8/6/15	75	JHU-17O-2383	Lake Junin pp434	Lake Junin carbonate	carbonate		-1.92	-3.90	-0.153	17.92	34.50	-0.139	Aug 2015_1
8/6/15	76	JHU-17O-2384	Lake Junin pp434	Lake Junin carbonate	carbonate		-2.09	-4.23	-0.149	17.74	34.16	-0.135	Aug 2015_1
Replaced septum													Aug 2015_1
8/6/15	77	JHU-17O-2385	Lake Junin pp426	Lake Junin carbonate	carbonate		-1.92	-3.90	-0.148	17.92	34.50	-0.135	Aug 2015_1
8/6/15	78	JHU-17O-2386	Lake Junin pp426	Lake Junin carbonate	carbonate		-1.82	-3.71	-0.148	18.02	34.69	-0.134	Aug 2015_1
8/6/15	79	JHU-17O-2387	Lake Junin pp439	Lake Junin carbonate	carbonate		-2.14	-4.34	-0.137	17.70	34.06	-0.123	Aug 2015_1
8/7/15	80	JHU-17O-2388	Lake Junin pp439	Lake Junin carbonate	carbonate		-2.93	-5.83	-0.143	16.91	32.56	-0.130	Aug 2015_1
8/7/15	81	JHU-17O-2389	VSMOW-2-052013-2a	water standard	water	Exclude	-17.42	-33.29					Aug 2015_1
8/7/15	82	JHU-17O-2390	VSMOW-2-052013-2a	water standard	water		-18.05	-34.48					Aug 2015_1
8/7/15	83	JHU-17O-2391	VSMOW-2-052013-2a	International Std	water		-18.37	-35.09					Aug 2015_1
8/8/15	84	JHU-17O-2392	NBS-18	International Std	CO3 international standard	Exclude	-11.41	-21.88	-0.098	8.51	16.37	-0.085	Aug 2015_1
8/8/15	85	JHU-17O-2393	NBS-18	International Std	CO3 international standard		-11.66	-22.34	-0.103	8.27	15.91	-0.089	Aug 2015_1
8/8/15	86	JHU-17O-2394	NBS-18	International Std	CO3 international standard		-11.83	-22.68	-0.099	8.09	15.57	-0.086	Aug 2015_1
8/8/15	87	JHU-17O-2395	L110813-D2#	Dinosaur Eggshell	CaCO3		-4.51	-8.65	-0.240	15.34	29.72	-0.227	Aug 2015_1
8/9/15	88	JHU-17O-2396	L110813-D2#	Dinosaur Eggshell	CaCO3		-3.67	-6.99	-0.269	16.18	31.39	-0.255	Aug 2015_1
8/9/15	89	JHU-17O-2397	L110813-D2#	Dinosaur Eggshell	CaCO3		-4.11	-7.81	-0.275	15.74	30.56	-0.262	Aug 2015_1
8/9/15	90	JHU-17O-2398	L120625-D3	Dinosaur Eggshell	CaCO3		-1.88	-3.61	-0.268	17.95	34.79	-0.254	Aug 2015_1
8/9/15	91	JHU-17O-2399	L120625-D3	Dinosaur Eggshell	CaCO3		-1.58	-3.03	-0.269	18.25	35.37	-0.256	Aug 2015_1
8/9/15	92	JHU-17O-2400	L120722-D3	Dinosaur Eggshell	CaCO3		-3.31	-6.35	-0.255	16.53	32.03	-0.241	Aug 2015_1
8/10/15	93	JHU-17O-2401	L120722-D3	Dinosaur Eggshell	CaCO3		-3.58	-6.86	-0.255	16.26	31.52	-0.242	Aug 2015_1
8/10/15	94	JHU-17O-2402	L101209-D2	Dinosaur Eggshell	CaCO3		-4.52	-8.76	-0.188	15.33	29.60	-0.175	Aug 2015_1
8/10/15	95	JHU-17O-2403	L101209-D2	Dinosaur Eggshell	CaCO3		-4.43	-8.60	-0.183	15.42	29.77	-0.170	Aug 2015_1
8/10/15	96	JHU-17O-2404	L100525-D2-1	Dinosaur Eggshell	CaCO3		-2.77	-5.39	-0.217	17.07	33.00	-0.203	Aug 2015_1
8/10/15	97	JHU-17O-2405	L100525-D2-1	Dinosaur Eggshell	CaCO3		-2.39	-4.69	-0.208	17.44	33.70	-0.195	Aug 2015_1
8/11/15	98	JHU-17O-2406	SLAP-2-A2	International Std.	H2O	Exclude	-44.03	-82.24					Aug 2015_1
8/11/15	99	JHU-17O-2407	SLAP-2-A2	International Std.	H2O	Exclude	-45.18	-84.39					Aug 2015_1
8/11/15	100	JHU-17O-2408	SLAP-2-A2	International Std.	H2O		-46.50	-86.84					Aug 2015_1
8/11/15	101	JHU-17O-2409	Tank #2 CO2	Lab Std	CO2	Exclude	-10.90	-20.74	-0.206	9.01	17.52	-0.193	Aug 2015_1
8/11/15	102	JHU-17O-2410	Tank #2 CO2	Lab Std	CO2	Exclude	-5.14	-9.99	-0.153	14.72	28.36	-0.139	Aug 2015_1
8/11/15	103	JHU-17O-2411	Tank #2 CO2	Lab Std	CO2		-2.95	-5.90	-0.127	16.90	32.49	-0.114	Aug 2015_1
8/12/15	104	JHU-17O-2412	S090723-D2#	Dinosaur Sample	CaCO3		-2.54	-4.94	-0.219	17.30	33.45	-0.205	Aug 2015_1
8/12/15	105	JHU-17O-2413	S090723-D2#	Dinosaur Sample	CaCO3		-3.01	-5.81	-0.235	16.83	32.57	-0.222	Aug 2015_1
8/12/15	106	JHU-17O-2414	L110702-D2	Dinosaur Sample	CaCO3		-4.79	-9.27	-0.186	15.07	29.09	-0.172	Aug 2015_1
8/12/15	107	JHU-17O-2415	L110702-D2	Dinosaur Sample	CaCO3		-4.92	-9.52	-0.178	14.94	28.84	-0.165	Aug 2015_1
8/12/15	108	JHU-17O-2416	L100510-D6#	Dinosaur Sample	CaCO3		-3.67	-7.15	-0.191	16.18	31.23	-0.177	Aug 2015_1
8/13/15	109	JHU-17O-2417	L100510-D6#	Dinosaur Sample	CaCO3		-2.97	-5.82	-0.189	16.87	32.56	-0.176	Aug 2015_1

Table S4.5: Analytical run data for sessions containing the newly analyzed enamel samples.[a]

							Voltage mismatch corrected data		Corrected carbonate data				
							d33 vs ref.	d34 vs ref.	$\Delta^{17}O$ (‰)	$\delta^{17}O$ (‰)	$\delta^{18}O$ (‰)	$\Delta^{17}O$ (‰)	
Date	**Rank in run**	**Analytical ID**	**Sample ID**	**Sample Description**	**Original Phase**	**Exclude?**	**R^2 > 0.6**	**R^2 > 0.6**				**(when CO_3 adjusted)**	**Session ID**
8/13/15	110	JHU-17O-2418	L100601-D5	Dinosaur Sample	CaCO3		-3.02	-5.88	-0.206	16.82	32.51	-0.193	Aug 2015_1
8/13/15	111	JHU-17O-2419	L100601-D5	Dinosaur Sample	CaCO3		-2.11	-4.16	-0.205	17.72	34.24	-0.191	Aug 2015_1
8/13/15	112	JHU-17O-2420	L100525-D2-2	Dinosaur Sample	CaCO3		-1.98	-3.89	-0.221	17.85	34.51	-0.208	Aug 2015_1
8/13/15	113	JHU-17O-2421	L100525-D2-2	Dinosaur Sample	CaCO3		-1.46	-2.90	-0.223	18.37	35.50	-0.209	Aug 2015_1
8/14/15	114	JHU-17O-2422	VSMOW-2-052013-2a	International Std	H2O	Exclude	-17.09	-32.64					Aug 2015_1
8/14/15	115	JHU-17O-2423	VSMOW-2-052013-2a	International Std	H2O		-17.53	-33.49					Aug 2015_1
8/14/15	116	JHU-17O-2424	VSMOW-2-052013-2a	International Std	H2O		-18.04	-34.48					Aug 2015_1
8/14/15	117	JHU-17O-2425	VSMOW-2-052013-2a	International Std	H2O		-18.12	-34.63					Aug 2015_1
8/15/15	1	JHU-17O-2426	VSMOW2-A2-12/02	International Std	H2O	Exclude	-18.29	-34.96					Aug 2015_2
8/15/15	2	JHU-17O-2427	VSMOW2-A2-12/02	International Std	H2O		-18.06	-34.52					Aug 2015_2
8/15/15	3	JHU-17O-2428	VSMOW2-A2-12/02	International Std	H2O		-17.99	-34.40					Aug 2015_2
8/16/15	4	JHU-17O-2429	Tank #2 CO2	Lab Std	CO2	Exclude	-4.59	-9.05	-0.126	15.56	29.92	-0.094	Aug 2015_2
8/16/15	5	JHU-17O-2430	Tank #2 CO2	Lab Std	CO2		-3.30	-6.55	-0.150	16.99	32.71	-0.119	Aug 2015_2
8/16/15	6	JHU-17O-2431	Tank #2 CO2	Lab Std	CO2		-3.00	-6.01	-0.139	17.31	33.31	-0.108	Aug 2015_2
8/16/15	7	JHU-17O-2432	L100509-D2C	Dinosaur Eggshell	CaCO3		-2.08	-4.07	-0.249	18.33	35.48	-0.218	Aug 2015_2
8/16/15	8	JHU-17O-2433	L100509-D2C	Dinosaur Eggshell	CaCO3		-1.54	-3.02	-0.265	18.92	36.66	-0.234	Aug 2015_2
8/17/15	9	JHU-17O-2434	L110816-D1	Dinosaur Eggshell	CaCO3		-2.45	-4.71	-0.291	17.91	34.77	-0.260	Aug 2015_2
8/17/15	10	JHU-17O-2435	L110816-D1	Dinosaur Eggshell	CaCO3		-3.27	-6.24	-0.296	17.02	33.06	-0.265	Aug 2015_2
8/17/15	11	JHU-17O-2436	L120630-D1#	Dinosaur Eggshell	CaCO3		-2.68	-5.24	-0.236	17.66	34.18	-0.205	Aug 2015_2
8/17/15	12	JHU-17O-2437	L120630-D1#	Dinosaur Eggshell	CaCO3		-2.69	-5.27	-0.230	17.65	34.15	-0.199	Aug 2015_2
8/17/15	13	JHU-17O-2438	L130605-D1	Dinosaur Eggshell	CaCO3		-3.30	-6.49	-0.192	16.98	32.78	-0.161	Aug 2015_2
8/18/15	14	JHU-17O-2439	L130605-D1	Dinosaur Eggshell	CaCO3		-3.19	-6.27	-0.192	17.11	33.03	-0.161	Aug 2015_2
8/18/15	15	JHU-17O-2440	S140514-7	Dinosaur Eggshell	CaCO3		-3.25	-6.29	-0.243	17.04	33.00	-0.212	Aug 2015_2
8/18/15	16	JHU-17O-2441	S140514-7	Dinosaur Eggshell	CaCO3		-2.60	-5.06	-0.252	17.75	34.38	-0.221	Aug 2015_2
8/18/15	17	JHU-17O-2442	SLAP2-A2-12/02	International Std	H2O	Exclude	-45.14	-84.30					Aug 2015_2
8/18/15	18	JHU-17O-2443	SLAP2-A2-12/02	International Std	H2O		-45.65	-85.27					Aug 2015_2
8/19/15	19	JHU-17O-2444	SLAP2-A2-12/02	International Std	H2O		-45.64	-85.26					Aug 2015_2
8/19/15	20	JHU-17O-2445	NBS-19	International Std	CaCO3	Exclude	4.51	-4.56	6.974	25.42	34.94	6.974	Aug 2015_2
8/19/15	21	JHU-17O-2446	NBS-19	International Std	CaCO3		-1.03	-2.22	-0.174	19.48	37.55	-0.174	Aug 2015_2
8/19/15	22	JHU-17O-2447	NBS-19	International Std	CaCO3		-0.23	-0.71	-0.170	20.36	39.24	-0.170	Aug 2015_2
8/19/15	23	JHU-17O-2448	S140519-1	Dinosaur Eggshell	CaCO3		-4.63	-8.97	-0.203	15.53	30.01	-0.172	Aug 2015_2
8/19/15	24	JHU-17O-2449	S140519-1	Dinosaur Eggshell	CaCO3		-4.48	-8.69	-0.204	15.69	30.32	-0.173	Aug 2015_2
8/20/15	25	JHU-17O-2450	S140515-9	Dinosaur Eggshell	CaCO3		-1.36	-2.74	-0.226	19.12	36.97	-0.195	Aug 2015_2
8/20/15	26	JHU-17O-2451	S140515-9	Dinosaur Eggshell	CaCO3		-1.98	-3.93	-0.225	18.43	35.64	-0.194	Aug 2015_2
8/20/15	27	JHU-17O-2452	S140515-16	Dinosaur Eggshell	CaCO3		-2.36	-4.65	-0.221	18.02	34.84	-0.190	Aug 2015_2
8/20/15	28	JHU-17O-2453	S140515-16	Dinosaur Eggshell	CaCO3		-1.87	-3.74	-0.217	18.55	35.86	-0.186	Aug 2015_2
8/20/15	29	JHU-17O-2454	S140517-4	Dinosaur Eggshell	CaCO3		0.06	-0.03	-0.238	20.68	39.99	-0.207	Aug 2015_2
8/20/15	30	JHU-17O-2455	S140517-4	Dinosaur Eggshell	CaCO3		0.01	-0.14	-0.242	20.62	39.88	-0.211	Aug 2015_2
8/21/15	31	JHU-17O-2456	G140616-A	Dinosaur Eggshell	CaCO3		-4.62	-9.02	-0.163	15.54	29.95	-0.132	Aug 2015_2
8/21/15	32	JHU-17O-2457	G140616-A	Dinosaur Eggshell	CaCO3		-4.45	-8.71	-0.165	15.72	30.30	-0.134	Aug 2015_2
8/21/15	33	JHU-17O-2458	VSMOW2-2A-12/02	International Std	H2O	Exclude	-17.64	-33.72					Aug 2015_2
8/21/15	34	JHU-17O-2459	VSMOW2-2A-12/02	International Std	H2O		-17.81	-34.04					Aug 2015_2
8/22/15	35	JHU-17O-2460	VSMOW2-2A-12/02	International Std	H2O		-17.96	-34.32					Aug 2015_2
8/22/15	36	JHU-17O-2461	102-GC-AZ01	Lab Std	CaCO3	Exclude	-9.05	-17.45	-0.113	10.67	20.53	-0.082	Aug 2015_2
8/22/15	37	JHU-17O-2462	102-GC-AZ01	Lab Std	CaCO3		-7.49	-14.51	-0.122	12.38	23.82	-0.091	Aug 2015_2
8/22/15	38	JHU-17O-2463	102-GC-AZ01	Lab Std	CaCO3		-7.16	-13.89	-0.120	12.75	24.51	-0.089	Aug 2015_2
8/22/15	39	JHU-17O-2464	17K4DC1	D. corbetti	CaCO3		0.26	0.26	-0.199	20.89	40.32	-0.168	Aug 2015_2
8/23/15	40	JHU-17O-2465	17K4DC1	D. corbetti	CaCO3		1.59	2.83	-0.215	22.36	43.19	-0.184	Aug 2015_2
8/23/15	41	JHU-17O-2466	45K1DL1	D. laini	CaCO3		2.36	4.33	-0.244	23.20	44.87	-0.213	Aug 2015_2
8/23/15	42	JHU-17O-2467	45K1DL1	D. laini	CaCO3		1.99	3.66	-0.254	22.80	44.12	-0.223	Aug 2015_2
8/23/15	43	JHU-17O-2468	20K1DS1	D. spaggiarii	CaCO3		1.00	1.72	-0.225	21.71	41.96	-0.194	Aug 2015_2
8/25/15	44	JHU-17O-2469	20K1DS1	D. spaggiarii	CaCO3		-1.32	-2.69	-0.217	19.16	37.02	-0.186	Aug 2015_2
8/25/15	45	JHU-17O-2470	175SCAW1C	S. camelus	CaCO3		6.40	12.19	-0.333	27.64	53.66	-0.302	Aug 2015_2
8/26/15	46	JHU-17O-2471	175SCAW1C	S. camelus	CaCO3		7.42	14.17	-0.353	28.76	55.87	-0.322	Aug 2015_2
8/26/15	47	JHU-17O-2472	193AW2DL1	D. laini	CaCO3		5.07	9.78	-0.397	26.18	50.96	-0.366	Aug 2015_2
8/26/15	48	JHU-17O-2473	193AW2DL1	D. laini	CaCO3		6.05	11.63	-0.391	27.26	53.03	-0.360	Aug 2015_2
8/26/15	49	JHU-17O-2474	SLAP	water std	H2O	Exclude	-44.49	-83.05					Aug 2015_2
8/26/15	50	JHU-17O-2475	SLAP	water std	H2O		-45.50	-84.96					Aug 2015_2
8/27/15	51	JHU-17O-2476	SLAP	water std	H2O		-45.44	-84.82					Aug 2015_2
8/27/15	52	JHU-17O-2477	NBS-19	CO3 std	CaCO3	Exclude	-4.13	-8.06	-0.182	16.08	31.02	-0.151	Aug 2015_2
8/28/15	53	JHU-17O-2478	NBS-19	CO3 std	CaCO3		-2.70	-5.38	-0.176	17.64	34.02	-0.145	Aug 2015_2
8/28/15	54	JHU-17O-2479	NBS-19	CO3 std	CaCO3		-1.77	-3.64	-0.162	18.66	35.96	-0.131	Aug 2015_2

Table S4.5: Analytical run data for sessions containing the newly analyzed enamel samples.[a]

							Voltage mismatch corrected data		Corrected carbonate data				
							d33 vs ref.	d34 vs ref.	$\Delta^{17}O$ (‰)	$\delta^{17}O$ (‰)	$\delta^{18}O$ (‰)	$\Delta^{17}O$ (‰)	
Date	**Rank in run**	**Analytical ID**	**Sample ID**	**Sample Description**	**Original Phase**	**Exclude?**	**R^2 > 0.6**	**R^2 > 0.6**				**(when CO_3 adjusted)**	**Session ID**
8/28/15	55	JHU-17O-2480	AA1 Finland Moose #1	moose enamel	moose enamel		-4.60	-8.96	-0.179	15.56	30.02	-0.147	Aug 2015_2
8/29/15	56	JHU-17O-2481	AA1 Finland Moose #1	moose enamel	moose enamel		-5.14	-9.97	-0.183	14.97	28.89	-0.152	Aug 2015_2
8/30/15	57	JHU-17O-2482	FT1 Finland deer#1	deer enamel	deer enamel		-5.42	-10.53	-0.171	14.65	28.27	-0.140	Aug 2015_2
8/30/15	58	JHU-17O-2483	FT1 Finland deer#1	deer enamel	deer enamel		-4.72	-9.18	-0.181	15.43	29.77	-0.150	Aug 2015_2
8/31/15	59	JHU-17O-2484	RT1 Finland deer#3	deer enamel	deer enamel		-4.98	-9.69	-0.175	15.14	29.20	-0.143	Aug 2015_2
8/31/15	60	JHU-17O-2485	RT1 Finland deer#3	deer enamel	deer enamel		-4.73	-9.21	-0.173	15.42	29.74	-0.142	Aug 2015_2
9/1/15	61	JHU-17O-2486	CF2 Finland Beaver#2	beaver enamel	beaver enamel		-5.55	-10.77	-0.170	14.52	28.00	-0.139	Aug 2015_2
9/1/15	62	JHU-17O-2487	CF2 Finland Beaver#2	beaver enamel	beaver enamel		-4.78	-9.32	-0.172	15.35	29.62	-0.141	Aug 2015_2
9/2/15	63	JHU-17O-2488	AA2 Finland Moose#2	moose enamel	moose enamel		-6.56	-12.64	-0.184	13.41	25.91	-0.153	Aug 2015_2
9/2/15	64	JHU-17O-2489	AA2 Finland Moose#2	moose enamel	moose enamel		-6.26	-12.10	-0.178	13.73	26.51	-0.147	Aug 2015_2
9/2/15	65	JHU-17O-2490	102GC-AZ-01	standard	CaCO3	Exclude	-6.73	-13.05	-0.133	13.22	25.45	-0.102	Aug 2015_2
9/3/15	66	JHU-17O-2491	102GC-AZ-01	standard	CaCO3		-7.72	-14.94	-0.125	12.13	23.34	-0.093	Aug 2015_2
9/3/15	67	JHU-17O-2492	BUR MH 70 White	soil carbonate	CaCO3		-1.87	-3.86	-0.140	18.56	35.71	-0.109	Aug 2015_2
9/3/15	68	JHU-17O-2493	BUR MH 70 White	soil carbonate	CaCO3		-1.30	-2.79	-0.146	19.18	36.92	-0.115	Aug 2015_2
9/4/15	69	JHU-17O-2494	SHP 100 Buff	soil carbonate	CaCO3		-2.19	-4.47	-0.144	18.21	35.04	-0.113	Aug 2015_2
9/4/15	70	JHU-17O-2495	SHP 100 Buff	soil carbonate	CaCO3		-1.50	-3.17	-0.145	18.96	36.49	-0.113	Aug 2015_2
9/6/15	71	JHU-17O-2496	Johnston lab O2	O2 - direct analysis, no extraction line	O2		-18.50	-40.42	2.948	0.24	-5.12		Aug 2015_2
11/15/15	1	JHU-17O-2495-ze	zero enrichment	ref gas	O2	Exclude	#DIV/0!	#DIV/0!					Nov 2015
11/15/15	2	JHU-17O-2495	ze2	zero enrichment	O2		0.05	0.11					Nov 2015
11/15/15	3	JHU-17O-2496	VSMOW2-A2-12-02	water	H2O	Exclude	-18.20	-34.83					Nov 2015
11/15/15	4	JHU-17O-2497	VSMOW2-A2-12-02	water	H2O	Exclude	-18.04	-34.54					Nov 2015
11/15/15	5	JHU-17O-2498	VSMOW2-A2-12-02	water	H2O	Exclude	-18.05	-34.56					Nov 2015
11/15/15	6	JHU-17O-2499	VSMOW2-A2-12-02	water	H2O	Exclude	-18.35	-35.11					Nov 2015
11/16/15	7	JHU-17O-2500	Eliye Spring, Lake Turkana	water	H2O		-16.32	-31.31					Nov 2015
11/16/15	8	JHU-17O-2501	Eliye Spring, Lake Turkana	water	H2O		-16.16	-30.98					Nov 2015
11/16/15	9	JHU-17O-2502	Lake Turkana Water	water	H2O		-15.84	-30.38					Nov 2015
11/16/15	10	JHU-17O-2503	Lake Turkana Water	water	H2O		-15.79	-30.28					Nov 2015
11/16/15	11	JHU-17O-2504	SLAP2-A2-12-02	water	H2O	Exclude	-45.25	-84.59					Nov 2015
11/17/15	12	JHU-17O-2505	SLAP2-A2-12-02	water	H2O		-45.88	-85.75					Nov 2015
11/17/15	13	JHU-17O-2506	SLAP2-A2-12-02	water	H2O		-46.39	-86.68					Nov 2015
11/17/15	14	JHU-17O-2507	SLAP2-A2-12-02	water	H2O		-46.55	-86.98					Nov 2015
11/17/15	15	JHU-17O-2508	NBS-19	carbonate	CaCO3	Exclude	-5.51	-10.72	-0.133	14.57	28.03	-0.132	Nov 2015
11/17/15	16	JHU-17O-2509	NBS-19	carbonate	CaCO3		-2.30	-4.65	-0.137	18.23	35.08	-0.136	Nov 2015
11/17/15	17	JHU-17O-2510	NBS-19	carbonate	CaCO3		-1.27	-2.69	-0.140	19.42	37.36	-0.138	Nov 2015
11/18/15	18	JHU-17O-2511	NBS-19	carbonate	CaCO3		-1.80	-3.72	-0.130	18.80	36.16	-0.129	Nov 2015
11/18/15	19	JHU-17O-2512	LJpp421	carbonate	CaCO3	Exclude - l	-1.86	-3.80	-0.143	18.74	36.07	-0.142	Nov 2015
11/18/15	20	JHU-17O-2513	LJpp421	carbonate	CaCO3		-3.28	-6.53	-0.126	17.11	32.91	-0.125	Nov 2015
11/18/15	21	JHU-17O-2514	LJpp405	carbonate	CaCO3	Exclude - l	-3.41	-6.74	-0.150	16.96	32.66	-0.148	Nov 2015
11/18/15	22	JHU-17O-2514	LJpp405	carbonate	CaCO3	REMOVE	-3.37	-6.72	-0.115	17.01	32.68	-0.114	Nov 2015
11/18/15	23	JHU-17O-2515	LJpp405	carbonate	CaCO3		-4.63	-9.10	-0.115	15.57	29.92	-0.113	Nov 2015
11/19/15	24	JHU-17O-2516	LJpp435	carbonate	CaCO3		-2.41	-4.86	-0.137	18.11	34.84	-0.135	Nov 2015
11/19/15	25	JHU-17O-2517	LJpp435	carbonate	CaCO3		-1.25	-2.66	-0.137	19.43	37.39	-0.135	Nov 2015
11/19/15	26	JHU-17O-2518	LJpp415	carbonate	CaCO3	duplicate v	-1.97	-4.03	-0.135	18.61	35.81	-0.133	Nov 2015
11/19/15	27	JHU-17O-2520	MD deer #1	carbonate	modern enamel		-1.71	-3.47	-0.177	18.91	36.46	-0.175	Nov 2015
11/20/15	28	JHU-17O-2521	MD deer #1	carbonate	modern enamel		-1.03	-2.16	-0.183	19.69	37.98	-0.181	Nov 2015
11/20/15	29	JHU-17O-2522	MD deer #2	carbonate	modern enamel		-2.40	-4.75	-0.193	18.12	34.97	-0.192	Nov 2015
11/20/15	30	JHU-17O-2523	MD deer #2	carbonate	modern enamel		-2.04	-4.06	-0.192	18.53	35.77	-0.190	Nov 2015
11/20/15	31	JHU-17O-2524	WV deer	carbonate	modern enamel		-1.50	-3.00	-0.207	19.16	37.00	-0.205	Nov 2015
11/20/15	32	JHU-17O-2525	WV deer	carbonate	modern enamel		-1.19	-2.43	-0.204	19.51	37.67	-0.203	Nov 2015
11/20/15	33	JHU-17O-2526	WI deer	carbonate	modern enamel		-3.43	-6.70	-0.189	16.95	32.71	-0.188	Nov 2015
11/20/15	34	JHU-17O-2527	WI deer	carbonate	modern enamel		-3.88	-7.56	-0.179	16.43	31.70	-0.178	Nov 2015
11/21/15	35	JHU-17O-2528	VSMOW-2A-12-02	water	modern enamel	Exclude	-13.00	-24.89					Nov 2015
11/21/15	36	JHU-17O-2529	VSMOW-2A-12-02	water	H2O		-17.22	-32.93					Nov 2015
11/21/15	37	JHU-17O-2530	VSMOW-2A-12-02	water	H2O		-17.72	-33.88					Nov 2015
11/21/15	38	JHU-17O-2531	VSMOW-2A-12-02	water	H2O		-17.73	-33.90					Nov 2015
New Fe filings in catalyst													Nov 2015
11/21/15	39	JHU-17O-2532	102-GC-AZ01	carbonate	CaCO3	Exclude	-8.39	-16.26	-0.077	11.27	21.60	-0.076	Nov 2015
11/21/15	40	JHU-17O-2533	102-GC-AZ01	carbonate	CaCO3		-7.10	-13.80	-0.092	12.74	24.45	-0.091	Nov 2015
11/22/15	41	JHU-17O-2534	102-GC-AZ01	carbonate	CaCO3		-7.14	-13.86	-0.097	12.70	24.38	-0.095	Nov 2015
11/22/15	42	JHU-17O-2535	ID deer	carbonate	modern enamel		-3.56	-6.93	-0.195	16.80	32.44	-0.193	Nov 2015
11/22/15	43	JHU-17O-2536	ID deer	carbonate	modern enamel		-2.72	-5.32	-0.212	17.76	34.31	-0.210	Nov 2015
11/22/15	44	JHU-17O-2537	WY deer	carbonate	modern enamel		-2.65	-5.18	-0.208	17.84	34.47	-0.206	Nov 2015

Table S4.5: Analytical run data for sessions containing the newly analyzed enamel samples.[a]

							Voltage mismatch corrected data		Corrected carbonate data				
							d33 vs ref.	d34 vs ref.	$\Delta^{17}O$ (‰)	$\delta^{17}O$ (‰)	$\delta^{18}O$ (‰)	$\Delta^{17}O$ (‰)	
Date	**Rank in run**	**Analytical ID**	**Sample ID**	**Sample Description**	**Original Phase**	**Exclude?**	**R^2 > 0.6**	**R^2 > 0.6**				**(when CO_3 adjusted)**	**Session ID**
11/22/15	45	JHU-17O-2538	WY deer	carbonate	modern enamel		-3.12	-6.08	-0.203	17.30	33.42	-0.202	Nov 2015
11/22/15	46	JHU-17O-2539	AK Caribou #1	carbonate	modern enamel		-6.47	-12.47	-0.171	13.47	26.00	-0.169	Nov 2015
11/23/15	47	JHU-17O-2540	AK Caribou #1	carbonate	modern enamel		-7.14	-13.73	-0.170	12.71	24.53	-0.169	Nov 2015
11/23/15	48	JHU-17O-2541	WY Yellowstone Moose #1	carbonate	modern enamel		-6.19	-11.96	-0.161	13.79	26.59	-0.160	Nov 2015
11/23/15	49	JHU-17O-2542	OK Bison #1	carbonate	modern enamel		-2.01	-4.07	-0.157	18.57	35.76	-0.155	Nov 2015
11/23/15	50	JHU-17O-2543	OK Bison #1	carbonate	modern enamel		-1.16	-2.45	-0.158	19.54	37.65	-0.156	Nov 2015
11/24/15	51	JHU-17O-2544	SLAP2-A2-12-02	water	H2O	Exclude	-43.20	-80.67					Nov 2015
11/24/15	52	JHU-17O-2544	SLAP2-A2-12-02	water	H2O	Exclude - l	-43.20	-80.68					Nov 2015
Replaced septum													Nov 2015
11/24/15	53	JHU-17O-2545	SLAP2-A2-12-02	water	H2O	Exclude	-44.60	-82.91					Nov 2015
11/24/15	54	JHU-17O-2545	SLAP2-A2-12-02	water	H2O	Exclude - l	-44.59	-83.28					Nov 2015
11/24/15	55	JHU-17O-2546	SLAP2-A2-12-02	water	H2O		-45.96	-85.81					Nov 2015
11/24/15	56	JHU-17O-2547	SLAP2-A2-12-02	water	H2O		-46.40	-86.62					Nov 2015
11/24/15	57	JHU-17O-2548	SLAP2-A2-12-02	water	H2O		-46.52	-86.85					Nov 2015
11/25/15	58	JHU-17O-2549	NBS-18	carbonate	CaCO3	Exclude	-12.27	-23.50	-0.097	6.84	13.19	-0.096	Nov 2015
11/25/15	59	JHU-17O-2550	NBS-18	carbonate	CaCO3		-11.50	-22.05	-0.097	7.73	14.88	-0.095	Nov 2015
11/25/15	60	JHU-17O-2551	NBS-18	carbonate	CaCO3		-11.59	-22.24	-0.091	7.62	14.65	-0.089	Nov 2015
11/25/15	61	JHU-17O-2552	ND bison #1	carbonate	modern enamel		-6.83	-13.20	-0.140	13.06	25.15	-0.139	Nov 2015
11/25/15	62	JHU-17O-2553	ND bison #1	carbonate	modern enamel		-6.26	-12.09	-0.158	13.71	26.44	-0.157	Nov 2015
11/25/15	63	JHU-17O-2554	ND bison #2	carbonate	modern enamel		-5.57	-10.77	-0.168	14.50	27.97	-0.167	Nov 2015
11/26/15	64	JHU-17O-2555	ND bison #2	carbonate	modern enamel		-5.94	-11.46	-0.171	14.08	27.17	-0.169	Nov 2015
11/29/15	65	JHU-17O-2556	SD bison #1	carbonate	modern enamel		-5.86	-11.30	-0.177	14.17	27.36	-0.176	Nov 2015
11/29/15	66	JHU-17O-2557	SD bison #1	carbonate	modern enamel		-5.30	-10.26	-0.168	14.81	28.57	-0.167	Nov 2015
11/29/15	67	JHU-17O-2558	VSMOW2-A2-12-02	water standard	H2O	Exclude	-17.68	-33.78					Nov 2015
11/30/15	68	JHU-17O-2559	VSMOW2-A2-12-02	water standard	H2O		-17.99	-34.37					Nov 2015
11/30/15	69	JHU-17O-2560	VSMOW2-A2-12-02	water standard	H2O		-18.45	-35.22					Nov 2015
11/30/15	70	JHU-17O-2561	LJpp415	carbonate	CaCO3	not primed	-5.71	-11.13	-0.120	14.33	27.55	-0.118	Nov 2015
11/30/15	71	JHU-17O-2562	LJpp415	carbonate	CaCO3		-3.24	-6.45	-0.128	17.16	32.99	-0.127	Nov 2015
11/30/15	72	JHU-17O-2563	62Q1W-43-45A	carbonate	CaCO3		-1.38	-2.95	-0.121	19.28	37.06	-0.120	Nov 2015
12/1/15	73	JHU-17O-2564	62Q1W-43-45B	carbonate	CaCO3		0.76	1.15	-0.140	21.73	41.83	-0.138	Nov 2015
12/1/15	74	JHU-17O-2565	62Q1W-43-45B	carbonate	CaCO3		1.00	1.61	-0.142	22.00	42.36	-0.141	Nov 2015
12/1/15	75	JHU-17O-2566	61Q3-61.5-64.5	carbonate	CaCO3		1.08	1.75	-0.141	22.09	42.53	-0.139	Nov 2015
12/1/15	76	JHU-17O-2567	61Q3-61.5-64.5	carbonate	CaCO3		0.87	1.36	-0.142	21.86	42.08	-0.140	Nov 2015
12/1/15	77	JHU-17O-2568	61Q1-7-10	carbonate	CaCO3		0.96	1.53	-0.143	21.95	42.27	-0.142	Nov 2015
12/1/15	78	JHU-17O-2569	61Q1-7-10	carbonate	CaCO3		-0.66	-1.53	-0.148	20.10	38.71	-0.147	Nov 2015
12/2/15	79	JHU-17O-2570	62Q2W-15-16	carbonate	CaCO3		-1.30	-2.81	-0.114	19.37	37.23	-0.113	Nov 2015
12/2/15	80	JHU-17O-2571	62Q2W-15-16	carbonate	CaCO3		-1.08	-2.37	-0.118	19.63	37.73	-0.117	Nov 2015
12/2/15	81	JHU-17O-2572	62Q1W-43-45A	carbonate	CaCO3		-1.06	-2.35	-0.113	19.65	37.76	-0.111	Nov 2015
12/2/15	82	JHU-17O-2573	LJpp415	carbonate	CaCO3		-1.97	-4.04	-0.131	18.61	35.80	-0.130	Nov 2015
12/3/15	83	JHU-17O-2574	NBS-19	carbonate	CaCO3	Exclude	-1.42	-2.99	-0.138	19.24	37.02	-0.136	Nov 2015
12/3/15	84	JHU-17O-2575	NBS-19	carbonate	CaCO3		-0.84	-1.90	-0.130	19.90	38.28	-0.128	Nov 2015
12/3/15	85	JHU-17O-2576	NBS-19	carbonate	CaCO3		-1.08	-2.35	-0.132	19.63	37.76	-0.130	Nov 2015
12/3/15	86	JHU-17O-2577	SLAP2-A2-12-02	carbonate	H2O	Exclude	-44.06	-82.27					Nov 2015
12/4/15	87	JHU-17O-2578	SLAP2-A2-12-02	water injection	H2O	Exclude - s	-44.51	-83.07					Nov 2015
Replaced septum - now yield is ~300mbr instead of ~160mbr													Nov 2015
12/4/15	88	JHU-17O-2579	SLAP2-A2-12-02	water injection	H2O		-45.71	-85.35					Nov 2015
12/4/15	89	JHU-17O-2580	SLAP2-A2-12-02	water injection	H2O		-46.32	-86.46					Nov 2015
12/4/15	90	JHU-17O-2581	O2 ref gas reduction line	O2 ref gas	O2		-9.48	-17.82	-0.337	10.06	19.79		Nov 2015
12/4/15	91	JHU-17O-2582	O2 ref gas reduction line	O2 ref gas	O2		-4.63	-8.73	-0.311	15.59	30.34		Nov 2015
12/4/15	92	JHU-17O-2583	O2 ref gas reduction line	O2 ref gas	O2		-1.22	-2.28	-0.318	19.48	37.84		Nov 2015
12/5/15	93	JHU-17O-2584	O2 ref gas reduction line	O2 ref gas	O2		-3.26	-6.16	-0.307	17.15	33.33		Nov 2015
12/5/15	94	JHU-17O-2585	O2 ref gas reduction line	O2 ref gas	O2		-2.39	-4.53	-0.302	18.14	35.23		Nov 2015
12/5/15	95	JHU-17O-2586	O2 ref gas reduction line	O2 ref gas	O2		-1.94	-3.67	-0.303	18.66	36.23		Nov 2015
12/6/15	96	JHU-17O-2587	O2 ref gas reduction line	O2 ref gas	O2		-1.53	-2.89	-0.305	19.12	37.13		Nov 2015
12/6/15	97	JHU-17O-2588	O2 ref gas fluorinated	O2 ref gas	O2		0.12	0.24					Nov 2015
12/6/15	98	JHU-17O-2589	O2 ref gas fluorinated	O2 ref gas	O2		0.04	0.08					Nov 2015
12/6/15	99	JHU-17O-2590	O2 ref gas fluorinated	O2 ref gas	O2		0.00	0.01					Nov 2015
12/7/15	100	JHU-17O-2591	O2 ref gas reduced	O2 ref gas	O2		-2.87	-5.43					Nov 2015
12/7/15	101	JHU-17O-2592	Zero Enrichment	O2 ref gas	O2		-0.01	0.00					Nov 2015
12/7/15	102	JHU-17O-2593	Zero Enrichment	O2 ref gas	O2		0.12	0.25					Nov 2015
12/8/15	103	JHU-17O-2594	II 193(1)	sandstone	sandstone		-2.19	-4.38	-0.169	18.36	35.39	-0.168	Nov 2015
12/8/15	104	JHU-17O-2595	II 193(1)	sandstone	sandstone		-1.15	-2.44	-0.159	19.55	37.65	-0.157	Nov 2015
12/8/15	105	JHU-17O-2596	102-GC-AZ01	carbonate	CaCO3	Exclude	-6.20	-12.02	-0.132	13.78	26.52	-0.130	Nov 2015

Table S4.5: Analytical run data for sessions containing the newly analyzed enamel samples.[a]

							Voltage mismatch corrected data		Corrected carbonate data				
							d33 vs ref.	d34 vs ref.	$\Delta'^{17}O$ (‰)	$\delta'^{17}O$ (‰)	$\delta^{18}O$ (‰)	$\Delta'^{17}O$ (‰)	
Date	**Rank in run**	**Analytical ID**	**Sample ID**	**Sample Description**	**Original Phase**	**Exclude?**	**R^2 > 0.6**	**R^2 > 0.6**				**(when CO_3 adjusted)**	**Session ID**
12/8/15	106	JHU-17O-2597	102-GC-AZ01	carbonate	CaCO3		-6.70	-12.98	-0.123	13.21	25.40	-0.121	Nov 2015
12/9/15	107	JHU-17O-2598	102-GC-AZ01	carbonate	CaCO3		-7.38	-14.31	-0.097	12.43	23.86	-0.096	Nov 2015
12/9/15	108	JHU-17O-2599	7/2DLRo1	carbonate	CaCO3		1.56	2.81	-0.216	22.65	43.76	-0.215	Nov 2015
12/9/15	109	JHU-17O-2601	7/2DLRo1	carbonate	CaCO3		4.96	9.34	-0.248	26.54	51.36	-0.247	Nov 2015
12/9/15	110	JHU-17O-2602	75Ro36DW1	carbonate	CaCO3		3.86	7.25	-0.252	25.28	48.93	-0.250	Nov 2015
12/9/15	111	JHU-17O-2603	75Ro36DW1	carbonate	CaCO3		3.58	6.70	-0.244	24.96	48.28	-0.242	Nov 2015
12/10/15	112	JHU-17O-2604	21K1DW1	carbonate	CaCO3		3.19	5.88	-0.207	24.51	47.34	-0.206	Nov 2015
12/10/15	113	JHU-17O-2605	21K1DW1	carbonate	CaCO3		1.88	3.40	-0.200	23.02	44.44	-0.198	Nov 2015
12/10/15	114	JHU-17O-2606	II-16-1	carbonate	CaCO3		1.97	3.46	-0.150	23.11	44.51	-0.148	Nov 2015
12/10/15	115	JHU-17O-2607	II-16-1	carbonate	CaCO3		2.31	4.11	-0.149	23.50	45.28	-0.147	Nov 2015
12/10/15	116	JHU-17O-2608	63Q2W-33-34A	lake carbonate	CaCO3		0.65	0.94	-0.146	21.60	41.59	-0.144	Nov 2015
12/11/15	117	JHU-17O-2609	63Q2W-33-34A	lake carbonate	CaCO3		-0.45	-1.16	-0.132	20.35	39.15	-0.130	Nov 2015
12/11/15	118	JHU-17O-2610	L J pp421	lake carbonate	CaCO3		-2.01	-4.11	-0.138	18.56	35.72	-0.137	Nov 2015
12/11/15	119	JHU-17O-2611	L J pp421	lake carbonate	CaCO3		-2.11	-4.29	-0.138	18.45	35.50	-0.136	Nov 2015
12/11/15	120	JHU-17O-2612	56Q2-92-95	lake carbonate	CaCO3		1.01	1.64	-0.148	22.02	42.40	-0.147	Nov 2015
12/11/15	121	JHU-17O-2613	56Q2-92-95	lake carbonate	CaCO3		1.35	2.29	-0.147	22.41	43.15	-0.146	Nov 2015
12/11/15	122	JHU-17O-2614	VSMOW2-A2-12-02	water	H2O	Exclude	-15.70	-30.02					Nov 2015
12/11/15	123	JHU-17O-2615	VSMOW2-A2-12-02	water	H2O		-16.79	-32.08					Nov 2015
12/11/15	124	JHU-17O-2616	VSMOW2-A2-12-02	water	H2O		-17.59	-33.59					Nov 2015
12/11/15	125	JHU-17O-2617	Lake Turkana water	water	H2O		-15.77	-30.21					Nov 2015
12/11/15	126	JHU-17O-2618	Lake Turkana water	water	H2O		-15.68	-30.02					Nov 2015

[a] Samples in each run that are not relevant to this study are in gray-colored text.

Sophie B. Lehmann

Birth Date: July 16th 1985
Birth Location: Toledo, Ohio, USA
Department of Earth and Planetary Sciences
The Johns Hopkins University, 301 Olin Hall, 3400 N. Charles Street, Baltimore, MD 21218
Phone: 1(419) 260-8866; Email: sophie.b.lehmann@gmail.com
Website: http://sites.krieger.jhu.edu/levin/people/sophie-b-lehmann/

RESEARCH INTERESTS

Evaluation of paleoclimate, paleovegetation and landscape using a multiproxy approach (e.g., isotopes, sediments, paleosols, mapping). Terrestrial response to global climate change. Development and application of methods in isotopic geochemistry to address questions about Earth history, including but not limited to conventional stable isotopes, clumped isotopes, triple oxygen isotopes and utilizing radiogenic isotopes for addressing questions of dating.

EDUCATION

Ph. D., Earth and Planetary Sciences, Johns Hopkins University, Baltimore Maryland, expected 2016
Thesis topic: Multiproxy reconstructions of Plio-Pleistocene climate, ecology and environment in the western coast of South Africa and triple oxygen isotopes in tooth enamel.
Advisor: Naomi E. Levin

M. S., Geology, Miami University of Ohio, Oxford Ohio, 2012
Thesis: Climatic and tectonic implications of a mid-Miocene landscape: examination of the Tarapacá Pediplain, northern Atacama Desert, Chile.
Advisor: Jason A. Rech

B. A., Geology, *magna cum laude*, The College of Wooster, Wooster Ohio, 2008
Thesis: Shallow marine paleoenvironments and paleocommunities of the Middle Jurassic (Callovian, Upper Zohar Formation and Lower Matmor Formation) within Hamakhtesh Hagadol in Israel's Negev Desert.
Advisor: Mark A. Wilson

Study abroad, Geological Sciences, University of Oxford, UK, 2006 - 2007
Advisors: Hugh Jenkins and Martin Brasier

PROFESSIONAL EXPERIENCE

Research Assistant, Teaching Assistant, 2011 - present
Department of Earth and Planetary Sciences, Johns Hopkins University

Research and Teaching Assistant, 2008 - 2011
Department of Geology, Miami University of Ohio

Student Advisor, Wiles Wooster Tree-Ring Lab, 2007 - 2008
Teaching Assistant, 2007 - 2008
Department of Geology, The College of Wooster

GRANTS, HONORS AND AWARDS

35th International Geological Congress Students and Early Career Scientists GSA Travel Grant, $3,500, 2016
Palmer Field Fund, Johns Hopkins University, $4,500, field and lab work in South Africa, 2014
Palmer Field Fund, Johns Hopkins University, $2,000, fieldtrip in Patagonia, 2014
Palmer Field Fund, Johns Hopkins University, $3,000, fieldwork in South Africa, 2012
NASA Graduate Fellowship, Sulfate soils and life on Earth and Mars, $90,000, 2011 (*declined*)
Phi Kappa Phi, Miami University of Ohio Chapter, 2010
Geological Society of America Graduate Grant, $2,690, 2010
Miami University of Ohio, Graduate Student Association, $500, 2009
Geological Society of America, Travel Grant, $600 each year, 2009 & 2010
College of Wooster, Ohio: Geology Departmental Honors & Independent Study Honors, 2008
College of Wooster Copland Fund, Independent Study, $2,000, National History Museum, London, 2008
The Robert W. McDowell Prize in Geology, The College of Wooster, 2008
College of Wooster Copland Fund, Independent Study, $2,000, fieldwork in Negev Desert, Israel, 2007
The Karl Ver Steeg Prize in Geology and Geography, The College of Wooster, 2007
Patricia E. Blosser Scholarship, The College of Wooster, 2005 - 2008
Edward S. Foster Scholarship, The College of Wooster, 2004 - 2008

PUBLICATIONS

Lehmann SB, Braun DR, Dennis KJ, Patterson DB, Stynder DD, Bishop LC, Forrest F, Levin NE, 2016, Stable isotopic composition of fossil mammal teeth and environmental change in southwestern South Africa during the Pliocene and Pleistocene. *Palaeogeography, Palaeoclimatology, Palaeoecology*, 457; 396-408

Patterson DB, **Lehmann SB**, Matthews T, Levin NE, Stynder D, Braun DR, 2016, Stable isotope ecology of Cape dune mole-rats (*Bathyergus suillus*) from Elandsfontein, South Africa: implications for C_4 vegetation and hominin paleoecology in the Cape Floral Region. *Palaeogeography, Palaeoclimatology, Palaeoecology*, 457; 409-421

Braun DR, Levin NE, Stynder D, Herries AIR, Archer W, Forrest F, Roberts DL, Bishop LC, Matthews T, **Lehmann SB**, Pickering R, Fitzsimmons KE, 2013, Mid-Pleistocene hominin occupation at Elandsfontein, Western Cape, South Africa. *Quaternary Science Reviews*, 82; 145-166.

Kirk-Lawlor NE, Jordan TE, Rech JA, **Lehmann SB**, 2013, Late Miocene to Early Pliocene paleohydrology and landscape evolution of northern Chile, 19° to 20° S. *Palaeogeography, Palaeoclimatology, Palaeoecology,* 387; 76-90.

Rech JA, Pigati JS, **Lehmann SB**, McGimpsey CN, Grimley DA, Nekola, JC, 2011, Assessing open-system behavior in of ^{14}C in terrestrial gastropod shells. *Radiocarbon*, 53; 325-335.

PUBLICATIONS – *in preparation*

Lehmann SB, Levin NE, Passey BP, Hu H, Miller JH, Hoppe KA, Arppe L, Hynek S, Cerling TE, *in prep*, Triple oxygen isotopes in bioapatite: modern range, primary influences and potential geological application, Target journals are *Earth and Planetary Science Letters* or *Geology*. Plan to submit in Fall 2016.

Lehmann SB, Braun, DR, Sealy J, le Roux P, Zhu M, Levin NE, *in prep*, Strontium isotope ratios of fossil herbivore and carnivore tooth enamel and the environment and ecology of mid-Pleistocene Elandsfontein and southwestern South Africa. Target journals are *Earth and Planetary Science Letters* or *Palaeogeography, Palaeoclimatology, Palaeoecology.* Plan to submit in Fall 2016.

ON-LINE REPORTS AND CONFERENCE PROCEEDINGS

Kirk-Lawlor NE, Jordan TE, Rech J, and **Lehmann SB**, 2012, Paleolago Tiliviche y sus relaciones estratigráficas y paleoclimáticas, Cuenca Pampa del Tamarugal, I Región, Chile. *Proceedings 13th Congreso Geológico Chileno*, 631-633.

Lehmann SB, Rech JA, 2009, NSF Vignette Online Contribution- Key Concepts in Geomorphology: Soils, relict landscapes and paleoclimate in the Atacama Desert, Chile. http://serc.carleton.edu/41080.

PRESENTATIONS – *first author only*

Lehmann SB, Levin NE, Passey BH, Cerling TE, Hu H, 2016, Evaluating aridity using triple oxygen isotopes in tooth enamel. *35th International Geological Congress, Cape Town, South Africa, 27 August – 4 September 2016*

Lehmann SB, Levin NE, Passey BH, Cerling TE, Hu H, 2015, Triple oxygen isotopes in teeth: implications for reconstructing paleoaridity. *Geological Society of America Annual Meeting, Baltimore, Maryland, USA, 1-4 November 2015. Geological Society of America Abstracts with Programs.* 47(7); 285

Lehmann SB, Levin NE, Braun DR, Dennis KJ, Stynder DD, Bishop LC, Forrest F, 2014, A Plio-Pleistocene record of vegetation, climate, and hydrology in western South Africa using carbon and oxygen isotopic composition of fossil tooth enamel. *4th Southern Deserts Conference, Mendoza, Argentina, November 2014.* Program page 17

Lehmann SB, Patterson DB, Braun DR, Stynder DD, Matthews T, Levin NE, 2013, Regional and landscape-scale Pleistocene paleoecology using carbon and oxygen isotopes from in situ macro- and micromammal tooth enamel at Elandsfontein, Western Cape, South Africa. *Society of Vertebrate Paleontology Annual Meeting, Los Angeles CA, Oct 30-Nov 2, 2013. Journal of Vertebrate Paleontology* 33: Program and Abstracts, p. 161

Lehmann SB, Levin NE, Dennis KJ, Bishop LC, Stynder DD, Braun DR, 2013, Trends in climate and vegetation of Plio-Pleistocene South Africa: using fossil enamel isotopic data to address questions of regional environmental change. *Geological Society of America Annual Meeting, Denver, CO, October 2013.* Abstract 187-15. *Geological Society of America Abstracts with Program.* 45(7): 458

Lehmann SB, Levin NE, Stynder DD, Bishop LC, Forrest F, Braun DR, 2012, New tooth enamel isotopic data from the West coast of South Africa and a comparison of terrestrial and marine records of Plio-Pleistocene climate change. *Annual Meeting of the American Geophysical Union, San Francisco CA, December 2012.* Abstract PP51B-2122

Lehmann SB, Rech JA, Currie BS, Jordan TE, Riquelme R, 2010, Climatic and tectonic implications of a mid Miocene landscape: examination of the Tarapacá Pediplain, northern Atacama Desert, Chile. *Geological Society of America Annual Meeting, Denver CO, October 2010*. Abstract 251-6. *Geological Society of America Abstracts with Program* 42(5): 597

Lehmann SB, Rech JA, Currie BS, Jordan TE, Riquelme R, 2009, Redefining the Tarapacá Pediplain; analysis of relict soils in the northern Atacama Desert, Chile. *Geological Society of America Annual Meeting, Denver CO, October 2009.* Abstract 244-33. *Geological Society of America Abstracts with Programs* 41(7): 624

Lehmann SB, Belding E, Wiles GC, Brush N, 2007, Development and climatic analysis of a 465-year tree ring chronology from northeast Ohio. *Geological Society of America Annual Meeting*, *Denver CO, October 2007.* Abstract 237-6. *Geological Society of America Abstracts with Program* 39(6): 637

Lehmann SB, Wiles GC, Cook ER, 2006, Use of stream flow and precipitation records for validating dendrochronological findings related to climate in Northeast Ohio. *Geological Society of America North-Central Session*, *Akron OH, April 2006*

Lehmann SB, Wiles GC, Cook ER. 2006. Extending drought-sensitive oak tree-ring chronologies by dating historical structures in Northeastern Ohio. Geological Society of America North Central Section, Akron Ohio, April 2006. Abstract 20-5. *Geological Society of America Abstracts with Programs, North-Central Section* 38(4): 27

Lehmann SB, Wiles GC, 2005, Dendroarchaeology: tree ring dating of historical structures in Northeastern Ohio. *Midwest Archaeological Conference, Dayton, OH, October 20-23, 2005.* Program and Abstracts page 68. http://www.midwestarchaeology.org/storage/2005Program.pdf

FIELD EXPERIENCE

Elandsfontein, Western Cape, South Africa, 2012 - 2016
Mapping, stratigraphy, and sample collection for isotopic analysis for Pleistocene paleoecology and various dating techniques

Montana, Wind River and Absaroka ranges, 2010
Miami University of Ohio Field Camp

Tarapacá Pediplain, northern Atacama Desert, Chile, 2008 and 2009
Landscape mapping of relict and buried landscapes, and collection of Neogene paleosol samples for elemental and isotopic geochemistry, petrography and detrital zircon dating

Negev Desert, Israel, 2007
Stratigraphic mapping and fossil collection for Jurassic shallow marine community ecological and paleontological analysis

Assynt, Scotland, and Pembrokeshire, Wales, 2006 and 2007
University of Oxford field camp

Glacier Bay National Park, Alaska, 2006
Field collection of subfossil trees for Holocene paleoclimatology and dendrochronology

Northeast and Southwest Ohio, 2006 - 2008
State-wide sampling of Oaks from historical structures and old-growth forests for dendrochronological and paleoprecipitation studies

Northern Kentucky, 2006
Outcrop collection for paleontological studies of shallow marine systems

LABORATORY EXPERIENCE

Levin & Passey Stable Isotope Laboratory, Johns Hopkins University, 2011 - 2016
Conventional and high precision stable isotopic measurements and method development, including triple oxygen isotopes and clumped isotopes of carbonates and bioapatites using a common acid bath peripheral and dual inlet mass spectrometer, laser ablation GC/IRMS system and cavity ring-down spectroscopy. Petrographic microscopy of cements and sand for sedimentological description and determination of environmental processes; XRD analysis of fossil enamel to determine mineralogical composition and degree of diagenesis.

Inductively-Coupled Mass Spectrometry (ICP-MS) Facilities, University of Cape Town, 2014
Clean lab sample preparation for $^{87}Sr/^{86}Sr$ determination in tooth enamel and rocks

Stable Isotope Ratio Facility for Environmental Research (SIRFER), University of Utah, 2013
Training in sample preparation (leaf water extraction, carbonate sampling, CO_2 digestion and glass tube formation), instrument use (IRMS and cavity ring-down mass spectroscopy) and spectrometer peripheral use (TC/EA, GasBench) for stable isotope research in geology, ecology and environmental science

Rech Geochemistry Laboratory, Miami University of Ohio, 2008 - 2011
Off line extraction of carbonate CO_2 and preparation of hyperarid paleosol samples for HPLC and direct current plasma (DCP) analysis
Zoology Microscopy Laboratory, Miami University of Ohio, 2008 - 2011
Electron microscopy (scanning EM: EDAX and BSE), transmission EM, light microscopy sample preparation and imaging

LaserChron Center, University of Arizona, 2009 & 2010
Zircon grain extraction and LA-ICPMS

Wiles Tree-Ring Laboratory, The College of Wooster, 2005 - 2008
Student manager, tree cross-section and core preparation, measurement and analysis of tree ring width

SERVICE

Student Organizer, Annual Geological Society of America meeting, 2015
Session Co-Chair, Annual Geological Society of America meeting, 2015
Session Title: African environments across space and through time: integrating modern and ancient climate data for insights into terrestrial ecosystem dynamics.
Department Representative in Graduate Organization, Johns Hopkins University, 2011 - 2016

TEACHING AND MENTORING EXPERIENCE

Preparing for an Academic Career in the Geosciences. Madison, Wisconsin, Summer 2015
Science Education Research Center (Carleton College) workshop on career development and teaching skills

Johns Hopkins University, Maryland, 2014-2015
Formation of lab course materials and syllabus and attendance at an introductory teaching course "*Introduction to Teaching at the College Level"*

Student mentor for undergraduates
Johns Hopkins University, sediment description and preparation, protocol development, 2013 - 2015
Miami University of Ohio, sample preparation, gastropod mineral composition and SEM imaging, 2009

The College of Wooster, Ohio, 2005 - 2008
Wiles Wooster Tree-Ring Lab Student Advisor for College of Wooster Environmental Analysis and Action Program and Research Project: Data collection and analysis for dating historical structures in NE and SW Ohio, trained students and community members basic techniques of dendrochronological collection and analysis, designed payment structure and wrote reports for clients during an entrepreneurial study and established a database of tree-ring widths from local Oaks

Teaching Assistant in courses (format is given as Course, the Professor, Date*)*

Johns Hopkins University, Department of Earth and Planetary Sciences
Introduction to Sustainability, Cindy Parker, Spring 2015
Guided Tour of the Solar System, Bruce Marsh, Spring 2013
Energy Resources in the Modern World, Linda Hinnov, Fall 2012, 2013 and 2014

Miami University of Ohio, Department of Geology
Introduction to Geology, Lab Course, 2009 - 2010
Introduction to Geology, Lecture Course, Brian Currie, 2009 - 2010

College of Wooster, Ohio, Department of Geology
Paleoclimate, Johannes Koch, 2007
Geomorphology and Hydrology, Johannes Koch, 2008